

Alma Mater Studiorum - Università di Bologna

DOTTORATO DI RICERCA IN  
CHIMICA

Ciclo 34

**Settore Concorsuale:** 03/C1 - CHIMICA ORGANICA

**Settore Scientifico Disciplinare:** CHIM/06 - CHIMICA ORGANICA

CO<sub>2</sub> UTILIZATION AND ALTERNATIVE SOLVENTS: EFFECTIVE TOOLS FOR  
SUSTAINABLE APPLICATIONS

**Presentata da:** Martina Vagnoni

**Coordinatore Dottorato**

Luca Prodi

**Supervisore**

Paola Galletti

**Co-supervisore**

Emilio Tagliavini

**Esame finale anno 2022**

# CONTENTS

<b>ABSTRACT</b>	<b>p.3</b>
<b>CHAPTER 1. INTRODUCTION</b>	<b>p.7</b>
<b>1.1 Carbon Dioxide and the greenhouse effect</b>	<b>p.7</b>
<b>1.2 Government policies for CO<sub>2</sub> reduction</b>	<b>p.9</b>
<b>1.3 Road to Net-zero: the role of carbon capture, utilization and storage (CCUS)</b>	<b>p.12</b>
<b>1.4 Green Chemistry to reduce CO<sub>2</sub> emissions</b>	<b>p.14</b>
<b>1.5 CO<sub>2</sub> utilization in industry and research</b>	<b>p.16</b>
<b>1.6 Synthesis of cyclic carbonates from CO<sub>2</sub> and epoxide</b>	<b>p.21</b>
<b>1.6.1 Homogeneous catalysts</b>	<b>p.23</b>
<b>1.6.2 Heterogeneous catalysts</b>	<b>p.24</b>
<b>1.7 Green Solvents: effective tools towards sustainable synthesis and extractions</b>	<b>p.25</b>
<b>1.7.1 Deep Eutectic Solvents</b>	<b>p.27</b>
<b>1.7.2 Linear and Cyclic Carbonates</b>	<b>p.28</b>
<b>1.7.2.1 Linear carbonates</b>	<b>p.28</b>
<b>1.7.2.2 Cyclic carbonates</b>	<b>p.29</b>
<b>1.7.3 Switchable Polarity Solvents (SPSs)</b>	<b>p.32</b>
<b>CHAPTER 2. AIM OF THE THESIS</b>	<b>p.39</b>
<b>CHAPTER 3. SYNTHESIS OF CYCLIC CARBONATES FROM EPOXIDES AND CO<sub>2</sub></b>	<b>p.41</b>
<b>3.1 Homogeneous catalysts: choline-based eutectic mixtures</b>	<b>p.41</b>
3.1.1 Introduction	p.41
3.1.2 Results and Discussion	p.42
3.1.3 Conclusions	p.51
3.1.4 Experimental section	p.51
<b>3.2 Heterogeneous catalysts: char-based bifunctional catalysts from biopolymers and waste</b>	<b>p.71</b>
3.2.1 Introduction	p.71

3.2.2 Results and Discussion	p.72
3.2.3 Conclusions	p.84
3.2.4 Experimental section	p.84
<b>CHAPTER 4. SYNTHESIS OF CYCLIC CARBONATES FROM DIOLS AND DIMETHYL CARBONATE</b>	<b>p.103</b>
<b>4.1 Homogeneous catalyst: DBU as switchable polarity catalyst</b>	<b>p.103</b>
4.1.1 Introduction	p.103
4.1.2 Results and Discussion	p.107
4.1.3 Conclusions	p.118
4.1.4 Experimental section	p.118
<b>4.2 Heterogeneous catalysts: char-based basic catalysts from potato starch</b>	<b>p.133</b>
4.2.1 Introduction	p.133
4.2.2 Results and Discussion	p.134
4.2.3 Conclusions	p.141
4.2.4 Experimental section	p.141
<b>CHAPTER 5. LIPASE CATALYSED EPOXIDATIONS IN A SUGAR-DERIVED NATURAL DEEP EUTECTIC SOLVENT</b>	<b>p.148</b>
5.1 Introduction	p.148
5.2 Results and Discussion	p.150
5.3 Conclusions	p.154
5.4 Experimental section	p.155
<b>CHAPTER 6. EXTRACTION OF ASTAXANTHIN FROM <i>HAEMATOCOCCUS PLUVIALIS</i> WITH HYDROPHOBIC DEEP EUTECTIC SOLVENTS BASED ON OLEIC ACID</b>	<b>p.168</b>
6.1 Introduction	p.168
6.2 Results and Discussion	p.171
6.3 Conclusions	p.179
6.4 Experimental section	p.180

## ABSTRACT

The growing concentration of CO<sub>2</sub> in the atmosphere and its harmful consequences has led the scientific community to direct its efforts towards a sustainable approach in the study of chemical processes. Among the possible approaches, the reuse of CO<sub>2</sub> and the use of alternative solvents are two strategies that are having widespread diffusion. Carbon capture, utilization and storage (CCUS) is considered a key point to achieve an effective reduction of the CO<sub>2</sub> emitted. In this work this strategy is expressed in the use of CO<sub>2</sub>: i) by using it as a reaction reagent; ii) as trigger to change the physical properties of a catalyst thus facilitating its recovery.

As regards the CO<sub>2</sub> incorporation into molecules, two catalytic systems have been developed for the conversion of CO<sub>2</sub> and epoxides into cyclic carbonates, which have potential applications in the synthesis of biocompatible polymers and linear dialkyl carbonates and as aprotic solvents, also used in lithium-ion batteries.

The first homogeneous catalytic system was composed by eutectic mixtures of choline salts and various H-bond donors (HBDs). The use of these mixtures presents several advantages: they are very easily synthesized from commercially available, inexpensive and non-toxic chemicals and do not require any particular purification step.

These catalysts worked in mild conditions of CO<sub>2</sub> pressure and temperature (1-4 bar, 80-100 °C) and they proved to be effective for the synthesis of terminal cyclic carbonates (giving yields from 80% to 88%). They also were recycled without loss of catalytic activity. In this context, the HBD, coupled with a choline salt, has a dual role: 1) to form a eutectic mixture with the choline salt, soluble in the starting materials in our reaction conditions; 2) to be the co-catalyst in the cycloaddition reaction, being able to stabilize a reaction intermediate. **(Figure 1)**

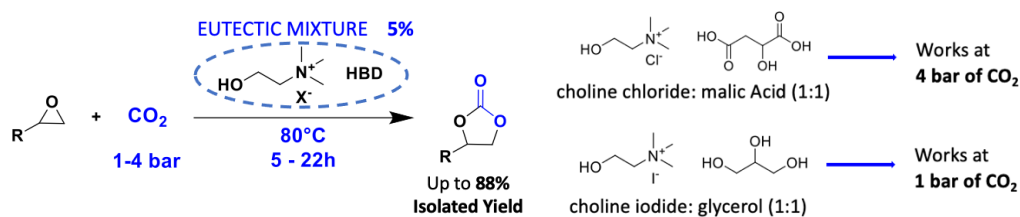


**Figure 1.** Use of choline-based eutectic mixture for the synthesis of cyclic carbonates from epoxides.

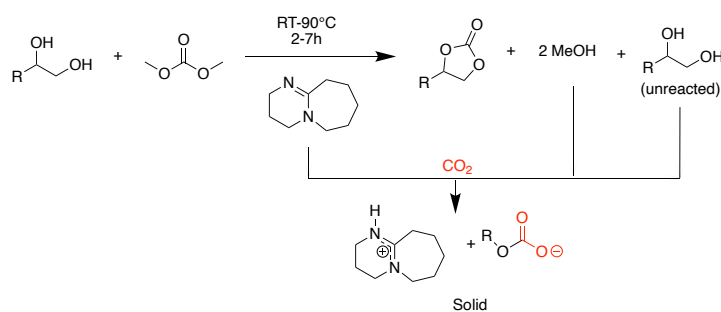
Moving to a heterogeneous version of the catalyst previously described, to improve the catalyst recycling method, we applied a four-steps derivatization method to six materials: i) pyrolysis ii) oxidation ii) introduction of an aminosilane group iv) quaternarization of the amine. With this synthetic pathway six char-catalysts from three different polysaccharides (cellulose, cellulose acetate and potato starch) and three types of waste mainly made from the same polysaccharides (fir sawdust, post-use cigarette filters and starch-based plastic bags) were prepared. The analysis (Raman, ATR-FTIR, XPS and SEM) made on these catalysts demonstrated the effectiveness of the derivatization methods showing no clear differences between the six materials. All the six catalysts proved to be very reactive towards the synthesis of terminal epoxides (from 76% to 91%) with a selectivity >99%. The catalysts have been recycled over five times without appreciable loss of catalytic activity. (**Figure 2**)

POLYMER		CORRESPONDING WASTE					
Cellulose	<b>HC- C</b>	Sawdust	<b>HC- FSD</b>	<b>CATALYST</b>	<b>Yield SC (%)</b>	<b>CATALYST</b>	<b>Yield SC (%)</b>
Cellulose acetate	<b>HC- CA</b>	Post-use Cigarette Filters	<b>HC- PUCF</b>	<b>HC- C</b>	<b>85.5</b>	<b>HC- FSD</b>	<b>91</b>
				<b>HC- CA</b>	<b>86.5</b>	<b>HC- PUCF</b>	<b>84</b>
Starch	<b>HC-PS</b>	Starch-based Plastic bags	<b>HC-SBPB</b>	<b>HC-PS</b>	<b>82</b>	<b>HC-SBPB</b>	<b>88</b>

Reaction conditions: 0,875 mmol SO (100  $\mu$ L), autoclave.

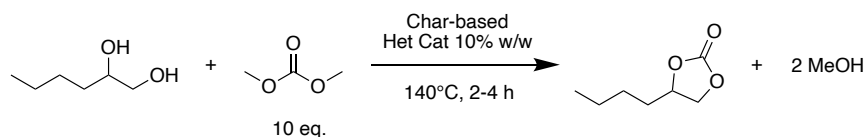
**Figure 2.** Synthesis of six char-catalysts made from biopolymers and waste and their application on the synthesis of cyclic carbonates from epoxides.

As the second application of CO<sub>2</sub> as polarity trigger, it was used for a catalyst recovery. Interestingly, DBU, as other amines, is part of the so called “switchable solvents”. These bases can pass from a less-polar to a more-polar form when reacting with CO<sub>2</sub> in presence of water or alcohols. In this work DBU was used to catalyze the transcobination reactions of various diols with dimethyl carbonate, which is another interesting route to obtain 5-membered cyclic carbonates. Bubbling CO<sub>2</sub> into the reaction vial at the end of the reaction, the catalyst formed a carbonate salt, thus becoming insoluble in the reaction mixture and easily separable. Different diols and conditions were tested obtaining good yields of products and DBU-recovery. (**Scheme 1**)



**Scheme 1.** Transcarbonation reaction scheme and catalyst recovery through CO<sub>2</sub> bubbling.

Wanting to develop a heterogeneous basic catalyst to run transcarbonations of diols and DMC, firstly we tested some catalysts obtained with the same procedure used for the synthesis of heterogeneous catalysts used for the synthesis of cyclic carbonates from epoxides and CO<sub>2</sub>. Although some catalysts seemed active, their poor stability in the new reaction conditions and their non-recyclability led us to study other kinds of functionalization. Starting from the pyrolysis of potato starch, a derivatization including an oxidation step and an amination step, with 1,2-hexanediamine, has been optimized. These new catalysts proved to be very effective in the synthesis of cyclic carbonates, and they have also been recycled over five times without any loss of catalytic activity. (**Scheme 2**)

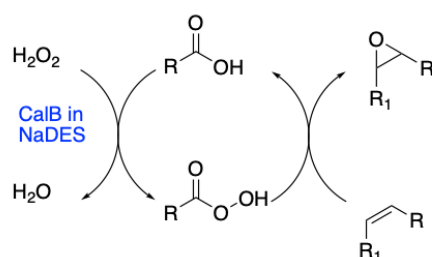


**Scheme 2.** New char-based heterogeneous catalysts for the synthesis of cyclic carbonates from diols and dimethyl carbonate.

As for the use of alternative solvents as tools to deliver more sustainable chemistry, this work focuses on the use of Deep Eutectic Solvents (DESs). They are a new generation of solvents composed by a mixture of two or more substances, liquid at room temperature, and non-volatile. Entropy of mixing, van der Waals interactions, and hydrogen bonding play a role in the formation of DESs. They respect all the requirements to be defined “green solvents” to the point that some of them are composed by natural products (NaDES). New and biobased DESs were here used: i) as reaction media to carry out chemoenzymatic epoxidation; ii) in the extraction of astaxanthin from microalgae culture.

The epoxidation systems used were composed by the alkene, the enzyme *Candida antarctica* lipase B (CALB), a long chain carboxylic acid and hydrogen peroxide. As described in **Scheme**

**3**, the enzyme is responsible for the synthesis in situ of the peracid, starting from the carboxylic acid and hydrogen peroxide, which is the compound that effectively makes the epoxidation on the alkene. Chemoenzymatic epoxidation in DES have been tested taking advantage of the fact that these sustainable solvents can increase the stability of the supported enzymes. The best yields in the reactions tested were obtained using a NaDES consisting of sugar mixtures, sucrose: fructose: glucose (1:1:1 mole ratio, 40% H<sub>2</sub>O). Specific conditions to perform the reaction on selected substrates (like limonene, *trans*-stilbene and oleic acid) in good conversion and selectivity were found.



**Scheme 3.** Chemoenzymatic pathway for epoxidation in DES.

In the last project, three novel DESs based on oleic acid and thymol (TAO), DL-menthol (MAO) and geraniol (GAO) have been here prepared for the first time and applied to the extraction of astaxanthin from *H. pluvialis*. Astaxanthin is an antioxidant produced by the metabolism of the *H. pluvialis* microalgae, and it is part of that pattern of high added value molecules that microalgae can synthesize starting from nutrients and CO<sub>2</sub>. All the DES tested gave good recovery percentages without any thermal, mechanical or chemical pre-treatment, both from dried biomass and directly from algal culture. Moreover, the eutectic mixture composed of thymol and oleic acid demonstrated to have an outstanding antioxidant potential and stabilizing power towards extracted astaxanthin was the best in this sense. (**Figure 3**)

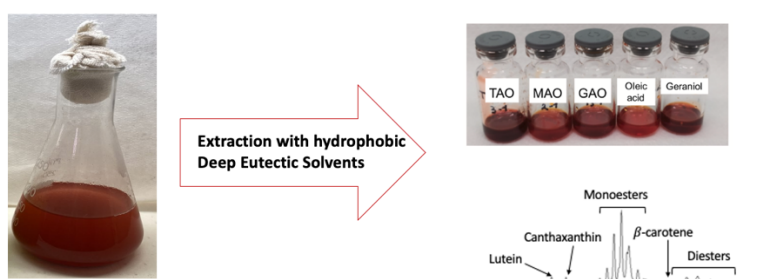


**Figure 3.** Extraction of astaxanthin and carotenoids with hydrophobic deep eutectic solvents.

# CHAPTER 1

## INTRODUCTION

### 1.1 Carbon Dioxide and the greenhouse effect

Carbon Dioxide (CO<sub>2</sub>) is a colorless and odorless gas at atmospheric temperatures and pressure. It is 1.53 times heavier than air, with a density of 1.98 kg/m<sup>3</sup>. It is a linear molecule, in which the carbon atom is the center of symmetry and is linked to the two oxygen atoms by double bonds.<sup>1</sup> It is a gas naturally present in the atmosphere as part of the Earth's carbon cycle (the natural circulation of carbon among soil, atmosphere, oceans, plants and animals). CO<sub>2</sub> produced in the geosphere originates from the degassing of magma, the metamorphism of carbonate rocks, the thermal alteration of coal, the biodegradation of oil and gas and the dissolution of carbonate rocks. The gas then reaches the Earth's surface being emitted within carbo-gaseous provinces commonly consisting of carbonated springs, mofettes (dry CO<sub>2</sub> gas emissions sites), volcanic and associated hydrothermal areas and geysers. Migrating CO<sub>2</sub> mixes readily with petroleum and is a common component of natural gas.<sup>2</sup> Terrestrial ecosystems play a key role in balancing the amount of CO<sub>2</sub> emitted and absorbed, in fact, in the face of many sources of CO<sub>2</sub>, there are also many natural "consumers". During the photosynthesis plants uses CO<sub>2</sub>, together with water and solar light, to produce chemical energy, under the form of sugars and starches. The marine water of the oceans takes up CO<sub>2</sub> in two steps: first, the CO<sub>2</sub> dissolves in the surface water. Afterwards, the ocean's overturning circulation distributes it: ocean currents and mixing processes transport the dissolved CO<sub>2</sub> from the surface deep into the ocean's interior, where it accumulates over time.<sup>3,4</sup>

CO<sub>2</sub>, together with aqueous vapor (H<sub>2</sub>O), methane (CH<sub>4</sub>), nitrous oxide (NO<sub>2</sub>) and ozone (O<sub>3</sub>), is a natural greenhouse gas, but it is also the primary greenhouse gas emitted through human activities. Greenhouse gases are gases in Earth's atmosphere that trap heat. They let most of the visible light coming from the Sun pass through the atmosphere, since they are not able to adsorb the radiation in the visible region (380-750 nm). Part of the radiation that reaches the Earth is reflected (55%) and another part (45%) is adsorbed and then converted in heat, released in the atmosphere as infrared radiation (IR). A minor part of them can pass the

atmosphere being released in the space, the rest remains trapped in the atmosphere causing an increasing of the temperature on the Earth (**Figure 1**).

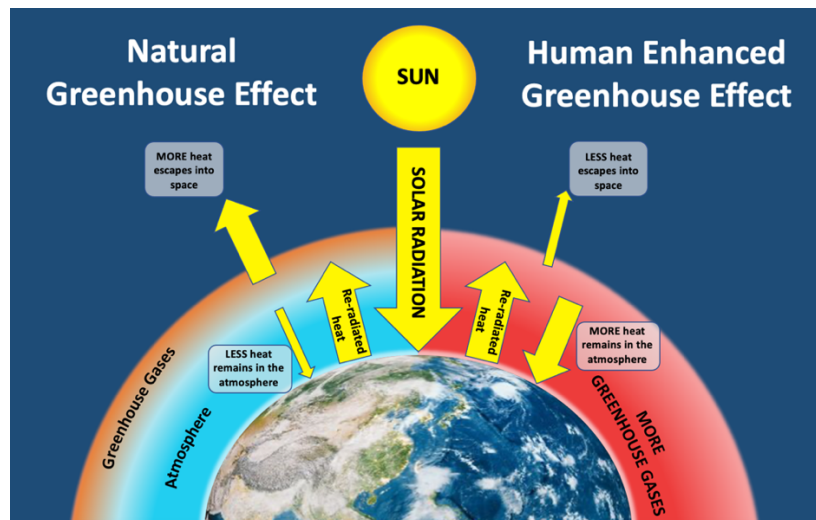


**Figure 1.** The greenhouse effect. Left - Regular levels of carbon dioxide (CO<sub>2</sub>), methane (CH<sub>4</sub>), and nitrous oxide (N<sub>2</sub>O) are created by normal life processes, trapping some of the sun's heat and preventing the planet from freezing. Right - The rampant emission of CO<sub>2</sub> from burning fossil fuels traps excess heat and results in an increase in the average temperature of our planet. Adapted from: Will Elder, NPS.

In fact CO<sub>2</sub> can adsorb the IR radiation because of its molecular structure which allows it to have many vibrational and rotational states. Molecules can only absorb photons energized with the same quantum of energy needed to elevate an electron to a higher energy state, or to elevate the entire molecule to a higher vibrational mode. There are three general vibrations for a CO<sub>2</sub> molecule: a symmetric mode, a bending mode, and an asymmetric mode. Each mode can absorb certain bands of wavelengths that in CO<sub>2</sub> spectrum are centered at 15, 4.3, 2.7, and 2 μm, all in the IR region of the electromagnetic spectrum. Ultimately, the energy from the photon can either be converted into thermal energy, by the conversion of the internal kinetic energy of the CO<sub>2</sub> molecule to the kinetic energy of a different, inert molecule such as N<sub>2</sub>, or the molecule can reemit a photon at a lower frequency. Also the other greenhouse gases, like H<sub>2</sub>O (as aqueous vapor), CH<sub>4</sub>, NO<sub>2</sub> and O<sub>3</sub> are able to adsorb radiation converting it into thermal energy, causing an increasing of the temperature in the troposphere, but CO<sub>2</sub> contributes nearly three-quarters of greenhouse gas emissions and so it is considered as the major gas responsible for the climate change.

In fact, an excessive level of CO<sub>2</sub> in the Earth's atmosphere is a direct cause of global warming and also of ocean acidification, that leads to the changes in seawater chemistry and shows

negative impacts on aquatic ecosystem and warm water stress, which in turn results in the extinction of microbial species in the oceans.<sup>5,6</sup>

As long as the levels of CO<sub>2</sub> in the world depend only on natural emissions, the carbon cycle maintains its balance thanks to the absorption of CO<sub>2</sub> by oceans and plants, but human activities are dramatically altering the carbon cycle-both by adding more CO<sub>2</sub> to the atmosphere, and by influencing the ability of natural sinks, like forests and soils, and oceans to remove and store CO<sub>2</sub> from the atmosphere.<sup>7</sup> Atmospheric CO<sub>2</sub> concentrations increased from ~280 ppm before the industrial revolution to almost 420 ppm in January 2022 (NOAA-GML, Mauna Loa Observatory, Hawaii).

The largest source of greenhouse gas emissions from human activities is from burning fossil fuels for electricity, heat, and transportation.<sup>8</sup>

The growing concentration of CO<sub>2</sub> in the atmosphere due to anthropogenic activities and the harmful consequences that are already pouring on the Earth in terms of climate change, which projections will worsen exponentially, have led the members of the major world economics to reflect on the current climate situation and on the future perspective. Studies and projections have highlighted an immediate need to act and regulate drastically all those polluting activities that cause this situation, bringing this issue to the attention of the governments of the countries, the world of science and the whole world community. The increased sensitivity on these themes has led, especially people in the most economically developed countries, to change their daily habits in the name of a more aware and responsible consumption.

## **1.2 Government policies for CO<sub>2</sub> reduction**

At the 1992 Earth Summit the United Nations Framework Convention on Climate Change (UNFCCC) laid the first foundations for a dialogue on climate change, stipulating that the countries should meet regularly at the COP (Conference of the Parties).<sup>9</sup>

In 1997, during the COP 3 of UNFCCC, 37 industrialized countries and the European Community (composed by 15 countries at that time) stipulated the Kyoto Protocol, to regulate themselves in the greenhouse gases emissions, valid from 2008 to 2012. The protocol was then extended until 2020 with the Doha Amendment. The main goal of the Kyoto Protocol was to control emissions of the main anthropogenic greenhouse gases (GHGs): CO<sub>2</sub>, CH<sub>4</sub>, N<sub>2</sub>O,

hydrofluorocarbons (HFCs), perfluorocarbons (PFCs), sulfur hexafluoride (SF<sub>6</sub>), nitrogen trifluoride (NF<sub>3</sub>). For each gas different levels of emissions reductions would be required to meet the objective of stabilizing atmospheric concentrations. An interesting feature of this Protocol is that the plans that each country had to submit reflected differences in greenhouse gases emissions, wealth, and capacity to make the reductions, underlying a clear difference between the actions to be made by developed and developing countries.<sup>10</sup>

The Paris Agreement was signed in 2016 by 196 countries during the COP 21 of UNFCCC. The main goal was to keep the global temperature below 2 °C above pre-industrial level, preferably limiting the increase to 1.5 °C, to avoid the worst global scenario for climate change. Contemporarily the plans should be set by each country to reach the net-zero emissions for 2050. Unlike the Kyoto protocol, in Paris Agreement there was no differences in the goal to be reach by major economics and less developed countries, all of them had to make plans for a future with zero emission.<sup>11</sup>

COP26 was held in Glasgow in 2021 and was organized with the aim and expectation that the countries could be involved in more ambitious goals than these set during the previous COPs, with always main hope always of limiting the rise in global temperature to 1.5 °C (**Figure 2**).

The work focused on delivering the Glasgow Climate Pact and driving action across the globe on mitigation (reducing emissions), adaptation (helping those already impacted by climate change), finance (enabling countries to deliver on their climate goals) and collaboration (working together to deliver even greater action). To deliver on these stretching targets, the COP has driven commitments to move away from coal power (immediately stopping the building of new coal power plants, scaling up clean power and retiring existing coal fleets, in advanced economies by 2030 and globally by 2040) halt and reverse deforestation (protecting and restoring ecosystems, and managing land sustainably), reduce methane emissions and speed up the switch to electric vehicles (with the aim to by fully electric by 2030).

The main issues and decisions taken during the Conference concern a change in the production and use of clean energy and in the respect for ecosystems; however, a topic that had a small space for discussion was certainly that of Carbon capture, utilization and storage

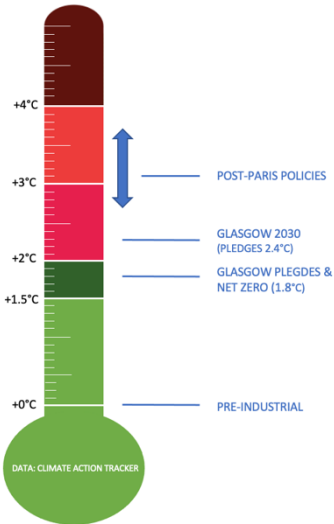


**Figure 2.** COP 26 aims. Adapted from: Climate Action Tracker

(CCUS), which instead is a point that has had a lot of relevance in the studies of the IEA (International Energy Agency). IEA is an autonomous intergovernmental organization born in 1973 after the oil crisis. Since then, it represents an advisor for firsts World economy (USA, Europe, China, etc.) as well as for emerging ones (Brazil, India, Indonesia, etc.) to support energy security and advance the clean energy transition worldwide. The World Energy Outlook (WEO), published every year and based on objective data and analysis, provides critical analysis and insights on trends in energy demand and supply, and what they mean for energy security, environmental protection and economic development. For 2021 the WEO responds to questions about the possibility of the new pledges made by different countries to be effective in reducing emissions and preventing global warming.

In COP26 several large economies have announced pledges to reach net zero emissions. The announcements have not been limited to CO<sub>2</sub> emissions, with more than 100 countries promising to cut emissions of methane by 30% by 2030, that could provide the most impactful way to limit near-term climate change. Nevertheless even if these new targets are met in full and on time, they would be enough to hold the rise in global temperatures to 1.8 °C by the end of the century, that is still above the Paris Agreement target of limiting global warming to well below 2 °C and pursuing efforts to limit it to 1.5 °C. This would require rapid progress and short-term actions on reducing emissions between now and 2030. We can read from IEA website “What is essential is for governments to turn their pledges into clear and credible policy actions and strategies today. Ambitions count for little if they are not implemented successfully. Tracking and accountability will be critical to ensure countries and companies are following through on their promises.”

For this reason, IEA drew a “Global Roadmap to Net Zero by 2050”, providing policy advice to governments on how they can bring their emissions in line with their pledges while still ensuring their clean energy transitions are secure, affordable and fair.

In the analysis the road to net-zero emissions in 2050 is anything but simple. In its report, more than 400 milestones, for what needs to be done and the timing to decarbonize the global economy in 30 years, are presented. Among the precise instructions given by the report, some general points could be summarized:

- Renewable energy technologies like solar and wind are the key to reducing emissions in the electricity sector, which is today the single largest source of CO<sub>2</sub> emissions. In

IEA's pathway to net zero, almost 90% of global electricity generation in 2050 comes from renewable sources, with solar photovoltaic and wind together accounting for nearly 70%.

- Many energy efficient solutions for buildings, vehicles, home appliances and industry are available today and should be scaled up quickly, creating lots of jobs in the process.
- As electricity generation becomes progressively cleaner, electrification of areas previously dominated by fossil fuels emerges as a crucial economy-wide tool for reducing emissions.
- Sustainable bioenergy delivers emissions reductions across a wide range of areas, including low-emissions fuels for planes, ships and other forms of transport, and the replacement of natural gas with biomethane to provide heating and electricity.
- Hydrogen and hydrogen-based fuels will need to fill the gaps where electricity cannot easily or economically replace fossil fuels and where limited sustainable bioenergy supplies cannot cope with demand.
- Achieving net zero by 2050 cannot be achieved without the sustained support and participation from citizens. Behavioral changes, particularly in advanced economies, provide around 4% of the cumulative emissions reductions.
- Carbon capture, utilization and storage (CCUS) contributes to the transition to net zero in multiple ways. These include tackling emissions from existing energy assets, providing solutions in some of the sectors where emissions are hardest to reduce like cement, supporting the rapid scaling up of low-emissions hydrogen production, and enabling some CO<sub>2</sub> to be removed from the atmosphere.

### **1.3 Road to Net-zero: the role of carbon capture, utilization and storage (CCUS) <sup>12</sup>**

The IEA has highlighted the important role of CCUS in achieving net zero emissions, which is relevant for tackling emissions from heavy industry sectors, as cement. CCUS also provides a key option to address emissions from existing energy assets, in the scale up of low-carbon hydrogen production, and to remove carbon from the atmosphere.

Many recent advances have been done in CCUS technology: more than 100 new facilities have been announced and the global project pipeline for CO<sub>2</sub> capture capacity is on track to quadruple. On average, capture capacity of less than 3 million tonnes of CO<sub>2</sub> (MtCO<sub>2</sub>) has been

added worldwide each year since 2010, with annual capture capacity now reaching over 40 MtCO<sub>2</sub>. This needs to increase to 1.6 billion tonnes (GtCO<sub>2</sub>) in 2030 to align with a pathway to net zero by 2050. This boost in CCUS project activity is due to three factors:

- A growing recognition of the relevance of CCUS to reach the net zero goals. For example, Copenhagen is aiming to be the world's first carbon-neutral city and companies such as Microsoft, United Airlines and others are investing in direct air capture technologies.
- The growing interest in producing low-carbon hydrogen. There are almost 50 facilities under development to capture CO<sub>2</sub> from hydrogen-related processes.
- The increasing numbers of investments made by the governments and industries, that since 2020 have committed more than USD 25 billion in funding specifically for CCUS projects and programs. CCUS projects are now operating or under development in 25 countries around the world, mainly from United States and Europe. Many countries are also offering expensive incentives for CCUS projects: USA, Norway, the Netherlands, United Kingdom, Canada and Australia.

Despite there has been some important progress since 2010, CCUS programs have had limited success until now. There are several issues for which CCUS projects are still far from being the key point to solving the problem of CO<sub>2</sub> concentration in the atmosphere: timing of their realizations, their costs and the still little fundings.

Anyway, from the IEA analysis it is clear that “net zero plans make CCUS a necessity, not an option”, especially after the strengthened climate goals. For this reason, in the report (Roadmap to Net Zero by 2050) a CCUS growing to 7.6 billion tonnes of CO<sub>2</sub> per year by 2050 is expected.

IEA analysis highlights the need for increased policy support together with accelerated efforts to identify and develop CO<sub>2</sub> re-utilization resources. Governments, industry and investors have a collective role and interest in ensuring this is the decade that CCUS delivers.

Boosting innovation will also be important for faster commercialization and applications, and this it is the point where science plays a role in making CO<sub>2</sub> technologies more and more efficient. For these reasons research has a duty to commit for an efficient and successful use of CO<sub>2</sub> which must be removed from the atmosphere.

## 1.4 Green Chemistry to reduce CO<sub>2</sub> emissions

It has been about 20 years since the 12 principles of green chemistry were published by Anastas and coworkers. (P. T. Anastas and J. C. Warner, *Green Chemistry: Theory and Practice*, Oxford University Press, Oxford, 1998)<sup>13,14</sup> The growing sensitivity towards the environmental sustainability asked chemistry to give itself principles and rules to be followed, in order to make more useful and applicable research in a World that wants to be clean. After their publication, a large part of the scientific community gathered around them, addressing new research topics and areas totally inspired by and consistent with the 12 principles. This is also demonstrated by the growing number of high-impact journals totally dedicated to the development of sustainable processes or, even more specifically, dedicated to the use of CO<sub>2</sub> or wastes.

For example, processes that include presence of wastes or CO<sub>2</sub> emissions, whether if it is a reaction by-product or produced by reaction energy consuming, is greatly discouraged by many principles:

- Principle 1: "It is better to prevent waste than to treat or clean up waste after it has been created".
- Principle 2: "Synthetic methods should be designed to maximize the incorporation of all materials used in the process into the final product".
- Principle 3: "Wherever practicable, synthetic methods should be designed to use and generate substances that possess little or no toxicity to human health and the environment".
- Principle 6: "Energy requirements of chemical processes should be recognized for their environmental and economic impacts and should be minimized. If possible, synthetic methods should be conducted at ambient temperature and pressure".
- Principle 8: "Unnecessary derivatization (use of blocking groups, protection/deprotection, temporary modification of physical/chemical processes) should be minimized or avoided, if possible, because such steps require additional reagents and can generate waste".

Also the role of process and product safety plays a pivotal role in the list, especially for what concern with the environmental and human safety:

- Principle 4: “Chemical products should be designed to affect their desired function while minimizing their toxicity”.
- Principle 10: “Chemical products should be designed so that at the end of their function they break down into innocuous degradation products and do not persist in the environment”.
- Principle 11: “Analytical methodologies need to be further developed to allow for real-time, in-process monitoring and control prior to the formation of hazardous substances”.
- Principle 12: “Substances and the form of a substance used in chemical processes should be chosen to minimize the potential for chemical accidents, including releases, explosions, and fires”.

On the other hand, the use of renewable resources, catalysts and solvents are allowed, but they should be as benign as possible:

- Principle 5: “The use of auxiliary substances (*e.g.*, solvents, separation agents, *etc.*) should be made unnecessary wherever possible and innocuous when used.
- Principle 7: “A raw material or feedstock should be renewable rather than depleting whenever technically and economically practicable.
- Principle 9: “Catalytic reagents (as selective as possible) are superior to stoichiometric reagents.”

Many examples adhering to these principles are widely present in the literature, especially for what concerns with the study of new and efficient catalysts (organocatalysts, metal catalysts, enzymes, *etc.*)<sup>15</sup> or the use of renewable resources, the prevention of wastes (also controlled by specific metrics, like atom economy<sup>16</sup> or E-factor<sup>17</sup>), the use of mild conditions (low temperature and pressures) and sustainable auxiliaries, like solvents. Especially as regards the latter aspects an interesting new field regards the synthesis of new sustainable solvents, like solvents derived from wastes and biomasses,<sup>18</sup> ionic liquids (ILs),<sup>19</sup> deep eutectic solvents (DESS)<sup>20</sup> and switchable hydrophilicity solvents (SHSs).<sup>21</sup> A total control of all these aspects in the study and set up of a process are what must guide the research for the future.

## 1.5 CO<sub>2</sub> utilization in industry and research

It is clear how chemistry can contribute to the reduction of CO<sub>2</sub> emitted into the atmosphere: by developing sustainable methods that avoid its production or by directly capturing and reusing the CO<sub>2</sub> already present in the atmosphere to convert it into valuable chemicals. The latter option falls within the field of the CCUS, in which the chemistry is giving nowadays the greatest contributions.

CO<sub>2</sub> can be used in different ways, mainly divided into two categories: the first is its use and transformation in chemicals and fuels, the second is its direct (physic) utilization as it is, mainly through its dissolution (**Figure 3**).<sup>22</sup> Poliakoff and Leitner defined twelve principles of CO<sub>2</sub> chemistry to assess the practicability of different reactions and processes that utilize CO<sub>2</sub>.<sup>23</sup>

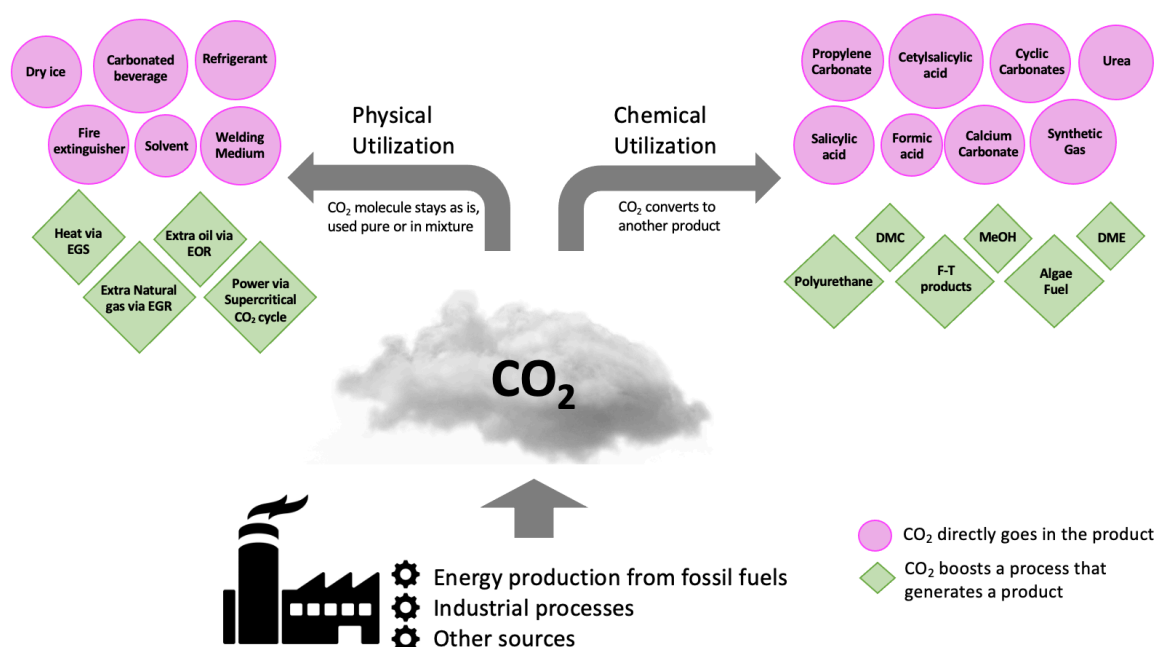


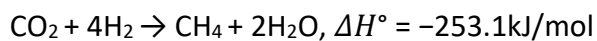
**Figure 3.** Different utilization of CO<sub>2</sub>. Adapted from: Trends in CO<sub>2</sub> Conversion and Utilization: A Review from Process Systems Perspective.<sup>22</sup>

In physical utilization, the CO<sub>2</sub> molecules remain pure or suspended in a solution without a chemical reaction. CO<sub>2</sub> can be physically used as dry ice, fire extinguisher, solvent in its supercritical form (scCO<sub>2</sub>), refrigerant, process fluid, welding medium. It can also be used in largescale industries to indirectly boost/enhance a process as in the enhanced oil recovery (EOR), enhanced gas recovery (EGR) and enhanced geothermal systems (EGS).

For chemical utilization, the bonds of CO<sub>2</sub> molecules often break in exothermic/endothermic reactions and eventually can be converted to various commodity chemicals, synthetic fuels,

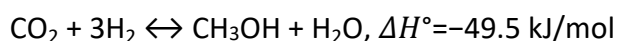
or building blocks. This practice will not only significantly reduce the resource intake and carbon emission but will also improve the sustainability of many chemical processes and industries. Here the main industrial utilization of CO<sub>2</sub>:

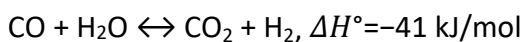
- **Synthesis of syngas:** reforming is the first step in converting raw materials, including fossil fuels, to value-added chemicals and fuels. Syngas (a mixture of CO and H<sub>2</sub>, with variable quantities of CH<sub>4</sub> and CO<sub>2</sub>) is the core intermediate product of reforming that can lead to the production of several end products. Historically steam has been used as a high-temperature medium to generate syngas, however CO<sub>2</sub> can also react with methane to generate syngas with a reaction called dry reforming; this reaction can indirectly lead to the production of several high-demand products such as diesel, naphtha, etc.
- **Methane production:** conversion of CO<sub>2</sub> to methane via catalytic hydrogenation reaction is called methanation or Sabatier process. This process involves the reaction of H<sub>2</sub> with CO<sub>2</sub> at the preferred temperature range of 300–400 °C and elevated pressures in the presence of transition metal catalysts to produce methane and water:



Among the transition metals catalyzing the Sabatier reaction, Ni and Ru are the most catalytically active metals. Currently, no large-scale industrial facilities solely dedicated to conversion of CO<sub>2</sub> to methane via the Sabatier process exist anywhere in the world, but this process is commonly used in the purification of hydrogen streams of CO<sub>x</sub> impurities.

- **Methanol production:** the production of methanol is currently in practice at large industrial scale: it can use CO<sub>2</sub> both indirectly (in reforming stage) and directly in the methanol reactor which converts syngas to methanol. The governing reactions in methanol synthesis from syngas are:





- **Synthesis of Dimethyl ether (DME):** it is an organic chemical compound with the formula  $\text{CH}_3\text{OCH}_3$ . There are two pathways for DME production: direct and indirect. DME can be produced indirectly by methanol synthesis at first step followed by the dehydration of two methanol molecules ( $2\text{CH}_3\text{OH} \leftrightarrow \text{CH}_3\text{OCH}_3 + \text{H}_2\text{O}$ ,  $\Delta H^\circ = -11.7 \text{ kJ/mol}$ ). It can also be produced directly from syngas in a single reactor.<sup>24</sup>
- **Synthesis of dimethyl carbonate (DMC):** it is a carbonate ester with a chemical formula of  $(\text{CH}_3\text{O})_2\text{CO}$ . It was initially produced by the reaction of phosgene ( $\text{COCl}_2$ ) with methanol with a base as catalyst ( $\text{COCl}_2 + 2 \text{CH}_3\text{OH} \rightarrow \text{CH}_3\text{OCO}_2\text{CH}_3 + 2\text{HCl}$ ). However, due to the toxicity of phosgene and the production of HCl in the process, over time this route was deserted, and other synthesis routes have been used. There are five other routes: oxidative carbonylation of methanol (Eni), oxidative carbonylation of methanol via methyl nitrite (Ube), ethylene carbonate transesterification (Asahi), urea transesterification, and direct synthesis from  $\text{CO}_2$ . Currently, the most popular industrial routes are: 1) direct production from methanol and  $\text{CO}_2$ ; 2) production from methanol,  $\text{CO}_2$ , and epoxides; 3) production from  $\text{CO}_2$  and ortho-ester or acetals. All these methods require a catalyst (**Table 1**).

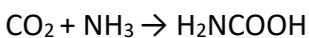
Route	Reaction conditions	Catalyst	Reaction phase
<b>1 Eni</b> $\text{CO} + 2\text{CH}_3\text{OH} + \text{O}_2 \rightarrow \text{DMC} + \text{H}_2\text{O}$	T = 70 – 200 °C P = 5 – 60 atm	CuCl	liquid
<b>2 Ube</b> $\text{N}_2\text{O}_3 + 2\text{CH}_3\text{OH} \rightarrow 2\text{CH}_3\text{ONO} + \text{H}_2\text{O}$ $2\text{CH}_3\text{ONO} + \text{CO} \rightarrow \text{DMC} + \text{NO}$	T = 50 – 150 °C P = 1 – 10 atm	supported Pd catalysts	gas
<b>3 Asahi</b> $(\text{CH}_2)_2\text{O} + \text{CO}_2 \rightarrow \text{C}_2\text{H}_4\text{O}$ $\text{C}_2\text{H}_4\text{O} + 2\text{CH}_3\text{OH} \rightarrow \text{DMC} + (\text{CH}_2\text{OH})_2$	T = 100 – 180 °C P = 40 – 60 atm	$\text{Me}_2\text{Sn}(\text{OMe})_2$	gas-liquid
<b>4 Urea transesterification</b> $2\text{NH}_3 + \text{CO}_2 \rightarrow (\text{NH}_2)_2\text{CO} + \text{H}_2\text{O}$ $(\text{NH}_2)_2\text{CO} + \text{CH}_3\text{OH} \rightarrow \text{CH}_3\text{OCONH}_2 + \text{NH}_3$ $\text{NH}_3\text{CH}_3\text{OCONH}_2 + \text{CH}_3\text{OH} \rightarrow \text{DMC} + \text{NH}_3$	T = 170 – 200 °C P = 1 – 30 atm	Zn salts, Pd salts and other oxides	gas
<b>5 Direct synthesis from methanol and <math>\text{CO}_2</math></b> $\text{CO}_2 + 2\text{CH}_3\text{OH} \rightarrow \text{DMC} + \text{H}_2\text{O}$	T = 160 – 180 °C P = 90 – 300 atm	organometallic compounds, metal tetra-alkoxides, $\text{K}_2\text{CO}_3$ , $\text{Ni}(\text{CH}_3\text{COO})_2$ , zirconia, $\text{CeO}_2$ , $\text{CeO}_2\cdot\text{ZrO}_2$ , $\text{H}_3\text{PW}_{12}\text{O}_{40}/\text{ZrO}_2$ , $\text{H}_3\text{PO}_4\cdot\text{ZrO}_4$ , $\text{H}_3\text{PO}_4\cdot\text{V}_2\text{O}_5$ and Cu-Ni/VSO	liquid
<b>6 Electrochemical reaction of <math>\text{CO}_2</math> and methanol</b>	T = 30 °C, P = 1 atm	$\text{CH}_3\text{OK}$ and the ionic liquid 1-butyl-3-methylimidazolium bromide (bmimBr)	liquid
<b>7 Methanol phosgenation</b> $\text{COCl}_2 + 2 \text{CH}_3\text{OH} \rightarrow \text{DMC} + \text{HCl}$	T = (-5) – 30 °C P = not reported	NaOH	liquid

**Table 1.** Methods for the synthesis of DMC. Source: Trends in  $\text{CO}_2$  conversion and utilization: A review from process systems perspective.<sup>22</sup>

- **Polymer production:** In the polycarbonates and polyurethane synthesis processes,  $\text{CO}_2$  substitutes traditionally used feedstocks. For example, polyethylene and

polypropylene carbonates (PEC and PPC, respectively) can be produced by copolymerization of CO<sub>2</sub> and ethylene oxide and propylene oxide respectively, in the presence of various metallic catalyst.<sup>25</sup> Such polymers (e.g., PEC) can contain up to 50 wt% of CO<sub>2</sub>; therefore, the replacement of traditional materials by these polymers would significantly reduce the carbon footprint (replacing traditional petroleum-based plastics such as polyethylene, polypropylene, polystyrene, and polyvinylchloride) and create a substantial demand for CO<sub>2</sub>.

- **Mineralization:** The CO<sub>2</sub> mineralization or carbonation reaction is a reaction in which CO<sub>2</sub> is converted into CO<sub>3</sub><sup>2-</sup> and the energy is released: high power density could be achieved at a high concentration of the CO<sub>2</sub>.<sup>26</sup> Moreover, CO<sub>2</sub> carbonation of fly ash from a power plant in Australia can be utilized in cement manufacturing in producing “green” building materials.<sup>27</sup>
- **Synthesis of urea:** Urea has various industrial applications and one of the most important is in fertilizers where it reacts with water, releasing CO<sub>2</sub> and ammonia to the soil. The basic urea process is the so-called Bosch-Meiser developed in 1922, which consists of two main reactions: the first reaction is fast exothermic and happens at high temperature and high pressure to produce ammonium carbamate (H<sub>2</sub>N-COONH<sub>4</sub>). This component is decomposed through a slow endothermic reaction in the second stage to form ammonia.



For producing one tonne of urea, 0.735–0.750 t CO<sub>2</sub> is consumed, but the amount of CO<sub>2</sub> emissions in the urea production process is 2.27 tonnes of CO<sub>2</sub>-eq. per tonne of CO<sub>2</sub> utilized. Consequently, the concept of CO<sub>2</sub> utilization in urea production is not recognized as a carbon reduction measure.<sup>28</sup>

- **Synthesis of other chemicals and other value-added products:** CO<sub>2</sub> is used as a building block in synthesizing various oxygen-rich chemical compounds and value-added products. For example, the members of propionic acid family could be synthesized from CO<sub>2</sub> and terminal alkynes via the carboxylation reaction in the presence of Cu-based catalysts.<sup>29</sup> Another CO<sub>2</sub> utilization includes the production of arylcarboxylic acids by carboxylation of aromatic compounds with CO<sub>2</sub> at mild conditions (20-80 °C)<sup>30</sup> or the reaction of CO<sub>2</sub> with CH<sub>4</sub> to produce acetic acid, an intermediate in the production of a variety of pharmaceuticals and polymers. One of the most industrially-relevant example of the use of CO<sub>2</sub> is its cycloaddition with epoxides to give cyclic carbonates, that are solvents and important building blocks for polymer synthesis (see section 5.1).<sup>31</sup>

- **Use in algal systems:**<sup>32</sup> Algae are one of the most abundant and highly adapted forms of life on the Earth playing an important role in the carbon cycle. Many algae are photosynthetic organisms capable of harvesting sunlight and converting CO<sub>2</sub> and water to oxygen and macromolecules such as carbohydrates, lipids, and proteins (together making up to 80 % of the dry algae mass basis). Certain microalgal species naturally accumulate large amounts of triacylglycerols (up to 60 % of dry weight), whereas macroalgae and cyanobacteria mostly accumulate carbohydrates, with lipid content being typically less than 5 %. Photoautotrophic organisms, that require light and CO<sub>2</sub> as carbon source to grow and create new biomass, have a unique capacity to capture CO<sub>2</sub> from both the atmosphere and industrial sources and transform it to biomass that can be further processed into transportation fuels, foodstuff, pharmaceuticals, and chemical products.

The efficiency of the photosynthesis process is a critical parameter related to the productivity of algae since it would ultimately affect the yields of CO<sub>2</sub> capture. To achieve high CO<sub>2</sub> uptake rates (and, hence, biomass production rates) microalgae has to be grown under the optimal conditions of light, temperature, pH, nutrient, and CO<sub>2</sub> concentrations. No single algal strain is known to satisfy all the production requirements but *Spirulina sp.*, *Chlorella vulgaris* demonstrated to have the highest CO<sub>2</sub> utilization capacity.

There are different products that can be obtained from algal cultivation, for example fuels. Technological pathways for the conversion of algae to biofuels fall into the following three main categories: direct production of biofuels from algae without the need for extractions or any other manipulation (e.g., such fuels as hydrogen, methane, ethanol, and alkanes), processing of whole algal biomass to biofuels (through pyrolysis, gasification, etc.), processing algal extracts (e.g., lipids, carbohydrates) to biofuel. Currently, most of the technological development and commercial activities in the algae-to-fuel area are concerned with the conversion of algal oil (or lipids, triacylglycerides) to biofuels, through transesterifications.

Although biofuels production is considered the primary objective of algae processing, the generation of other coproducts could significantly enhance the economics of the process. Indeed, algae is a unique resource in its capacity to address CO<sub>2</sub> mitigation, wastewater treatment (nutrients removal), and deliver a wide range of valuable products: human food supplement (*Spirulina*, *Chlorella*, *Dunaliella*, etc.), animal feed additive (mainly, *Spirulina*, *Chlorella* has been used with good results as a food additive for cows, horses, pigs, poultry, etc.), polyunsaturated fatty acids (e.g., arachidonic, docosahexaenoic acids are health-promoting additives to human food and animal feed), antioxidants (the most common is  $\beta$ -carotene that is produced from *Dunaliella salina* sold on a health-food market), coloring agents and pigments, like astaxanthin (used as natural dyes for food, cosmetics, and as pigments in animal feed, i.e. to obtain the red color in salmon), fertilizers and soil conditioners, specialty products (biofloculants, biopolymers and biodegradable plastics, cosmetics, pharmaceuticals and bioactive compounds, polysaccharides, and stable isotopes for research).

Differently from biodiesel production, in which the storage is temporary because CO<sub>2</sub> is re-released as soon as fuel is burnt in a diesel engine, other algal products which have longer live than fuels, and can be considered a semipermanent storage.

## 1.6 Synthesis of cyclic carbonates from CO<sub>2</sub> and epoxide

The synthesis of cyclic carbonates (CCs) from CO<sub>2</sub> and epoxides is an interesting solution for the reuse of CO<sub>2</sub> and moreover it is a 100% Atom Economy reaction (**scheme 1.**). It is also a green alternative to the synthesis of CCs from diols and phosgene, which have several toxicity

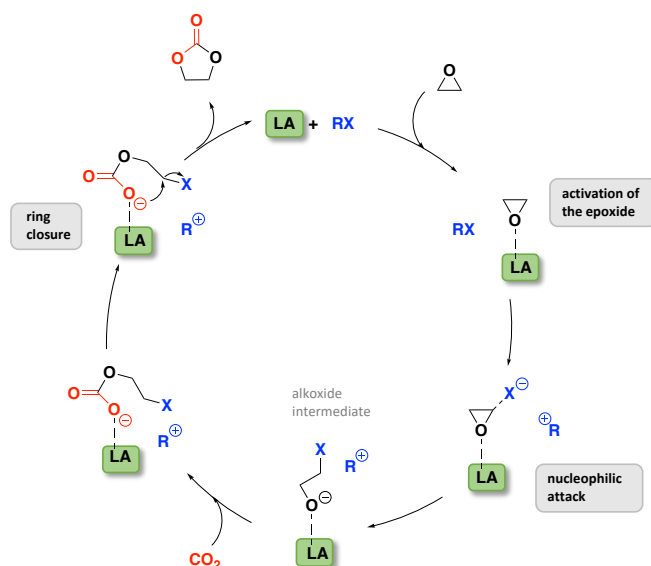
problems. Another interesting routes to obtain CCs is the use of transcarbonation reaction between a diol and a linear carbonate (see section 1.7.2.1). Moreover synthesis of CCs from epoxides and CO<sub>2</sub> can be easily carried out in solvent-free conditions.



**Scheme 1.** Cycloaddition of CO<sub>2</sub> with epoxides to obtain cyclic carbonates.

CCs have a potential applications in the synthesis of biocompatible polymers and linear dialkyl carbonates and as aprotic solvents, also used in lithium-ion batteries.<sup>31,33–35</sup> This reaction has been the focus of many research studies, being an efficient and straightforward mean to reuse CO<sub>2</sub>. Nevertheless, the direct synthesis of CCs from CO<sub>2</sub> is still challenging because, being CO<sub>2</sub> a kinetically and thermodynamically stable molecule, the systems used often require high-energy oxiranes or very strong reaction conditions, both in terms of CO<sub>2</sub> pressure and temperature.<sup>36</sup>

The nature of the catalyst, the nature of the epoxide and the reaction conditions, play a crucial role also in determining the selectivity between the two possible products of the reaction of CO<sub>2</sub> with epoxides, that are CCs and polycarbonates. So, the design and development of active and selective catalytic systems are central topics of research in the domain of the conversion of CO<sub>2</sub> into CCs. The most common and active catalytic systems for this reaction have a Lewis acid site (a metallic center or an H-bond donor) that activates the epoxide, through coordination to the O atom, and a Lewis base (generally a halide) that is responsible for the ring-opening of the epoxide through a nucleophilic attack. After the formation of the alkoxide intermediate, the insertion of CO<sub>2</sub> occurs, followed by the intramolecular ring closure to yield the cyclic carbonate product (**Scheme 2.**)<sup>37</sup>



**Scheme 2.** General mechanism for the synthesis of CCs from epoxides.

The need for two different active species often requires the use of a bi-component catalytic system in which the Lewis base is considered the main catalyst, since it is responsible for the epoxy-ring opening (the rate-determining step of the reaction), and the Lewis acid is considered a co-catalyst. Moreover, the two active species can be present within a bifunctional single-component catalyst or in a binary system consisting of two separate components. Complete selectivity towards the cyclic carbonate product is generally achieved with metal-free catalysts, whereas for metal-containing catalysts the selectivity between cyclic and polymeric carbonate typically depends on the nature of the nucleophilic species and of the metal, on the nucleophile-to-metal ratio and on the reaction conditions.<sup>25</sup>

Several homogeneous and heterogeneous catalysts have been studied for CO<sub>2</sub> conversion in CCs.

### 1.6.1 Homogeneous catalysts

Among homogenous catalysts there are both metal and organocatalysts.

As for metal catalysts they generally consist of metal complexes bearing both the active sites or requiring a co-catalyst. Recent trends regard the use of earth-abundant, non-toxic and cheap metals, which must be air- and moisture- stable; various Al and Fe complexes have been synthesized and studied to this scope.<sup>38–48</sup> North and coworkers studied the first bimetallic aluminium (scorpionate) complex that catalyzes, with tetrabutylammonium bromide, the formation of CC from terminal and internal epoxides and CO<sub>2</sub> under mild reaction conditions.

<sup>44</sup> Among the cited examples, many of them present very active catalysts, which gave high

yields for a broad substrate scope, at low catalyst loading (<1%) and mild reaction conditions ( $T < 100\text{ }^{\circ}\text{C}$  and  $p(\text{CO}_2) < 10\text{ bar}$ ). Nevertheless, the problems that hamper the industrial use of these catalysts and the scalability of such processes are the long process for catalysts synthesis and the relative high costs.

As for organocatalysts, they generally consist of one or two molecules bearing an H-bond donor and an halide salt, with  $\text{Cl}^-$ ,  $\text{Br}^-$  or  $\text{I}^-$  as anion, and generally ammonium or phosphonium as cation.<sup>49</sup> Quaternary ammonium salts are among the most studied organocatalysts for the conversion of  $\text{CO}_2$  into CCs, i.e. tetraethylammonium bromide (TEABr) is industrially used to promote the synthesis of ethylene or propylene carbonate from  $\text{CO}_2$  and epoxides since 1950s.<sup>50</sup> Although they demonstrated to generally require higher catalyst loading, most of them gave very high yield and selectivity in mild reaction conditions. While the use of the ammonium and phosphonium salts are quite common in these organocatalysts, research is focusing on the study of bio-based and sustainable H-bond donor, until studying the role of water.<sup>51,52</sup> Notably, also ionic-liquid (IL) type organocatalyst is gaining large attention, having high thermal stability, low vapor pressure and a unique tunable structure. In this background, various functionalized ILs are widely investigated, such as hydroxyl functionalized ILs, carboxy functionalized ILs, urea derivative-based ILs, and porous ionic polymers.<sup>53,54</sup>

### 1.6.2 Heterogeneous catalysts

The most important heterogeneous catalysts consist of silica-based catalysts, metal organic frameworks (MOF), metal oxides, carbon-based materials, functionalized polymers and zeolites.<sup>55</sup>

Silica materials can be functionalized with amine group and possessing organo-basic sites on the surface and acidic metal or silanol groups with the material framework, represent a valid kind of catalyst for CC formation.<sup>56</sup>

MOFs demonstrated to be promising catalysts for CC synthesis. The porosity and the Lewis acidic sites (unsaturated metal cations) make MOFs ideal candidates for epoxide activation. A serious drawback is the poor availability and accessibility of active sites, so it is often necessary to use Lewis basic co-catalysts, to synthesize CC.<sup>57</sup>

Metal oxides, like  $\text{MgO}$ , have been tested as catalysts for cyclic carbonate formation as they contain both acidic and basic sites and have redox properties, which can create defects and thus oxygen vacancies, in the catalyst. These oxides constitute the largest family of catalysts in heterogeneous catalysis.

Carbon materials (like graphitic carbon nitride) have a high surface area, good chemical and mechanical stability, as well as high conductivity. Pure carbon materials, like graphite, are often inert in the conversion of CO<sub>2</sub>, so its derivatization is necessary to obtain active sites on its surface: by inserting heteroatoms, such as nitrogen, into these materials, basic sites are introduced into the matrix, increasing CO<sub>2</sub> absorption, stability, and facilitating their use as catalysts.<sup>58</sup>

An emerging type of porous materials is porous organic polymers (POPs), which are useful materials for gas storage, pollutant removal, heterogeneous catalysis and CO<sub>2</sub> absorption. Factors such as high thermal and chemical stability enable these materials also to be used in strenuous reaction conditions if required, and therefore they often exhibit high catalytic activity and long durability.<sup>59</sup>

Zeolites, zeolite-based MOFs and amine-functionalized mesoporous materials have large surface areas combined with thermal and chemical stability. They also consist of large pores, which in terms of size can be easily adjusted. These materials can have many active functional sites, which can act as Brønsted acidic, Lewis acidic or Lewis basic sites. This makes these materials good adsorbents and catalysts for CO<sub>2</sub> conversion.<sup>60</sup>

### **1.7 Green Solvents: effective tools towards sustainable synthesis and extractions**

As described in section 1.4, green solvents could be effective tools to make chemical processes more sustainable, and for this reason they are a relevant research topic.<sup>61,62</sup> Green solvents can be divided into classes: solvents derived from cellulose and starch, ionic liquids (ILs), liquid polymers, deep eutectic solvents (DESs), linear and cyclic carbonates and CO<sub>2</sub> tunable solvents. The latter class contains other subclasses: supercritical CO<sub>2</sub> (scCO<sub>2</sub>), CO<sub>2</sub> expanded liquids and Switchable solvents.

- The hydrolysis of starch and cellulose may be achieved chemically or enzymatically to produce glucose. Subsequent chemical transformations of glucose can provide a wide range of value-added chemical products, such as 2-methyl tetrahydrofuran (2-MeTHF), and  $\gamma$ -valerolactone (GVL), used as solvents for chemical processes. 2-MeTHF is now being used as a renewable alternative to THF. It can be synthesized from xylose and glucose, both of which are derived from biomass via other feedstock intermediates such as levulinic acid and furfural.<sup>63</sup> GVL is a sustainable alternative to toxic dipolar

aprotic solvents such as acetonitrile, dimethylformamide (DMF), or N,N-dimethylacetamide. It may also be used as a renewable fuel. GVL can be produced from cellulose via the production of hydroxymethylfurfural to levulinic acid, or via furfural from hemicellulose.<sup>64</sup>

- Ionic liquids (ILs) are salts that are molten at, or close to, room temperature. They are composed of discrete anions and cations and have extremely high enthalpies of vaporization making them effectively nonvolatile. Moreover, ionic liquids have high chemical and thermal stabilities and remarkable solvating power. Their physical and chemical properties can vary changing anion–cation combinations. Several drawbacks in their use regard the relatively high cost of starting materials and preparation and their toxicity profile.<sup>19</sup>
- Liquid polymers (LPs) have the inherent advantage of negligible volatility. Polyethylene glycol (PEG) and the structurally similar polypropylene glycol (PPG) are the most extensively studied LPs: they are ubiquitous in both chemistry and biology, with commercial applications ranging from personal care products to food additives.<sup>65</sup>
- Deep eutectic solvents (DESs) are a very new generation of solvents, formed from mixtures of Brønsted or Lewis acids and bases. The melting points of DES are lower than the individual components, presenting a deviation from ideality, and they are often prepared by mixing two solid reagents to form a liquid product. Different types of DES have been described, and most contain hydrogen-bond acceptors (HBAs) such as choline chloride and hydrogen-bond donors (HBDs) such as urea. Alternatively, they may also contain metal salts or hydrated metal salts. More in-depth discussion in section 1.7.1.<sup>66</sup>
- Dimethyl Carbonate (DMC) is the most important linear dialkyl carbonate, used both as solvent and electrophilic reagent in various reactions.<sup>66</sup> Among cyclic carbonates, propylene carbonate (PC), ethylene carbonate (EC) and glycerol carbonate (GC) are the one most commonly used as green solvents and reagents. More in depth discussion in section 1.7.2.1.<sup>36</sup>
- Supercritical CO<sub>2</sub> has been used extensively as an extraction solvent in the food, beverage, flavor, and cosmetic industries, most famously for the decaffeination of coffee, which is carried out without subsidy.<sup>67</sup> However, its use requires high capital installation and running costs. Because of the good miscibility of gases with CO<sub>2</sub>,

hydrogenation reactions in scCO<sub>2</sub> have been extensively studied. One example of a hydrogenation in scCO<sub>2</sub> used CO<sub>2</sub> itself as the substrate, which was reduced to methanol and formic acid. The hydrogenation of alkenes in scCO<sub>2</sub> has also been investigated.<sup>68</sup>

- In CO<sub>2</sub> expanded liquids, the ability of CO<sub>2</sub> to dissolve in various solvents is exploited to modify their behavior. CO<sub>2</sub> addition leads to the volumetric expansion of the liquid phase, whose physicochemical properties can be controlled by altering the pressure, temperature, or amount of gas in the system. A wide range of chemical reactions have been performed in CO<sub>2</sub> expanded liquids, for example, hydrogenations, oxidations, and hydroformylations. As compared to traditional liquid-phase processes, expanded liquids offer higher diffusivity, lower viscosity, and increased safety due to the nonflammable medium (inerted by the CO<sub>2</sub> atmosphere). CO<sub>2</sub> expanded liquids have also been identified as promising solvents for biomass-based extractions allowing temperature sensitive medium-to-high polarity compounds to be extracted without thermal decomposition. Wang *et al.* performed LCAs for microalgae oil extraction using CO<sub>2</sub> expanded methanol and ethanol.<sup>69</sup>
- Switchable solvents are capable of modifying their polarity and consequently their solvent capacities in the presence of a trigger. The concept was first presented by Jessop and co-workers using organic bases that became more polar forming a carbonate salt in the presence of CO<sub>2</sub> and water or alcohol. The change of polarity was exploited both in the extraction field, avoiding distillation processes, and in organic synthesis. More information in the section 6.2.<sup>70-72</sup>

### 1.7.1 Deep Eutectic Solvents

Deep eutectic solvents (DESs) are a new generation of solvents described for the first time by Abbott *et al.* (2001).<sup>79</sup> They are composed of a hydrogen bond acceptor (HBA) like choline chloride or betaine and a hydrogen-bond donor (HBD) (such as amides, amines, alcohols, and carboxylic acids) that self-associate through hydrogen bonds and other non-covalent interactions making them liquid at or below 100 °C. For a “deep eutectic solvent” to be significantly different from any other eutectic mixture, and to grant any meaning to the “deep” qualificative, it should be defined as a mixture of pure compounds for which the eutectic point temperature is below that of an ideal liquid mixture. The temperature depression should be defined as the difference ( $\Delta T_2$ ) between the ideal (TE, ideal) and the real (TE) eutectic point

and not as the difference ( $\Delta T_1$ ) between the linear combination of the melting points of the pure components and the real eutectic point (**Figure 4**).<sup>80</sup>

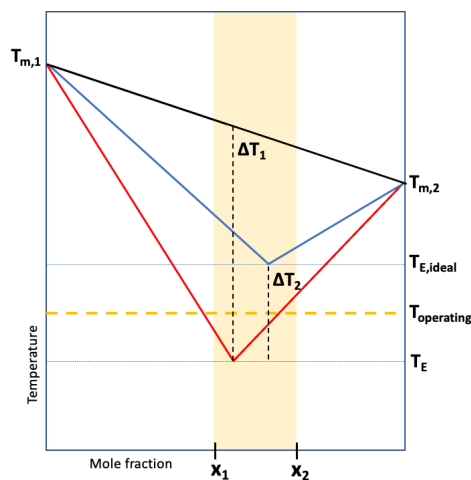


**Figure 4.** Schematic representation of the comparison of the SLE of a simple ideal eutectic mixture (red line) and a deep eutectic mixture (blue line). Adapted from: Insights into the Nature of Eutectic and Deep Eutectic Mixtures.<sup>80</sup>

DESs have become quite popular in the scenario of “green solvents”, especially if composed by non-toxic and biocompatible hydrogen bond donors and acceptors (HBD and HBA, respectively). DESs have been initially considered as an improvement of ILs in terms of sustainability, but the characteristics that these two families of neoteric solvents have in common are few, like the non-volatility and the tunability of the properties as a function of different combinations of the components.

Among the great family of DESs there are some subgroups, like the NaDESs (Natural DESs), prepared using plant metabolites, the TheDESs (Therapeutic DESs) prepared using therapeutic agents, and the Lipophilic DESs, that are a new class of hydrophobic DESs.

They have been used mainly in extractions but also as reaction media (in alkylations, brominations, aminations, for the synthesis of polymers and HMF, etc.).

### 1.7.2 Linear and Cyclic Carbonates

Organic carbonates are diesters of carbonic acid. They can be linear or cyclic, symmetrical or non-symmetrical, they are typically very stable molecules and widely used in industries.<sup>73</sup>

#### 1.7.2.1 Linear carbonates

Linear carbonates are carbonic acid diesters obtained from the reaction between CO or CO<sub>2</sub> and alcohols; they could be symmetrical or non-symmetrical. The most widely used linear organic carbonate is DMC (dimethyl carbonate) obtained from the reaction between CO or

CO<sub>2</sub> with methanol. The first industrial synthesis of the DMC used phosgene and methanol, but this method was replaced by other non-toxic solutions, like the oxidative carbonylation of methanol using metal catalysts such as copper oxides. The synthesis was subsequently studied and implemented in the early 2000s by Asahi-Kasei Corp for the in-situ production of DMC, which includes the use of CO<sub>2</sub>, used for the synthesis of polycarbonates (see section 1.5, **Table 1**). Its production starting from CO<sub>2</sub>, its lack of toxicity, and its versatile reactivity, make DMC an ideal vector of both CO and the methyl function for bio-based building block upgrading and valorization.<sup>74</sup>

In most of the synthetic processes in which DMC is involved, it acts as both solvent and (electrophilic) reagent to transform highly functionalized bio-based chemicals into other molecules. DMC can react on the carbonyl carbon or on one of its methyl groups, and the chemoselectivity depends on several factors, including the nature of the nucleophile, reaction conditions and structure of the products.

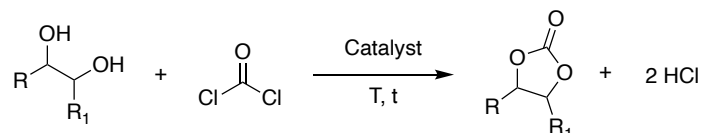
DMC is used as a transesterification reagent for the preparation of cyclic and linear carbonates, as a methylation reagent for the etherification of glycerol acetals, sugars and polysaccharides and other derivatives such as cellulose, starch, isosorbide, lignin and lignin-based phenolics. It is also used for the synthesis of renewable based monomers, for the synthesis of polyurethanes and polycarbonates, but also as solvent for metathesis reactions and Michael condensations of long chain unsaturated acids and glycerol derivatives, as well as for the extraction of biopolymers. Other important linear carbonates are diphenyl carbonate and diethyl carbonate, used as building blocks for the synthesis of other linear and cyclic carbonates and polycarbonates.<sup>74</sup>

#### **1.7.2.2 Cyclic carbonates**

Cyclic carbonates (CC) are used in various fields as solvents, additives for fuels, paint thinners, monomers, liquids for lithium batteries, reagents for fine chemicals and for the synthesis of drugs.<sup>33</sup> The most important CCs have been identified as possible more green solvents alternative to common aprotic organic solvents (such as DMF, THF, etc.), but without the same toxicity problems. In 2004 cyclic carbonates were used as a means of transporting ions inside lithium batteries: the use of these compared to traditional solvents has advantages such as high thermal stability (essential feature for the safety of the product), the low bio-toxicity, the total or partial biodegradability, the competitive price and the high availability. Many of today's batteries have five-term cyclic carbonates inside, such as propylene carbonate or

ethylene carbonate.<sup>35</sup> Among cyclic carbonates, propylene carbonate is the most used as green solvent. Ethylene carbonate has similar properties to propylene carbonate but is a solid at room temperature ( $T_m = 36\text{ }^\circ\text{C}$ ), which makes it less suitable for application as a solvent. To overcome this limitation, ethylene carbonate is generally used as solvent in combination with other compounds (e.g. DMC).

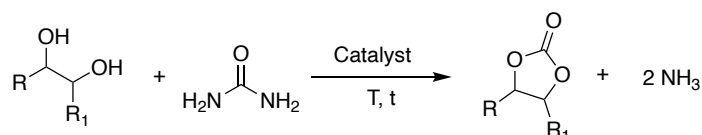
The first industrial process for the synthesis of cyclic carbonates uses phosgene as a donor of the carbonyl group, which in the presence of diols forms cyclic carbonates and two equivalents of hydrochloric acid. The two equivalents of hydrochloric acid (corrosive gas) that are formed must be recycled or neutralized as salts, usually using pyridine. The use of toxic substances and the production of corrosive gases in an industrial process entail enormous risks for operators and the surrounding environment. (**Scheme 3.**)



**Scheme 3.** Reaction of diols with phosgene to give CC.

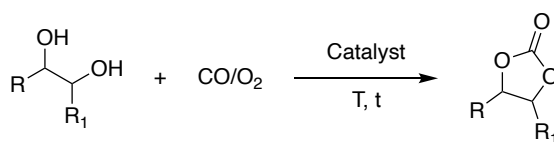
The most recent techniques for the synthesis of these compounds are:

(i) the reaction of diols with metal-catalyzed urea, that requires heat and complexes of zinc, magnesium, aluminum, iron and zirconium as catalysts (**Scheme 4.**). These methods often involve drastic reaction conditions giving low yields.



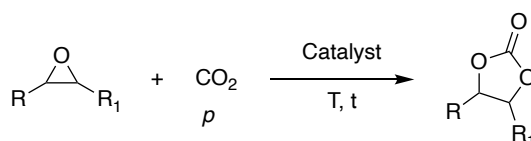
**Scheme 4.** Synthesis reaction of CCs using urea and diols as starting materials.

(ii) electrosynthesis starting from carbon monoxide and alcohols catalyzed by copper oxides or oxidative carbonylation of diols with carbon monoxide Pd/C with KI and sodium acetate or copper halides (**Scheme 5**).<sup>75,76</sup>



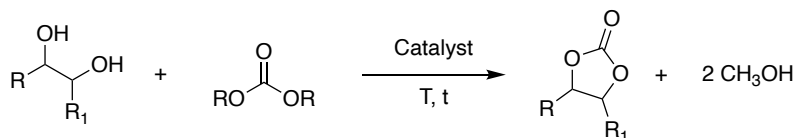
**Scheme 5.** Oxidative carbonylation reaction of diols to give CCs.

(iii) Reaction of  $\text{CO}_2$  with epoxides. (see section 5.1) The catalyst can be metallic (complexes of Iron, Cobalt, Zinc and Aluminum are well studied) or organocatalysts, such as quaternary ammonium salts (**Scheme 6**).



**Scheme 6.** Reaction of carbonation of epoxides.

(iv) Transcarbonation reaction of diols with cyclic or linear carbonates (**Scheme 7**).



**Scheme 7.** Reaction of transcarbonation of a diol with a carbonate.

The transcarbonation of a diol with a carbonate (Carbonate Interchange) (**Scheme 7**) is an interesting and currently much studied alternative for the synthesis of cyclic carbonates. They consist in the exchange of the carbonyl group between a carbonate, typically the DMC, and a diol in the presence of a catalyst.

Glycerol carbonate (GC) is used as a non-volatile organic solvent, as a reagent for synthesis in mild conditions of epichlorohydrin and other products, can be used as an intermediate for the synthesis of polymers or as a plasticizer and as a liquid electrolyte for lithium-ion batteries. Moreover, glycerol (GLY) is a biobased material widely available as a waste product from triglyceride processing, such as in the production of biodiesel. GC can be synthesized from GLY with two possible pathways: (i) carbonation, using glycerol and carbon monoxide CO or carbon dioxide  $\text{CO}_2$  as starting material; (ii) transcarbonation, exchange reaction between a carbonate

and glycerol (the carbonates that are used in this type of reactions can be alkylene carbonates or dialkyl carbonates). The second pathway is the most convenient both in terms of yield, catalysts and conditions used.

### 1.7.3 Switchable Polarity Solvents (SPSs)

The so-called “Switchables” are a category of compounds that can reversibly change their physical properties.

More specifically, Switchable polarity solvents (SPSs) are defined as all those compounds capable of changing their polarity if subjected to an external stimulus (trigger), that can be a gas, light or other. These classes of molecules were initially investigated by Jessop *et al.* in 2005, specifically their aim was to find a solvent capable of modifying its polarity.<sup>62,70</sup> The most common switchable solvents are derivatives of amines, amidines or guanidines: some of these, being non-polar, are not very soluble in water and therefore form a biphasic mixture with it. If they react with the trigger, which is a gas such as CO<sub>2</sub>, they modify their polarity becoming totally miscible with water (**Figure 5**).

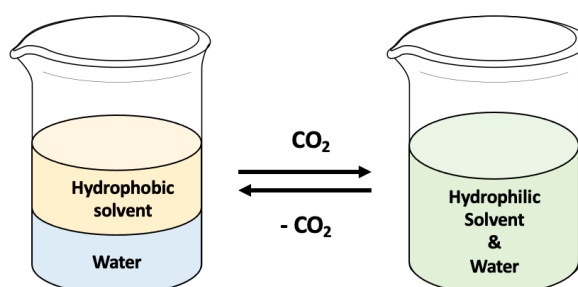
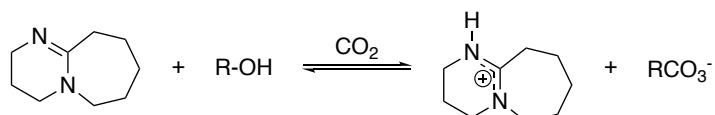


**Figure 5.** Switchable solvents. Adapted from: A solvent having switchable hydrophilicity.<sup>21</sup>

This peculiar ability to vary the polarity and consequently the solubility of some compounds in the various solvents is because the molecules, typically neutral (as they do not have net charges), of the switchable react with CO<sub>2</sub> (trigger), in presence of water or alcohol, to form ionic species, intrinsically polar.

Moreover, the process proved to be totally reversible by removing the CO<sub>2</sub> from the system by means of thermal and / or mechanical processes. The most used process to remove CO<sub>2</sub> from the salt and thus reform the free base is to heat the compound while stirring. Another

possible method to reform the free base is to insufflate nitrogen. There have been many SPS's reported to date. The first SPS was a low-polarity liquid mixture of 1-hexanol and an amidine called DBU (1,8-diazabicyclo[5.4.0]undec-7-ene) (**Scheme 8.**). Other groups have reported many new examples of SPS's: binary liquid mixtures such as glycerol–amidine, alcohol–guanidine, or amidine–primary amine mixtures and single-component SPS's such as diamines, hydroxyamidines, hydroxyguanidines, secondary amines, and primary amines.



**Scheme 8.** Polarity switch of DBU with CO<sub>2</sub> and alcohols.

The use of SPSs is ideal in multi-step syntheses: a solvent that proved to be “ideal” for one reaction step, often is not the same for the next; for this reason, the common practice is to add / remove a solvent after each step (using distillation, an extremely energy-intensive process) thus making the process disadvantageous from an economic and sustainability point of view. In this context it is therefore useful to be able to vary the properties of a solvent making it optimal for different steps. As seen before, the reuse of CO<sub>2</sub> must be particularly encouraged, also because if inserted in a closed system, can be reused for subsequent switches of polarity, without any emission. The switchable solvents were initially tested in liquid-liquid (l-l) or solid-liquid (s-l) extractions. Using the SPSs it is instead possible to extract the product by skipping the distillation step: a product of polarity similar to the solvent (tendentially lipophilic) can be extracted from its matrix obtaining a solvent-product mixture. By inserting CO<sub>2</sub> into the mixture, the switchable solvent will become more polar, losing its solvent capacity towards the product, which therefore, being no longer dissolved, can be easily separated from the mixture. The ionized version of the solvent (liquid or solid) can be restored to its original form, for possible reuse, by heating the solution or blowing nitrogen, as previously described. In the years research group of Galletti and Samorì have used this technique for various purposes: the extraction of hydrocarbons (lipids) from microalgal cultures (**Figure n.6**),<sup>71</sup> for the extraction of PHA (polyhydroxyalkanoates) from microbial cultures<sup>77</sup> and for the recycling of components in multilayer packaging.<sup>78</sup>

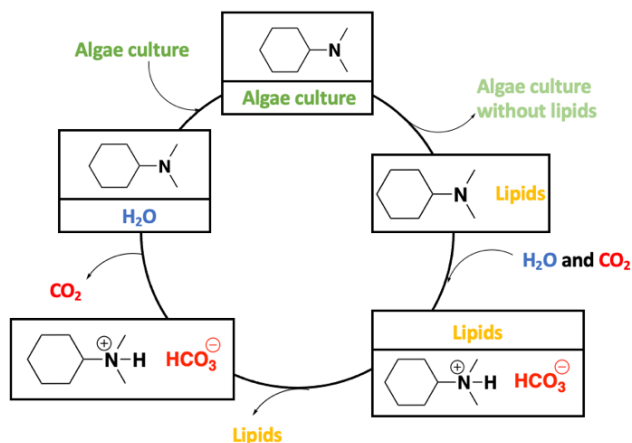


**Figure 6.** Scheme of algae cultures extraction based on N,N-dimethylcyclohexylamine switchable solvents. Adapted from: Effective Lipid Extraction from Algae Cultures Using Switchable Solvents.<sup>71</sup>

Other research groups worked on other extraction: crude oil or bitumen from oil sands or oil shale, hemicellulose and lignin from wood, etc. SPSs have also been employed as media for many reactions, including the polymerization of styrene, aldolic condensation, Claisen–Schmidt condensation, cyanosilylation, Michael addition, and the Heck reaction. They have also been used as solvents for the post-reaction separation of catalysts from products in some of those reactions and in the copolymerization of epoxide and CO<sub>2</sub>. In biomass conversion, they have been utilized in the acylation of cellulose, activation of microcrystalline cellulose toward hydrolysis, transesterification of soybean oil and other triacylglycerides.

## BIBLIOGRAPHY

- (1) PubChem. Carbon dioxide <https://pubchem.ncbi.nlm.nih.gov/compound/280> (accessed 2022 -01 -03).
- (2) Holloway, S.; Pearce, J. M.; Hards, V. L.; Ohsumi, T.; Gale, J. Natural Emissions of CO<sub>2</sub> from the Geosphere and Their Bearing on the Geological Storage of Carbon Dioxide. *Energy* **2007**, *32* (7), 1194–1201. <https://doi.org/10.1016/j.energy.2006.09.001>.
- (3) Gruber, N.; Clement, D.; Carter, B. R.; Feely, R. A.; van Heuven, S.; Hoppema, M.; Ishii, M.; Key, R. M.; Kozyr, A.; Lauvset, S. K.; Lo Monaco, C.; Mathis, J. T.; Murata, A.; Olsen, A.; Perez, F. F.; Sabine, C. L.; Tanhua, T.; Wanninkhof, R. The Oceanic Sink for Anthropogenic CO<sub>2</sub> from 1994 to 2007. *Science* **2019**, *363* (6432), 1193–1199. <https://doi.org/10.1126/science.aau5153>.
- (4) DeVries, T.; Holzer, M.; Primeau, F. Recent Increase in Oceanic Carbon Uptake Driven by Weaker Upper-Ocean Overturning. *Nature* **2017**, *542* (7640), 215–218. <https://doi.org/10.1038/nature21068>.
- (5) Boyd, P. W. Beyond Ocean Acidification. *Nat. Geosci.* **2011**, *4* (5), 273–274. <https://doi.org/10.1038/ngeo1150>.
- (6) Riebesell, U.; Gattuso, J.-P. Lessons Learned from Ocean Acidification Research. *Nat. Clim. Change* **2015**, *5* (1), 12–14. <https://doi.org/10.1038/nclimate2456>.
- (7) AR5 Climate Change 2013: The Physical Science Basis — IPCC.
- (8) US EPA, O. Sources of Greenhouse Gas Emissions <https://www.epa.gov/ghgemissions/sources-greenhouse-gas-emissions> (accessed 2022 -01 -03).
- (9) Rio Earth Summit — European Environment Agency <https://www.eea.europa.eu/help/glossary/chm-biodiversity/rio-earth-summit> (accessed 2022 -01 -09).
- (10) UNFCCC (1997) Kyoto Protocol to the United Nations Framework Convention on Climate Change adopted at COP3 in Kyoto, Japan, on 11 December 1997 — European Environment Agency <https://www.eea.europa.eu/data-and-maps/indicators/primary-energy-consumption-by-fuel/unfccc-1997-kyoto-protocol-to> (accessed 2022 -01 -09).
- (11) UNFCCC, 2015, The Paris Agreement, — European Environment Agency <https://www.eea.europa.eu/data-and-maps/indicators/atmospheric-greenhouse-gas-concentrations-7/unfccc-2015-the-paris-agreement> (accessed 2022 -01 -09).
- (12) IEA (2021), Carbon Capture in 2021: Off and Running or Another False Start?, IEA, Paris <https://www.iea.org/commentaries/carbon-capture-in-2021-off-and-running-or-another-false-start>.
- (13) Anastas, P.; Eghbali, N. Green Chemistry: Principles and Practice. *Chem. Soc. Rev.* **2010**, *39* (1), 301–312. <https://doi.org/10.1039/B918763B>.
- (14) Erythropel, H. C.; Zimmerman, J. B.; Winter, T. M. de; Petitjean, L.; Melnikov, F.; Lam, C. H.; Lounsbury, A. W.; Mellor, K. E.; Janković, N. Z.; Tu, Q.; Pincus, L. N.; Falinski, M. M.; Shi, W.; Coish, P.; Plata, D. L.; Anastas, P. T. The Green ChemisTREE: 20 Years after Taking Root with the 12 Principles. *Green Chem.* **2018**, *20* (9), 1929–1961. <https://doi.org/10.1039/C8GC00482J>.
- (15) Meninno, S. Valorization of Waste: Sustainable Organocatalysts from Renewable Resources. *ChemSusChem* **2020**, *13* (3), 439–468. <https://doi.org/10.1002/cssc.201902500>.
- (16) Trost, B. M. Atom Economy—A Challenge for Organic Synthesis: Homogeneous Catalysis Leads the Way. *Angew. Chem. Int. Ed. Engl.* **1995**, *34* (3), 259–281. <https://doi.org/10.1002/anie.199502591>.
- (17) Sheldon, R. A. The E Factor 25 Years on: The Rise of Green Chemistry and Sustainability. *Green Chem.* **2017**, *19* (1), 18–43. <https://doi.org/10.1039/C6GC02157C>.
- (18) Gevorgyan, A.; Hopmann, K. H.; Bayer, A. Exploration of New Biomass-Derived Solvents: Application to Carboxylation Reactions. *ChemSusChem* **2020**, *13* (8), 2080–2088. <https://doi.org/10.1002/cssc.201903224>.
- (19) Introduction: Ionic Liquids. *Chem. Rev.* **2017**, *117* (10), 6633–6635. <https://doi.org/10.1021/acs.chemrev.7b00246>.
- (20) Paiva, A.; Craveiro, R.; Aroso, I.; Martins, M.; Reis, R. L.; Duarte, A. R. C. Natural Deep Eutectic Solvents – Solvents for the 21st Century. *ACS Sustain. Chem. Eng.* **2014**, *2* (5), 1063–1071. <https://doi.org/10.1021/sc500096j>.
- (21) G. Jessop, P.; Phan, L.; Carrier, A.; Robinson, S.; J. Dürr, C.; R. Harjani, J. A Solvent Having Switchable Hydrophilicity. *Green Chem.* **2010**, *12* (5), 809–814. <https://doi.org/10.1039/B926885E>.
- (22) Rafiee, A.; Rajab Khalilpour, K.; Milani, D.; Panahi, M. Trends in CO<sub>2</sub> Conversion and Utilization: A Review from Process Systems Perspective. *J. Environ. Chem. Eng.* **2018**, *6* (5), 5771–5794. <https://doi.org/10.1016/j.jece.2018.08.065>.
- (23) Poliakoff, M.; Leitner, W.; Streng, E. S. The Twelve Principles of CO<sub>2</sub> CHEMISTRY. *Faraday Discuss.* **2015**, *183* (0), 9–17. <https://doi.org/10.1039/C5FD90078F>.
- (24) Catizzone, E.; Bonura, G.; Migliori, M.; Frusteri, F.; Giordano, G. CO<sub>2</sub> Recycling to Dimethyl Ether:

- State-of-the-Art and Perspectives. *Molecules* **2018**, *23* (1), 31. <https://doi.org/10.3390/molecules23010031>.
- (25) J. Kamphuis, A.; Picchioni, F.; P. Pescarmona, P. CO<sub>2</sub>-Fixation into Cyclic and Polymeric Carbonates: Principles and Applications. *Green Chem.* **2019**, *21* (3), 406–448. <https://doi.org/10.1039/C8GC03086C>.
- (26) Xie, H.; Wang, Y.; He, Y.; Gou, M.; Liu, T.; Wang, J.; Tang, L.; Jiang, W.; Zhang, R.; Xie, L.; Liang, B. Generation of Electricity from CO<sub>2</sub> Mineralization: Principle and Realization. *Sci. China Technol. Sci.* **2014**, *57* (12), 2335–2343. <https://doi.org/10.1007/s11431-014-5727-6>.
- (27) Ebrahimi, A.; Saffari, M.; Milani, D.; Montoya, A.; Valix, M.; Abbas, A. Sustainable Transformation of Fly Ash Industrial Waste into a Construction Cement Blend via CO<sub>2</sub> Carbonation. *J. Clean. Prod.* **2017**, *156*, 660–669. <https://doi.org/10.1016/j.jclepro.2017.04.037>.
- (28) Muradov, N. Industrial Utilization of CO<sub>2</sub>: A Win–Win Solution. In *Liberating Energy from Carbon: Introduction to Decarbonization*; Muradov, N., Ed.; Lecture Notes in Energy; Springer: New York, NY, 2014; pp 325–383. [https://doi.org/10.1007/978-1-4939-0545-4\\_9](https://doi.org/10.1007/978-1-4939-0545-4_9).
- (29) Yu, D.; Zhang, Y. Copper- and Copper–N-Heterocyclic Carbene-Catalyzed C–H Activating Carboxylation of Terminal Alkynes with CO<sub>2</sub> at Ambient Conditions. *Proc. Natl. Acad. Sci.* **2010**, *107* (47), 20184–20189. <https://doi.org/10.1073/pnas.1010962107>.
- (30) Olah, G. A.; Török, B.; Joschek, J. P.; Bucsi, I.; Esteves, P. M.; Rasul, G.; Surya Prakash, G. K. Efficient Chemoselective Carboxylation of Aromatics to Arylcarboxylic Acids with a Superelectrophilically Activated Carbon Dioxide–Al<sub>2</sub>Cl<sub>6</sub>/Al System. *J. Am. Chem. Soc.* **2002**, *124* (38), 11379–11391. <https://doi.org/10.1021/ja020787o>.
- (31) North, M.; Pasquale, R.; Young, C. Synthesis of Cyclic Carbonates from Epoxides and CO<sub>2</sub>. *Green Chem.* **2010**, *12* (9), 1514–1539. <https://doi.org/10.1039/C0GC00065E>.
- (32) Kishimoto, M.; Okakura, T.; Nagashima, H.; Minowa, T.; Yokoyama, S.-Y.; Yamaberi, K. CO<sub>2</sub> Fixation and Oil Production Using Micro-Algae. *J. Ferment. Bioeng.* **1994**, *78* (6), 479–482. [https://doi.org/10.1016/0922-338X\(94\)90052-3](https://doi.org/10.1016/0922-338X(94)90052-3).
- (33) Rollin, P.; Soares, L. K.; Barcellos, A. M.; Araujo, D. R.; Lenardão, E. J.; Jacob, R. G.; Perin, G. Five-Membered Cyclic Carbonates: Versatility for Applications in Organic Synthesis, Pharmaceutical, and Materials Sciences. *Appl. Sci.* **2021**, *11* (11), 5024. <https://doi.org/10.3390/app11115024>.
- (34) Schöffner, B.; Schöffner, F.; Verevkin, S. P.; Börner, A. Organic Carbonates as Solvents in Synthesis and Catalysis. *Chem. Rev.* **2010**, *110* (8), 4554–4581. <https://doi.org/10.1021/cr900393d>.
- (35) Xu, K. Nonaqueous Liquid Electrolytes for Lithium-Based Rechargeable Batteries. *Chem. Rev.* **2004**, *104* (10), 4303–4418. <https://doi.org/10.1021/cr030203g>.
- (36) Pescarmona, P. P. Cyclic Carbonates Synthesized from CO<sub>2</sub>: Applications, Challenges and Recent Research Trends. *Curr. Opin. Green Sustain. Chem.* **2021**, *29*, 100457. <https://doi.org/10.1016/j.cogsc.2021.100457>.
- (37) Monica, F. D.; W. Kleij, A. Mechanistic Guidelines in Nonreductive Conversion of CO<sub>2</sub>: The Case of Cyclic Carbonates. *Catal. Sci. Technol.* **2020**, *10* (11), 3483–3501. <https://doi.org/10.1039/D0CY00544D>.
- (38) Rintjema, J.; Kleij, A. W. Aluminum-Mediated Formation of Cyclic Carbonates: Benchmarking Catalytic Performance Metrics. *ChemSusChem* **2017**, *10* (6), 1274–1282. <https://doi.org/10.1002/cssc.201601712>.
- (39) Wu, X.; North, M. A Bimetallic Aluminium(Salphen) Complex for the Synthesis of Cyclic Carbonates from Epoxides and Carbon Dioxide. *ChemSusChem* **2017**, *10* (1), 74–78. <https://doi.org/10.1002/cssc.201601131>.
- (40) Castro-Osma, J. A.; North, M.; Wu, X. Development of a Halide-Free Aluminium-Based Catalyst for the Synthesis of Cyclic Carbonates from Epoxides and Carbon Dioxide. *Chem. – Eur. J.* **2014**, *20* (46), 15005–15008. <https://doi.org/10.1002/chem.201404117>.
- (41) Taherimehr, M.; Sertã, J. P. C. C.; Kleij, A. W.; Whiteoak, C. J.; Pescarmona, P. P. New Iron Pyridylamino-Bis(Phenolate) Catalyst for Converting CO<sub>2</sub> into Cyclic Carbonates and Cross-Linked Polycarbonates. *ChemSusChem* **2015**, *8* (6), 1034–1042. <https://doi.org/10.1002/cssc.201403323>.
- (42) Della Monica, F.; Buonerba, A.; Paradiso, V.; Milione, S.; Grassi, A.; Capacchione, C. [OSSO]-Type Fe(III) Metallate as Single-Component Catalyst for the CO<sub>2</sub> Cycloaddition to Epoxides. *Adv. Synth. Catal.* **2019**, *361* (2), 283–288. <https://doi.org/10.1002/adsc.201801240>.
- (43) W. Comerford, J.; V. Ingram, I. D.; North, M.; Wu, X. Sustainable Metal-Based Catalysts for the Synthesis of Cyclic Carbonates Containing Five-Membered Rings. *Green Chem.* **2015**, *17* (4), 1966–1987. <https://doi.org/10.1039/C4GC01719F>.
- (44) Martínez, J.; Castro-Osma, J. A.; Earlam, A.; Alonso-Moreno, C.; Otero, A.; Lara-Sánchez, A.; North, M.; Rodríguez-Diéguez, A. Synthesis of Cyclic Carbonates Catalysed by Aluminium Heteroscorpionate Complexes. *Chem. – Eur. J.* **2015**, *21* (27), 9850–9862. <https://doi.org/10.1002/chem.201500790>.
- (45) Castro-Osma, J. A.; North, M.; Wu, X. Synthesis of Cyclic Carbonates Catalysed by Chromium and

- Aluminium Salphen Complexes. *Chem. – Eur. J.* **2016**, *22* (6), 2100–2107.  
<https://doi.org/10.1002/chem.201504305>.
- (46) Panza, N.; di Biase, A.; Gallo, E.; Caselli, A. Unexpected “Ferrate” Species as Single-Component Catalyst for the Cycloaddition of CO<sub>2</sub> to Epoxides. *J. CO<sub>2</sub> Util.* **2021**, *51*, 101635.  
<https://doi.org/10.1016/j.jcou.2021.101635>.
- (47) Andrea, K. A.; Butler, E. D.; Brown, T. R.; Anderson, T. S.; Jagota, D.; Rose, C.; Lee, E. M.; Goulding, S. D.; Murphy, J. N.; Kerton, F. M.; Kozak, C. M. Iron Complexes for Cyclic Carbonate and Polycarbonate Formation: Selectivity Control from Ligand Design and Metal-Center Geometry. *Inorg. Chem.* **2019**, *58* (16), 11231–11240. <https://doi.org/10.1021/acs.inorgchem.9b01909>.
- (48) Seong, E. Y.; Kim, J. H.; Kim, N. H.; Ahn, K.-H.; Kang, E. J. Multifunctional and Sustainable Fe-Iminopyridine Complexes for the Synthesis of Cyclic Carbonates. *ChemSusChem* **2019**, *12* (2), 409–415.  
<https://doi.org/10.1002/cssc.201802563>.
- (49) Fiorani, G.; Guo, W.; W. Kleij, A. Sustainable Conversion of Carbon Dioxide: The Advent of Organocatalysis. *Green Chem.* **2015**, *17* (3), 1375–1389. <https://doi.org/10.1039/C4GC01959H>.
- (50) Poppel, W. J. Preparation and Properties of the Alkylene Carbonates. *Ind. Eng. Chem.* **1958**, *50* (5), 767–770. <https://doi.org/10.1021/ie50581a030>.
- (51) Arayachukiat, S.; Kongtes, C.; Barthel, A.; Vummaleti, S. V. C.; Poater, A.; Wannakao, S.; Cavallo, L.; D’Elia, V. Ascorbic Acid as a Bifunctional Hydrogen Bond Donor for the Synthesis of Cyclic Carbonates from CO<sub>2</sub> under Ambient Conditions. *ACS Sustain. Chem. Eng.* **2017**, *5* (8), 6392–6397.  
<https://doi.org/10.1021/acssuschemeng.7b01650>.
- (52) Alassmy, Y.; Pescarmona, P. The Role of Water Revisited and Enhanced: A Sustainable, Affordable Catalytic System for the Conversion of CO<sub>2</sub> into Cyclic Carbonates under Mild Conditions. *ChemSusChem* **2019**, *12*. <https://doi.org/10.1002/cssc.201901124>.
- (53) Li, C.; Liu, F.; Zhao, T.; Gu, J.; Chen, P.; Chen, T. Highly Efficient CO<sub>2</sub> Fixation into Cyclic Carbonate by Hydroxyl-Functionalized Protic Ionic Liquids at Atmospheric Pressure. *Mol. Catal.* **2021**, *511*, 111756.  
<https://doi.org/10.1016/j.mcat.2021.111756>.
- (54) Zhang, Z.; Fan, F.; Xing, H.; Yang, Q.; Bao, Z.; Ren, Q. Efficient Synthesis of Cyclic Carbonates from Atmospheric CO<sub>2</sub> Using a Positive Charge Delocalized Ionic Liquid Catalyst. *ACS Sustain. Chem. Eng.* **2017**, *5* (4), 2841–2846. <https://doi.org/10.1021/acssuschemeng.7b00513>.
- (55) Marciniak, A. A.; Lamb, K. J.; Ozorio, L. P.; Mota, C. J. A.; North, M. Heterogeneous Catalysts for Cyclic Carbonate Synthesis from Carbon Dioxide and Epoxides. *Curr. Opin. Green Sustain. Chem.* **2020**, *26*, 100365.  
<https://doi.org/10.1016/j.cogsc.2020.100365>.
- (56) Udayakumar, S.; Raman, V.; Shim, H.-L.; Park, D.-W. Cycloaddition of Carbon Dioxide for Commercially-Imperative Cyclic Carbonates Using Ionic Liquid-Functionalized Porous Amorphous Silica. *Appl. Catal. Gen.* **2009**, *368* (1), 97–104. <https://doi.org/10.1016/j.apcata.2009.08.015>.
- (57) Pal, T. K.; De, D.; Bharadwaj, P. K. Metal–Organic Frameworks for the Chemical Fixation of CO<sub>2</sub> into Cyclic Carbonates. *Coord. Chem. Rev.* **2020**, *408*, 213173. <https://doi.org/10.1016/j.ccr.2019.213173>.
- (58) Vidal, J. L.; Andrea, V. P.; MacQuarrie, S. L.; Kerton, F. M. Oxidized Biochar as a Simple, Renewable Catalyst for the Production of Cyclic Carbonates from Carbon Dioxide and Epoxides. *ChemCatChem* **2019**, *11* (16), 4089–4095. <https://doi.org/10.1002/cctc.201900290>.
- (59) Liang, J.; Huang, Y.-B.; Cao, R. Metal–Organic Frameworks and Porous Organic Polymers for Sustainable Fixation of Carbon Dioxide into Cyclic Carbonates. *Coord. Chem. Rev.* **2019**, *378*, 32–65.  
<https://doi.org/10.1016/j.ccr.2017.11.013>.
- (60) Hwang, G.-Y.; Roshan, R.; Ryu, H.-S.; Jeong, H.-M.; Ravi, S.; Kim, M.-I.; Park, D.-W. A Highly Efficient Zeolitic Imidazolate Framework Catalyst for the Co-Catalyst and Solvent Free Synthesis of Cyclic Carbonates from CO<sub>2</sub>. *J. CO<sub>2</sub> Util.* **2016**, *15*, 123–130. <https://doi.org/10.1016/j.jcou.2016.02.005>.
- (61) Jessop, P. G. Searching for Green Solvents. *Green Chem.* **2011**, *13* (6), 1391–1398.  
<https://doi.org/10.1039/C0GC00797H>.
- (62) Clarke, C. J.; Tu, W.-C.; Levers, O.; Bröhl, A.; Hallett, J. P. Green and Sustainable Solvents in Chemical Processes. *Chem. Rev.* **2018**, *118* (2), 747–800. <https://doi.org/10.1021/acs.chemrev.7b00571>.
- (63) Pace, V.; Hoyos, P.; Castoldi, L.; Domínguez de María, P.; Alcántara, A. R. 2-Methyltetrahydrofuran (2-MeTHF): A Biomass-Derived Solvent with Broad Application in Organic Chemistry. *ChemSusChem* **2012**, *5* (8), 1369–1379. <https://doi.org/10.1002/cssc.201100780>.
- (64) Alonso, D. M.; Wettstein, S. G.; Dumesic, J. A. Gamma-Valerolactone, a Sustainable Platform Molecule Derived from Lignocellulosic Biomass. *Green Chem.* **2013**, *15* (3), 584–595.  
<https://doi.org/10.1039/C3GC37065H>.
- (65) Heldebrant, D. J.; Witt, H. N.; Walsh, S. M.; Ellis, T.; Rauscher, J.; Jessop, P. G. Liquid Polymers as

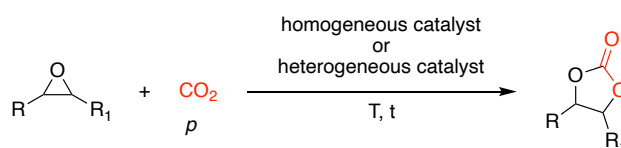
- Solvents for Catalytic Reductions. *Green Chem.* **2006**, *8* (9), 807–815. <https://doi.org/10.1039/B605405F>.
- (66) Smith, E. L.; Abbott, A. P.; Ryder, K. S. Deep Eutectic Solvents (DESs) and Their Applications. *Chem. Rev.* **2014**, *114* (21), 11060–11082. <https://doi.org/10.1021/cr300162p>.
- (67) Raventós, M.; Duarte, S.; Alarcón, R. Application and Possibilities of Supercritical CO<sub>2</sub> Extraction in Food Processing Industry: An Overview. *Food Sci. Technol. Int.* **2002**, *8* (5), 269–284. <https://doi.org/10.1106/108201302029451>.
- (68) Jessop, P. G.; Joó, F.; Tai, C.-C. Recent Advances in the Homogeneous Hydrogenation of Carbon Dioxide. *Coord. Chem. Rev.* **2004**, *248* (21), 2425–2442. <https://doi.org/10.1016/j.ccr.2004.05.019>.
- (69) Wang, T.; Hsu, C.-L.; Huang, C.-H.; Hsieh, Y.-K.; Tan, C.-S.; Wang, C.-F. Environmental Impact of CO<sub>2</sub>-Expanded Fluid Extraction Technique in Microalgae Oil Acquisition. *J. Clean. Prod.* **2016**, *137*, 813–820. <https://doi.org/10.1016/j.jclepro.2016.07.179>.
- (70) Jessop, P. G.; Heldebrant, D. J.; Li, X.; Eckert, C. A.; Liotta, C. L. Reversible Nonpolar-to-Polar Solvent. *Nature* **2005**, *436* (7054), 1102–1102. <https://doi.org/10.1038/4361102a>.
- (71) Samorì, C.; Barreiro, D. L.; Vet, R.; Pezzolesi, L.; F. Brilman, D. W.; Galletti, P.; Tagliavini, E. Effective Lipid Extraction from Algae Cultures Using Switchable Solvents. *Green Chem.* **2013**, *15* (2), 353–356. <https://doi.org/10.1039/C2GC36730K>.
- (72) Großeheilmann, J.; Vanderveen, J. R.; Jessop, P. G.; Kragl, U. Switchable-Hydrophilicity Solvents for Product Isolation and Catalyst Recycling in Organocatalysis. *ChemSusChem* **2016**, *9* (7), 696–702. <https://doi.org/10.1002/cssc.201501654>.
- (73) Shaikh, A.-A. G.; Sivaram, S. Organic Carbonates. *Chem. Rev.* **1996**, *96* (3), 951–976. <https://doi.org/10.1021/cr950067i>.
- (74) Fiorani, G.; Perosa, A.; Selva, M. Dimethyl Carbonate: A Versatile Reagent for a Sustainable Valorization of Renewables. *Green Chem.* **2018**, *20* (2), 288–322. <https://doi.org/10.1039/C7GC02118F>.
- (75) Uozumi, Y.; Pan, S. Oxidative Carbonylation of Diols Using Palladium on Carbon. *Synfacts* **2014**, *10* (4), 442–442. <https://doi.org/10.1055/s-0033-1340917>.
- (76) Giannoccaro, P.; Casiello, M.; Milella, A.; Monopoli, A.; Cotugno, P.; Nacci, A. Synthesis of 5-Membered Cyclic Carbonates by Oxidative Carbonylation of 1,2-Diols Promoted by Copper Halides. *J. Mol. Catal. Chem.* **2012**, *365*, 162–171. <https://doi.org/10.1016/j.molcata.2012.08.026>.
- (77) Samorì, C.; Basaglia, M.; Casella, S.; Favaro, L.; Galletti, P.; Giorgini, L.; Marchi, D.; Mazzocchetti, L.; Torri, C.; Tagliavini, E. Dimethyl Carbonate and Switchable Anionic Surfactants: Two Effective Tools for the Extraction of Polyhydroxyalkanoates from Microbial Biomass. *Green Chem.* **2015**, *17* (2), 1047–1056. <https://doi.org/10.1039/C4GC01821D>.
- (78) Samorì, C.; Cespi, D.; Blair, P.; Galletti, P.; Malferrari, D.; Passarini, F.; Vassura, I.; Tagliavini, E. Application of Switchable Hydrophilicity Solvents for Recycling Multilayer Packaging Materials. *Green Chem.* **2017**, *19* (7), 1714–1720. <https://doi.org/10.1039/C6GC03535C>.
- (79) Abbott, A. P.; Capper, G.; Davies, D. L.; Munro, H. L.; Rasheed, R. K.; Tambyrajah, V. Preparation of Novel, Moisture-Stable, Lewis-Acidic Ionic Liquids Containing Quaternary Ammonium Salts with Functional Side Chains. *Chem. Commun.* **2001**, No. 19, 2010–2011. <https://doi.org/10.1039/B106357J>.
- (80) Martins, M. A. R.; Pinho, S. P.; Coutinho, J. A. P. Insights into the Nature of Eutectic and Deep Eutectic Mixtures. *J. Solut. Chem.* **2019**, *48* (7), 962–982. <https://doi.org/10.1007/s10953-018-0793-1>.

## CHAPTER 2

### AIM OF THE THESIS

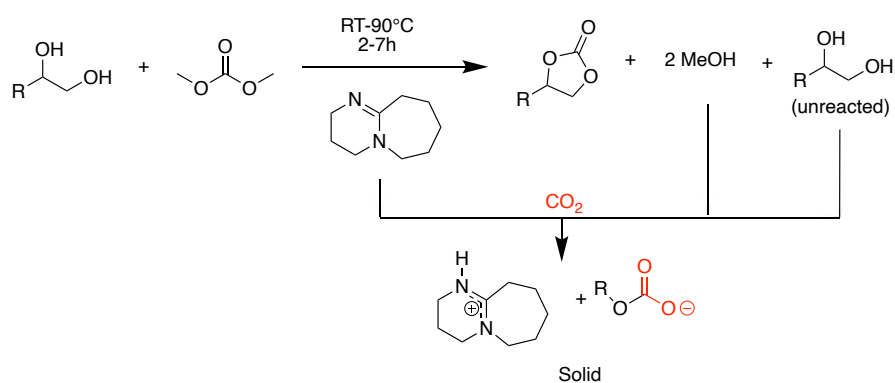
This thesis has been devoted to CO<sub>2</sub> utilization, both as a reactant and a reagent together with the exploitation of alternative solvent in new sustainable processes. This first key point has been addressed from different points of view: by incorporating CO<sub>2</sub> into valuable products, as a trigger to change the physical properties of a catalyst thus facilitating its recovery, as carbon source in microalgae cultivation. The use of alternative solvents was exploited and merged in these processes: new and biobased Deep Eutectic Solvents were used both as reaction media to carry out chemoenzymatic epoxidation and in the extraction of astaxanthin from microalgae culture.

As regards the CO<sub>2</sub> incorporation into molecules, two catalytic systems have been developed for the conversion of CO<sub>2</sub> and epoxides into cyclic carbonates (**Scheme 2.1**). The first group of catalysts, homogeneous, consists of eutectic mixtures based on choline and various compounds with H-bond donor groups. As regards the heterogeneous catalysts, various materials were pyrolyzed, including wastes, and the chars thus obtained were functionalized, using for all of them the same protocol, adding the same groups that proved reactive in homogeneous catalysis (quaternary ammonium and H-bond donor groups).



**Scheme 2.1** Reaction of epoxides with CO<sub>2</sub> to give cyclic carbonates, catalyzed by both homogeneous and heterogeneous catalysts.

As the second field of application, CO<sub>2</sub> was used for a catalyst recovery. DBU was used to catalyze the transcaponation reactions of various diols with dimethyl carbonate; bubbling CO<sub>2</sub> into the reaction vial at the end of the reaction, the catalyst formed a carbonate salt, thus becoming insoluble in the reaction mixture and being easily separable (**Scheme 2.2**).

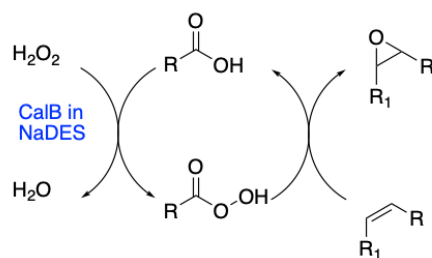


**Scheme 2.2** Trans-carbonation reaction scheme and catalyst recovery through CO<sub>2</sub> bubbling.

All these reactions were carried out in solventless conditions, except for transcarbonation reaction of diols, in which dimethyl carbonate (one of the most promising green solvents) is used in excess with the role of both reagent and solvent.

Deep Eutectic solvents were used, always with a view to using sustainable methods aimed at reducing CO<sub>2</sub> emissions, both in the synthetic and extractive fields.

In a first reaction project epoxidation of alkenes using a chemoenzymatic method was carried out in a sugar-based Deep Eutectic Solvent. The epoxidation systems used were composed by the alkene, the enzyme *Candida antarctica lipase B* (CALB), a long chain carboxylic acid and hydrogen peroxide (**Scheme 2.3**).



**Scheme 2.3** Chemoenzymatic pathway for epoxidation in DES.

Finally, extraction of astaxanthin from *Haematococcus Pluvialis* was achieved via hydrophobic DES based on oleic acid. In microalgae CO<sub>2</sub> is used during cultivation process, that in specific conditions transform nutrients in various molecules, including antioxidants.

## CHAPTER 3

### SYNTHESIS OF CYCLIC CARBONATES FROM EPOXIDES AND CO<sub>2</sub>

#### 3.1 HOMOGENEOUS CATALYSTS: CHOLINE-BASED EUTECTIC MIXTURE <sup>1</sup>

##### 3.1.1 Introduction

Among the large amount of organocatalysts, used for the synthesis of CCs from epoxides and CO<sub>2</sub>, quaternary ammonium salts are surely ones of the most common and known for a long time.<sup>2-11</sup> Nevertheless, their use in neat reactions, without any co-catalysts, usually requires high catalyst loading<sup>12,13</sup> or high temperature and CO<sub>2</sub> pressure.<sup>5,6</sup> Recently many improvements and insights have been made in this context, above all in terms of reaction conditions due to the growing attention towards sustainable synthesis;<sup>8,11,13-16</sup> nowadays it quite well known the beneficial role of an alcoholic or acid component that can be used as a co-catalyst or included in the aliphatic quaternary ammonium salt. In fact, the role of both the hydroxyl group and the hydrogen bonds that can be formed in the stabilization of the intermediate after the epoxy-ring opening, proved to be crucial.<sup>7,17-20</sup> Choline (2-hydroxy-*N,N,N*-trimethylethan-1-aminium) is a non-toxic compound, it is naturally present in human and other animals metabolism and it is used as dietary supplements, although it cannot be considered a bio-based product as nowadays it is industrially synthesized from fossil fuels. Choline chloride, bromide or iodide have been largely used for the coupling of various terminal epoxides with CO<sub>2</sub>, bearing both the ammonium and the alcoholic moieties.<sup>21-25</sup> However, Büttner *et al.* showed that choline halides are ineffective for the synthesis of cyclic carbonates in solventless conditions (2h, 90 °C, 1MPa) and an elongation of the alkyl chains of the ammonium ion is required for reaching good conversions.<sup>21</sup> Amaral *et al.* obtained good results using Choline Iodide (ChI) when ethanol was used as solvent (6h, 85 °C, 1 MPa).<sup>22</sup> Interestingly choline derivatives are able to form strong hydrogen bonds acting as hydrogen bond acceptors (HBA), in the presence of a great variety of hydrogen bond donors (HBD). The mixture of the two components (HDB and HBA) has a lower melting point than the components alone, and, in some cases, constitutes a Deep Eutectic Solvent (DES).<sup>26-28</sup> H-bonds have a crucial role in the stabilization of the reaction intermediate formed in the epoxide-to-

carbonate cyclization mechanism so the presence of HBD could be useful to further improve catalytic efficiency of choline salts. Various research groups have used DES-based systems to catalyze the synthesis of CCs from epoxides:<sup>29–33</sup> Wu *et al.* used a choline chloride-PEG<sub>200</sub> (poly ethylene glycol) DES to catalyze the carbonation reaction using a CO<sub>2</sub> pressure of 0.8 MPa and 150 °C,<sup>24</sup> while Zhu *et al.* used choline chloride/urea supported on molecular sieves as heterogeneous catalyst to promote the carbonation reaction with a molar ratio of CO<sub>2</sub>: epoxide = 1.5–1.87 at 110 °C.<sup>25</sup>

In this work the double ability of biobased, non-toxic, recyclable choline-based HBD-HBA pairs are exploited both to form eutectic mixtures and to catalyze under homogeneous conditions the synthesis of cyclic carbonates from epoxides. The carbonation protocols here developed foresee solventless reactions that work in mild conditions of temperature and CO<sub>2</sub> pressure, thus combining efficiency and sustainability.

### 3.1.2 Results and Discussion

The reaction between CO<sub>2</sub> and epoxide catalyzed by eutectic mixtures has been initially studied with styrene oxide (SO) **1a** as model substrate at different temperatures and CO<sub>2</sub> pressures.

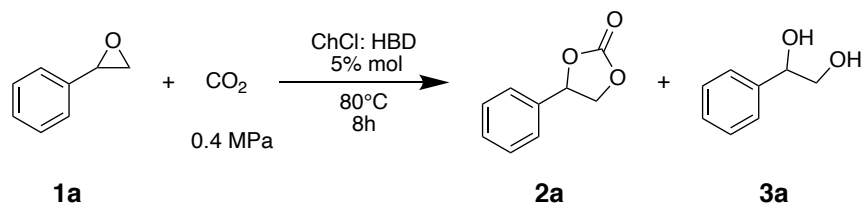
Under the tested reaction conditions, ChCl and ChI were both insoluble in styrene oxide, but their solubilization increased by coupling them with a hydrogen bond donor (HBD). Thus, several choline-based eutectic mixtures were prepared and their ability to catalyze epoxides carbonation was tested. Urea, glycerol, ethylene glycol, water and several carboxylic acids (oxalic, citric, maleic, malonic, tartaric, malic, fumaric, 3- hydroxybutyric, alpha-hydroxyisobutyric, crotonic, benzoic, octanoic, butanoic, and acetic acid), were all tested as HBD. Most of the chosen HBDs are non-toxic and biobased.

#### Choline chloride-based catalysts

The activity of ChCl-based catalysts was tested in stainless steel autoclave at maximum p(CO<sub>2</sub>)=0.4 MPa and T= 80°C (**Table 3.1**), as described in the experimental section. Eutectic mixtures were initially screened in sub-stoichiometric amounts (5 mol% in terms of choline component with respect to the starting material). A 5%, or even higher, catalyst loading is quite common when carbonation reactions are performed under mild conditions, especially

in DES or ILs-type catalyst; moreover such amounts of catalysts allowed us to easily carry out the subsequent recyclability tests on this small scale.<sup>5,10,13,15,21,22,30,32–38</sup>

**Table 3.1** Synthesis of styrene carbonate (SC) **2a** catalyzed by ChCl-HBD catalysts.



Entry	Catalyst ChCl:HBD	Conversion % <sup>e</sup>	Selectivity % <sup>e</sup> 2a:3a
<b>1</b>	ChCl	0	-
<b>2<sup>a</sup></b>	ChCl: Urea (1:2)	33	>99
<b>3<sup>a</sup></b>	ChCl: Ethylene Glycol (1:2)	82	93:7
<b>4<sup>b</sup></b>	ChCl and Ethylene Glycol (1:2)	80	89:11
<b>5<sup>a</sup></b>	ChCl: Glycerol (1:2)	93	98:2
<b>6<sup>b</sup></b>	ChCl and Glycerol (1:2)	72	92:8
<b>7<sup>a</sup></b>	ChCl: Oxalic Acid (1:1)	76	93:7
<b>8<sup>a</sup></b>	ChCl: Citric Acid (1:1)	95	98:2
<b>9<sup>a</sup></b>	ChCl: Maleic Acid (1:1)	97	98:2
<b>10<sup>a,c</sup></b>	ChCl: Maleic Acid (1:1)	91	99:1
<b>11<sup>a</sup></b>	ChCl: Malonic Acid (1:1)	97	99:1
<b>12<sup>b</sup></b>	ChCl and Malonic Acid (1:1)	92	99:1
<b>13<sup>a</sup></b>	ChCl: Tartaric Acid (1:1)	95	95:5
<b>14<sup>b</sup></b>	ChCl and Tartaric Acid (1:1)	83	95:5
<b>15<sup>a</sup></b>	ChCl: Malic Acid (1:1)	97	99:1
<b>16<sup>a,c</sup></b>	ChCl: Malic Acid (1:1)	91	98:2
<b>17<sup>a,d</sup></b>	ChCl: Malic Acid (1:1)	26	98:2
<b>18<sup>b,d</sup></b>	ChCl and Malic Acid (1:1)	22	98:2
<b>19<sup>a</sup></b>	1.5% ChCl: Malic Acid (1:1)	95	98:2
<b>20<sup>a</sup></b>	3% ChCl: Malic Acid (1:1)	96	98:2

Reaction conditions: 1.3 mmol SO **1a** (148.6  $\mu$ L),  $p(\text{CO}_2) = 0.4$  MPa, neat.

<sup>a</sup> Catalyst was pre-formed as eutectic mixture and then added to **1a**;

<sup>b</sup> Catalyst components were added separately in the reaction mixture;

<sup>c</sup>  $p(\text{CO}_2) = 0.2$  MPa;

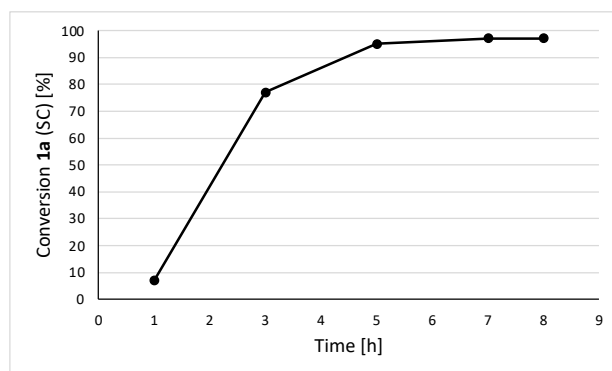
<sup>d</sup>  $p(\text{CO}_2) = 0.1$  MPa (balloon);

<sup>e</sup> Conversions and selectivity calculated by GC-MS (see experimental section).

As already observed, ChCl alone had no catalytic effect being very scarcely soluble in the reaction mixture (SO and CO<sub>2</sub>) within 8 h (entry 1); ChCl:Urea (1:1) eutectic mixture behaved slightly better than ChCl alone (entry 2) but definitely better results have been obtained with catalysts containing acidic or alcoholic groups as HBD. All dicarboxylic acids here tested had an excellent activity in terms of both conversion and selectivity; the only exception was oxalic acid (entry 7). All the other ChCl: acids mixtures gave an almost quantitative conversion of SO **1a** into SC **2a** (entries 8 -20), with a very good selectivity for the formation of SC **2a**. When polyols were used as HBD, different behaviors were observed: glycerol had an activity similar to that of carboxylic acids (entry 5), while ethylene glycol (entry 3) was less reactive and less selective.

The activity of the catalysts when ChCl-eutectic mixture was pre-formed, as described in experimental section, (entries 3, 5, 11, 13, the two components are separated by the colon “:”) in comparison to its formation in situ by adding the components separately inside the reaction mixture (entries 4, 6, 12, 14, the two components are separated by “and”) was also analyzed. In some cases, the differences in terms of conversion between the two strategies were negligible (entries 3 and 4, 11 and 12), in other cases they were more relevant (entries 5 and 6, 13 and 14). In terms of selectivity for SC formation, the two strategies gave similar results with acids-based mixtures (entries 11 and 12, 13 and 14), but better results were achieved when polyol-based mixture were preformed than when they were formed in situ (entries 3 and 4, 5 and 6). The reaction between CO<sub>2</sub> and SO was also tested in presence of betaine, a zwitterion, containing both a quaternary ammonium salt, as choline, and an acidic group, but without the halide and hydroxyl groups. As ChCl tested alone (entry 1), also betaine was totally ineffective (data not shown).

Variations of pressure, time and amount of catalyst were further tested by using ChCl: Malic acid (1:1) as catalyst. A decrease in CO<sub>2</sub> pressure proved to be detrimental (entries 16, 17, 18) especially with the system operating at 0.1 MPa (balloon). The addition of the catalyst in the preformed eutectic mixture or as two separate components did not affect conversion if CO<sub>2</sub> pressure was kept at 0.1 MPa (balloon) (entry 17 and 18), whereas a slight decrease in both conversion and selectivity was observed by lowering the catalyst amount (entries 19, 20). An in-depth study of the initial reaction rate demonstrated that 5-7 hours were enough to get an almost quantitative conversion of SO **1a** (**Figure 3.1**, conditions of entry 15).

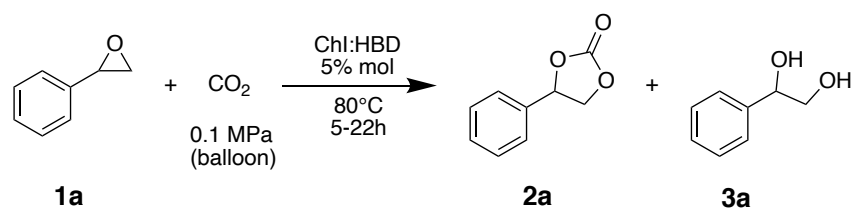


**Figure 3.1** Effect of the time on **1a** conversion using 5% ChCl:Malic acid (1:1), 80 °C,  $p(\text{CO}_2)$ = 0.4 MPa.

### Choline iodide-based catalysts

Being iodide a better leaving group than chloride, despite its worse nucleophilicity in such an aprotic environment, ChI-based catalysts were tested. As done for ChCl-HBD mixtures, ChI-HBD mixtures were firstly tested on **1a** (**Table 3.2**) as described in the experimental section. ChI-based mixtures have higher melting points than ChCl-based ones; for avoiding any possible thermal degradation of the catalyst, that could happen when HBD and HBA were mixed at quite high temperature, the two components (ChI and HBD) were added separately in the reaction mixture (when the two components of the catalysts are added separately their names are divided by “and” instead of the colon, as in **Table 3.1**).

From previous studies ChI proved to be ineffective as catalyst at low reaction times (2h), even with a  $\text{CO}_2$  pressure of 1MPa, in solventless system,<sup>21</sup> while Amaral *et al.* instead demonstrated that it showed a good reactivity in reaction with protic solvents (1MPa, 6h).<sup>22</sup> In our conditions ChI alone could effectively catalyze the reaction (5% mol, entry 1) giving a 95% conversion of **1a** into **2a** but at longer reaction times (22 h); the most commonly used TBAI (Tetrabutylammonium Iodide) did not give a complete conversion in 7 h (entry 21). The coupling of ChI with a HDB forms a homogenous mixture in a short time, significantly decreasing the carbonatation time (entries 2-19, **Table 3.2**). Moreover, ChI-based mixtures proved to catalyze the reaction in milder conditions than what found with ChCl-based mixtures, allowing to decrease  $\text{CO}_2$  pressure from 0.4 MPa to 0.1 MPa (balloon). Notably, very good results and selectivity were found also by adding the components of the mixture separately inside the reaction system; being iodide a better leaving group than chloride despite the presence of water, the product ring-closure is achieved despite the presence of water (**Table 3.2**, entry 14).

**Table 3.2** Synthesis of styrene carbonate **2a** catalyzed by ChI-HBD catalysts.

Entry	Catalysts ChI:HBD	Time (h)	Conversion % <sup>a</sup>	Selectivity % <sup>a</sup> 2a:3a
<b>1</b>	ChI	5	16	99:1
		7	35	
		22	95	
<b>2</b>	ChI and Malic Acid (1:1)	5	88	99:1
		22	95	
<b>3</b>	ChI and Maleic Acid (1:1)	5	87	99:1
		22	95	
<b>4</b>	ChI and Fumaric Acid (1:1)	5	87	98:2
		22	96	
<b>5</b>	ChI and Tartaric Acid (1:1)	5	85	99:1
		22	94	
<b>6</b>	ChI and 3- Hydroxybutyric Acid (1:1)	5	86	99:1
		22	97	
<b>7</b>	ChI and alpha- Hydroxyisobutyric Acid (1:1)	5	77	99:1
		22	97	
<b>8</b>	ChI and Crotonic Acid (1:1)	5	88	>99
<b>9</b>	ChI and Benzoic Acid (1:1)	5	87	>99
<b>10</b>	ChI and Octanoic Acid (1:1)	5	87	>99
<b>11</b>	ChI and Butanoic Acid (1:1)	5	76	>99
<b>12</b>	ChI and Acetic Acid (1:1)	5	90	98:2
<b>13</b>	ChI and Ethylene Glycol (1:1)	5	91	>99
<b>14</b>	ChI 5% and H <sub>2</sub> O 10%	5	88	>99
<b>15</b>	ChI and Glycerol (1:1)	5	96	98:2
		7	99	
<b>16</b>	ChI and Glycerol (1:1), 2%	7	90	97:3
<b>17</b>	ChI and Glycerol (1:1), 4%	7	94	96:4
<b>18</b>	ChI and Glycerol (1:1), 5% rt	7	0	0
<b>19</b>	ChI and Glycerol (1:1), 5% 50 °C	7	50	93:7

<b>20</b>	Glycerol 5%	22	0 0 0	-
<b>21</b>	TBAI 5%	7	64	>99

Reaction conditions: 2.6 mmol **1a** (297.2  $\mu\text{L}$ ),  $p(\text{CO}_2) = 0.1 \text{ MPa}$  (balloon), neat.

<sup>a</sup>Conversions and selectivity calculated by GC-MS (see experimental section).

Several HBD were tested in combination with ChI. When dicarboxylic acids were used as HBD (entries 2, 3, 4, 5), better conversions (close to 90%) than those achieved with ChI alone (entry 1) were obtained in shorter reaction times (5 h), demonstrating that the presence of the HBD enhanced ChI activity. High conversions were reached also with other hydroxy-substituted carboxylic acids (entries 6 and 7), crotonic acid (entry 8), benzoic acid (entry 9) and some aliphatic acids (entries 10, 11, 12). Among the various acids, acetic acid seemed to be the most effective. The carboxylic acids tested alone were ineffective (data not shown). When polyols (glycerol and ethylene glycol, entries 13 and 15) or water (entry 14) were used as HBD, very good results were obtained. The best conversion (99% in 7 h) was obtained with glycerol as HBD, whereas glycerol used alone (entry 20) was ineffective even after 22 h. By studying in more detail the effect of the catalyst amount, temperature and time it was found that: i) a slight decrease in product conversion was observed by decreasing the catalyst amount (entries 16 and 17); ii) the reaction did not run at rt (entry 18) and just 50% conversion was achieved at 50 °C after 7h (entry 19); iii) a conversion of 90% was got after 3 h, becoming quantitative in 7 h (**Figure 3.2**).

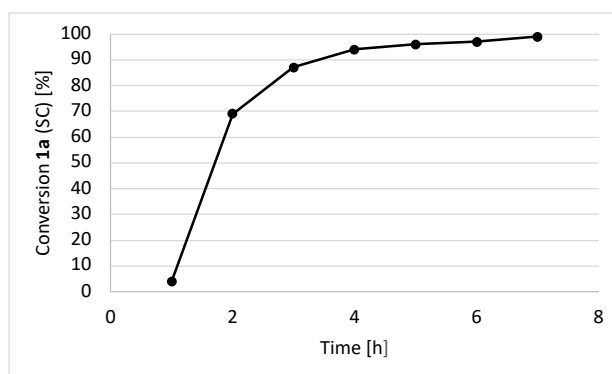


**Figure 3.2** Effect of time on **1a** conversion using 5% ChI:Glycerol (1:1), 80 °C,  $p(\text{CO}_2) = 0.1 \text{ MPa}$  (balloon).

### Substrate screening

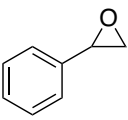
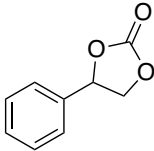
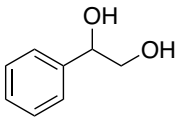
The catalysts and conditions that gave the overall best results in the carbonatation of **1a** (ChCl-Malic Acid under  $p\text{CO}_2=0.4$  MPa; ChI-Glycerol under  $p\text{CO}_2=0.1$  MPa) were used for substrate scope (**Table 3.3**). Although many other HBDs performed well with ChCl and others with ChI, Malic Acid and Glycerol have been chosen because they are non-toxic, widely available and cheap.

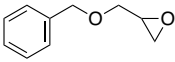
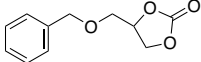
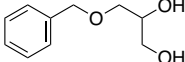
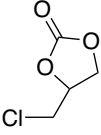
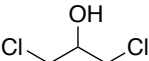
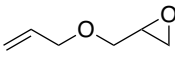
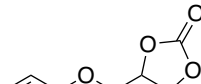
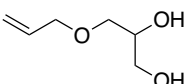
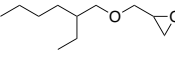
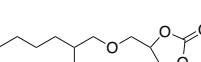
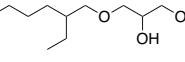
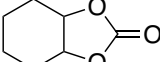
Due to the different volatility of the substrates, the reaction with **1c** and **1d** was carried out inside the steel autoclave, in the condition optimized for ChCl-based eutectic mixtures ( $p\text{CO}_2=0.4$  MPa,  $70^\circ\text{C}$ ); this approach guaranteed a greater insulation of the system than the Schlenk tube equipped with  $\text{CO}_2$  balloon. In this case it was not possible to carry out reactions inside the autoclave at lower pressures because the small size apparatus would have limited  $\text{CO}_2$  amount.

Generally, terminal epoxides could be transformed into the corresponding cyclic carbonates with good to very good yields (entries 1–5); more lipophilic substrate **1e** required a prolonged reaction time. Conversions were quantitative in most cases, just traces (<1%) of the starting materials were visible at GC-MS. The non-quantitative yields were due to the formation of the corresponding diols of each species as by-product or 1,3-dichloropropan-2-ol for reaction of **1c**.

For internal epoxides (entry 6), no conversion and selectivity were obtained, even when the reaction time was prolonged to 23 h; this discouraged us from studying further non-activated, bio-based or more internal epoxides.

**Table 3.3** Reaction of various substrates with  $\text{CO}_2$  using choline-based catalysts.

Entry	Substrate	Product	By-product	Time (h)	Yield <b>2</b> [%] <sup>c</sup>	Yield <b>3 or 4</b> [%] <sup>c</sup>
<b>1<sup>a</sup></b>				7	90 (88)	9

<b>2<sup>a</sup></b>				7	94 (87)	5
<b>3<sup>b</sup></b>				7	80 (80)	10
<b>4<sup>b</sup></b>				5	91 (80)	8
<b>5<sup>a</sup></b>				22	95 (83)	4
<b>6<sup>a,b</sup></b>			-	23	0	-

<sup>a</sup> Reaction conditions: 2.6 mmol of substrate, ChI: Glycerol (1: 1) 5%, 80 °C (5<sup>a</sup> 100°C), p(CO<sub>2</sub>) = 0.1 MPa (balloon);

<sup>b</sup> Reaction conditions: 1.3 mmol of substrate, ChCl: Malic Acid (1:1) 5%, 80 °C, p(CO<sub>2</sub>) = 0.4 MPa (autoclave);

<sup>c</sup> Calculated by <sup>1</sup>H-NMR (see experimental part), isolated yields in parentheses.

### Catalyst recycles

The recycle of the catalyst ChI: Glycerol (1:1) (5 mol%) was tested in the conversion of **1b** into **2b** in the conditions described above (Table 3.3, entry 2). After the reaction was completed, ethyl acetate was added to the crude together with a small amount of water. The components of the eutectic mixture are very soluble in water and insoluble in ethyl acetate, in which the synthesized carbonate is soluble instead. The organic phase was collected to recover the product while the aqueous phase was collected to recover the catalyst after removal of water by distillation. The recovered catalyst was used for next run without further purification. The catalyst could be recycled over four times without appreciable loss of catalytic activity (Figure 3.3).

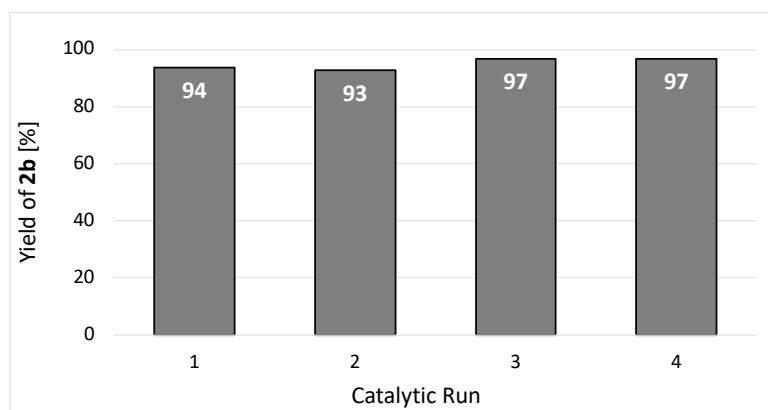
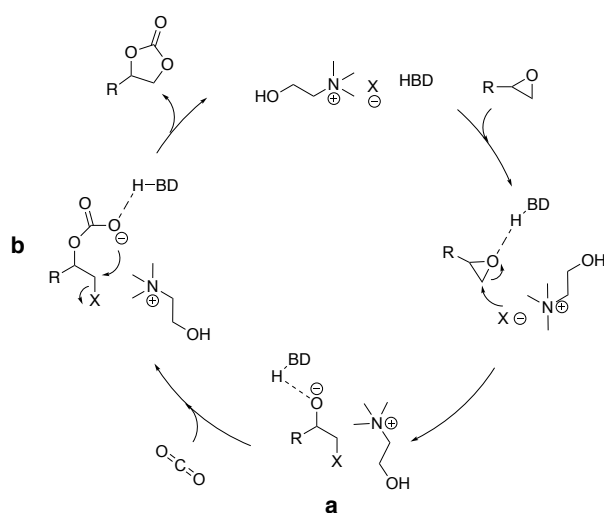


**Figure 3.3** Catalyst recycling for the conversion of **1b** into **2b**. Yield calculated by GC-MS (see experimental section).

### Reaction mechanism

The experimental evidences here found let us hypothesize a plausible mechanism, which confirms the most commonly reported in literatures, in case of catalytic systems composed by a couple of quaternary ammonium salts and H-bond donors are used (**Scheme 3.1**). After the epoxide activation by the HBD, the nucleophilic attack of the choline halide occurs, forming intermediate **a**. The latter, reacting with CO<sub>2</sub>, forms intermediate **b** that cyclizes to give the cyclic carbonate via halide elimination. The boosting activity of the HBD to the choline catalyst is demonstrated by the inactivity of ChCl and ChI alone. Moreover the role of the anion, that must be a good leaving group, is shown by the increased activity of the ChI-based catalyst respect to the ChCl-based ones.



**Scheme 3.1** Proposed mechanism for Choline halides-based eutectic catalysts.

### 3.1.3 Conclusions

Herein sustainable catalysts composed by eutectic mixtures of choline salts and various bio based HBDs have been proved to be effective and recyclable catalysts for the synthesis of terminal cyclic carbonates from CO<sub>2</sub> and epoxides. The HBD, coupled with a choline salt has a dual role: 1) to form an eutectic mixture with the choline salt, soluble in the starting materials in our reaction conditions; 2) to be the co-catalyst in the cycloaddition reaction, being able to stabilize the alkoxide intermediate **a** (**Scheme 3.1**). Very good conversions of various terminal epoxides into the corresponding cyclic carbonates were obtained with choline chloride and choline iodide-based catalysts. With both catalysts carbonatation reactions were conducted under solvent-free conditions, at 80 °C, in 7-22h. While using choline chloride-based mixture a pressure of 0.4 MPa of CO<sub>2</sub> was required to obtain appreciable conversions, with iodide-based mixtures atmospheric pressure of CO<sub>2</sub> (balloon) has been successfully used.

The novelty of the present work in the wide panorama of previous studies about choline-based, ionic liquid- or DES- based catalysts is represented by the very mild conditions used (atmospheric CO<sub>2</sub> pressure and temperature below 100 °C) and the simplicity of the catalysts used. In fact, the use of these mixtures presents several advantages: they are very easily synthesized from commercially available, inexpensive and bio-based, non-toxic chemicals and do not require any particular purification step.

### 3.1.4 Experimental section

#### Material

All chemicals and solvents were purchased from Sigma-Aldrich or Alfa Aesar and used without any further purification. Particularly hygroscopic reagents (quaternary ammonium salts, glycerol, ethylene glycol and carboxylic acids) were used after vacuum drying and kept in a dryer. CO<sub>2</sub> with  $\geq 99.5\%$  purity was purchased from Siad, Italy.

#### Synthesis of choline chloride Choline Chloride (ChCl)-based DES

Choline Chloride (ChCl) was mixed with various HBDs in the appropriate molar ratios, heated at about 80-90 °C (60 °C when the HBD was a dicarboxylic acid)<sup>39</sup> and magnetically stirred until

homogeneous liquids were obtained. DES were cooled to rt before the use and stored in the fridge.

Representative procedure for the synthesis of carbonates at 0.4 MPa of CO<sub>2</sub> and at 0.1 MPa of CO<sub>2</sub> (balloon)

The reaction at 0.4 MPa was conducted in a stainless-steel, self-made, 25 mL autoclave equipped with a heating mantle. The preformed eutectic mixtures, or the two components of the same (5% mol in terms of ChCl respect to the epoxide), were weighed inside a 2 mL vial equipped with a magnetic stirring bar; then the epoxide (1.3 mmol) was added. The air in the reactor was firstly replaced with CO<sub>2</sub>, then the vial was placed inside the steel autoclave. The autoclave was heated and filled with CO<sub>2</sub> (0.4 MPa), and the vial placed inside was kept stirring for the whole reaction time. After the completion of the reaction, the autoclave was cooled to rt and slowly depressurized.

The reaction at 0.1 MPa was conducted in a 25 ml Schlenk tube equipped with a CO<sub>2</sub> balloon. The two components of the eutectic mixture (5% mol respect to the epoxide) were weighed and put inside the Schlenk with the epoxide (2.6 mmol). The air in the Schlenk tube was firstly replaced with CO<sub>2</sub>, then the Schlenk was placed in an oil bath heated at 80 °C. The CO<sub>2</sub> of the balloon was then allowed to flow into the flask. After the completion of the reaction, the Schlenk tube was cooled to rt.

In both cases crudes were weighted to check CO<sub>2</sub> incorporation or any reagent loss, and then analyzed by Gas Chromatography – Mass Spectrometry (GC-MS) after dilution in ethyl acetate. Conversions reported in Tables 3.1 and 3.2 were calculated by GC-MS using a calibration curve of the starting material in 20-400 ppm range, whereas the selectivity was calculated as ratio between the chromatographic peak of carbonate and the peaks of all by-products detectable by GC-MS. Yields reported in Table 3.3 were calculated by NMR using mesitylene as internal standard (see supplementary material for more details); isolated yields are also reported in Table 3.3. <sup>1</sup>H and <sup>13</sup>C NMR spectra of the purified products have been acquired after purification of the crude by flash-column chromatography. All obtained carbonates are known,<sup>40,41</sup> thus they were recognized by comparison with standards or through NMR and mass spectra, matching to what reported in NIST database.<sup>42</sup> The formation of by-products was checked by GC-MS and NMR (See Appendix A3.1).

### Procedure for catalyst recycle

The recycle of the catalyst was tested with the best performing mixture choline iodide (ChI): glycerol (1:1) (5 mol%) in the conversion of benzyl glycidyl ether **1b** (2.6 mmol) into the corresponding cyclic carbonate **2b** at  $p(\text{CO}_2) = 0.1 \text{ MPa}$  (balloon),  $80 \text{ }^\circ\text{C}$ , for 7 h. After the reaction was completed, ethyl acetate was added to the crude together with a small amount of water. The organic phase was collected to recover the product while the aqueous phase was collected to recover the catalyst after removal of water by distillation. The recovered catalyst was used for next runs without further purification. The organic phase containing the product was analyzed by GC-MS, after dilution as before.

### Instrumentation

GC-MS analyses of reaction mixtures were performed using an Agilent HP 6850 gas chromatograph connected to an Agilent HP 5975 quadrupole mass spectrometer. Analytes were separated on a HP-5MS fused-silica capillary column (stationary phase 5%-Phenyl)-methylpolysiloxane, 30 m, 0.25 mm i.d., 0.25  $\mu\text{m}$  film thickness), with helium as the carrier gas (at constant pressure,  $36 \text{ cm s}^{-1}$  linear velocity at  $200 \text{ }^\circ\text{C}$ ). Mass spectra were recorded under electron ionization (70 eV) at a frequency of  $1 \text{ scan s}^{-1}$  within the 12–600  $m/z$  range. The injection port temperature was  $250 \text{ }^\circ\text{C}$ . The temperature of the column was kept at  $50 \text{ }^\circ\text{C}$  for 5 minutes, then increased from 50 to  $250 \text{ }^\circ\text{C}$  at  $10 \text{ }^\circ\text{C min}^{-1}$  and the final temperature of  $250 \text{ }^\circ\text{C}$  was kept for 12 minutes. Epichlorohydrin **1c** and allyl glycidyl ether **1d** (more volatile than the other substrates) were analyzed through the following thermal program: the temperature of the column was kept at  $40 \text{ }^\circ\text{C}$  for 6 minutes, then increased from 50 to  $250 \text{ }^\circ\text{C}$  at  $10 \text{ }^\circ\text{C min}^{-1}$  until the final temperature of  $250 \text{ }^\circ\text{C}$ .  $^1\text{H}$  spectra were recorded on Varian 400 (400 MHz) spectrometers.  $^{13}\text{C}$  NMR spectra were recorded on a Varian 400 (100 MHz) spectrometers. Chemical shifts are reported in ppm from TMS with the solvent resonance as the internal standard (deuteriochloroform: 7.26 ppm). Mesitylene (1,3,5 trimethylbenzene) was used as internal standard (see supplementary material for more details).

### Characterization data of **2a-2e** and **3a-3e** (Spectra in Appendix 3.1)

**2a. 4-Phenyl-1,3-dioxolan-2-one**  $^1\text{H}$  NMR (400 MHz,  $\text{CDCl}_3$ )  $\delta$  7.50 – 7.33 (m, 5H), 5.68 (t,  $J = 8.0 \text{ Hz}$ , 1H), 4.80 (t,  $J = 8.4 \text{ Hz}$ , 1H), 4.35 (dd,  $J = 8.5, 8.0 \text{ Hz}$ , 1H).  $^{13}\text{C}$  NMR (100 MHz,  $\text{CDCl}_3$ )  $\delta$

154.77, 135.76, 129.71, 129.21, 125.83, 77.96, 71.1. m/z (EI): 164 [M], 119 [M-COO], 105 [M-COOO], 91 [Tropylium cation], 78 [Benzene].

**3a. 1-Phenyl-1,2-ethanediol** (diagnostic signals)  $^1\text{H}$  NMR (400 MHz,  $\text{CDCl}_3$ )  $\delta$  7.49 – 7.42 (m, 3H), 7.39 – 7.35 (m, 2H),  $\delta$  4.49 (m, 1H), 3.81 – 3.73 (m, 1H), 3.73 – 3.64 (m, 1H). m/z (EI): 138 [M], 192 [M+  $\text{CH}_2\text{CH}_3+\text{CH}_2\text{CH}_3$ , from the solvent EtOAc], 107 [M-OH-OH], 91 [Tropylium cation], 78 [Benzene].

**2b. 4-Phenylmethoxymethyl-1,3-dioxolan-2-one**  $^1\text{H}$  NMR (400 MHz,  $\text{CDCl}_3$ )  $\delta$  7.41 – 7.28 (m, 5H), 4.81 (ddt,  $J = 7.9, 6.1, 3.9$  Hz, 1H), 4.60 (m, 2H), 4.48 (t,  $J = 8.4$  Hz, 1H), 4.39 (dd,  $J = 8.4, 6.1$  Hz, 1H), 3.71 (dd,  $J = 10.9, 4.0$  Hz, 1H), 3.62 (dd,  $J = 10.9, 3.8$  Hz, 1H).  $^{13}\text{C}$  NMR (100 MHz,  $\text{CDCl}_3$ )  $\delta$  154.87, 137.00, 128.56, 128.08, 127.74, 74.93, 73.70, 68.79, 66.2. m/z (EI): 208 [M], 164 [M-COO], 148 [M-COOO], 107 [M- COOO- $\text{CH}_2\text{-CH-CH}_2$ ], 91[Tropylium cation], 78 [Benzene].

**3b. 3-Benzyloxypropan-1,2-diol** (diagnostic signals)  $^1\text{H}$  NMR (400 MHz,  $\text{CDCl}_3$ )  $\delta$  3.94 – 3.89 (m, 1H), 3.61 – 3.55 (m, 2H). m/z (EI): 182 [M], 163 [M-OH], 143 [M-OH- OH- $\text{CH}_2$ ], 121[M-OH-OH- $\text{CH}_2\text{-CH}$ ], 107 [M- COOO- $\text{CH}_2\text{-CH-CH}_2$ ], 91 [Tropylium cation], 78 [Benzene].

**2c. 4-(Chloromethyl)-1,3-dioxolan-2-one**  $^1\text{H}$  NMR (400 MHz,  $\text{CDCl}_3$ )  $\delta$  4.96 (m, 1H), 4.59 (t,  $J = 8.6$  Hz, 1H), 4.41 (dd,  $J = 8.9, 5.7$  Hz, 1H), 3.75 (m, 2H).  $^{13}\text{C}$  NMR (100 MHz,  $\text{CDCl}_3$ )  $\delta$  154.08, 74.20, 66.95, 43.57. m/z (EI): 135 [M], 91.

**3c. 1,3-Dichloro-2-propanol:** 4c. (diagnostic signals)  $^1\text{H}$  NMR (400 MHz,  $\text{CDCl}_3$ )  $\delta$  4.07 (m, 1H). m/z (EI): 127 [M].

**2d. 4-Allyloxymethyl-1,3-dioxolan-2-one**  $^1\text{H}$  NMR (400 MHz,  $\text{CDCl}_3$ )  $\delta$  5.87 (ddd,  $J = 22.8, 10.8, 5.6$  Hz, 1H), 5.33 – 5.19 (m, 2H), 4.82 (ddt,  $J = 8.1, 6.1, 3.9$  Hz, 1H), 4.50 (t,  $J = 8.4$  Hz, 1H), 4.40 (dd,  $J = 8.3, 6.1$  Hz, 1H), 4.10 – 4.00 (m, 2H), 3.69 (dd,  $J = 11.0, 4.0$  Hz, 1H), 3.62 (dd,  $J = 11.0, 3.8$  Hz, 1H).  $^{13}\text{C}$  NMR (100 MHz,  $\text{CDCl}_3$ )  $\delta$  154.86, 133.60, 117.95, 74.95, 72.60, 68.81, 66.26. m/z (EI): 158 [M], 102 [M- $\text{CH}_2=\text{CH-CH}_2\text{-O}$ ], 117 [M-  $\text{CH}_2=\text{CH-CH}_2$ ], 58 [ $\text{CH}_2=\text{CH-CH}_2\text{-O}$ ].

**3d. 3-Allyloxy-1,2-propanediol** (diagnostic signals)  $^1\text{H}$  NMR (400 MHz,  $\text{CDCl}_3$ )  $\delta$  3.90 (m, 1H), 3.59 – 3.51 (m, 2H).  $m/z$  (EI): 132 [M], 58 [ $\text{CH}_2=\text{CH}-\text{CH}_2-\text{O}$ ].

**2e. 4-(((2-Ethylhexyl)oxy)methyl)-1,3-dioxolan-2-one**  $^1\text{H}$  NMR (400 MHz,  $\text{CDCl}_3$ )  $\delta$  4.83 – 4.73 (m, 1H), 4.48 (t,  $J = 8.3$  Hz, 1H), 4.39 (dd,  $J = 8.3, 6.0$  Hz, 1H), 3.62 (m, 2H), 3.39 (dd,  $J = 5.7, 2.0$  Hz, 2H), 1.55 – 1.45 (m, 1H), 1.40 – 1.26 (m, 8H), 0.87 (dt,  $J = 10.2, 7.0$  Hz, 6H).  $^{13}\text{C}$  NMR (100 MHz,  $\text{CDCl}_3$ )  $\delta$  154.91, 75.02, 74.83, 69.87, 66.28, 39.55, 30.37, 29.02, 23.72, 22.98, 14.03, 11.02.  $m/z$  (EI): 230 [M], 201 [M- $\text{CH}_3-\text{CH}_2$ ], 118 [M- $\text{CH}_3(\text{x}2)-\text{CH}_2(\text{x}5)-\text{CH}$ ], 102 [ $\text{CH}_2-\text{CH}-\text{CH}_2-\text{COOO}$ ], 57 [ $\text{CH}_3-\text{CH}_2\text{x}3$ ].

**3e. 3-[(2-Ethylhexyl)oxy]-1,2-propanediol** (diagnostic signals)  $^1\text{H}$  NMR (400 MHz,  $\text{CDCl}_3$ )  $\delta$  3.53 – 3.49 (m, 2H), 1.50 (dt,  $J = 12.0, 6.0$  Hz, 14H).  $m/z$  (EI): 173 [M- $\text{CH}_3-\text{CH}_2$ ], 143 [ $\text{CH}_3(\text{x}2)-\text{CH}_2(\text{x}5)-\text{CH}-\text{O}-\text{CH}_2$ ], 129 [ $\text{CH}_3(\text{x}2)-\text{CH}_2(\text{x}5)-\text{CH}-\text{O}$ ], 113 [ $\text{CH}_3(\text{x}2)-\text{CH}_2(\text{x}5)-\text{CH}$ ], 57 [ $\text{CH}_3-\text{CH}_2\text{x}3$ ].

## BIBLIOGRAPHY

- (1) Vagnoni, M.; Samorì, C.; Galletti, P. Choline-Based Eutectic Mixtures as Catalysts for Effective Synthesis of Cyclic Carbonates from Epoxides and CO<sub>2</sub>. *J. CO<sub>2</sub> Util.* **2020**, *42*, 101302. <https://doi.org/10.1016/j.jcou.2020.101302>.
- (2) Peppel, W. J. Preparation and Properties of the Alkylene Carbonates. *Ind. Eng. Chem.* **1958**, *50* (5), 767–770. <https://doi.org/10.1021/ie50581a030>.
- (3) Abbott, A. P.; Capper, G.; Davies, D. L.; Munro, H. L.; Rasheed, R. K.; Tambyrajah, V. Preparation of Novel, Moisture-Stable, Lewis-Acidic Ionic Liquids Containing Quaternary Ammonium Salts with Functional Side Chains. *Chem. Commun.* **2001**, No. 19, 2010–2011. <https://doi.org/10.1039/B106357J>.
- (4) Du, Y.; Wang, J. Q.; Chen, J. Y.; Cai, F.; Tian, J. S.; Kong, D. L.; He, L. N. A Poly(Ethylene Glycol)-Supported Quaternary Ammonium Salt for Highly Efficient and Environmentally Friendly Chemical Fixation of CO<sub>2</sub> with Epoxides under Supercritical Conditions. *Tetrahedron Lett.* **2006**, *47* (8), 1271–1275. <https://doi.org/10.1016/j.tetlet.2005.12.077>.
- (5) Ju, H.-Y.; Manju, M. D.; Kim, K.-H.; Park, S.-W.; Park, D.-W. Catalytic Performance of Quaternary Ammonium Salts in the Reaction of Butyl Glycidyl Ether and Carbon Dioxide. *J. Ind. Eng. Chem. - J IND ENG CHEM* **2008**, *14*, 157–160. <https://doi.org/10.1016/j.jiec.2007.12.001>.
- (6) Wang, J.-Q.; Dong, K.; Cheng, W.-G.; Sun, J.; Zhang, S.-J. Insights into Quaternary Ammonium Salts-Catalyzed Fixation Carbon Dioxide with Epoxides. *Catal. Sci. Technol.* **2012**, *2* (7), 1480. <https://doi.org/10.1039/c2cy20103h>.
- (7) Cheng, W.; Xiao, B.; Sun, J.; Dong, K.; Zhang, P.; Zhang, S.; Ng, F. T. T. Effect of Hydrogen Bond of Hydroxyl-Functionalized Ammonium Ionic Liquids on Cycloaddition of CO<sub>2</sub>. *Tetrahedron Lett.* **2015**, *56* (11), 1416–1419. <https://doi.org/10.1016/j.tetlet.2015.01.174>.
- (8) Fiorani, G.; Guo, W.; Kleij, A. W. Sustainable Conversion of Carbon Dioxide: The Advent of Organocatalysis. *Green Chem.* **2015**, *17* (3), 1375–1389. <https://doi.org/10.1039/C4GC01959H>.
- (9) Cokoja, M.; Wilhelm, M. E.; Anthofer, M. H.; Herrmann, W. A.; Kühn, F. E. Synthesis of Cyclic Carbonates from Epoxides and Carbon Dioxide by Using Organocatalysts. *ChemSusChem* **2015**, *8* (15), 2436–2454. <https://doi.org/10.1002/cssc.201500161>.
- (10) Toda, Y.; Komiyama, Y.; Kikuchi, A.; Suga, H. Tetraarylphosphonium Salt-Catalyzed Carbon Dioxide Fixation at Atmospheric Pressure for the Synthesis of Cyclic Carbonates. *ACS Catal.* **2016**, *6* (10), 6906–6910. <https://doi.org/10.1021/acscatal.6b02265>.
- (11) Zhang, Y.-Y.; Yang, G.-W.; Xie, R.; Yang, L.; Li, B.; Wu, G.-P. Scalable, Durable, and Recyclable Metal-Free Catalysts for Highly Efficient Conversion of CO<sub>2</sub> to Cyclic Carbonates. *Angew. Chem. Int. Ed.* **2020**, *59* (51), 23291–23298. <https://doi.org/10.1002/anie.202010651>.
- (12) Caló, V.; Nacci, A.; Monopoli, A.; Fanizzi, A. Cyclic Carbonate Formation from Carbon Dioxide and Oxiranes in Tetrabutylammonium Halides as Solvents and Catalysts. *Org. Lett.* **2002**, *4* (15), 2561–2563. <https://doi.org/10.1021/ol026189w>.
- (13) Kumatabara, Y.; Okada, M.; Shirakawa, S. Triethylamine Hydroiodide as a Simple Yet Effective Bifunctional Catalyst for CO<sub>2</sub> Fixation Reactions with Epoxides under Mild Conditions. *ACS Sustain. Chem. Eng.* **2017**, *5* (8), 7295–7301. <https://doi.org/10.1021/acssuschemeng.7b01535>.
- (14) Pescarmona, P. P. Cyclic Carbonates Synthesised from CO<sub>2</sub>: Applications, Challenges and Recent Research Trends. *Curr. Opin. Green Sustain. Chem.* **2021**, *29*, 100457. <https://doi.org/10.1016/j.cogsc.2021.100457>.
- (15) Wang, L.; Zhang, G.; Kodama, K.; Hirose, T. An Efficient Metal- and Solvent-Free Organocatalytic System for Chemical Fixation of CO<sub>2</sub> into Cyclic Carbonates under Mild Conditions. *Green Chem.* **2016**, *18* (5), 1229–1233. <https://doi.org/10.1039/C5GC02697K>.
- (16) Yang, H.; Gu, Y.; Deng, Y.; Shi, F. Electrochemical Activation of Carbon Dioxide in Ionic Liquid: Synthesis of Cyclic Carbonates at Mild Reaction Conditions. *Chem. Commun.* **2002**, No. 3, 274–275. <https://doi.org/10.1039/B108451H>.
- (17) Alves, M.; Grignard, B.; Mereau, R.; Jerome, C.; Tassaing, T.; Detrembleur, C. Organocatalyzed Coupling of Carbon Dioxide with Epoxides for the Synthesis of Cyclic Carbonates: Catalyst Design and Mechanistic Studies. *Catal. Sci. Technol.* **2017**, *7* (13), 2651–2684. <https://doi.org/10.1039/C7CY00438A>.
- (18) Sun, J.; Zhang, S.; Cheng, W.; Ren, J. Hydroxyl-Functionalized Ionic Liquid: A Novel Efficient Catalyst for Chemical Fixation of CO<sub>2</sub> to Cyclic Carbonate. *Tetrahedron Lett.* **2008**, *22* (49), 3588–3591. <https://doi.org/10.1016/j.tetlet.2008.04.022>.
- (19) Arayachukiat, S.; Kongtes, C.; Barthel, A.; Vummaleti, S. V. C.; Poater, A.; Wannakao, S.; Cavallo, L.; D'Elia, V. Ascorbic Acid as a Bifunctional Hydrogen Bond Donor for the Synthesis of Cyclic Carbonates from CO<sub>2</sub>

- under Ambient Conditions. *ACS Sustain. Chem. Eng.* **2017**, *5* (8), 6392–6397. <https://doi.org/10.1021/acssuschemeng.7b01650>.
- (20) Alassmy, Y. A.; Pescarmona, P. P. The Role of Water Revisited and Enhanced: A Sustainable Catalytic System for the Conversion of CO<sub>2</sub> into Cyclic Carbonates under Mild Conditions. *ChemSusChem* **2019**, *12* (16), 3856–3863. <https://doi.org/10.1002/cssc.201901124>.
- (21) Büttner, H.; Lau, K.; Spannenberg, A.; Werner, T. Bifunctional One-Component Catalysts for the Addition of Carbon Dioxide to Epoxides. *ChemCatChem* **2015**, *7* (3), 459–467. <https://doi.org/10.1002/cctc.201402816>.
- (22) Amaral, A. J. R.; Coelho, J. F. J.; Serra, A. C. Synthesis of Bifunctional Cyclic Carbonates from CO<sub>2</sub> Catalysed by Choline-Based Systems. *Tetrahedron Lett.* **2013**, *54* (40), 5518–5522. <https://doi.org/10.1016/j.tetlet.2013.07.152>.
- (23) He, Q.; O'Brien, J. W.; Kitselman, K. A.; Tompkins, L. E.; Curtis, G. C. T.; Kerton, F. M. Synthesis of Cyclic Carbonates from CO<sub>2</sub> and Epoxides Using Ionic Liquids and Related Catalysts Including Choline Chloride–Metal Halide Mixtures. *Catal. Sci. Technol.* **2014**, *4* (6), 1513–1528. <https://doi.org/10.1039/C3CY00998J>.
- (24) Wu, K.; Su, T.; Hao, D.; Liao, W.; Zhao, Y.; Ren, W.; Deng, C.; Lü, H. Choline Chloride-Based Deep Eutectic Solvents for Efficient Cycloaddition of CO<sub>2</sub> with Propylene Oxide. *Chem. Commun.* **2018**, *54* (69), 9579–9582. <https://doi.org/10.1039/C8CC04412K>.
- (25) Zhu, A.; Jiang, T.; Han, B.; Zhang, J.; Xie, Y.; Ma, X. Supported Choline Chloride/Urea as a Heterogeneous Catalyst for Chemical Fixation of Carbon Dioxide to Cyclic Carbonates. *Green Chem.* **2007**, *9* (2), 169–172. <https://doi.org/10.1039/B612164K>.
- (26) Dai, Y.; van Spronsen, J.; Witkamp, G.-J.; Verpoorte, R.; Choi, Y. H. Natural Deep Eutectic Solvents as New Potential Media for Green Technology. *Anal. Chim. Acta* **2013**, *766*, 61–68. <https://doi.org/10.1016/j.aca.2012.12.019>.
- (27) Martins, M. A. R.; Pinho, S. P.; Coutinho, J. A. P. Insights into the Nature of Eutectic and Deep Eutectic Mixtures. *J. Solut. Chem.* **2019**, *48* (7), 962–982. <https://doi.org/10.1007/s10953-018-0793-1>.
- (28) Zhang, Q.; Vigier, K. D. O.; Royer, S.; Jérôme, F. Deep Eutectic Solvents: Syntheses, Properties and Applications. *Chem. Soc. Rev.* **2012**, *41* (21), 7108–7146. <https://doi.org/10.1039/C2CS35178A>.
- (29) García-Argüelles, S.; Ferrer, M. L.; Iglesias, M.; Del Monte, F.; Gutiérrez, M. C. Study of Superbase-Based Deep Eutectic Solvents as the Catalyst in the Chemical Fixation of CO<sub>2</sub> into Cyclic Carbonates under Mild Conditions. *Materials* **2017**, *10* (7), 759. <https://doi.org/10.3390/ma10070759>.
- (30) Yang, X.; Zou, Q.; Zhao, T.; Chen, P.; Liu, Z.; Liu, F.; Lin, Q. Deep Eutectic Solvents as Efficient Catalysts for Fixation of CO<sub>2</sub> to Cyclic Carbonates at Ambient Temperature and Pressure through Synergetic Catalysis. *ACS Sustain. Chem. Eng.* **2021**, *9* (31), 10437–10443. <https://doi.org/10.1021/acssuschemeng.1c03187>.
- (31) Lü, H.; Wu, K.; Zhao, Y.; Hao, L.; Liao, W.; Deng, C.; Ren, W. Synthesis of Cyclic Carbonates from CO<sub>2</sub> and Propylene Oxide (PO) with Deep Eutectic Solvents (DESS) Based on Amino Acids (AAs) and Dicarboxylic Acids. *J. CO<sub>2</sub> Util.* **2017**, *22*, 400–406. <https://doi.org/10.1016/j.jcou.2017.10.024>.
- (32) Liu, Y.; Cao, Z.; Zhou, Z.; Zhou, A. Imidazolium-Based Deep Eutectic Solvents as Multifunctional Catalysts for Multisite Synergistic Activation of Epoxides and Ambient Synthesis of Cyclic Carbonates. *J. CO<sub>2</sub> Util.* **2021**, *53*, 101717. <https://doi.org/10.1016/j.jcou.2021.101717>.
- (33) Wang, S.; Zhu, Z.; Hao, D.; Su, T.; Len, C.; Ren, W.; Lü, H. Synthesis Cyclic Carbonates with BmimCl-Based Ternary Deep Eutectic Solvents System. *J. CO<sub>2</sub> Util.* **2020**, *40*, 101250. <https://doi.org/10.1016/j.jcou.2020.101250>.
- (34) Coulembier, O.; Moins, S.; Lemaur, V.; Lazzaroni, R.; Dubois, P. Efficiency of DBU/Iodine Cooperative Dual Catalysis for the Solvent-Free Synthesis of Five-Membered Cyclic Carbonates under Atmospheric CO<sub>2</sub> Pressure. *J. CO<sub>2</sub> Util.* **2015**, *10*, 7–11. <https://doi.org/10.1016/j.jcou.2015.02.002>.
- (35) Meng, X.; Ju, Z.; Zhang, S.; Liang, X.; Solms, N. von; Zhang, X.; Zhang, X. Efficient Transformation of CO<sub>2</sub> to Cyclic Carbonates Using Bifunctional Protic Ionic Liquids under Mild Conditions. *Green Chem.* **2019**, *21* (12), 3456–3463. <https://doi.org/10.1039/C9GC01165J>.
- (36) Wang, L.; Kodama, K.; Hirose, T. DBU/Benzyl Bromide: An Efficient Catalytic System for the Chemical Fixation of CO<sub>2</sub> into Cyclic Carbonates under Metal- and Solvent-Free Conditions. *Catal. Sci. Technol.* **2016**, *6* (11), 3872–3877. <https://doi.org/10.1039/C5CY01892G>.
- (37) Wang, Z.; Li, D.; Chen, S.; Hu, J.; Gong, Y.; Guo, Y.; Deng, T. Ionic Liquid [DBUH][BO<sub>2</sub>]: An Excellent Catalyst for Chemical Fixation of CO<sub>2</sub> under Mild Conditions. *New J. Chem.* **2021**, *45* (10), 4611–4616. <https://doi.org/10.1039/D0NJ04631K>.
- (38) Liu, F.; Gu, Y.; Zhao, P.; Xin, H.; Gao, J.; Liu, M. N-Hydroxysuccinimide Based Deep Eutectic Catalysts as a Promising Platform for Conversion of CO<sub>2</sub> into Cyclic Carbonates at Ambient Temperature. *J. CO<sub>2</sub> Util.* **2019**, *33*, 419–426. <https://doi.org/10.1016/j.jcou.2019.07.017>.

- (39) Rodriguez Rodriguez, N.; van den Bruinhorst, A.; Kollau, L. J. B. M.; Kroon, M. C.; Binnemans, K. Degradation of Deep-Eutectic Solvents Based on Choline Chloride and Carboxylic Acids. *ACS Sustain. Chem. Eng.* **2019**, *7* (13), 11521–11528. <https://doi.org/10.1021/acssuschemeng.9b01378>.
- (40) Zhang, Z.; Fan, F.; Xing, H.; Yang, Q.; Bao, Z.; Ren, Q. Efficient Synthesis of Cyclic Carbonates from Atmospheric CO<sub>2</sub> Using a Positive Charge Delocalized Ionic Liquid Catalyst. *ACS Sustain. Chem. Eng.* **2017**, *5* (4), 2841–2846. <https://doi.org/10.1021/acssuschemeng.7b00513>.
- (41) Lai, S.; Gao, J.; Xiong, X. Rosin-Based Porous Heterogeneous Catalyst Functionalized with Hydroxyl Groups and Triazole Groups for CO<sub>2</sub> Chemical Conversion under Atmospheric Pressure Condition. *React. Funct. Polym.* **2021**, *165*, 104976. <https://doi.org/10.1016/j.reactfunctpolym.2021.104976>.
- (42) Informatics, N. O. of D. and. *NIST Chemistry WebBook*. <https://webbook.nist.gov/chemistry/> (accessed 2022-05-11). <https://doi.org/10.18434/T4D303>.

## APPENDIX 3.1

### Contents

**A3.1** GC-MS chromatogram,  $^1\text{H}$  NMR spectrum of reaction crude for conversion of 1a into 2a (Table 3.3, entry 1<sup>a</sup>),  $^1\text{H}$  and  $^{13}\text{C}$  NMR spectra of isolated PRODUCT 2a (Table 3.3, entry 1<sup>a</sup>).

**A3.2** GC-MS chromatogram,  $^1\text{H}$  NMR spectrum of reaction crude for conversion of 1b into 2b (Table 3.3, entry 2<sup>a</sup>),  $^1\text{H}$  and  $^{13}\text{C}$  NMR spectra of isolated PRODUCT 2b (Table 3.3, entry 2<sup>a</sup>).

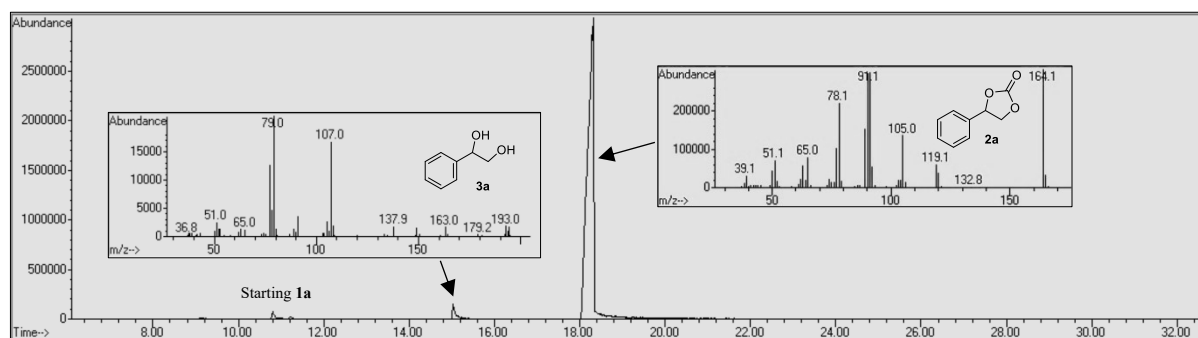
**A3.2** GC-MS chromatogram,  $^1\text{H}$  NMR spectrum of reaction crude for conversion of 1c into 2c (Table 3.3, entry 3<sup>b</sup>),  $^1\text{H}$  and  $^{13}\text{C}$  NMR spectra of isolated PRODUCT 2c (Table 3.3, entry 3<sup>b</sup>).

**A3.3** GC-MS chromatogram,  $^1\text{H}$  NMR spectrum of reaction crude for conversion of 1d into 2d (Table 3.3, entry 4<sup>b</sup>),  $^1\text{H}$  and  $^{13}\text{C}$  NMR spectra of isolated PRODUCT 2d (Table 3.3, entry 4<sup>b</sup>).

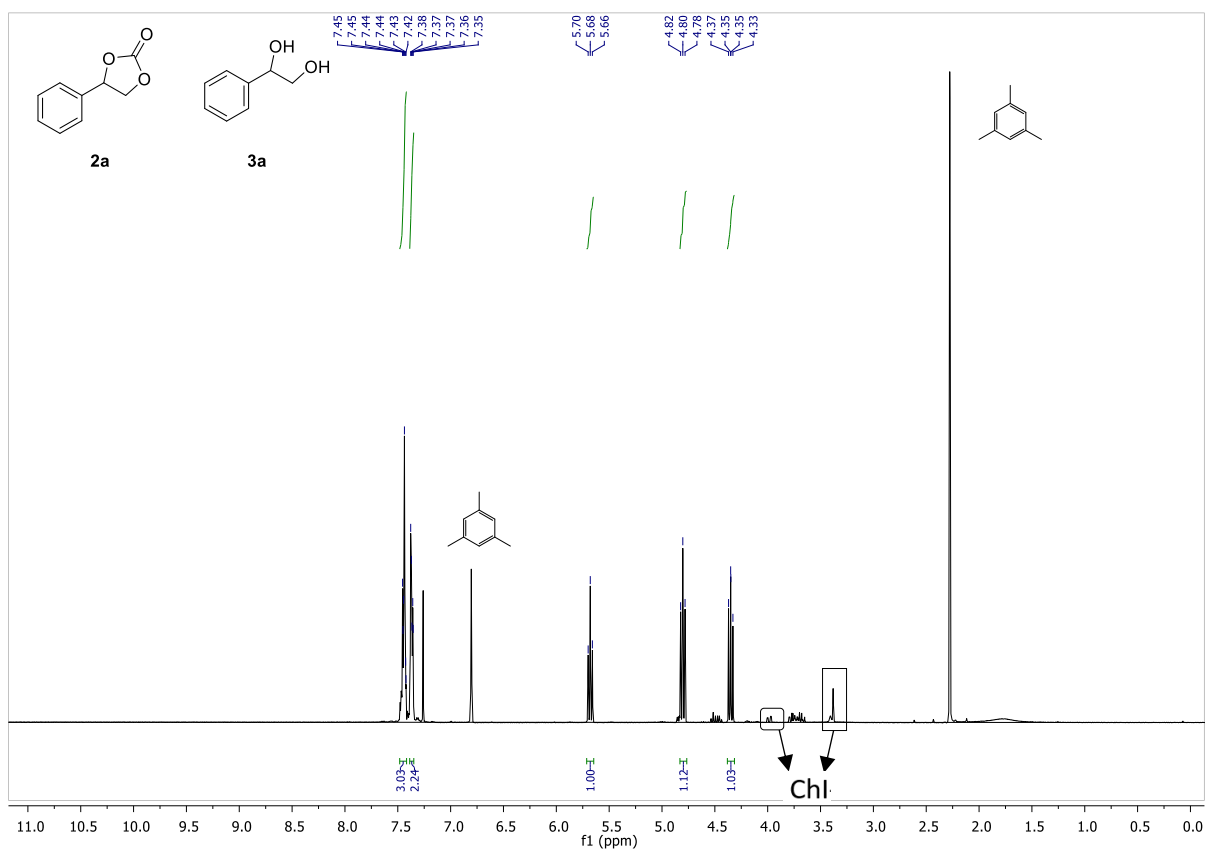
**A3.4** GC-MS chromatogram,  $^1\text{H}$  NMR spectrum of reaction crude for conversion of 1e into 2e (Table 3.3, entry 5<sup>a</sup>),  $^1\text{H}$  and  $^{13}\text{C}$  NMR spectra of isolated PRODUCT 2e (Table 3.3, entry 5<sup>a</sup>).

### A3.1 PRODUCT 2a

GC-MS chromatogram of reaction crude for conversion of 1a into 2a (Table 3.3, entry 1<sup>a</sup>)



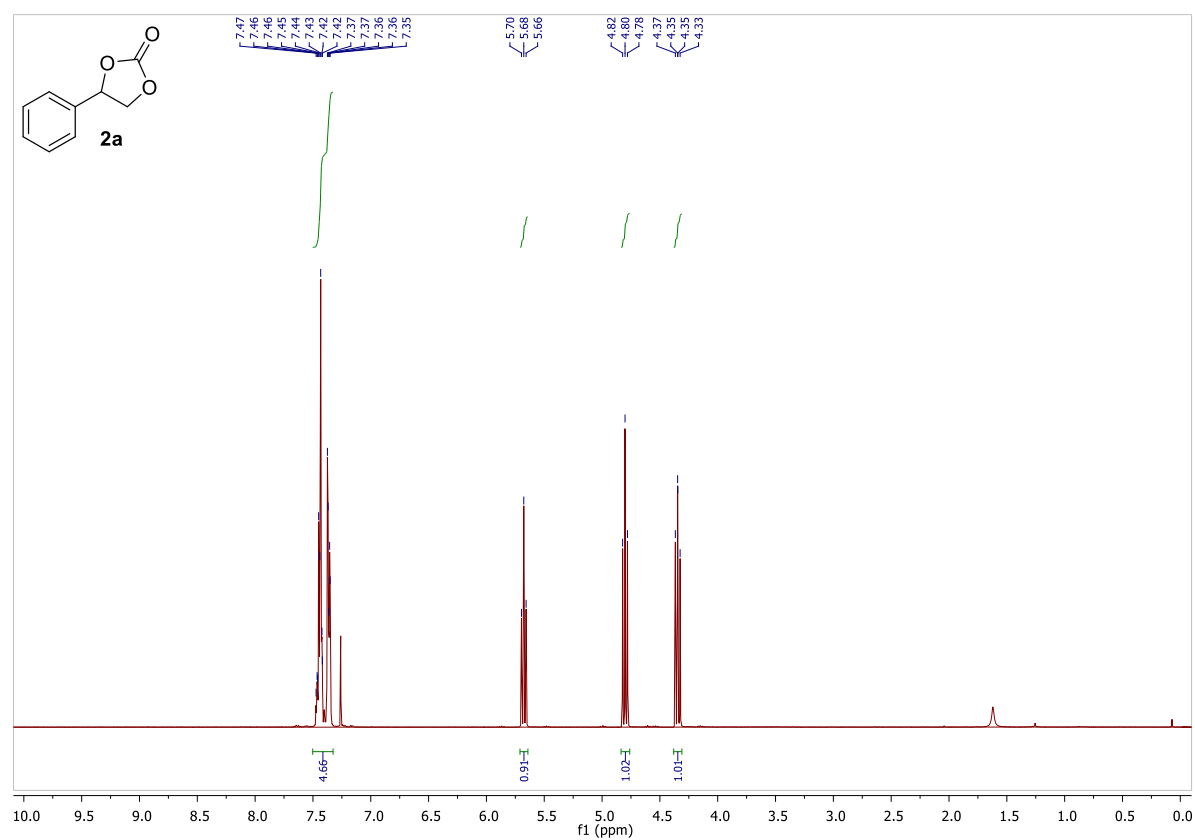
<sup>1</sup>H NMR spectrum of reaction crude for conversion of 1a into 2a (Table 3.3, entry 1<sup>a</sup>)



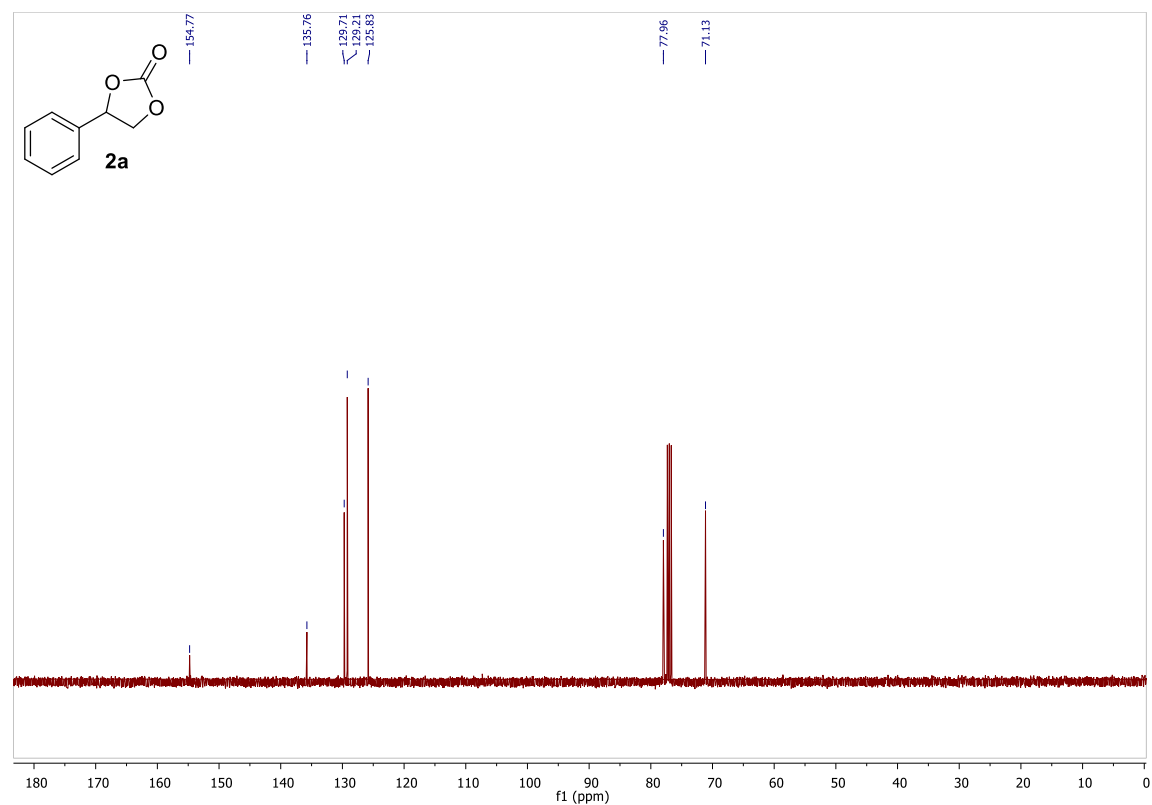
**2a.** <sup>1</sup>H NMR (400 MHz, CDCl<sub>3</sub>) δ 7.49 – 7.42 (m, 3H), 7.39 – 7.35 (m, 2H), 5.68 (t, *J* = 8.0 Hz, 1H), 4.80 (dd, *J* = 8.4, 7.7 Hz, 1H), 4.35 (dd, *J* = 8.6, 7.9 Hz, 1H).

**3a.** (diagnostic signals) <sup>1</sup>H NMR (400 MHz, CDCl<sub>3</sub>) δ 7.49 – 7.42 (m, 3H), 7.39 – 7.35 (m, 2H), δ 4.49 (m, 1H), 3.81 – 3.73 (m, 1H), 3.73 – 3.64 (m, 1H).

<sup>1</sup>H and <sup>13</sup>C NMR spectra of isolated product **2a** (Table 3.3, entry 1<sup>a</sup>)



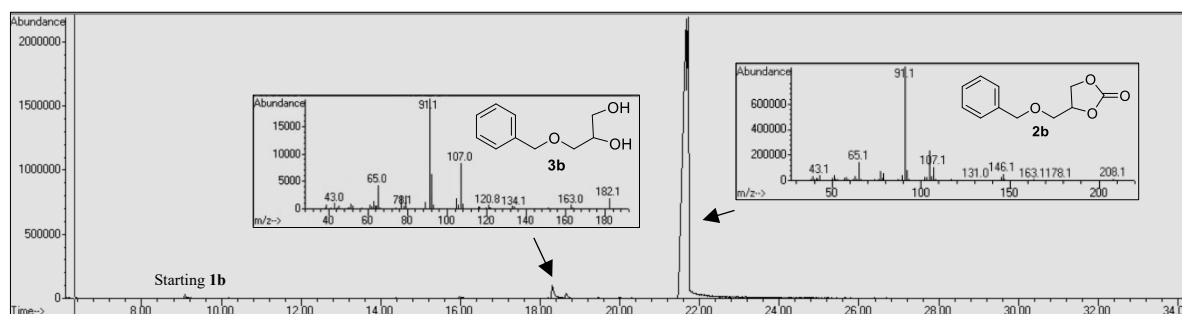
**2a.** <sup>1</sup>H NMR (400 MHz, CDCl<sub>3</sub>) δ 7.50 – 7.33 (m, 5H), 5.68 (t, *J* = 8.0 Hz, 1H), 4.80 (t, *J* = 8.4 Hz, 1H), 4.35 (dd, *J* = 8.5, 8.0 Hz, 1H).



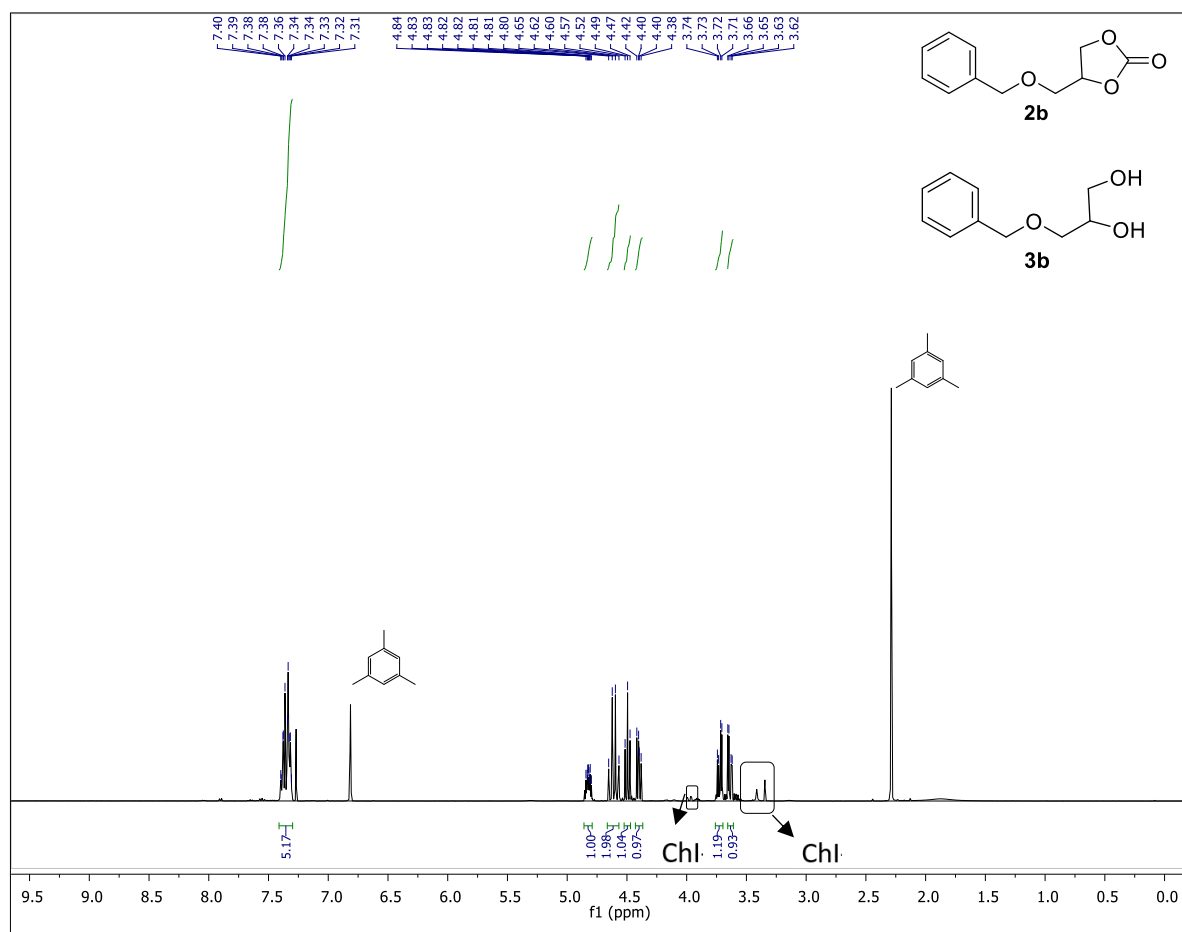
**2a.** <sup>13</sup>C NMR (100 MHz, CDCl<sub>3</sub>) δ 154.77, 135.76, 129.71, 129.21, 125.83, 77.96, 71.1

### A3.2. PRODUCT 2b

GC-MS chromatogram and of reaction crude for conversion of 1b into 2b (Table 3.3, entry 2<sup>a</sup>)



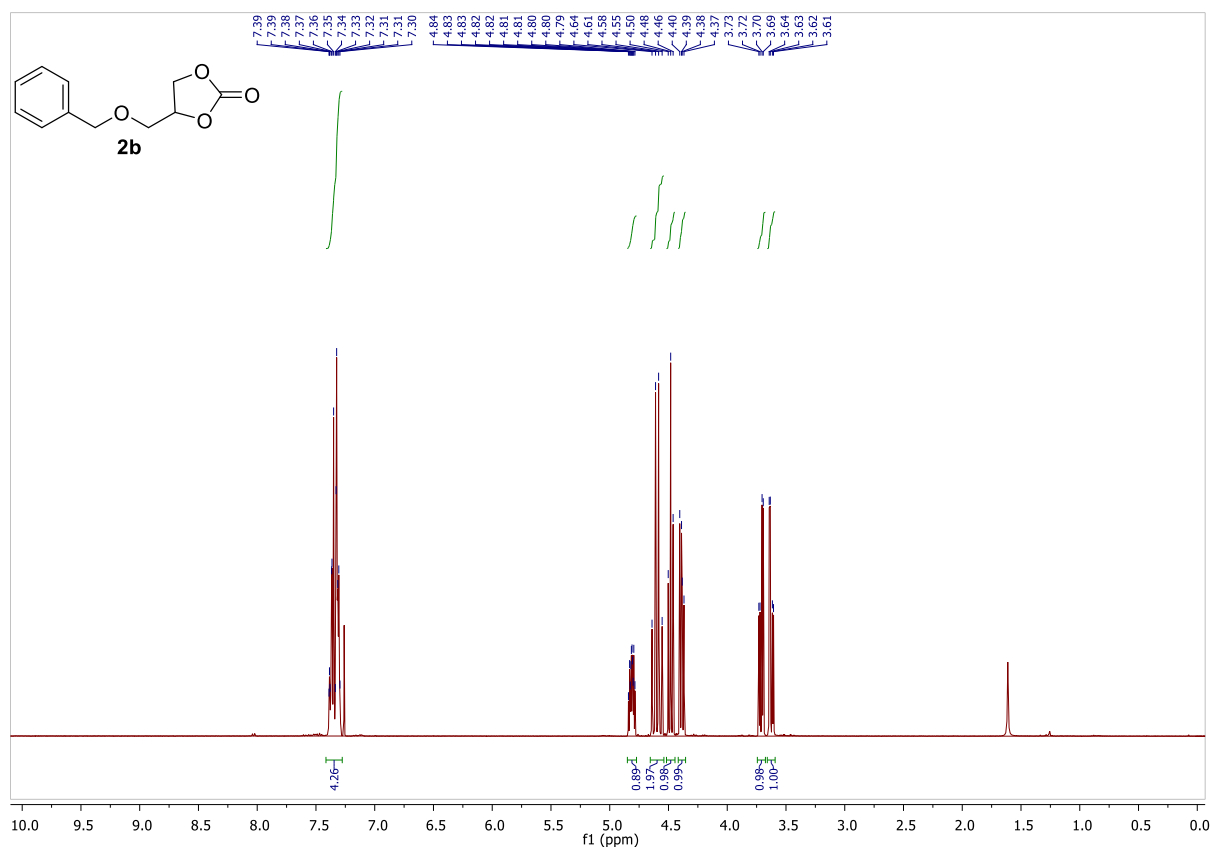
<sup>1</sup>H NMR spectrum of reaction crude for conversion of 1b into 2b (Table 3.3, entry 2<sup>a</sup>)



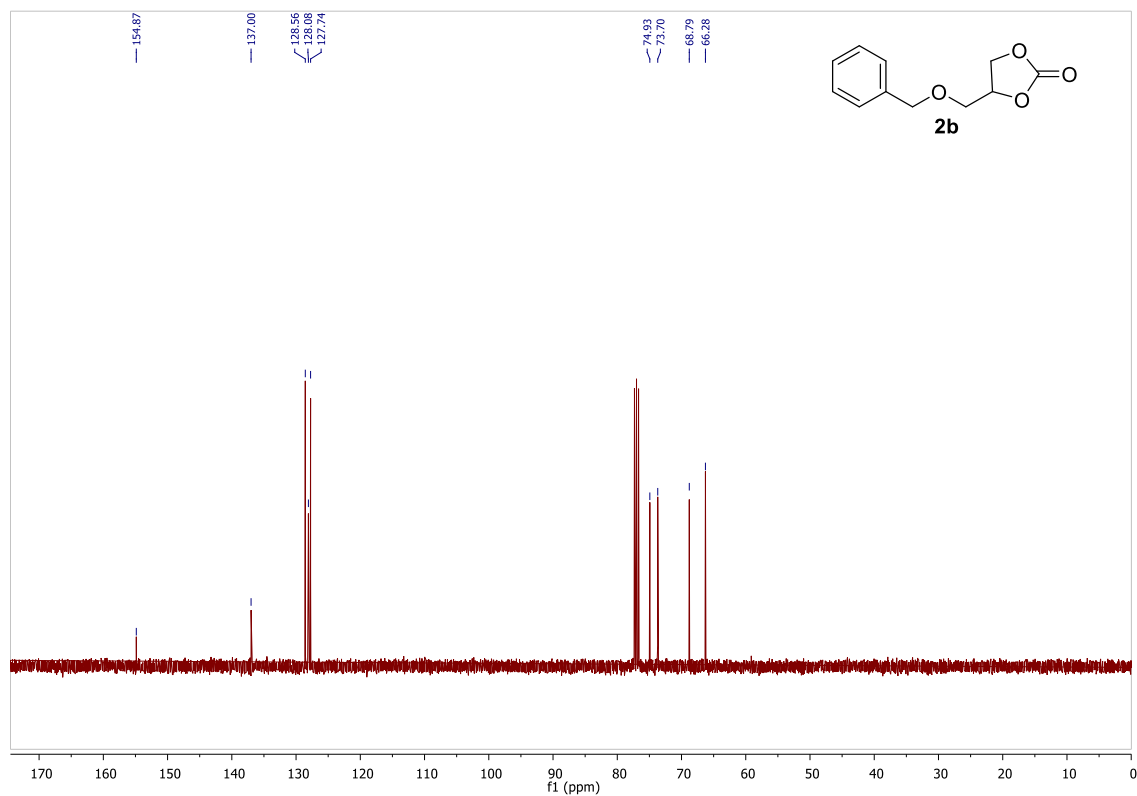
**2b.** <sup>1</sup>H NMR (400 MHz, CDCl<sub>3</sub>) δ 7.35 (m, 5H), 4.82 (ddt, *J* = 8.1, 6.0, 4.1 Hz, 1H), 4.66 – 4.57 (m, 2H), 4.49 (t, *J* = 8.4 Hz, 1H), 4.40 (dd, *J* = 8.4, 6.1 Hz, 1H), 3.72 (dd, *J* = 10.9, 4.1 Hz, 1H), 3.64 (dd, *J* = 10.9, 3.7 Hz, 1H).

**3b.** (diagnostic signals) <sup>1</sup>H NMR (400 MHz, CDCl<sub>3</sub>) δ 3.94 – 3.89 (m, 1H), 3.61 – 3.55 (m, 2H).

<sup>1</sup>H and <sup>13</sup>C NMR spectra of isolated product **2b** (Table 3.3, entry 2<sup>a</sup>)



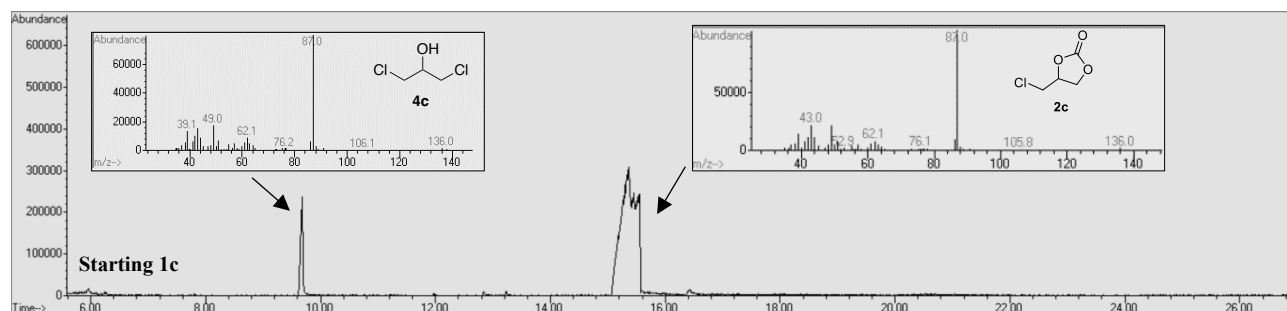
**2b.** <sup>1</sup>H NMR (400 MHz, CDCl<sub>3</sub>) δ 7.41 – 7.28 (m, 5H), 4.81 (ddt, *J* = 7.9, 6.1, 3.9 Hz, 1H), 4.60 (m, 2H), 4.48 (t, *J* = 8.4 Hz, 1H), 4.39 (dd, *J* = 8.4, 6.1 Hz, 1H), 3.71 (dd, *J* = 10.9, 4.0 Hz, 1H), 3.62 (dd, *J* = 10.9, 3.8 Hz, 1H).



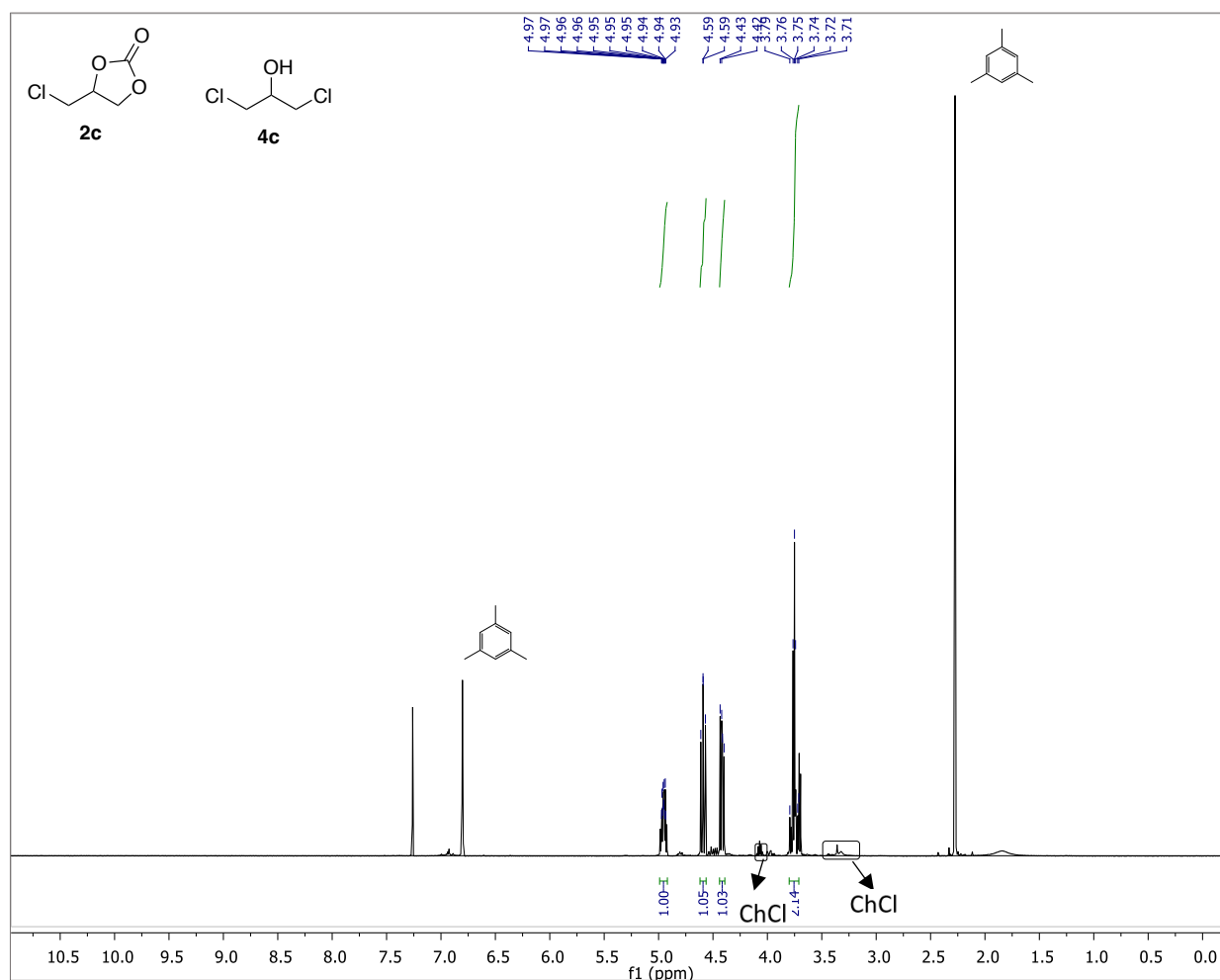
**2b.** <sup>13</sup>C NMR (100 MHz, CDCl<sub>3</sub>) δ 154.87, 137.00, 128.56, 128.08, 127.74, 74.93, 73.70, 68.79, 66.2

### A3.3. PRODUCT 2c

GC-MS chromatogram and of reaction crude for conversion of 1c into 2c (Table 3.3, entry 3<sup>b</sup>)



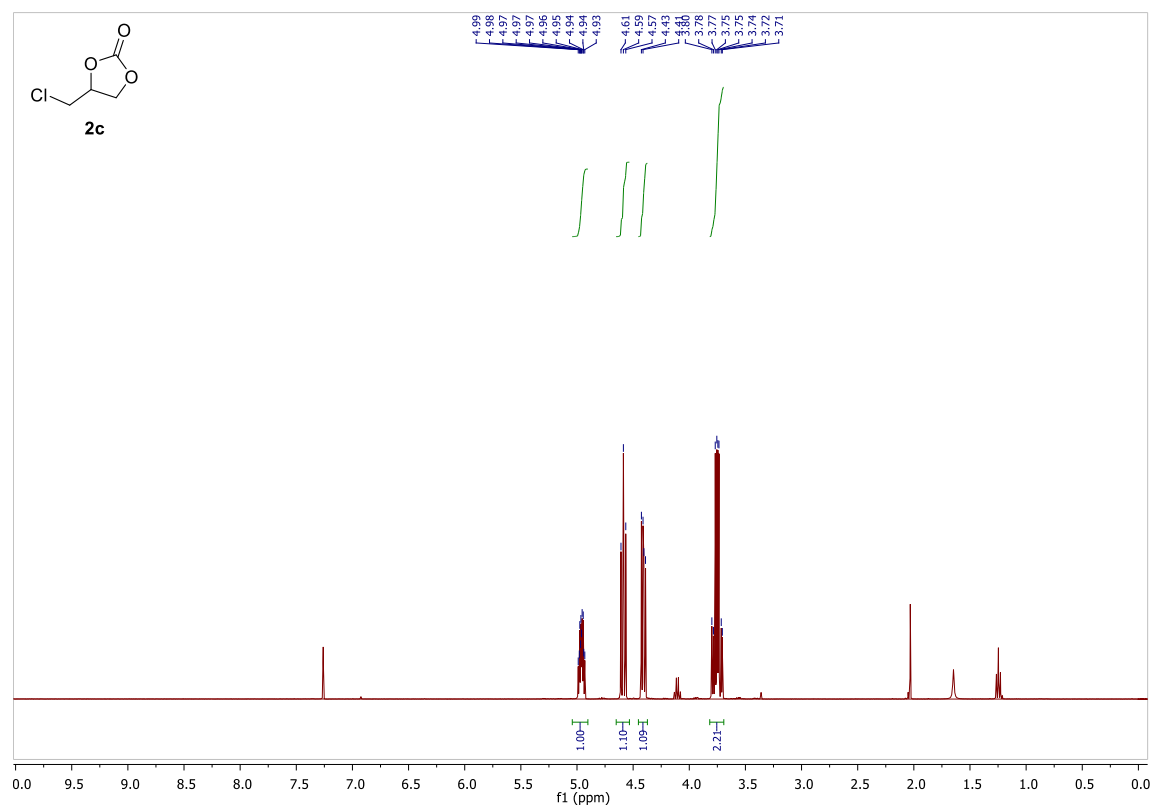
<sup>1</sup>H NMR spectrum and of reaction crude for conversion of 1c into 2c (Table 3.3, entry 3<sup>b</sup>)



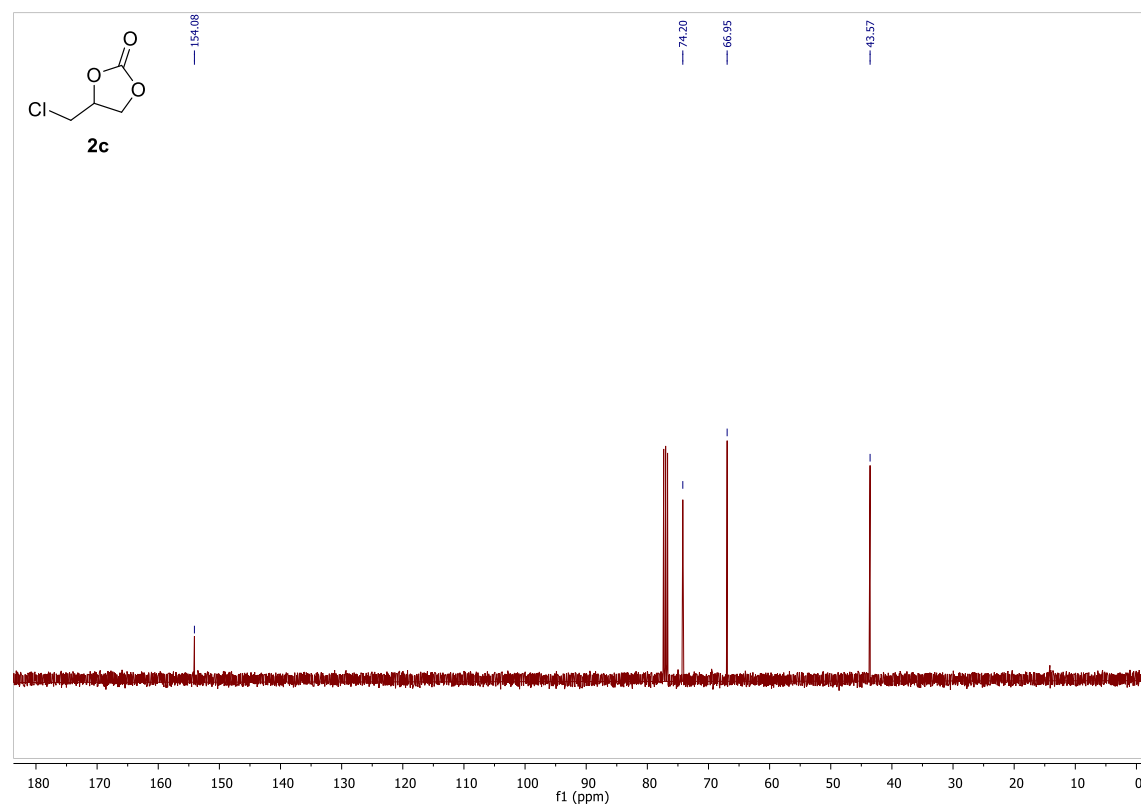
**2c.** <sup>1</sup>H NMR (400 MHz, CDCl<sub>3</sub>) δ 4.97 – 4.93 (m, 1H), 4.59 (dd, *J* = 8.8, 8.3 Hz, 1H), 4.42 (dd, *J* = 8.9, 5.7 Hz, 1H), 3.80 – 3.71 (m, 2H).

**4c.** (diagnostic signals) <sup>1</sup>H NMR (400 MHz, CDCl<sub>3</sub>) δ 4.07 (m, 1H).

$^1\text{H}$  and  $^{13}\text{C}$  NMR spectra of isolated product **2c** (Table 3.3, entry 3<sup>b</sup>)



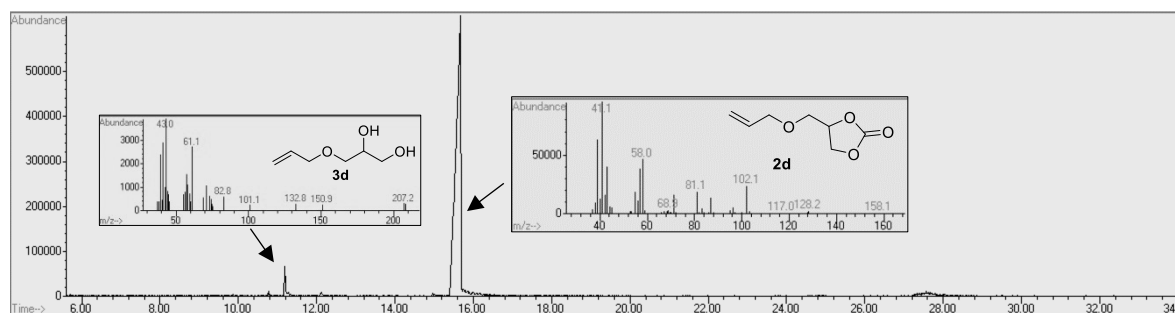
**2c.**  $^1\text{H}$  NMR (400 MHz,  $\text{CDCl}_3$ )  $\delta$  4.96 (m, 1H), 4.59 (t,  $J = 8.6$  Hz, 1H), 4.41 (dd,  $J = 8.9, 5.7$  Hz, 1H), 3.75 (m, 2H).



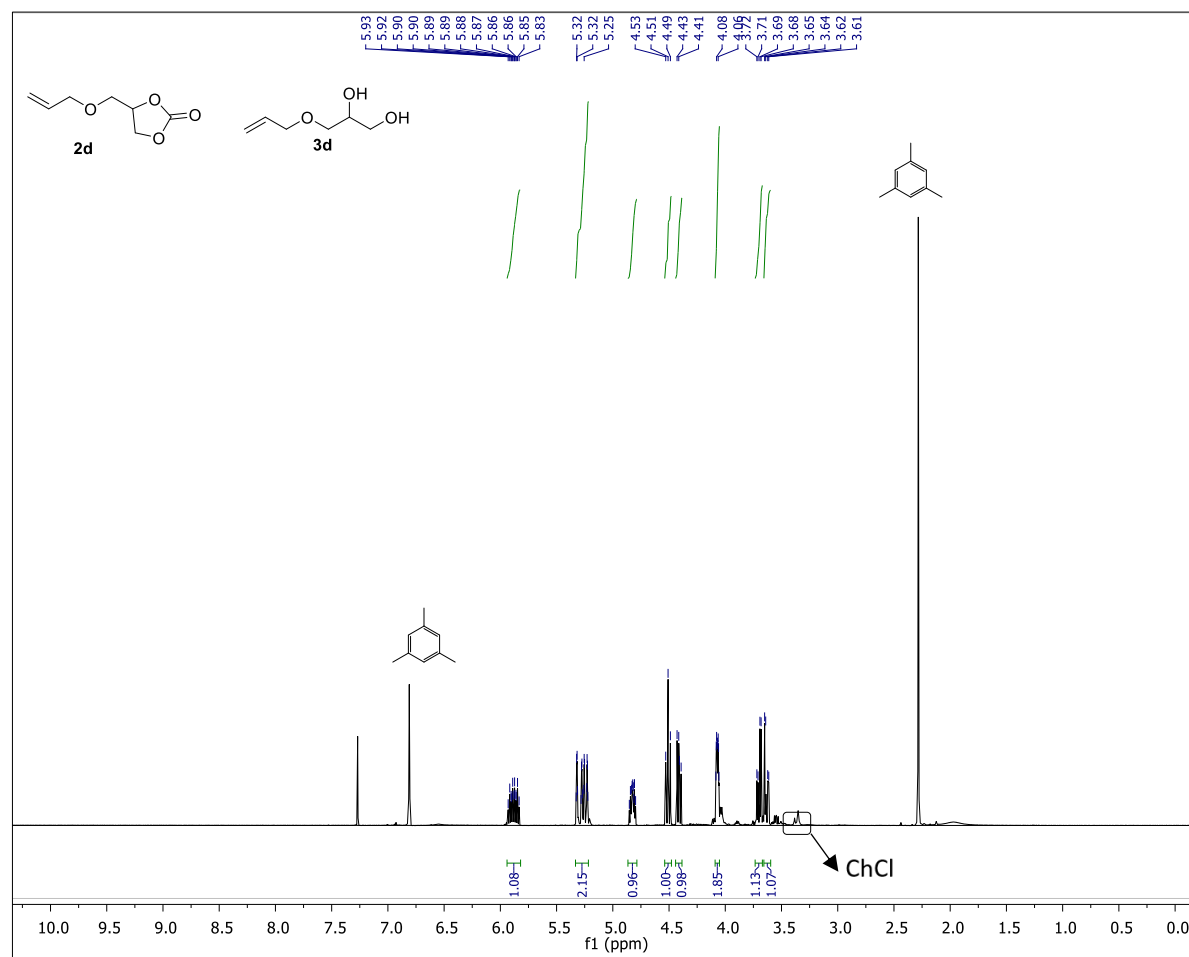
**2c.**  $^{13}\text{C}$  NMR (100 MHz,  $\text{CDCl}_3$ )  $\delta$  154.08, 74.20, 66.95, 43.57.

### A3.4 PRODUCT 2d

GC-MS chromatogram of reaction crude for conversion of 1d into 2d (Table 3.3, entry 4<sup>b</sup>)



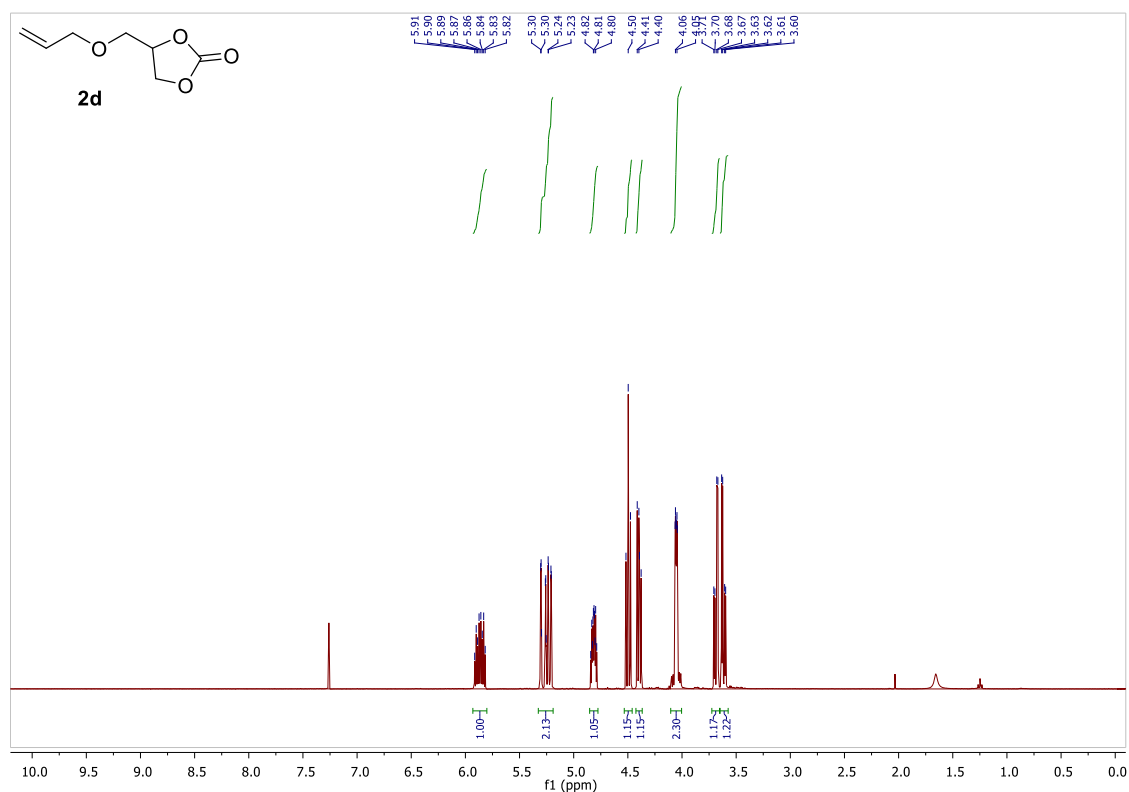
<sup>1</sup>H NMR spectrum of reaction crude for conversion of 1d into 2d (Table 3.3, entry 4<sup>b</sup>)



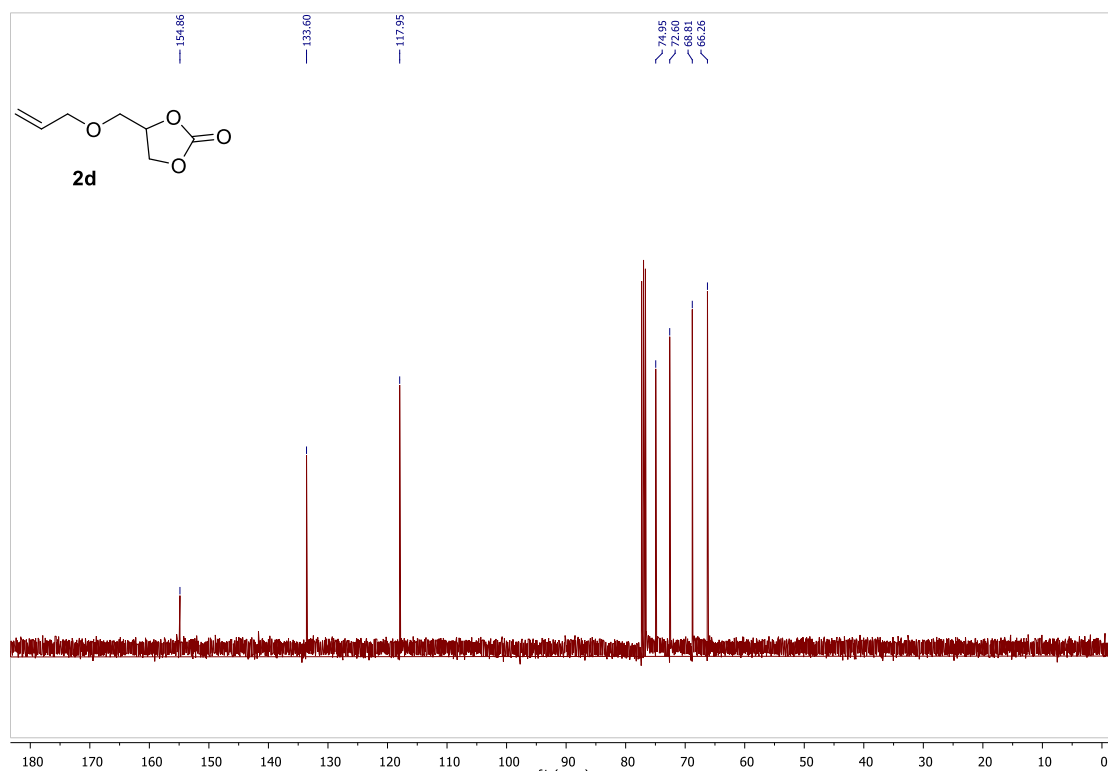
**2d.** <sup>1</sup>H NMR (400 MHz, CDCl<sub>3</sub>) δ 5.88 (ddt, *J* = 17.1, 10.5, 5.7 Hz, 1H), 5.33 – 5.22 (m, 2H), 4.87 – 4.79 (m, 1H), 4.51 (t, *J* = 8.3 Hz, 1H), 4.41 (dd, *J* = 8.4, 6.1 Hz, 1H), 4.07 (m, 2H), 3.70 (dd, *J* = 11.0, 4.1 Hz, 1H), 3.63 (dd, *J* = 11.0, 3.8 Hz, 1H).

**3d.** (diagnostic signals) <sup>1</sup>H NMR (400 MHz, CDCl<sub>3</sub>) δ 3.90 (m, 1H), 3.59 – 3.51 (m, 2H).

$^1\text{H}$  and  $^{13}\text{C}$  NMR spectra of isolated product **2d** (Table 3.3, entry 4<sup>b</sup>)



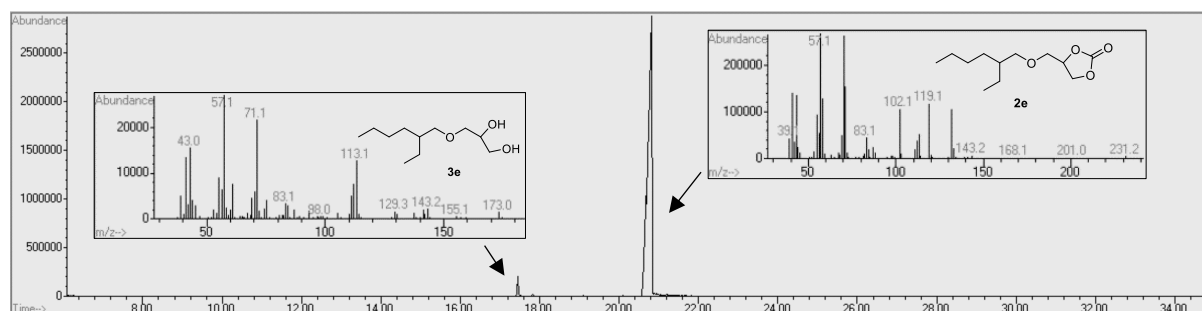
**2d.**  $^1\text{H}$  NMR (400 MHz,  $\text{CDCl}_3$ )  $\delta$  5.87 (ddd,  $J = 22.8, 10.8, 5.6$  Hz, 1H), 5.33 – 5.19 (m, 2H), 4.82 (ddt,  $J = 8.1, 6.1, 3.9$  Hz, 1H), 4.50 (t,  $J = 8.4$  Hz, 1H), 4.40 (dd,  $J = 8.3, 6.1$  Hz, 1H), 4.10 – 4.00 (m, 2H), 3.69 (dd,  $J = 11.0, 4.0$  Hz, 1H), 3.62 (dd,  $J = 11.0, 3.8$  Hz, 1H).



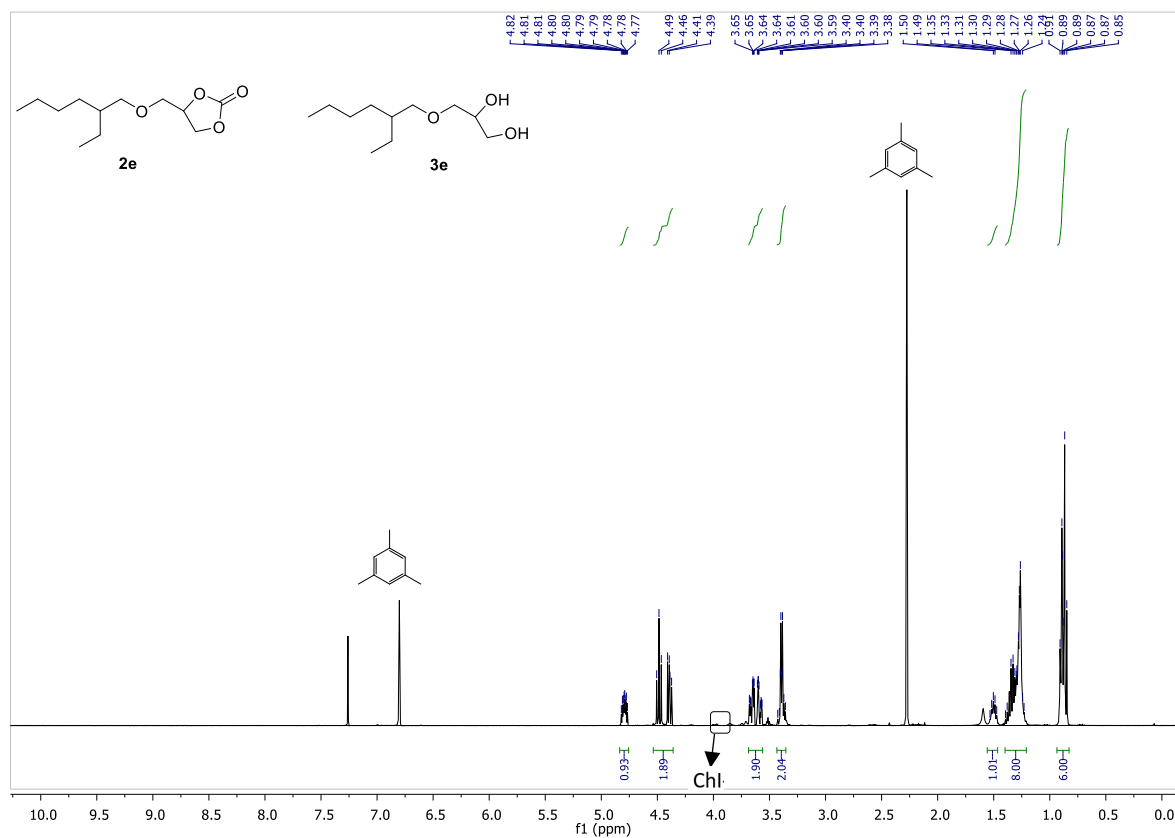
**2d.**  $^{13}\text{C}$  NMR (100 MHz,  $\text{CDCl}_3$ )  $\delta$  154.86, 133.60, 117.95, 74.95, 72.60, 68.81, 66.26

### A3.5. PRODUCT 2e

GC-MS chromatogram of reaction crude for conversion of 1e into 2e (Table 3.3, entry 5<sup>a</sup>)



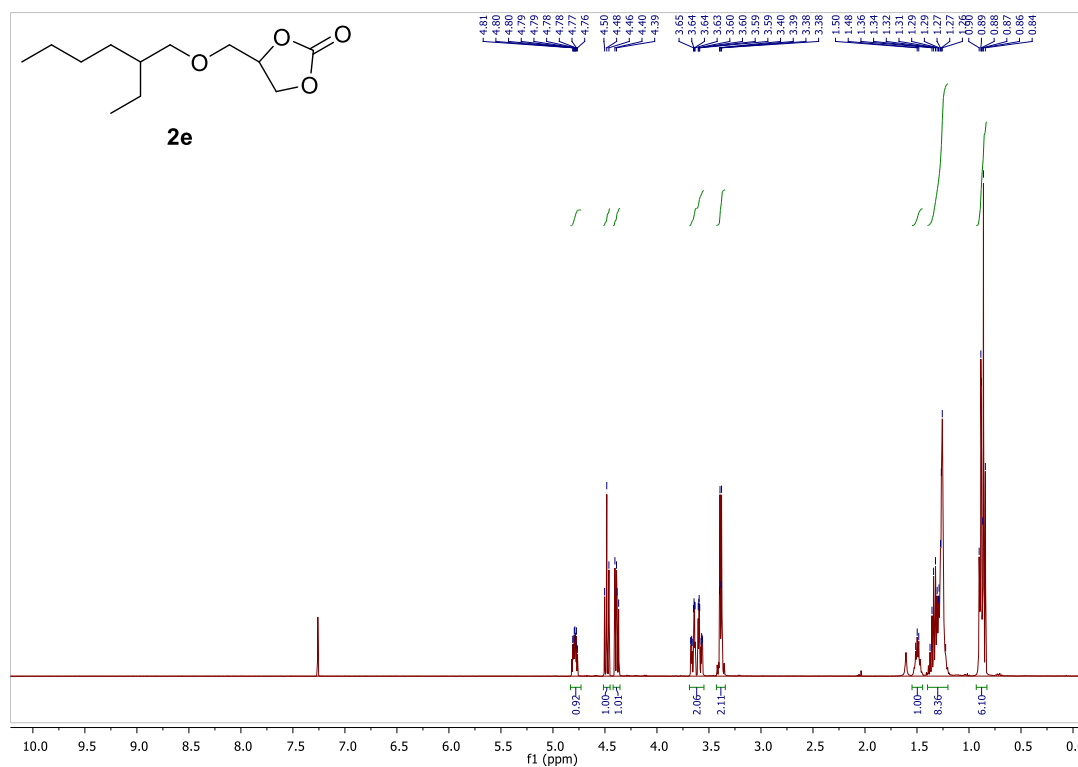
<sup>1</sup>H NMR spectrum of reaction crude for conversion of 1e into 2e (Table 3.3, entry 5<sup>a</sup>)



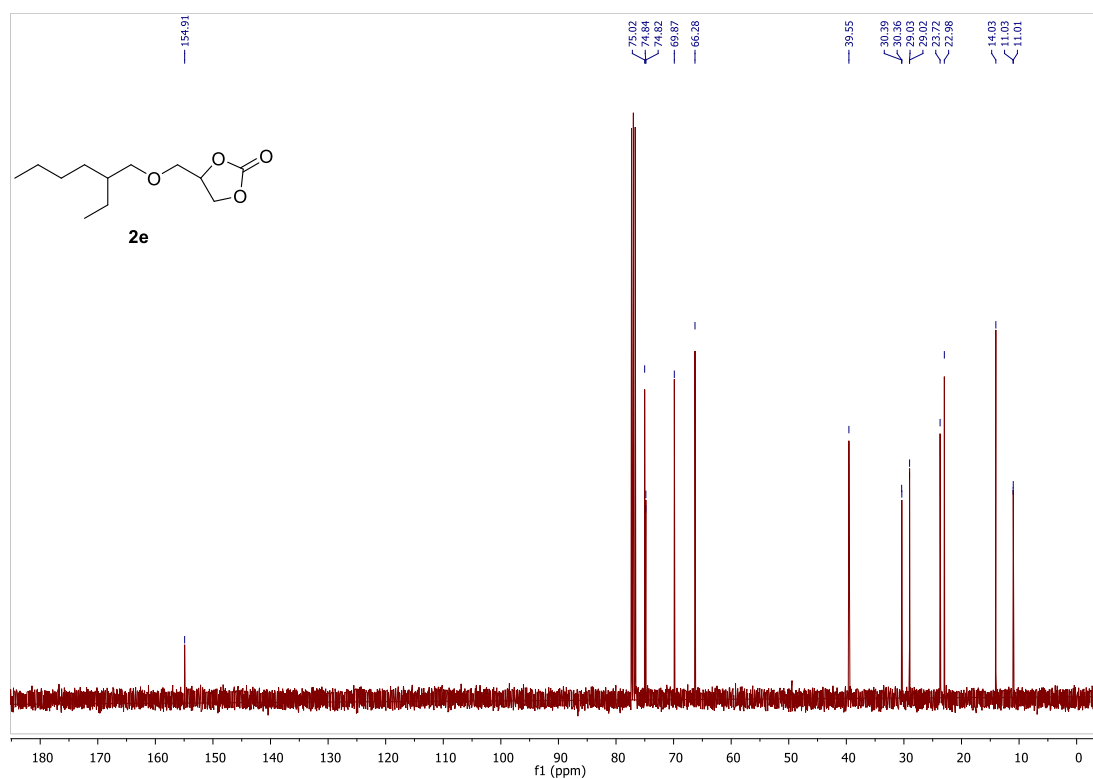
**2e.** <sup>1</sup>H NMR (400 MHz, CDCl<sub>3</sub>) δ 4.82 – 4.76 (m, 1H), 4.51 – 4.36 (m, 2H), 3.62 (m, 2H), 3.39 (dd, *J* = 5.7, 1.9 Hz, 2H), 1.55 – 1.45 (m, 1H), 1.40 – 1.20 (m, 8H), 0.88 (dt, *J* = 10.6, 7.0 Hz, 6H).

**3e.** (diagnostic signals) <sup>1</sup>H NMR (400 MHz, CDCl<sub>3</sub>) δ 3.53 – 3.49 (m, 2H), 1.50 (dt, *J* = 12.0, 6.0 Hz, 14H).

$^1\text{H}$  and  $^{13}\text{C}$  NMR spectra of isolated product **2e** (Table 3.3, entry 5<sup>a</sup>)



**2e.**  $^1\text{H}$  NMR (400 MHz,  $\text{CDCl}_3$ )  $\delta$  4.83 – 4.73 (m, 1H), 4.48 (t,  $J$  = 8.3 Hz, 1H), 4.39 (dd,  $J$  = 8.3, 6.0 Hz, 1H), 3.62 (m, 2H), 3.39 (dd,  $J$  = 5.7, 2.0 Hz, 2H), 1.55 – 1.45 (m, 1H), 1.40 – 1.26 (m, 8H), 0.87 (dt,  $J$  = 10.2, 7.0 Hz, 6H).



**2e.**  $^{13}\text{C}$  NMR (100 MHz,  $\text{CDCl}_3$ )  $\delta$  154.91, 75.02, 74.83, 69.87, 66.28, 39.55, 30.37, 29.02, 23.72, 22.98, 14.03, 11.02

**Published as:** Vagnoni, M.; Samorì, C.; Galletti, P. Choline-Based Eutectic Mixtures as Catalysts for Effective Synthesis of Cyclic Carbonates from Epoxides and CO<sub>2</sub>. *J. CO<sub>2</sub> Util.* **2020**, *42*, 101302. <https://doi.org/10.1016/j.jcou.2020.101302>.

## 3.2 HETEROGENEOUS CATALYSTS: CHAR-BASED BIFUNCTIONAL CATALYSTS FROM BIOPOLYMERS AND WASTE

### 3.2.1 Introduction

As stated and demonstrated in chapter 3.1, the synthesis of CCs from epoxides requires the use of two different active species as catalysts. To this scope, is very common in literature to find bi-component catalytic systems, in which there are: a Lewis base, responsible for the epoxy-ring opening (the rate-determining step of the reaction), and a Lewis acid, mainly considered as a co-catalyst, responsible for the epoxide activation and for the stabilization of alkoxide intermediate. It is more difficult to have a single catalyst bearing the two active sites, both homogeneous and heterogeneous reactions, and it is still a challenging task to find a non-metallic, effective and recyclable catalyst that works under mild conditions.<sup>1</sup> Another interesting feature is that, since these reactions are carried out in solvent-free conditions, a bifunctional heterogeneous catalysts could allow a simple product separation and a facile catalyst recovery and reuse for multiple cycles.<sup>2,3</sup>

Several biobased polymeric materials (cellulose, lignin, chitosan or chitin, lignocellulose, etc.) have been used for this kind of reaction, working as:

- (i) Lewis acids, through the -OH groups present on their surfaces, while, as Lewis base, tetrabutylammonium halides or KI were always added;<sup>4-7</sup>
- (ii) heterogeneous supports for ionic liquids or deep eutectic solvents, mainly bearing an imidazolium chain (as Lewis base);<sup>8-13</sup>
- (iii) functionalized materials (i.e. with a quaternary ammonium salt).<sup>14-18</sup>

Being these catalysts non-bifunctional, a common drawback to all these biobased polymeric materials is the need of a co-catalysts (both Lewis acids and Lewis bases) to perform the reaction.

Moreover, from a circular economy perspective and for environmental sustainability purposes, the production of bifunctional heterogeneous catalysts made from wastes could represent a step forward in this framework. The valorization of waste has been carried out over the years through various chemical, biological and thermochemical processes (e.g. pyrolysis, gasification or hydrothermal conversion).<sup>19,20</sup> Specifically, through thermochemical

processes, various biofuels or biochemicals, such as syngas, bio-oil, biochar/char and platform chemicals can be obtained.<sup>21</sup> Biochar is a carbonaceous material whose physicochemical properties varies significantly according to the feedstock in input, the carbonization process, and the activation or functionalization methods.<sup>22</sup> Thanks to the porous structure, the large surface area and the high quantity of functional groups on the surface, activated or functionalized bio-chars are widely used as activated carbons, soil amendments, carbon sequestration agents and environmental adsorbents for organic and heavy metal removal.<sup>23,24</sup> More importantly, due to the possibility of covalently adding different functional groups on their surface, bio-chars can be used as versatile catalysts and/or catalyst supports in many chemical processes, such as biodiesel production.<sup>25,26</sup>

In the literature only one report deals with the conversion of CO<sub>2</sub> and epoxides into cyclic carbonates using oxidized biochar with alcoholic or carboxylic groups. These moieties work as H-bond donors on the surface of biochar behaving as Lewis acid co-catalyst, with the addition of the catalyst tetrabutylammonium bromide (TBAB) as a Lewis base.<sup>27</sup>

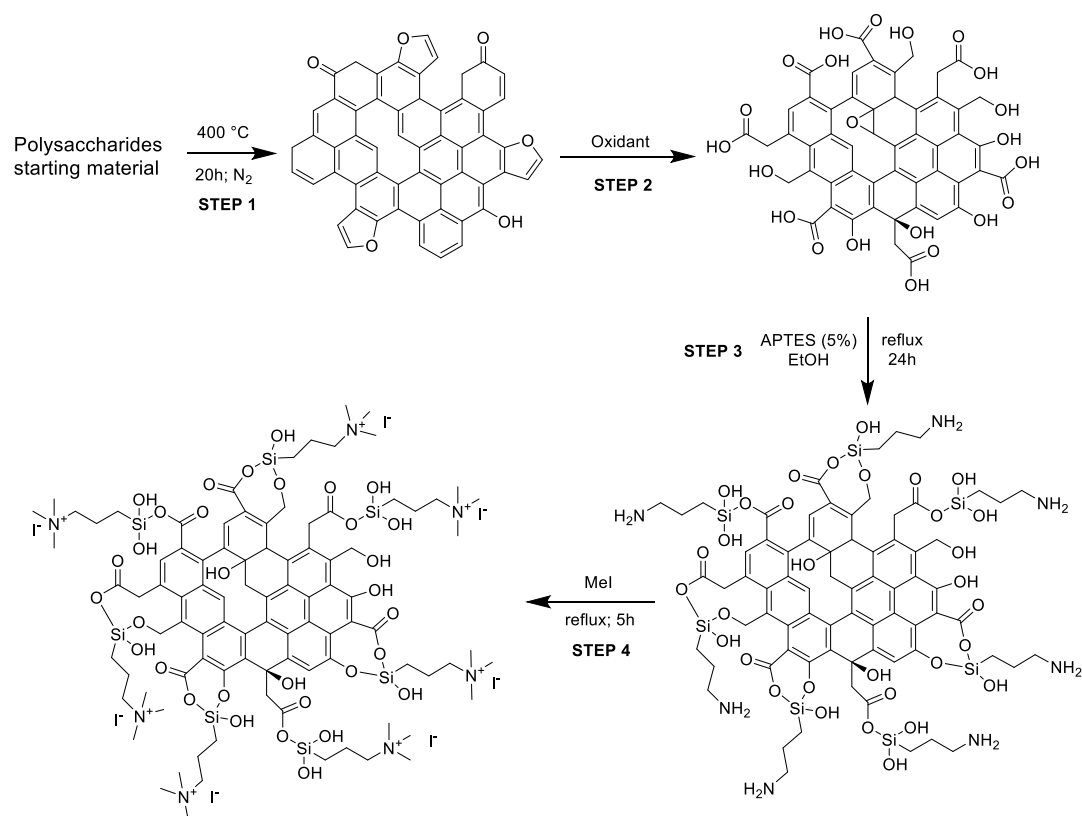
Here, various bio-chars made from three different polysaccharides (cellulose, cellulose acetate, and starch) and corresponding waste (fir sawdust, post-use cigarette filters, and starch-based plastic bags) were derivatized with a new protocol to obtain bifunctional heterogeneous catalysts. Such catalysts were then applied in the synthesis of cyclic carbonates by incorporating CO<sub>2</sub> into epoxides in mild conditions. An extensive characterization of the final catalysts and the materials obtained after each functionalization step was also performed.

### **3.2.2 Result and discussion**

#### Bifunctional heterogeneous catalysts synthesis

The optimization of the synthesis of the heterogeneous catalysts was made in collaboration with Dr. A.Parodi. The procedure adopted for the production of the bifunctional catalysts from different polysaccharides and waste is a 4-step synthetic pathway consisting of: a) carbonization of the starting material to give a char; b) oxidation of the char with H<sub>2</sub>O<sub>2</sub> to give an oxidized char (OC); c) functionalization of OC through the introduction of amine moieties by anchoring of (3-Aminopropyl)triethoxysilane (APTES) to give an amine-functionalized char (AC); d) quaternarization of the amine functionality into ammonium iodide salt to give the

final catalyst (**Scheme 3.1**). Preliminary studies for the optimization of the procedure were performed on cellulose and sawdust and monitored through the elemental analysis (CHN) of the functionalized char. Pyrolysis of the starting material was crucial to achieving an effective oxidation of the obtained char: the higher was the temperature, the less oxidizable was the carbonaceous material. In fact, higher temperatures create more aromatic and robust chars that need more energy and time to reach the same oxidation degree as a char obtained with lower pyrolysis temperatures (see Appendix A3.1). On the other hand, shorter times or lower temperatures gave too fragile materials that were not able to maintain their 3D-structure after the oxidation step. The best conditions corresponded to a pyrolysis at 400 °C for 15 h.<sup>28,29</sup> Oxidation was performed screening several oxidizing agents, such as HNO<sub>3</sub>, H<sub>2</sub>O<sub>2</sub> or KMnO<sub>4</sub> at different times and temperatures (see Appendix A3.1 and A3.2). H<sub>2</sub>O<sub>2</sub> was selected for the optimized methodology (85 °C for 24h) because of its higher sustainability and safety, and also because, unlike HNO<sub>3</sub>, it cannot give side reactions such as nitration of the char. KMnO<sub>4</sub> did not work efficiently, maintaining almost unaltered the elemental composition of the char (see Appendix A3.1 and A3.2). The oxidation significantly changes the surface of the char, increasing its oxygen content (**Table 3.1**, step 2) through alcoholic and carboxylic functionalities (see characterization paragraph), essential for the further amination step. After oxidation, the anchoring of APTES on the surface of the char was performed under various conditions (see Appendix A3.1), and it was found that a little amount of water was mandatory to produce an active catalyst, since water hydrolyzes the ethoxy groups<sup>30</sup> to hydroxyl group, an active Lewis acid species in the carbonation of epoxides mechanism. The increased nitrogen content of the OCs testified the performances of this step (**Table 3.1**, step 3). The last step was optimized to minimize the amount of methyl iodide (MeI) necessary for the quaternarization of the amine based on the effectively anchored amine group (quantified through XPS analysis). As alternatives to MeI, longer chain alkyl iodides (butyl and octyl iodide) were successfully used even if higher reaction temperatures were needed for an effective quaternarization of the amine (see Appendix A3.2).



**Scheme 3.1** 4-steps catalyst synthesis. A tentative model structures of chars at each reaction step was given on the basis of elemental analysis results.

**Table 3.1** Elemental composition of the functionalized chars derived from cellulose and sawdust for each optimized reaction step (mean  $\pm$  standard deviation of three independent replicates).

Reaction step	Cellulose			Sawdust		
	N [%]	C [%]	H [%]	N [%]	C [%]	H [%]
Starting Material	-	40.5 $\pm$ 0.7	6.5 $\pm$ 0.1	-	45.7 $\pm$ 0.6	6.4 $\pm$ 0.1
Step 1 -Pyrolysis (C)	-	85.0 $\pm$ 0.3	2.9 $\pm$ 0.1	-	79.3 $\pm$ 0.2	2.9 $\pm$ 0.1
Step 2 -Oxidation (OC)	-	58.2 $\pm$ 0.4	2.8 $\pm$ 0.2	-	56.6 $\pm$ 0.5	2.9 $\pm$ 0.2
Step 3 - APTES anchoring (AC)	7.1 $\pm$ 0.1	42.1 $\pm$ 0.5	6.0 $\pm$ 0.1	6.7 $\pm$ 0.2	41.3 $\pm$ 0.4	5.5 $\pm$ 0.1
Step 4 - Quaternarization	5.0 $\pm$ 0.1	29.3 $\pm$ 0.6	4.4 $\pm$ 0.3	4.9 $\pm$ 0.1	31.2 $\pm$ 0.3	4.3 $\pm$ 0.1

The optimized procedure was applied on six different starting materials: three polysaccharides (potato starch, cellulose and cellulose acetate) and the three corresponding post-use wastes (starch-based plastics bags, fir sawdust and wasted cigarette filters). All the catalysts obtained have the appearance of black powders. The versatility of the method was checked through elemental analysis and it was found that all the materials tested behaved similarly, since the final elemental composition of all the catalysts is very close one another (**Table 3.2**).

**Table 3.2** Elemental composition of the final catalysts derived from different materials (mean  $\pm$  standard deviation of three independent replicates).

Label	Starting Material	N	C	H
HC-PS	Potato Starch	4.7 $\pm$ 0.1	31.8 $\pm$ 0.2	4.5 $\pm$ 0.2
HC-SBPB	Starch Based Plastic Bags	4.4 $\pm$ 0.2	28.2 $\pm$ 0.8	3.8 $\pm$ 0.2
HC-C	Cellulose	5.0 $\pm$ 0.1	29.3 $\pm$ 0.6	4.4 $\pm$ 0.3
HC-FSD	Fir Sawdust	4.9 $\pm$ 0.1	31.2 $\pm$ 0.3	4.3 $\pm$ 0.1
HC-CA	Cellulose Acetate	5.0 $\pm$ 0.2	31.3 $\pm$ 0.4	4.4 $\pm$ 0.2
HC-PUCF	Post Use Cigarette Filters	4.9 $\pm$ 0.1	33.8 $\pm$ 0.3	4.6 $\pm$ 0.1

### Bifunctional heterogeneous catalysts characterization

Characterization of the final catalysts and of cellulose and sawdust after each reaction step were performed by two research groups from “Institute of nanostructured materials (ISMN) - National Research Council (CNR)”. ATR-FTIR and SEM analysis were carried out by the group of Doc. F. De Giorgio and Doc. G. Ruani, while XPS analyses have been done by Doc. A. Mezzi. The comparison of the ATR-FTIR spectra of cellulose- and sawdust-derived materials shown in **Figure 3.1** suggests that no differences are observed between the cellulose- and sawdust-derived materials at each reaction step (band assignments for cellulose-based catalyst, thus valid also for fir sawdust-based, are described in Appendix A3.3). Irrespective of the different starting materials (see appendix A3.4), no differences are evinced in the peak positions of the ATR-FTIR spectra of the catalysts, i.e., the last step of the synthesis, thus demonstrating the versatility of the derivatization procedure in order to obtain similarly functionalized catalysts (**Figure 3.2**). Analyses of HC-C and HC-CA coming from different batch of starting materials and synthesized in different moments have been also performed, showing the same peak positions and thus the high reproducibility of the synthesis (see appendix A3.5).

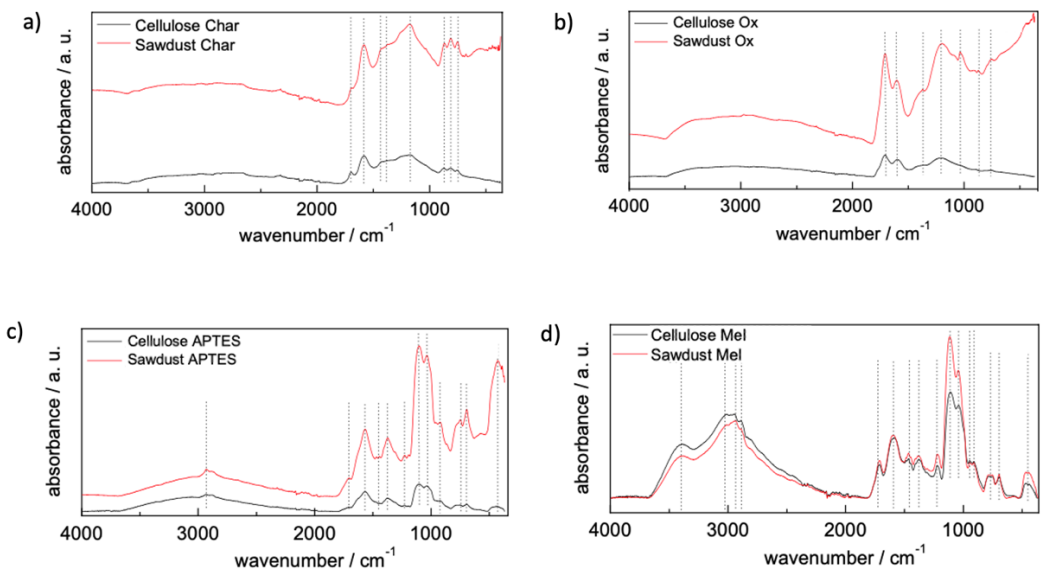


**Figure 3.1** ATR-FTIR spectra of cellulose- and sawdust-derived materials at each reaction step.

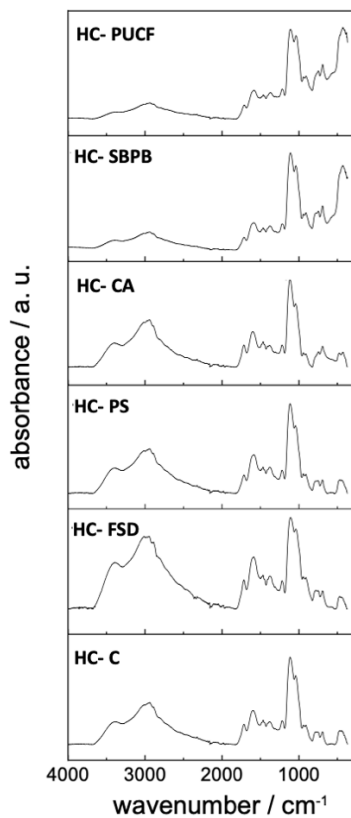


**Figure 3.2** ATR-FTIR spectra of all the catalysts.

The XPS measurements revealed the presence of C, O, Si, I and F, characteristic for each product during the preparation process of HC-C and HC-FSD (**Figure 3.3 a and b**). The presence of F can be considered a contamination, as well Si in form of silicates. The chars contain C and O whose atomic ratio is almost the same of the stoichiometric value (C:O = 10:1). The effect of the oxidation step is evident because the C/O ratio immediately decreases to  $\sim 2.2$  and it never changes for the rest of the samples. The following step was the reaction with APTES, which was successfully added as it is testified by the presence of Si and N. The Si 2p signal is characterized by the presence of two components, one assigned to APTES and the other one to silicates, respectively. Even the N 1s signal is characterized by the presence of two components, which are assigned to amine and ammonium groups, respectively. It is worth to mention that  $N(\text{amine}) > N(\text{ammonium})$ . Interestingly, when Mel was added to the reaction in the last step, this ratio is inverted. Comparing the composition of all the HCs, they are quite similar (**Figure 3.3 c**), even though it is remarkable to note that the amine contribution almost disappears in the HC-FSD and HC-SBPB samples. Small differences are also registered on the C 1s spectra (**Figure 3.3 d**).

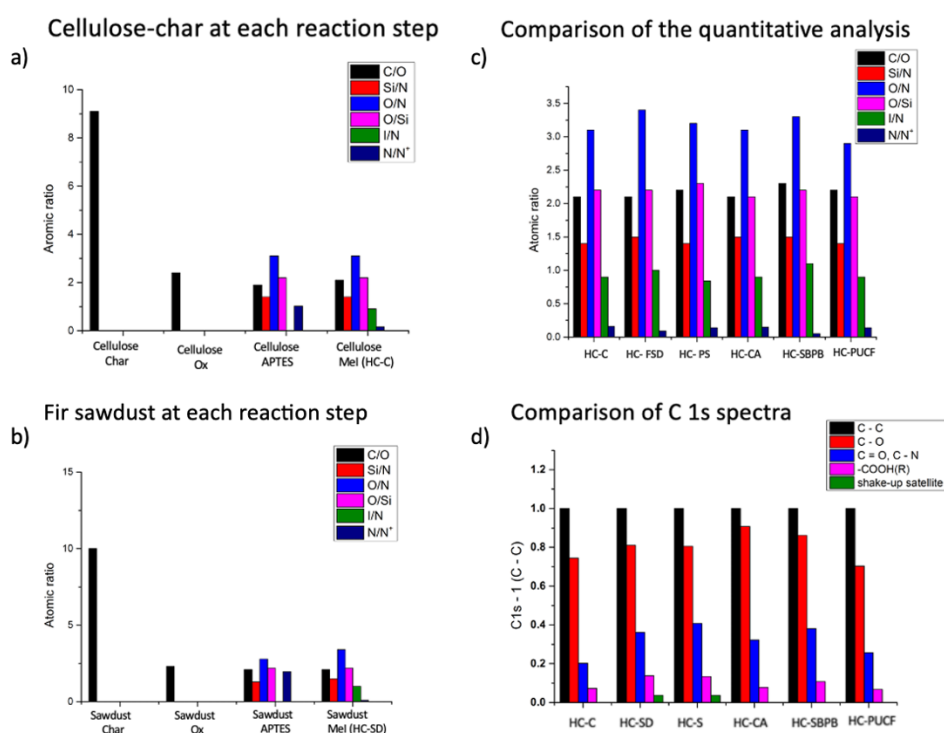


**Figure 3.3** a) XPS quantitative analysis for the Cellulose batch at each reaction step; b) XPS quantitative analysis for the fir sawdust batch at each reaction step; c) comparison of the quantitative analysis for all HCs samples; d) components distribution in C 1s spectra of all HCs.

SEM images of all the catalysts were collected for evaluating if their morphologies may affect their potential activity. **Figure 3.4** shows the SEM images of the catalysts collected at low magnification (x 80). The images suggest that morphologies are divided into three categories: small-medium aggregates with crystal-like shape (a, b, c), big aggregates with crystal-like shape (d, f) and big aggregates with no regular shape (e). Neither of these morphologies suggests a potential greater activity of some of these HCs.

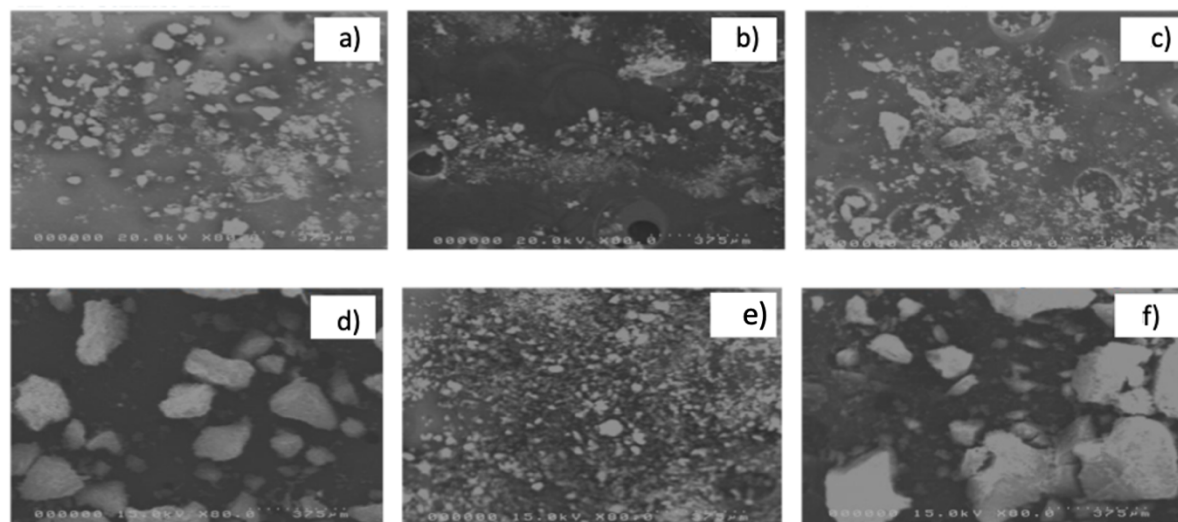


**Figure 3.4** SEM images (x 80) of the catalysts: (a) HC-C; (b) HC-FSD; (c) HC-PS; (d) HC-CA; (e) HC-PUCF; (f) HC-SBPB.

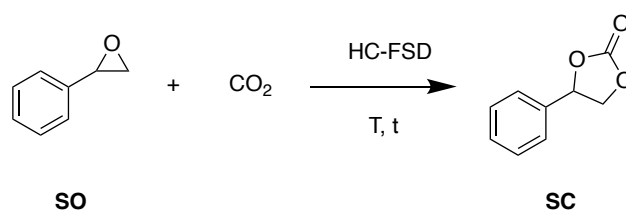
### Bifunctional heterogeneous catalysts in the synthesis of cyclic carbonates

Considering the demonstrated functionalization of the different chars with both ammonium and Lewis acid groups, all the heterogeneous catalysts here prepared were tested in the conversion of CO<sub>2</sub> and epoxides into cyclic carbonates. The cycloaddition of CO<sub>2</sub> to styrene oxide (SO) catalyzed by HC-FSD was firstly selected as a model reaction to optimize the reaction conditions. The activity of HC-FSD was tested in a stainless-steel autoclave at maximum p (CO<sub>2</sub>)= 5 bar and T= 70 °C. As shown in **Table 3.3**, 5% of HC-SD had an efficient catalytic activity with a yield of SC of 80%, and a TON of 45.7, at 70 °C and 3 bar of CO<sub>2</sub> (entry 1). Increasing the amount of catalyst to 10%, the yield reached 91% (entry 2); in both cases the selectivity towards the formation of SC was 99%. An increase of CO<sub>2</sub> pressure to 5 bar didn't improve the yield (entry 3), while conducting the reaction at 1 bar, in a Schlenk tube using a balloon as source of CO<sub>2</sub> (entry 6), decreased the yield to 41%, even after prolonging

reaction time to 24 h. For what concerns the temperature, the reaction didn't proceed at room temperature even for prolonged time (entry 4), at 50 °C there was a slight increase in yield (entry 5).

Also heterogeneous catalysts functionalized with longer alkyl iodide (butyl iodide and octyl iodide) have been successfully tested in the cycloaddition of SO with CO<sub>2</sub> giving very good yields and selectivity (see Appendix A3.2).

**Table 3.3** Results for the coupling of SO and CO<sub>2</sub> catalyzed by HC-SD.



Entry <sup>a</sup>	Catalyst amount [% w/w]	p [bar]	T [°C]	t [h]	Yield [%] <sup>b</sup>	Selectivity [%] <sup>c</sup>	TON <sup>e</sup>	TOF [h <sup>-1</sup> ] <sup>f</sup>
<b>1</b>	5	3	70	7	80	99	45.7	6.5
<b>2</b>	10	3	70	7	91	99	26	3.7
<b>3</b>	10	5	70	7	91	99	26	3.7
<b>4</b>	10	5	25	24	0	-	-	-
<b>5</b>	10	3	50	7	13	98	3.7	0.5
<b>6<sup>d</sup></b>	10	1	70	24	41	95	11.7	1.7

<sup>a</sup> Reaction conditions: 0.875 mmol SO (100 µL), autoclave.

<sup>b</sup> Isolated yields after purification of the reaction crude by flash column chromatography. Yields are expressed as mean of two independent replicates.

<sup>c</sup> Selectivity calculated by GC-MS and NMR on crude products.

<sup>d</sup> Carried out using a CO<sub>2</sub> balloon.

<sup>e</sup> Turnover number, defined as mol<sub>SC</sub>/mol<sub>iodide</sub>

<sup>f</sup> TOF= TON/h

A typical kinetic profile of the cycloaddition reaction of CO<sub>2</sub> with SO in the presence of HC-FSD at 70 °C and 3 bar of CO<sub>2</sub> pressure is shown in **Figure 3.5**. In the model reaction, the yield of the product increased with increasing reaction time until 7 h, after which it did not increase anymore.

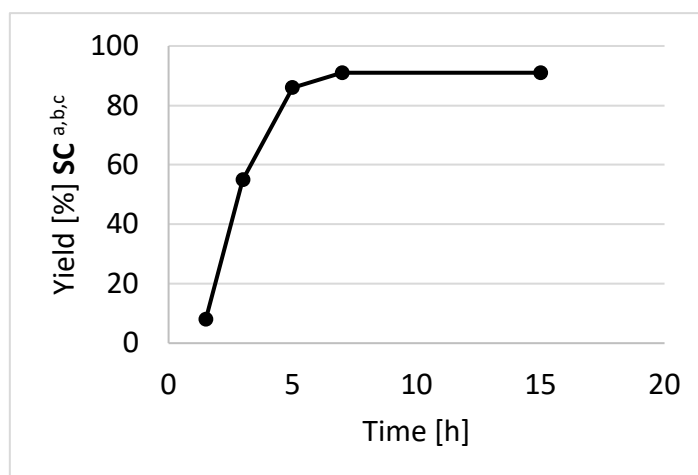


**Figure 3.5** Reaction rate for the conversion of SO into SC catalyzed by HC-FSD.

<sup>a</sup> Reaction conditions: 0,875 mmol SO (100  $\mu$ L), autoclave.

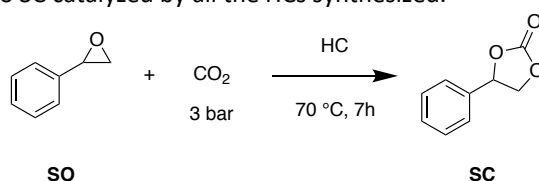
<sup>b</sup> Isolated yields after purification of the reaction crude by flash column chromatography. Yields are expressed as mean of two independent replicates.

<sup>c</sup> Selectivity was >99% for all entries.

After achieving high catalytic activity of HC-FSD for SC formation, we explored the activity of catalysts synthesized from post-use cigarette filters (HC-PUCF) and starch-based plastic bags (HC-SBPB), and from the biopolymers they are mainly composed: cellulose (HC-C), cellulose acetate (HC-CA) and potato starch (HC-PS) (**Table 3.4**). All of them have been tested at 5% and 10% w/w using the conditions optimized for HC-FSD (entries 1 and 2), 70 °C, 3 bar of CO<sub>2</sub>, 7 h. They all proved to have similar and very good activity in the cycloaddition reaction. The similar activity can be explained by the physical analysis made on all the HCs that do not put in evidence significant differences.

HC-PS catalyst proved to be the less reactive one giving 82% yield at 10% w/w (entry 10), respect HC-FSD in the same conditions (entry 2). Using HC-C (entries 3 and 4) and HC-CA (entries 5 and 6) identical yields have been obtained. As demonstrated by chemical-physical analysis, regardless from the starting material, the derivatization method used for the six chars creates almost identical catalysts. This shows the viability and versatility of the method to valorize different kinds of wastes.

**Table 3.4** Conversion of SO into SC catalyzed by all the HCs synthesized.



Entry <sup>a</sup>	Catalyst	Catalyst amount [% w/w]	Yield [%] <sup>b, c</sup>	TON <sup>d</sup>	TOF [h <sup>-1</sup> ] <sup>e</sup>
1	HC-FSD	5	80	45.7	6.5

<b>2</b>	HC-FSD	10	91	26	3.7
<b>3</b>	HC-C	5	77	45.1	6.4
<b>4</b>	HC- C	10	85.5	25.1	3.6
<b>5</b>	HC- CA	5	77	45.7	6.5
<b>6</b>	HC- CA	10	86.5	25.6	3.7
<b>7</b>	HC- PUCF	5	76.5	43.7	6.2
<b>8</b>	HC- PUCF	10	84	24	3.4
<b>9</b>	HC-PS	5	72	44.6	6.4
<b>10</b>	HC-PS	10	82	25.4	3.6
<b>11</b>	HC-SBPB	5	79.5	44.1	6.3
<b>12</b>	HC-SBPB	10	88	24.4	3.5

<sup>a</sup> Reaction conditions: 0,875 mmol SO (100 uL), autoclave, p (CO<sub>2</sub>) 3 bar, Temperature 70°C, 7 hours.

<sup>b</sup> Isolated yields are given, after purification of the reaction crude by flash column chromatography. Yield of SC was the average after two runs.

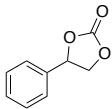
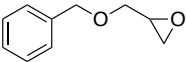
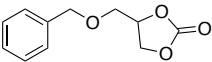
<sup>c</sup> Selectivity was >99% for all entries. It was determined by <sup>1</sup>H NMR spectroscopy using mesitylene as internal standard

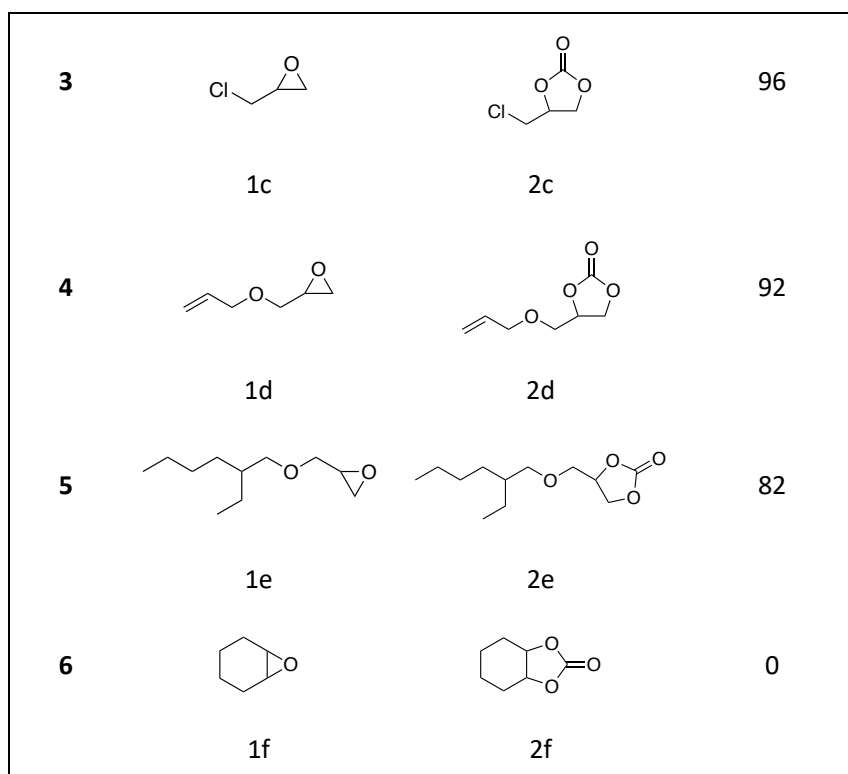
<sup>d</sup> Turnover number, defined as mol<sub>SC</sub>/mol<sub>iodide</sub>

<sup>e</sup> TOF = TON/h

HC-FSD proved to be more reactive than the other catalysts, thus it was used to explore the substrate scope under CO<sub>2</sub> pressure in the optimized reaction conditions previously described (**Table 3.5**). Generally, all the terminal epoxides tested could be transformed into the corresponding cyclic carbonates. Very good yields have been obtained for carbonation of epichlorohydrin **1c** (entry 3) and allyl glycidyl ether **1d** (entry 4). Lower but still good yields have been obtained for the reaction of benzyl glycidyl ether **1b** (entry 2) and 2-ethylhexyl glycidyl ether **1e** (entry 5). The selectivity toward the formation of the cyclic carbonate is 99% in all cases. As expected, for internal epoxides (entry 6), no conversion was obtained, due to the steric hindrance on both carbons.

**Table 3.5** Cycloaddition of CO<sub>2</sub> with different substituted epoxides to form cyclic carbonates over HC-FSD catalyst.

Entry <sup>a</sup>	Substrate	Product	Yield [%] <sup>b,c</sup>
<b>1</b>	 1a (SO)	 2 <sup>a</sup> (SC)	91
<b>2</b>	 1b	 2b	76



<sup>a</sup> Reaction conditions: 0,875 mmol Substrate (100  $\mu$ L), autoclave, p (CO<sub>2</sub>) 3 bar, Temperature 70°C, 7 hours.

<sup>b</sup> Isolated yields after purification of the reaction crude by flash column chromatography. Yields are expressed as mean of two independent replicates.

<sup>c</sup> Selectivity was >99% for all catalytic runs. It was determined by <sup>1</sup>H NMR spectroscopy using mesitylene as internal standard.

Recyclability of the catalyst HC-FSD was tested using the model reaction of SO into SC, in the conditions described above. After the reaction completion ethyl acetate was added, and catalyst was separated from the crude by centrifugation as described in experimental section. HC-FSD could be recycled over five times without appreciable loss of catalytic activity both in term of conversion and selectivity (**Figure 3.6**). Also HC-PS (slightly less reactive) and HC-CA were fully recyclable over five times.

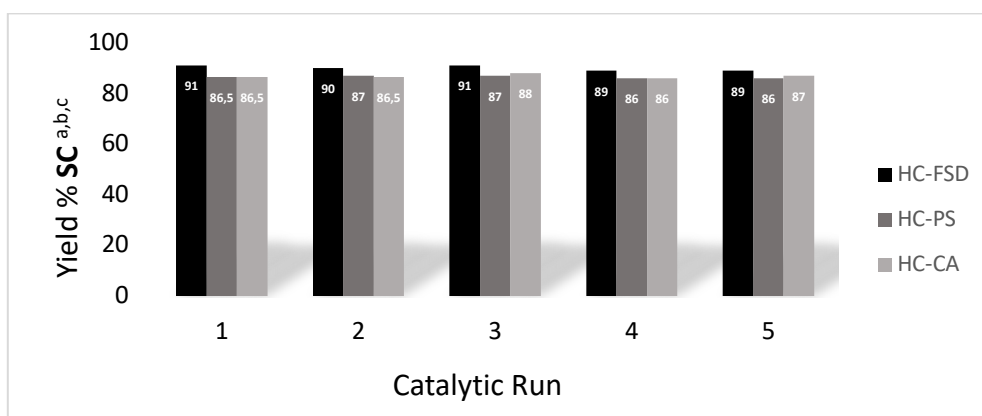


**Figure 3.6** Recycling catalytic test for the coupling of SO and CO<sub>2</sub> catalyzed by HC-FSD, HC-PS and HC-CA.

<sup>a</sup> Reaction conditions: 0,875 mmol SO (100 μL), autoclave, p (CO<sub>2</sub>) 3 bar, Temperature 70 °C, 7 h.

<sup>b</sup> Isolated yields after purification of the reaction crude by flash column chromatography. Yields are expressed as mean of two independent replicates.

<sup>c</sup> Selectivity was >99% for all catalytic runs. It was determined by <sup>1</sup>H NMR spectroscopy using mesitylene as internal standard.

The analysis carried out on the HC-FSD catalyst before use were repeated on the catalyst after its reuse for 5 cycles. In **Figure 3.7** a) are shown ATR-FTIR spectra of the HC-FSD before use and HC-FSD recycled after five recycling runs. As for the fresh fir sawdust-based catalyst, the recycled catalyst displays the same characteristic peaks, suggesting that the recycled catalyst does not suffer from degradation processes over repeated cycles of catalytic reactions and maintain the structural stability. In b) the quantitative XPS analysis on HC-FSD after five cycles are compared to the fresh HC-FSD. The chemical composition of the HC-FSD after 5 cycle sample is a little bit different from the catalyst before-use: comparing the tables, while the amount of I and N was reduced, the amount of Si appears unchanged. In **Figure 3.7** c) and d) there are the SEM images of the two catalysts where there are no obvious morphological differences.

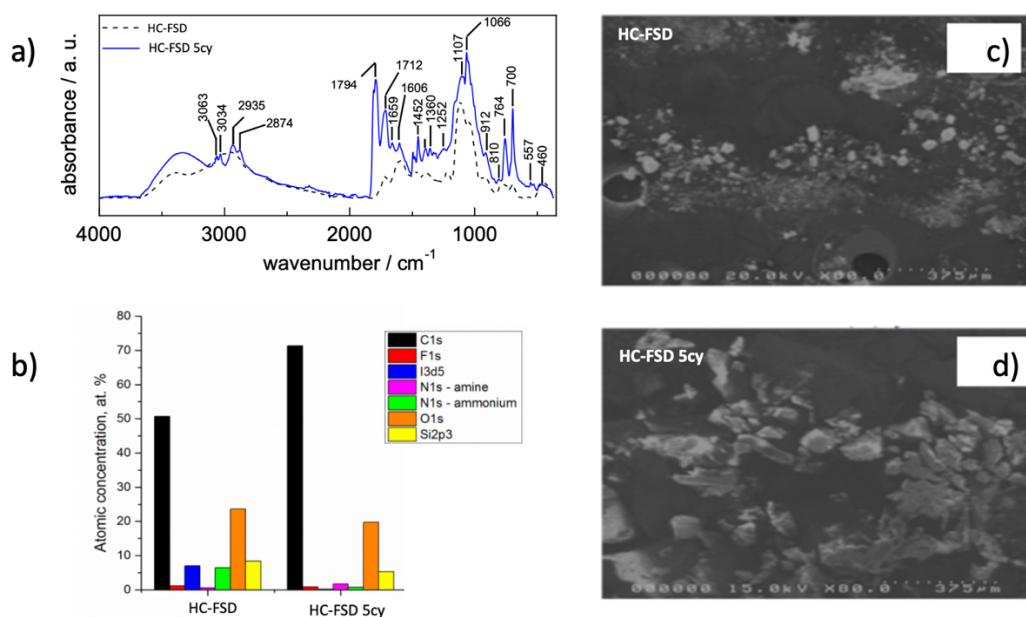


**Figure 3.7** a) ATR-FTIR spectra of the HC-FSD before use and HC-FSD recycled after five recycling runs; b) quantitative XPS analysis on HC-FSD after five cycles are compared to the fresh HC-FSD; c) SEM image of fresh HC-FSD d) SEM image of HC-FSD after 5 cycles.

### 3.2.3 Conclusions

Six different materials were subjected to the same four-steps procedure (i) pyrolysis of the starting material at 400 °C ii) oxidation with a sustainable oxidant as H<sub>2</sub>O<sub>2</sub> iii) introduction of an aminosilane group, using APTES iv) quaternarization of the amino group with methyl iodide. With this synthetic pathway six catalysts from three different polysaccharides (cellulose, cellulose acetate and starch) and three types of waste mainly made from the same polysaccharides (fir sawdust, post-use cigarette filters and starch-based plastic bags) were produced. The analysis (ATR-FTIR, XPS and SEM) made on these catalysts and their precursors demonstrate that: (i) each reaction step was successfully performed; (ii) there are no clear differences in the functional groups present on the surface of the different materials; (iii) both iodide and various types of H-bond donor functionalities are present (i.e., -NH<sub>2</sub>, -COOH, Si-OH), thus demonstrating the bi-functionality of the catalysts. All the six catalysts proved to be very reactive towards the synthesis of styrene carbonate from styrene oxide, giving a yield >82%, up to 91% obtained with fir sawdust-based catalyst (selectivity >99% in all cases). The catalysts have been recycled over five times without appreciable loss of catalytic activity. We also tested the more reactive catalyst, the sawdust-based one, on the carbonation of different terminal epoxide, obtaining yields from 76% to 96% of the cyclic carbonate.

### 3.2.4 Experimental Section

#### Materials

All chemicals were purchased from Sigma-Aldrich and used without further purification. CO<sub>2</sub> with ≥99.5% purity was purchased from Siad, Italy. Starch-based plastic bags (SBPB) were got from a local supermarket (Ravenna, Italy). Post-use cigarette filters (PU-CF) were self-obtained after smoking cigarettes. Fir Sawdust (FSD) was purchased by a woodworking company (Salati e Montepietra s.r.l., Reggio Emilia, Italy).

#### Catalysts synthesis procedure

All the catalysts reported in this work were synthesized following an optimized experimental procedure based on 4 steps as reported below. Optimization phases are described in the Appendix.

1. *Pyrolysis of polysaccharides and waste.* Starting materials were pyrolyzed following a previously reported procedure.<sup>29</sup> Hence, cellulose acetate (CA), cellulose (C), starch-based plastic bags (SBPB), post-use cigarette filters (PU-CF), fir sawdust (FSD) (5 g) or potato starch (PS) (3 g) were subjected to bench-scale pyrolysis, using an apparatus consisting of a sliding sample carrier placed in a heated quartz tube connected to ice traps and a settling chamber. The quartz tube was heated by a cylindrical co-axial furnace and purged by 1.5 L min<sup>-1</sup> N<sub>2</sub> flow. Samples were moved into the heated zone of the quartz tube and heated for 15 h at 420 °C (measured temperature) under N<sub>2</sub> flow. The resulting char was collected, ground to powder in a mortar and used for the next steps without further purification.
2. *Oxidation of chars.* In a 50 mL round bottomed flask, chars (500 mg) were stirred in H<sub>2</sub>O<sub>2</sub> (25 mL) at 85 °C for 24 h. After that time, the reaction mixture was cooled to rt and a solution of HCl 1M (5 mL) was added, then the suspension was filtered and washed several times with H<sub>2</sub>O to recover oxidized chars (OC), that were dried overnight at 70 °C under reduced pressure (100 mbar).
3. *Anchoring of amine functionality.* In a 25 mL round-bottomed flask equipped with a reflux condenser, OC (80 mg) was added to a solution of aminopropyltriethoxysilane (APTES, 4.4 v/v%) in a mixture EtOH/H<sub>2</sub>O 96:4 (5 mL). The mixture was stirred at 85 °C for 4 h, then the solution was filtered and washed three times with ethanol (EtOH) (10 mL). The resulting amine-functionalized char (AC) was dried overnight at 70 °C under reduced pressure (100 mbar).

Drying procedure for steps 2 and 3 could be avoided, with no change in activity. Here it has been performed in case of complete characterization of catalyst intermediates.

4. *Amine quaternarization.* In a sealed tube the selected AC (100 mg) was put in EtOH (1 mL) and methyl iodide (MeI, 0.11 mL, 246 mg) or longer alkyl iodides were added. The reaction was stirred at 45 °C for 15 h, then the resulting mixture was filtered and washed with EtOH (2 x 5 mL) and ethyl acetate (2 x 5 mL). The resulting ammonium iodide functionalized char (AIC) was dried overnight under reduced pressure (100 mbar).

### Representative procedure for the synthesis of cyclic carbonates

The tests with CO<sub>2</sub> at 3-5 bar were carried out in a stainless-steel, self-made, 25 mL autoclave equipped with a heating mantle. In a typical experiment, the epoxide (0.875 mmol) and the catalyst (5-10% w/w respect to the epoxide), were weighed into a 2 mL glass vial equipped with a magnetic stirring bar and closed with a PTFE septum pierced with a needle to let CO<sub>2</sub> flow inside the vial. Then the vial was placed inside the steel autoclave. The air in the reactor was firstly replaced with CO<sub>2</sub> and then the autoclave was heated and pressurized with CO<sub>2</sub>; the vial placed inside was kept stirring for the whole reaction time. After the completion of the reaction, the autoclave was cooled to RT in 30 min and slowly depressurized.

Reactions at 1 bar were conducted in a 25 mL Schlenk tube equipped with a CO<sub>2</sub> balloon. The epoxide (0.875 mmol) and the catalyst (5-10% w/w respect to the epoxide) were weighed and put inside the Schlenk tube. The air in the Schlenk tube was firstly replaced with CO<sub>2</sub>, then the Schlenk tube was placed in an oil bath heated at 70 °C. The CO<sub>2</sub> in the balloon was then allowed to flow into the flask. After reaction completion, the Schlenk tube was cooled to RT. In both cases, reaction crudes were diluted with ethyl acetate (1 mL) and the catalyst was separated from the crudes by centrifugation. The recovered catalyst was then washed twice with ethyl acetate. Crudes were weighted to check CO<sub>2</sub> incorporation or any reagent loss, and then analyzed by GC-MS after further dilution in ethyl acetate. Products have been isolated by flash column chromatography; the isolated yields are reported in Table 3.5. All obtained carbonates are known;<sup>31,32</sup> thus they were recognized by comparison with standards or through NMR and mass spectra, matching to what reported in NIST database.<sup>33</sup> Selectivity was determined by <sup>1</sup>H NMR spectroscopy using mesitylene as the internal standard. TONs have been calculated for each entry as mol of SC obtained on moles of iodide contained in the amount of HC-SD used. The moles of iodide on grams of HC-SD have been determined through XPS analysis.

### Catalysts recycling

The recycling of the catalysts was tested in the conversion of styrene oxide **1a** (0.875 mmol) into the corresponding cyclic carbonate **2a** using HC-FSD (10% w/w), using 3 bar of CO<sub>2</sub>, 70 °C, in 7 h. After the reaction completion, ethyl acetate (1 mL) was added to the crude and catalyst was separated from the crude by centrifugation. The catalyst was then washed twice with ethyl acetate. The organic phase was collected to isolate the product by flash column

chromatography, while the solid catalyst was kept under vacuum for one night to remove any traces of solvents. The recovered catalyst was weighted to check its total recovery and it was used for next runs without further purification.

### Instrumentation

GC-MS analyses of reaction mixtures were performed using an Agilent HP 6850 gas chromatograph connected to an Agilent HP 5975 quadrupole mass spectrometer. Analytes were separated on a HP-5MS fused-silica capillary column (stationary phase 5%-Phenyl)-methylpolysiloxane, 30 m, 0.25 mm i.d., 0.25  $\mu\text{m}$  film thickness), with helium as the carrier gas (at constant pressure, 36  $\text{cm s}^{-1}$  linear velocity at 200  $^{\circ}\text{C}$ ). Mass spectra were recorded under electron ionization (70 eV) at a frequency of 1 scan  $\text{s}^{-1}$  within the 12–600  $m/z$  range. The injection port temperature was 250  $^{\circ}\text{C}$ . The temperature of the column was kept at 50  $^{\circ}\text{C}$  for 5 min, then increased from 50 to 250  $^{\circ}\text{C}$  at 10  $^{\circ}\text{C min}^{-1}$  and the final temperature of 250  $^{\circ}\text{C}$  was kept for 12 min. Epichlorohydrin **1c** and allyl glycidyl ether **1d** (more volatile than the other substrates) were analyzed through the following thermal program: 40  $^{\circ}\text{C}$  for 6 min, then increased from 50 to 250  $^{\circ}\text{C}$  at 10  $^{\circ}\text{C min}^{-1}$  until the final temperature of 250  $^{\circ}\text{C}$ .  $^1\text{H}$  NMR spectra were recorded on Varian 400 (400 MHz) spectrometer.  $^{13}\text{C}$  NMR spectra were recorded on a Varian 400 (100 MHz) spectrometer. Chemical shifts are reported in ppm from TMS with the solvent resonance as the internal standard (deuteriochloroform: 7.26 ppm). The elemental composition of the starting materials, the chars at each derivatization step and the final catalysts was determined using an elemental analyzer (Thermo Scientific, Flash 2000, Organic Elemental Analyzer) through the flash combustion technique.

### Characterization of starting materials, bio-chars and catalysts

Attenuated Total Reflectance Fourier Transform (ATR-FTIR) measurements were performed with a  $\text{N}_2$  purged Bruker Vertex 70 interferometer using a single reflection Platinum-ATR accessory (diamond crystal), a DLaTGS detector and a KBr beamsplitter. The spectra were recorded from 4000  $\text{cm}^{-1}$  to 370  $\text{cm}^{-1}$  with 4  $\text{cm}^{-1}$  resolution at room temperature. The ATR-FTIR spectra correction was carried out.

The surface chemical composition of the samples was investigated by XPS. The XPS experiments were carried out by using an ESCALAB 250 Xi spectrometer, equipped with a monochromatic Al X-ray source and six channeltrons as detection system. In order to avoid any charging effect, the

measurements were performed by using a flood gun, neutralizing the charge induced by the photoelectrons emission. All samples were mounted fixing the powder on Au foil by mechanical pressure.

Scanning Electron Microscopy (SEM) analyses were performed with a SEM-FEG Hitachi S-4000 instrument. The images were collected with an acceleration voltage of 10-20 kV. Before the analysis, the samples were covered with an Au coating of a few nm by sputtering using a Q150R - Rotary Pumped Coater, except sawdust char.

#### Characterization data of 2a-2e (Spectra in Appendix 3.2)

**2a. 4-Phenyl-1,3-dioxolan-2-one**  $^1\text{H}$  NMR (400 MHz,  $\text{CDCl}_3$ )  $\delta$  7.46 -7.33 (m, 5H), 5.66 (t,  $J$  = 8.0 Hz, 1H), 4.78 (t,  $J$  = 8.4 Hz, 1H), 4.33 (dd,  $J$  = 8.5, 8.0 Hz, 1H).  $^{13}\text{C}$  NMR (100 MHz,  $\text{CDCl}_3$ )  $\delta$  154.77, 135.76, 129.71, 129.21, 125.83, 77.96, 71.1.  $m/z$  (EI): 164 [M], 119 [M-COO], 105 [M-COOO], 91 [Tropylium cation], 78 [Benzene].

**2b. 4-Phenylmethoxymethyl-1,3-dioxolan-2-one 2b**  $^1\text{H}$  NMR (400 MHz,  $\text{CDCl}_3$ )  $\delta$  7.37 – 7.24 (m, 5H), 4.879 (ddt,  $J$  = 7.9, 6.1, 3.9 Hz, 1H), 4.60 (m, 2H), 4.49 (t,  $J$  = 8.4 Hz, 1H), 4.37 (dd,  $J$  = 8.4, 6.1 Hz, 1H), 3.70 (dd,  $J$  = 10.9, 4.0 Hz, 1H), 3.61 (dd,  $J$  = 10.9, 3.8 Hz, 1H).  $^{13}\text{C}$  NMR (100 MHz,  $\text{CDCl}_3$ )  $\delta$  154.88, 137.01, 128.56, 128.08, 127.74, 74.94, 73.70, 68.79, 66.28.  $m/z$  (EI): 208 [M], 164 [M-COO], 148 [M-COOO], 107 [M- COOO-CH<sub>2</sub>-CH-CH<sub>2</sub>], 91 [Tropylium cation], 78 [Benzene].

**2c. 4-(Chloromethyl)-1,3-dioxolan-2-one**  $^1\text{H}$  NMR (400 MHz,  $\text{CDCl}_3$ )  $\delta$  4.96 (m, 1H), 4.59 (t,  $J$  = 8.6 Hz, 1H), 4.41 (dd,  $J$  = 8.9, 5.7 Hz, 1H), 3.75 (m, 2H).  $^{13}\text{C}$  NMR (100 MHz,  $\text{CDCl}_3$ )  $\delta$  154.08, 74.20, 66.95, 43.57.  $m/z$  (EI): 135 [M], 91.

**2d. 4-Allyloxymethyl-1,3-dioxolan-2-one**  $^1\text{H}$  NMR (400 MHz,  $\text{CDCl}_3$ )  $\delta$  5.87 (ddd,  $J$  = 22.8, 10.8, 5.6 Hz, 1H), 5.29 -5.20 (m, 2H), 4.8 (ddt,  $J$  = 8.1, 6.1, 3.9 Hz, 1H), 4.48 (t,  $J$  = 8.4 Hz, 1H), 4.38 (dd,  $J$  = 8.3, 6.1 Hz, 1H), 4.04 (m, 2H), 3.70-3.59 (m, 2H).  $^{13}\text{C}$  NMR (100 MHz,  $\text{CDCl}_3$ )  $\delta$  154.75, 133.60, 117.96, 74.95, 72.61, 68.81, 66.27.  $m/z$  (EI): 158 [M], 102 [M-CH<sub>2</sub>=CH-CH<sub>2</sub>-O], 117 [M- CH<sub>2</sub>=CH-CH<sub>2</sub>], 58 [CH<sub>2</sub>=CH-CH<sub>2</sub>-O].

**2e. 4-(((2-Ethylhexyl)oxy)methyl)-1,3-dioxolan-2-one**  $^1\text{H}$  NMR (400 MHz,  $\text{CDCl}_3$ )  $\delta$  4.82 -4.76 (m, 1H), 4.50 -4.37 (m, 2H), 3.62 (m, 2H), 3.39 (dd,  $J = 5.7, 1.9$  Hz, 2H), 1.55 -1.45 (m, 1H), 1.40 -1.20 (m, 8H), 0.88 (dt,  $J = 10.6, 7.0$  Hz, 6H).  $^{13}\text{C}$  NMR (100 MHz,  $\text{CDCl}_3$ )  $\delta$  154.90, 75.02, 74.85, 74.82, 69.88, 66.28, 39.56, 30.40, 30.37, 29.03, 29.02, 23.73, 22.98, 14.03, 11.03, 11.01.  
 $m/z$  (EI): 230 [M], 201 [M-CH<sub>3</sub>-CH<sub>2</sub>], 118 [M- CH<sub>3</sub>(x2)-CH<sub>2</sub>(x5)-CH], 102 [CH<sub>2</sub>-CH-CH<sub>2</sub>-COOO], 57 [CH<sub>3</sub>-CH<sub>2</sub>x3].

## BIBLIOGRAPHY

- (1) Pescarmona, P. P. Cyclic Carbonates Synthesised from CO<sub>2</sub>: Applications, Challenges and Recent Research Trends. *Curr. Opin. Green Sustain. Chem.* **2021**, *29*, 100457. <https://doi.org/10.1016/j.cogsc.2021.100457>.
- (2) Saptal, V. B.; Bhanage, B. M. Current Advances in Heterogeneous Catalysts for the Synthesis of Cyclic Carbonates from Carbon Dioxide. *Curr. Opin. Green Sustain. Chem.* **2017**, *3*, 1–10. <https://doi.org/10.1016/j.cogsc.2016.10.006>.
- (3) Calabrese, C.; Giacalone, F.; Aprile, C. Hybrid Catalysts for CO<sub>2</sub> Conversion into Cyclic Carbonates. *Catalysts* **2019**, *9* (4), 325. <https://doi.org/10.3390/catal9040325>.
- (4) Liang, S.; Liu, H.; Jiang, T.; Song, J.; Yang, G.; Han, B. Highly Efficient Synthesis of Cyclic Carbonates from CO<sub>2</sub> and Epoxides over Cellulose/KI. *Chem. Commun.* **2011**, *47* (7), 2131–2133. <https://doi.org/10.1039/C0CC04829A>.
- (5) Wu, Z.; Xie, H.; Yu, X.; Liu, E. Lignin-Based Green Catalyst for the Chemical Fixation of Carbon Dioxide with Epoxides To Form Cyclic Carbonates under Solvent-Free Conditions. *ChemCatChem* **2013**, *5* (6), 1328–1333. <https://doi.org/10.1002/cctc.201200894>.
- (6) Díaz Velázquez, H.; Guzmán Pantoja, J.; Meneses Ruiz, E.; García de León, R.; Martínez Palou, R. Efficient Synthesis of Organic Carbonates to the Multigram Level from CO<sub>2</sub> Using a New Chitin-Supported Catalyst. *Catal. Lett.* **2017**, *147* (9), 2260–2268. <https://doi.org/10.1007/s10562-017-2123-4>.
- (7) Chen, W.; Zhong, L.; Peng, X.; Sun, R.; Lu, F. Chemical Fixation of Carbon Dioxide Using a Green and Efficient Catalytic System Based on Sugarcane Bagasse—An Agricultural Waste. *ACS Sustain. Chem. Eng.* **2015**, *3* (1), 147–152. <https://doi.org/10.1021/sc5006445>.
- (8) Roshan, K. R.; Mathai, G.; Kim, J.; Tharun, J.; Park, G.-A.; Park, D.-W. A Biopolymer Mediated Efficient Synthesis of Cyclic Carbonates from Epoxides and Carbon Dioxide. *Green Chem.* **2012**, *14* (10), 2933–2940. <https://doi.org/10.1039/C2GC35942A>.
- (9) Wu, X.; Wang, M.; Xie, Y.; Chen, C.; Li, K.; Yuan, M.; Zhao, X.; Hou, Z. Carboxymethyl Cellulose Supported Ionic Liquid as a Heterogeneous Catalyst for the Cycloaddition of CO<sub>2</sub> to Cyclic Carbonate. *Appl. Catal. Gen.* **2016**, *519*, 146–154. <https://doi.org/10.1016/j.apcata.2016.04.002>.
- (10) Xiong, X.; Zhang, H.; Lai, S. L.; Gao, J.; Gao, L. Lignin Modified by Deep Eutectic Solvents as Green, Reusable, and Bio-Based Catalysts for Efficient Chemical Fixation of CO<sub>2</sub>. *React. Funct. Polym.* **2020**, *149*, 104502. <https://doi.org/10.1016/j.reactfunctpolym.2020.104502>.
- (11) Sun, J.; Wang, J.; Cheng, W.; Zhang, J.; Li, X.; Zhang, S.; She, Y. Chitosan Functionalized Ionic Liquid as a Recyclable Biopolymer-Supported Catalyst for Cycloaddition of CO<sub>2</sub>. *Green Chem.* **2012**, *14* (3), 654–660. <https://doi.org/10.1039/C2GC16335G>.
- (12) Lai, S.; Gao, J.; Zhang, H.; Cheng, L.; Xiong, X. Luffa Sponge Supported Dendritic Imidazolium ILs with High-Density Active Sites as Highly Efficient and Environmentally Friendly Catalysts for CO<sub>2</sub> Chemical Fixation. *J. CO<sub>2</sub> Util.* **2020**, *38*, 148–157. <https://doi.org/10.1016/j.jcou.2020.01.004>.
- (13) Jing-Xian, C.; Bi, J.; Wei-Li, D.; Sen-Lin, D.; Liu-Ren, C.; Zong-Jie, C.; Sheng-Lian, L.; Xu-Biao, L.; Xin-Man, T.; Chak-Tong, A. Catalytic Fixation of CO<sub>2</sub> to Cyclic Carbonates over Biopolymer Chitosan-Grafted Quarternary Phosphonium Ionic Liquid as a Recyclable Catalyst. *Appl. Catal. Gen.* **2014**, *484*, 26–32. <https://doi.org/10.1016/j.apcata.2014.07.008>.
- (14) Zhao, Y.; Tian, J.-S.; Qi, X.-H.; Han, Z.-N.; Zhuang, Y.-Y.; He, L.-N. Quaternary Ammonium Salt-Functionalized Chitosan: An Easily Recyclable Catalyst for Efficient Synthesis of Cyclic Carbonates from Epoxides and Carbon Dioxide. *J. Mol. Catal. Chem.* **2007**, *271* (1), 284–289. <https://doi.org/10.1016/j.molcata.2007.03.047>.
- (15) Tharun, J.; Hwang, Y.; Roshan, R.; Ahn, S.; Kathalikkattil, A. C.; Park, D.-W. A Novel Approach of Utilizing Quaternized Chitosan as a Catalyst for the Eco-Friendly Cycloaddition of Epoxides with CO<sub>2</sub>. *Catal. Sci. Technol.* **2012**, *2* (8), 1674–1680. <https://doi.org/10.1039/C2CY20137B>.
- (16) Roshan, K. R.; Jose, T.; Kathalikkattil, A. C.; Kim, D. W.; Kim, B.; Park, D. W. Microwave Synthesized Quaternized Celluloses for Cyclic Carbonate Synthesis from Carbon Dioxide and Epoxides. *Appl. Catal. Gen.* **2013**, *467*, 17–25. <https://doi.org/10.1016/j.apcata.2013.07.007>.
- (17) Kohrt, C.; Werner, T. Recyclable Bifunctional Polystyrene and Silica Gel-Supported Organocatalyst for the Coupling of CO<sub>2</sub> with Epoxides. *ChemSusChem* **2015**, *8* (12), 2031–2034. <https://doi.org/10.1002/cssc.201500128>.
- (18) Alassmy, Y. A.; Asgar Pour, Z.; Pescarmona, P. P. Efficient and Easily Reusable Metal-Free Heterogeneous Catalyst Beads for the Conversion of CO<sub>2</sub> into Cyclic Carbonates in the Presence of Water as Hydrogen-Bond Donor. *ACS Sustain. Chem. Eng.* **2020**, *8* (21), 7993–8003.

<https://doi.org/10.1021/acssuschemeng.0c02265>.

- (19) Czajczyńska, D.; Anguilano, L.; Ghazal, H.; Krzyżyńska, R.; Reynolds, A. J.; Spencer, N.; Jouhara, H. Potential of Pyrolysis Processes in the Waste Management Sector. *Therm. Sci. Eng. Prog.* **2017**, *3*, 171–197. <https://doi.org/10.1016/j.tsep.2017.06.003>.
- (20) Ma, L.; Wang, T.; Liu, Q.; Zhang, X.; Ma, W.; Zhang, Q. A Review of Thermal–Chemical Conversion of Lignocellulosic Biomass in China. *Biotechnol. Adv.* **2012**, *30* (4), 859–873. <https://doi.org/10.1016/j.biotechadv.2012.01.016>.
- (21) Zhou, C.-H.; Xia, X.; Lin, C.-X.; Tong, D.-S.; Beltramini, J. Catalytic Conversion of Lignocellulosic Biomass to Fine Chemicals and Fuels. *Chem. Soc. Rev.* **2011**, *40* (11), 5588–5617. <https://doi.org/10.1039/C1CS15124J>.
- (22) Cao, X.; Sun, S.; Sun, R. Application of Biochar-Based Catalysts in Biomass Upgrading: A Review. *RSC Adv.* **2017**, *7* (77), 48793–48805. <https://doi.org/10.1039/C7RA09307A>.
- (23) Yang, X.; Wan, Y.; Zheng, Y.; He, F.; Yu, Z.; Huang, J.; Wang, H.; Ok, Y. S.; Jiang, Y.; Gao, B. Surface Functional Groups of Carbon-Based Adsorbents and Their Roles in the Removal of Heavy Metals from Aqueous Solutions: A Critical Review. *Chem. Eng. J.* **2019**, *366*, 608–621. <https://doi.org/10.1016/j.cej.2019.02.119>.
- (24) Kołtowski, M.; Charmas, B.; Skubiszewska-Zięba, J.; Oleszczuk, P. Effect of Biochar Activation by Different Methods on Toxicity of Soil Contaminated by Industrial Activity. *Ecotoxicol. Environ. Saf.* **2017**, *136*, 119–125. <https://doi.org/10.1016/j.ecoenv.2016.10.033>.
- (25) Toda, M.; Takagaki, A.; Okamura, M.; Kondo, J. N.; Hayashi, S.; Domen, K.; Hara, M. Biodiesel Made with Sugar Catalyst. *Nature* **2005**, *438* (7065), 178–178. <https://doi.org/10.1038/438178a>.
- (26) Samorì, C.; Parodi, A.; Tagliavini, E.; Galletti, P. Recycling of Post-Use Starch-Based Plastic Bags through Pyrolysis to Produce Sulfonated Catalysts and Chemicals. *J. Anal. Appl. Pyrolysis* **2021**, *155*, 105030. <https://doi.org/10.1016/j.jaap.2021.105030>.
- (27) Vidal, J. L.; Andrea, V. P.; MacQuarrie, S. L.; Kerton, F. M. Oxidized Biochar as a Simple, Renewable Catalyst for the Production of Cyclic Carbonates from Carbon Dioxide and Epoxides. *ChemCatChem* **2019**, *11* (16), 4089–4095. <https://doi.org/10.1002/cctc.201900290>.
- (28) Samorì, C.; Torri, C.; Fabbri, D.; Falini, G.; Faraloni, C.; Galletti, P.; Spera, S.; Tagliavini, E.; Torzillo, G. Unusual Catalysts from Molasses: Synthesis, Properties and Application in Obtaining Biofuels from Algae. *ChemSusChem* **2012**, *5* (8), 1501–1512. <https://doi.org/10.1002/cssc.201100822>.
- (29) Samorì, C.; Parodi, A.; Tagliavini, E.; Galletti, P. Recycling of Post-Use Starch-Based Plastic Bags through Pyrolysis to Produce Sulfonated Catalysts and Chemicals. *J. Anal. Appl. Pyrolysis* **2021**, *155* (October 2020), 105030. <https://doi.org/10.1016/j.jaap.2021.105030>.
- (30) Pinheiro, A. F. de M.; Nijmeijer, A.; Sripathi, V. G. P.; Winnubst, L. Chemical Modification/Grafting of Mesoporous Alumina with Polydimethylsiloxane (PDMS). *Eur. J. Chem.* **2015**, *6* (3), 287–295. <https://doi.org/10.5155/eurjchem.6.3.287-295.1258>.
- (31) Zhang, Z.; Fan, F.; Xing, H.; Yang, Q.; Bao, Z.; Ren, Q. Efficient Synthesis of Cyclic Carbonates from Atmospheric CO<sub>2</sub> Using a Positive Charge Delocalized Ionic Liquid Catalyst. *ACS Sustain. Chem. Eng.* **2017**, *5* (4), 2841–2846. <https://doi.org/10.1021/acssuschemeng.7b00513>.
- (32) Lai, S.; Gao, J.; Xiong, X. Rosin-Based Porous Heterogeneous Catalyst Functionalized with Hydroxyl Groups and Triazole Groups for CO<sub>2</sub> Chemical Conversion under Atmospheric Pressure Condition. *React. Funct. Polym.* **2021**, *165*, 104976. <https://doi.org/10.1016/j.reactfunctpolym.2021.104976>.
- (33) Informatics, N. O. of D. and. *NIST Chemistry WebBook*. <https://webbook.nist.gov/chemistry/> (accessed 2022-05-11). <https://doi.org/10.18434/T4D303>.

## APPENDIX 3.2

### Contents

**A3.1** Elemental analysis of the functionalized char over different reaction conditions (Table 1) and their application in the synthesis of SC (Table 2).

**A3.2** Elemental analysis of the char functionalized with butyl iodide (Bul) and octyl iodide (OctI) over different conditions (Table 1) and their application in the synthesis of SC (Table 2).

**A3.3** Bands assignments for cellulose-based char after each reaction steps.

**A3.4** The ATR-FTIR spectra of the starting materials: (a) cellulose; (b) cellulose acetate; (c) fir sawdust; (d) potato starch; (e) starch-based plastic bag; (f) cigarette filter and band assignment.

**A3.5** The ATR-FTIR spectra of two different batch of HC-C and of two different batch of HC-CA showing the same peak positions.

**A3.6**  $^1\text{H}$  and  $^{13}\text{C}$  NMR spectra of isolated PRODUCT 2a (Table 3.5, entry 1).

**A3.7**  $^1\text{H}$  and  $^{13}\text{C}$  NMR spectra of isolated PRODUCT 2b (Table 3.5, entry 2).

**A3.8**  $^1\text{H}$  and  $^{13}\text{C}$  NMR spectra of isolated PRODUCT 2c (Table 3.5, entry 3).

**A3.9**  $^1\text{H}$  and  $^{13}\text{C}$  NMR spectra of isolated PRODUCT 2d (Table 3.5, entry 4).

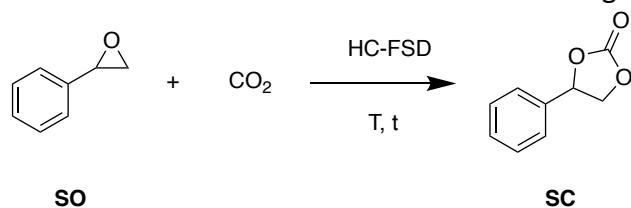
**A3.10**  $^1\text{H}$  and  $^{13}\text{C}$  NMR spectra of isolated PRODUCT 2e (Table 3.5, entry 5).

### A3.1 Elemental analysis of the functionalized char over different reaction conditions and their application in the synthesis of SC.

Table 1. Elemental composition of the functionalized chars in different reaction conditions derived from cellulose and sawdust for each optimized reaction step (mean  $\pm$  standard deviation of three independent replicates).

Label	Conditions	N	C	H
A	1) HNO <sub>3</sub> , 80°C, 2days; 2)WET, APTES, EtOH, 80°C reflux, 24H; 3) MeI, EtOH 40°C, 16H	5.9 $\pm$ 0.1	34.7 $\pm$ 0.3	4.4 $\pm$ 0.2
B	1) H <sub>2</sub> SO <sub>4</sub> , KMnO <sub>4</sub> , reflux, 5h; 2) WET, APTES, EtOH, 80°C reflux, 24H; 3) MeI, EtOH 40°C, 16H	0.4 $\pm$ 0.1	63.5 $\pm$ 0.4	2.6 $\pm$ 0.1
C	1) HNO <sub>3</sub> /H <sub>2</sub> SO <sub>4</sub> (1:3), 80°C, 6H; 2) WET, APTES, EtOH, 80°C reflux, 24H; 3) MeI, EtOH 40°C, 16H	4.3 $\pm$ 0.2	51.8 $\pm$ 0.5	3.8 $\pm$ 0.2
D	1)Starch Char (550 °C), H <sub>2</sub> O <sub>2</sub> 24h 2) APTES, EtOH:H <sub>2</sub> O (95/5), 80°C 3) MeI, EtOH 40°C, 16H	0.6 $\pm$ 0.2	81.8 $\pm$ 0.6	1.4 $\pm$ 0.1
E	1) Starch Char (420 °C), H <sub>2</sub> O <sub>2</sub> 24h 2) APTES, EtOH (no H <sub>2</sub> O), 80°C; 3) MeI, EtOH 40°C, 16H	3.1 $\pm$ 0.1	36.0 $\pm$ 0.4	4.7 $\pm$ 0.1
F	1) Starch Char (420 °C), H <sub>2</sub> O <sub>2</sub> 24h 2) APTES, EtOH:H <sub>2</sub> O (90/10), 80°C ; 3) MeI, EtOH 40°C, 16H	5.6 $\pm$ 0.1	31.9 $\pm$ 0.6	4.3 $\pm$ 0.2

Table 2. Results for carbonation reaction using catalyst produced over different conditions



Entry	Catalyst	Cyclic Carbonate [%] <sup>b,c</sup>
1 <sup>a</sup>	A	86
2	B	0
3	C	71
4	D	0
5	E	21
6	F	14

<sup>a</sup> Reaction conditions: 0.875 mmol SO (100  $\mu$ L), autoclave.

<sup>b</sup> Isolated yields after purification of the reaction crude by flash column chromatography. Yields are expressed as mean of two independent replicates

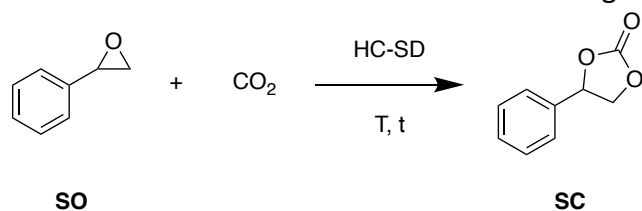
<sup>c</sup> Selectivity was >99% for all entries. It was determined by <sup>1</sup>H NMR spectroscopy using mesitylene as internal standard.

### A3.2 Elemental analysis of the char functionalized with Bul and OctI over different conditions (Table 1) and their application in the synthesis of SC (Table 2).

Table 1. Elemental composition of the functionalized chars in derived from cellulose and sawdust, functionalized with Bul and OctI at different conditions (mean  $\pm$  standard deviation of three independent replicates).

Label	Conditions	N	C	H
G	Bul, EtOH 40°C, 16H	6.3 $\pm$ 0.2	39.6 $\pm$ 0.3	5.2 $\pm$ 0.2
H	OctI, EtOH 40°C, 16H	6.3 $\pm$ 0.1	40.3 $\pm$ 0.2	5.3 $\pm$ 0.2
I	Bul, 80°C, 16H	5.2 $\pm$ 0.1	33.0 $\pm$ 0.4	4.5 $\pm$ 0.1
J	OctI, 80°C, 16H	5.4 $\pm$ 0.2	36.3 $\pm$ 0.3	4.9 $\pm$ 0.2
K	Bul, 120°C, 16H	4.7 $\pm$ 0.1	34.2 $\pm$ 0.2	4.7 $\pm$ 0.1
L	OctI, 120°C, 16H	4.9 $\pm$ 0.1	41.2 $\pm$ 0.5	5.4 $\pm$ 0.2

Table 2. Results for carbonation reaction using Bul and OctI functionalized catalysts.



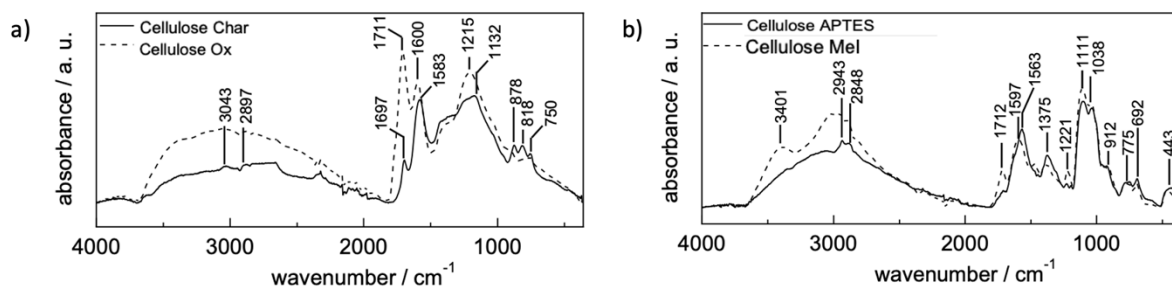
Entry <sup>a</sup>	Catalyst	Cyclic Carbonate [%] <sup>b,c</sup>
1	G	26
2	H	15
3	I	65
4	J	61
5	K	79
6	L	84

<sup>a</sup> Reaction conditions: 0.875 mmol SO (100  $\mu$ L), autoclave.

<sup>b</sup> Isolated yields after purification of the reaction crude by flash column chromatography. Yields are expressed as mean of two independent replicates

<sup>c</sup> Selectivity was >99% for all entries. It was determined by <sup>1</sup>H NMR spectroscopy using mesitylene as internal standard.

### A3.3 Bands assignments for cellulose-based char after each reaction steps.



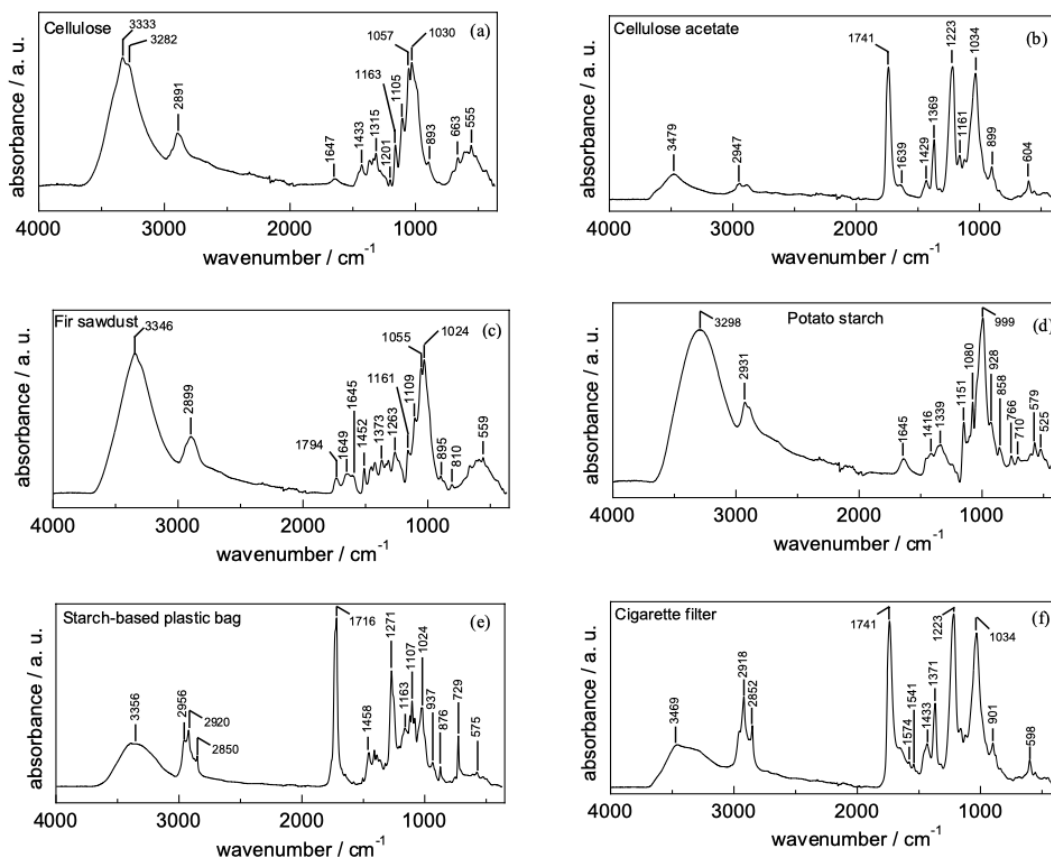
a) The spectra show similar peaks and small changes in the wavenumbers. The broad absorption band with weak peaks observable at 3043 cm<sup>-1</sup> and 2897 cm<sup>-1</sup> mainly for the char are attributed to the stretching of C-H aromatic and aliphatic, respectively, while no stretching of -OH (phenolic or aliphatic) near 3300 cm<sup>-1</sup> is detected in both spectra. The peaks at 1697 cm<sup>-1</sup>/1710 cm<sup>-1</sup> can be assigned to the conjugate C=O and those at 1583 cm<sup>-1</sup>/1600 cm<sup>-1</sup> to the (C-H)<sub>ar</sub> polyaromatic systems, benzene rings and to the asymmetric COO<sup>-</sup> stretch (1600 cm<sup>-1</sup>) for the cellulose Ox. The band between 1450 and 1320 cm<sup>-1</sup> can be related to the bending of C-H aliphatic and to the symmetric deformation -CH<sub>2</sub>- (bending). The peaks at 1215 and 1132 cm<sup>-1</sup> can be attributed to the C=O stretching and to the -CO and -CC stretch, and -COH and -CCH bend. The peaks between 878 and 750 cm<sup>-1</sup> can be related to the aromatic-carbon-carbon (HCC) rocking vibrations. The peak at 750 cm<sup>-1</sup> can be also related to the benzene ring and condensed ring system.

b) The peak at 3401 cm<sup>-1</sup>, well observable in the spectrum of cellulose Mel is attributed to the stretching vibration of Si-OH silanol group and to the N-H bending vibration. The peak at 2943 cm<sup>-1</sup> can be attributed to the stretching of C-H aromatic and aliphatic and that at 2848 cm<sup>-1</sup> can be related to the RCH<sub>2</sub>- symmetric stretching. For the APTES- and Mel-based samples no stretching of -OH (phenolic or aliphatic) near 3300 cm<sup>-1</sup> is detected.

The peaks at 1712 cm<sup>-1</sup> can be assigned to the conjugate C=O, while those at 1597 cm<sup>-1</sup>/1563 cm<sup>-1</sup> to the (C-H)<sub>ar</sub> polyaromatic systems, benzene rings and to the asymmetric COO<sup>-</sup> stretch. It is worth noting that the peaks at 1597 cm<sup>-1</sup> and 1563 cm<sup>-1</sup> can also be attributed to the NH<sub>2</sub> scissor vibrations indicating the presence of the NH<sub>2</sub> terminal group of APTES.

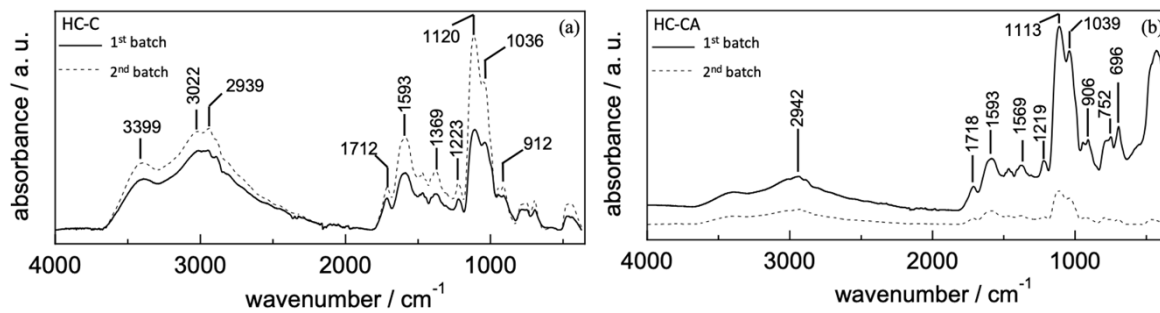
The weak peaks at 1221 cm<sup>-1</sup> can be attributed to the C=O stretching. The spectra show some peaks that can be related to the absorption bands of the siloxane groups (Si-O-Si), specifically those at around 1111 cm<sup>-1</sup> and 1038 cm<sup>-1</sup> can be related to the stretching vibration, while that at 775 cm<sup>-1</sup> to the bending vibration of the siloxane groups. The peak at 912 cm<sup>-1</sup> can be attributed to the aromatic-carbon-carbon (HCC) rocking vibrations.

**A3.4** The ATR-FTIR spectra of the starting materials: (a) cellulose; (b) cellulose acetate; (c) fir sawdust; (d) potato starch; (e) starch-based plastic bag; (f) cigarette filter and band assignment.

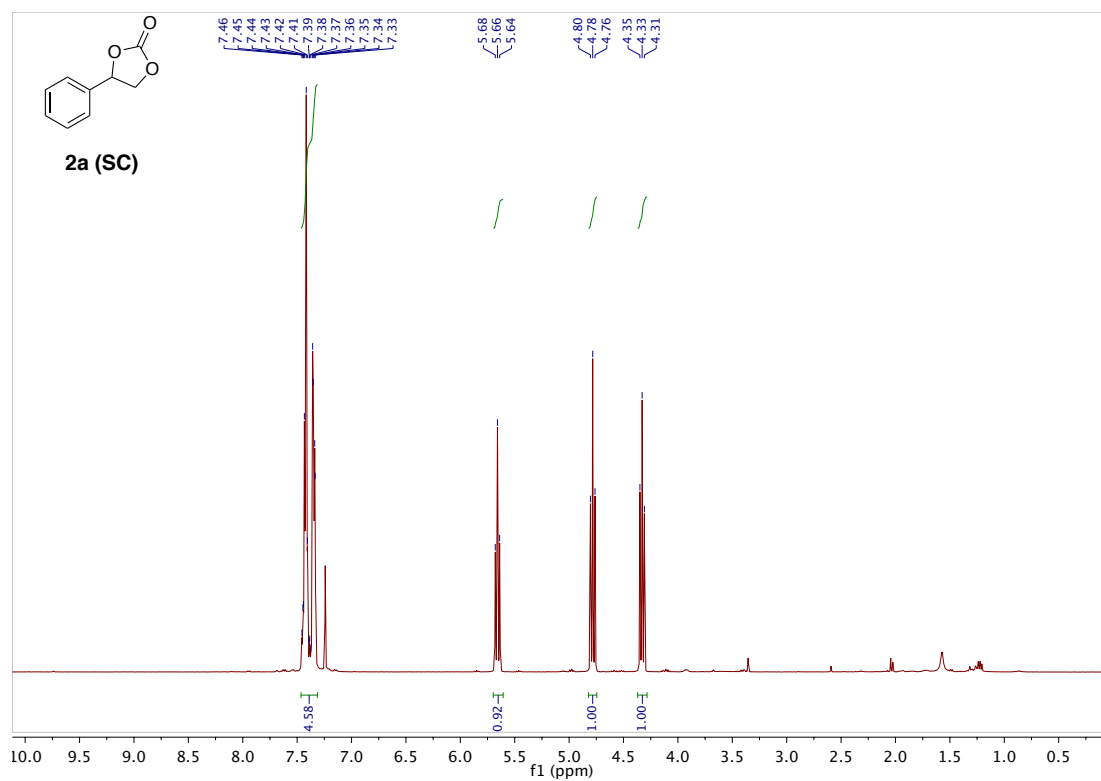


Band position (cm <sup>-1</sup> )	Assignment	Attributed to
3300 – 3200	Hydroxyl (-OH) groups, mainly of phenolic OH or alkyl hydroxyls, intramolecular H-bonding	Lignin (sawdust), cellulose, cellulose acetate, starch
2917, 2852	-CH stretching modes	Cigarette filter
1400 – 1700	Common lignin bands	Sawdust
1716	C=O group in the structure of bioplastic polymers	PBAT (polybutylene adipate terephthalate) present in the polymer (starch-based plastic bag)
1741	C=O stretching modes	Cellulose acetate, cigarette filter
1452	C=C and C-H bond and O-H in plane deformation	Lignin
1433, 1429	CH <sub>2</sub> bending	Cellulose, cellulose acetate, cigarette filter
1271	Starch in the polymer	Starch-based plastic bag
1263	G-ring plus C=O stretch	Sawdust
1223, 1034	C-O single bond stretching modes	Cellulose acetate, cigarette filter
1105, 1109, 1107	C-C and C-O stretch	Cellulose, sawdust, starch-based plastic bag
890 – 1400	Side groups C-OH and C-O-C glycosidic bond vibrations	Specific polysaccharide bands
1373, 1369	Symmetric C-H deformation vibration (bending)	Sawdust, cellulose acetate
1315	CH <sub>2</sub> wagging	Cellulose
1163, 1161, 1151	C-O-C symmetric stretching	Cellulose, cellulose acetate, sawdust, starch
1105, 1109	Ring asymmetric valence vibration	Cellulose, sawdust
1024	C-O stretch	Cellulose, sawdust, starch-based plastic bag
893, 899, 895, 901	Aromatic C-H out of plane deformation	Cellulose, cellulose acetate, sawdust, cigarette filter

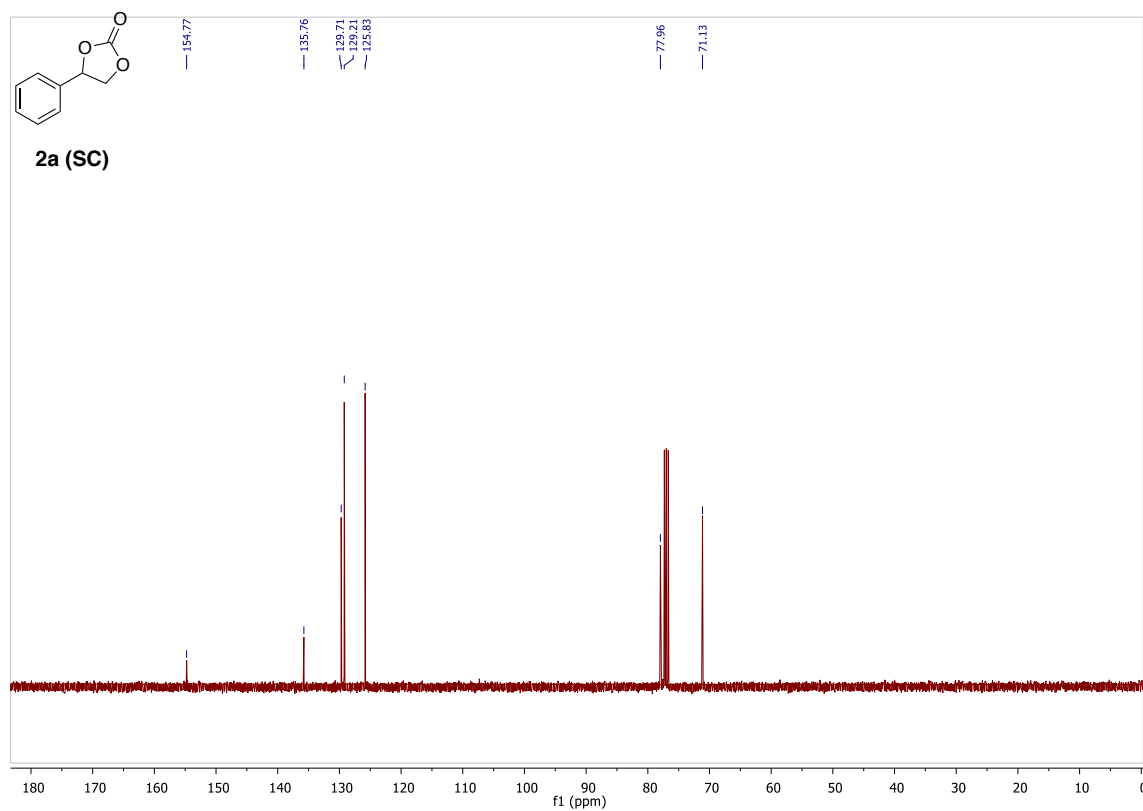
**A3.5** The ATR-FTIR spectra of two different batch of HC-C and of two different batch of HC-CA showing the same peak positions.



A3.6  $^1\text{H}$  and  $^{13}\text{C}$  NMR spectra of isolated **PRODUCT 2a** (Table 3.5, entry 1).

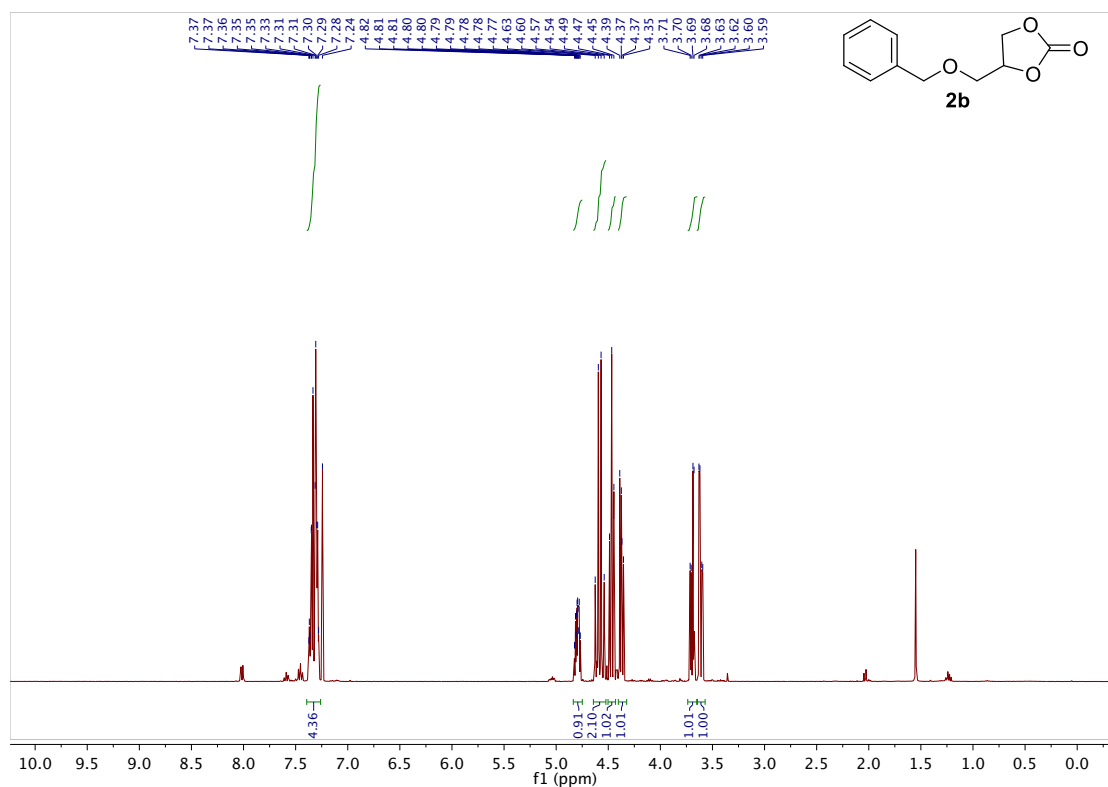


**2a.**  $^1\text{H}$  NMR (400 MHz,  $\text{CDCl}_3$ )  $\delta$  7.46–7.33 (m, 5H), 5.66 (t,  $J$  = 8.0 Hz, 1H), 4.78 (t,  $J$  = 8.4 Hz, 1H), 4.33 (dd,  $J$  = 8.5, 8.0 Hz, 1H).

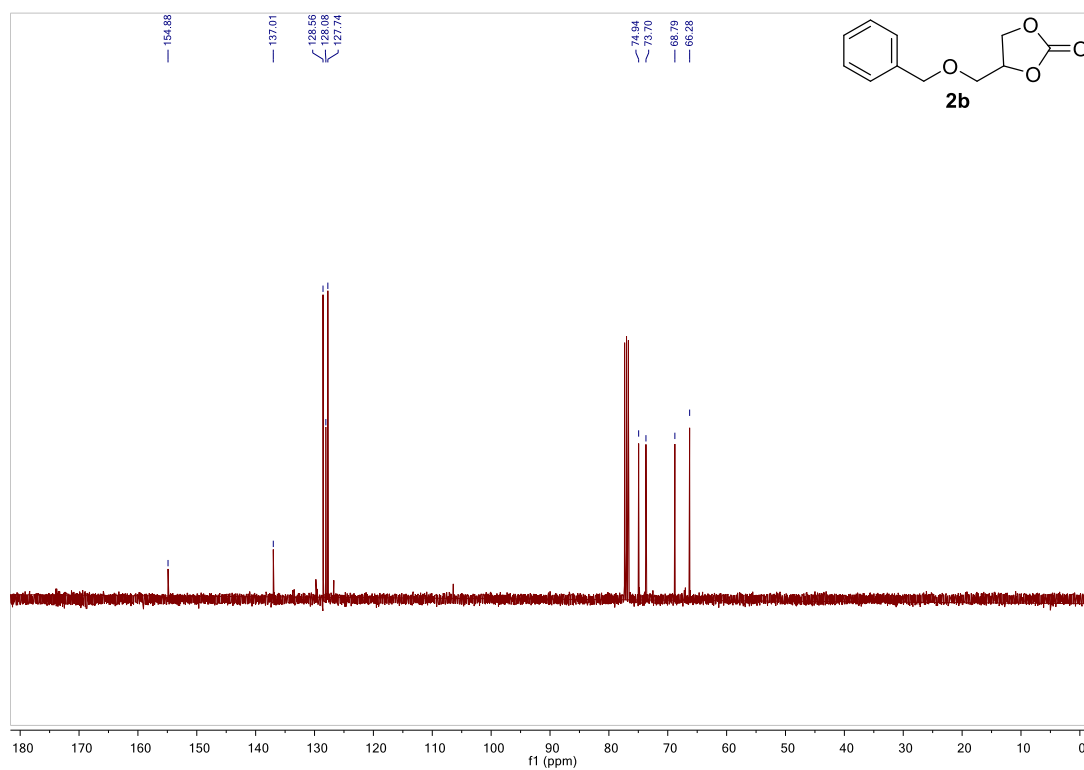


**2a.**  $^{13}\text{C}$  NMR (100 MHz,  $\text{CDCl}_3$ )  $\delta$  154.77, 135.76, 129.71, 129.21, 125.83, 77.96, 71.1

A3.7  $^1\text{H}$  and  $^{13}\text{C}$  NMR spectra of isolated **PRODUCT 2b** (Table 3.5, entry 2).

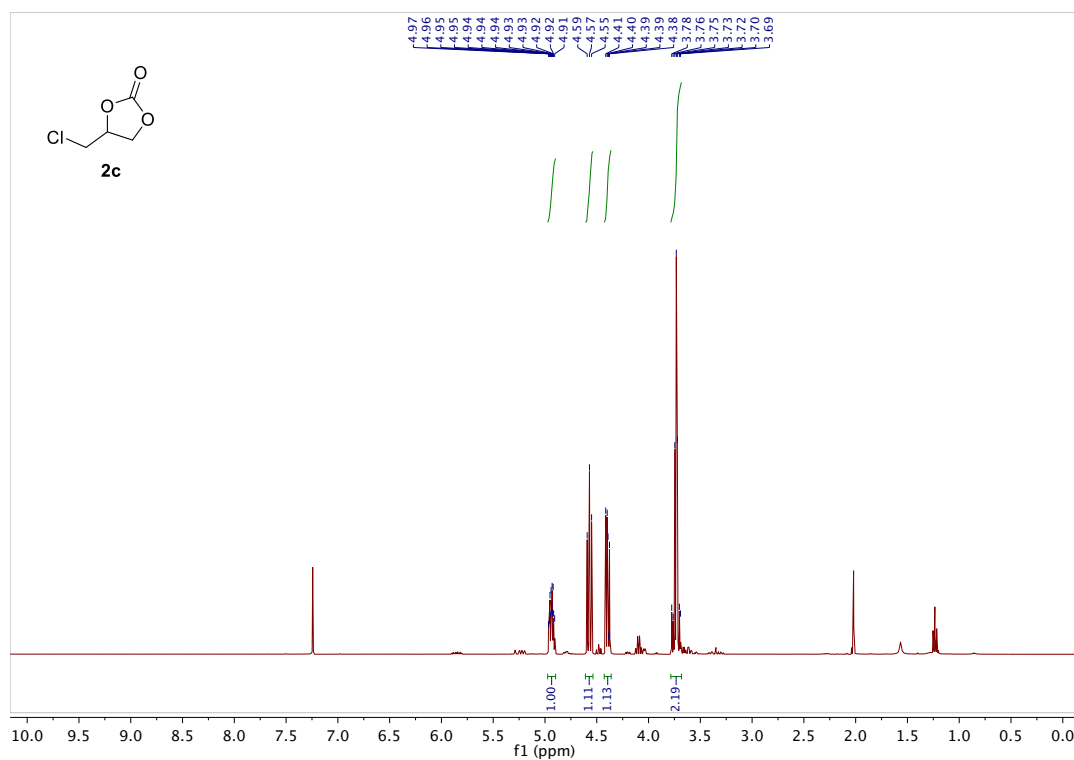


**2b.**  $^1\text{H}$  NMR (400 MHz,  $\text{CDCl}_3$ )  $\delta$  7.37 – 7.24 (m, 5H), 4.879 (ddt,  $J = 7.9, 6.1, 3.9$  Hz, 1H), 4.60 (m, 2H), 4.49 (t,  $J = 8.4$  Hz, 1H), 4.37 (dd,  $J = 8.4, 6.1$  Hz, 1H), 3.70 (dd,  $J = 10.9, 4.0$  Hz, 1H), 3.61 (dd,  $J = 10.9, 3.8$  Hz, 1H).

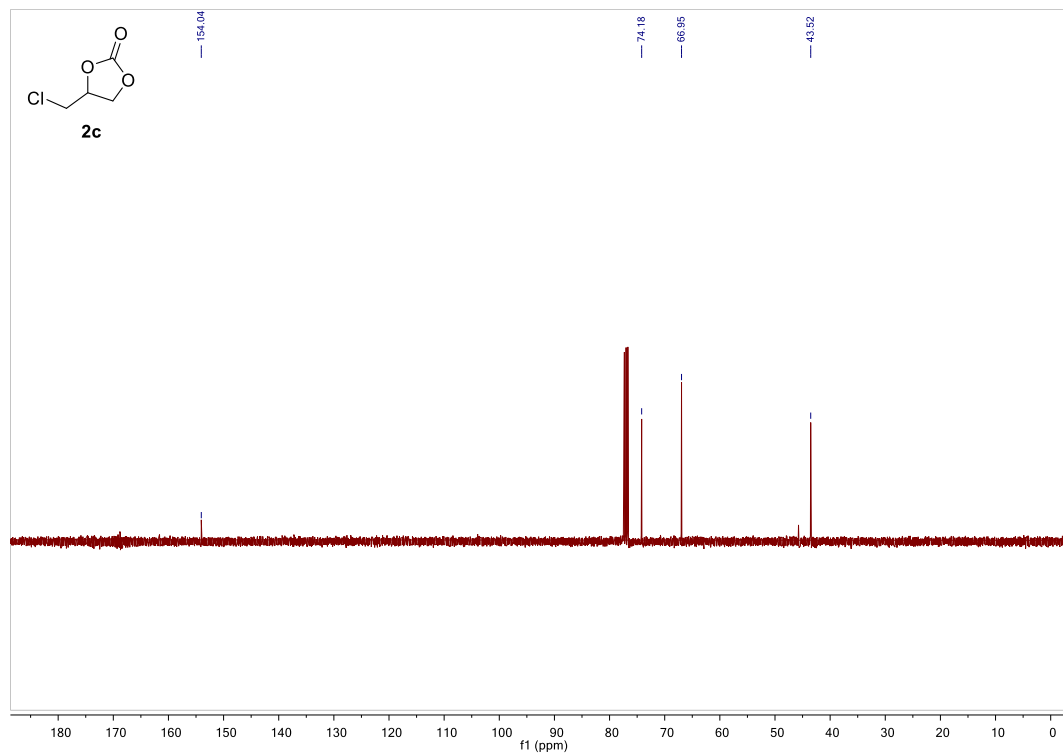


**2b.**  $^{13}\text{C}$  NMR (100 MHz,  $\text{CDCl}_3$ )  $\delta$  154.88, 137.01, 128.56, 128.08, 127.74, 74.94, 73.70, 68.79, 66.28.

A3.8  $^1\text{H}$  and  $^{13}\text{C}$  NMR spectra of isolated PRODUCT 2c (Table 3.5, entry 3).

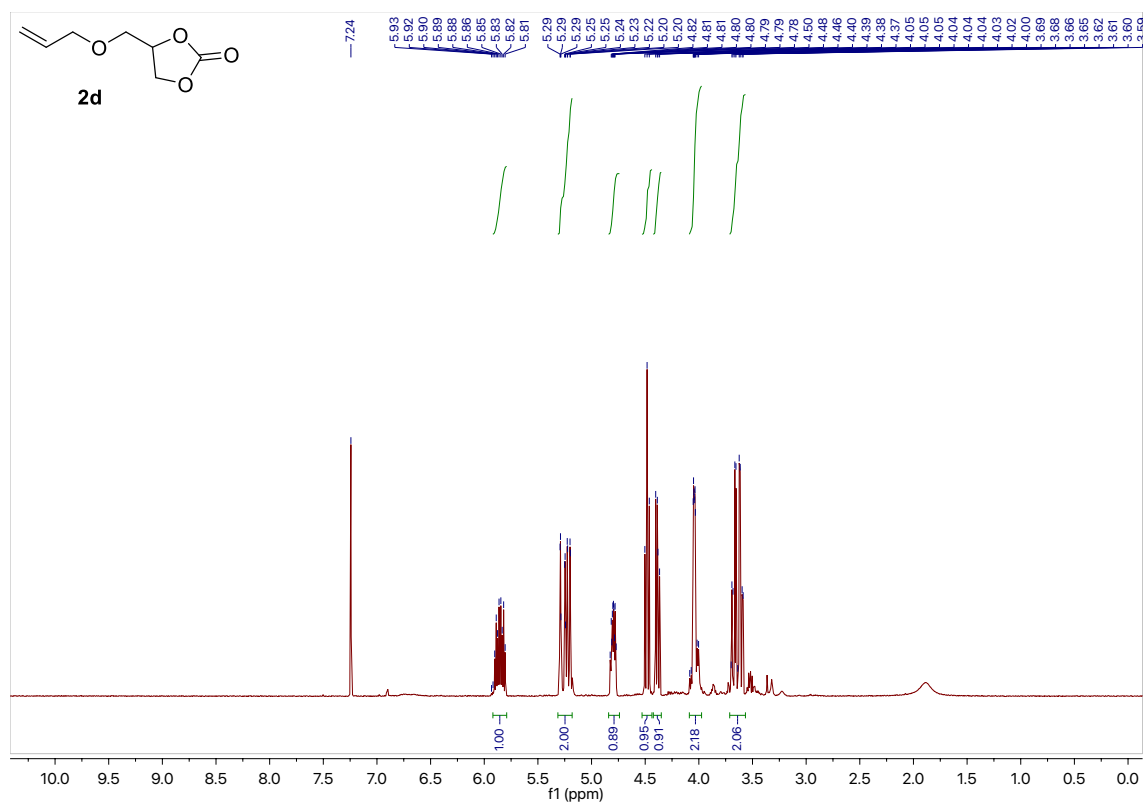


**2c.**  $^1\text{H}$  NMR (400 MHz,  $\text{CDCl}_3$ )  $\delta$  4.94 (m, 1H), 4.57 (t,  $J = 8.6$  Hz, 1H), 4.40 (dd,  $J = 8.9, 5.7$  Hz, 1H), 3.74 (m, 2H).

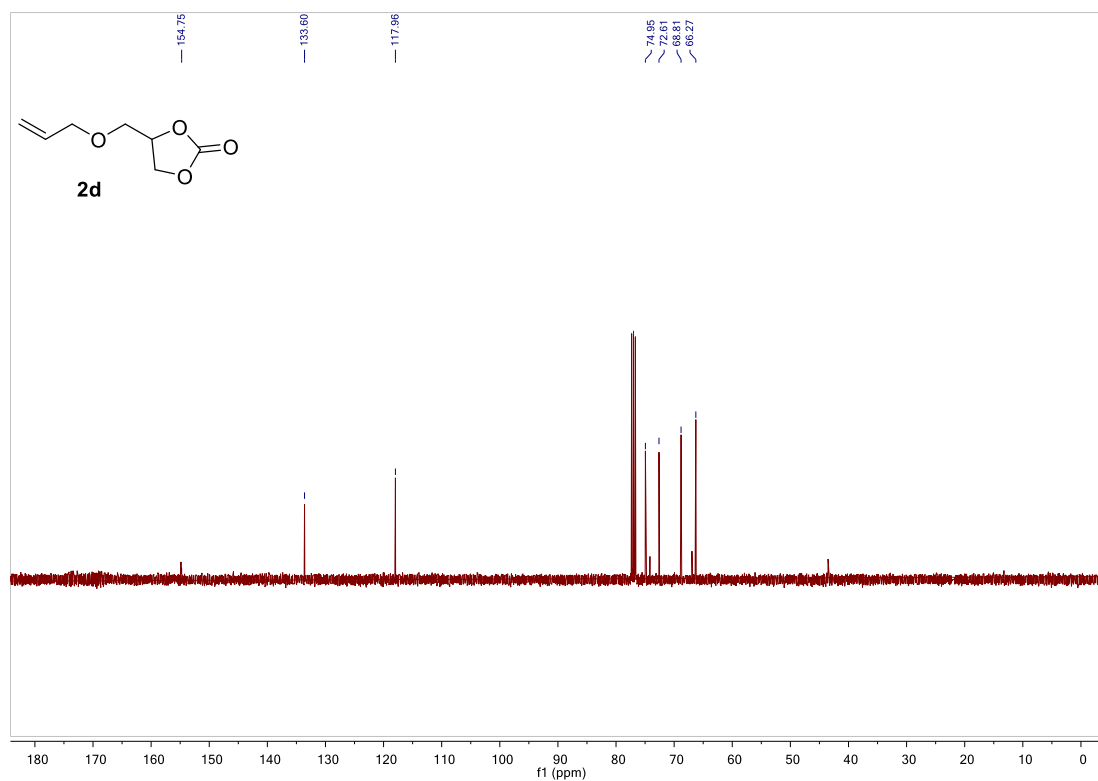


**2c.**  $^{13}\text{C}$  NMR (100 MHz,  $\text{CDCl}_3$ )  $\delta$  154.04, 74.18, 66.95, 43.52.

A3.9  $^1\text{H}$  and  $^{13}\text{C}$  NMR spectra of isolated **PRODUCT 2d** (Table 3.5, entry 4).

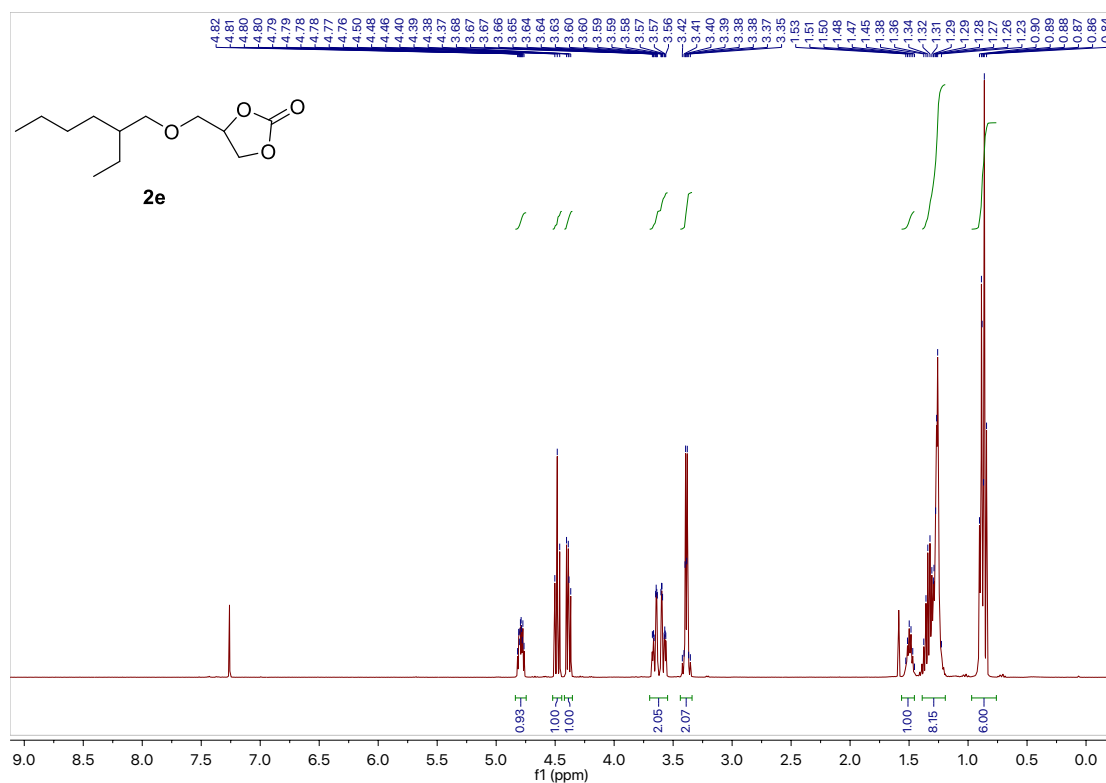


**2d.**  $^1\text{H}$  NMR (400 MHz,  $\text{CDCl}_3$ )  $\delta$  5.87 (ddd,  $J = 22.8, 10.8, 5.6$  Hz, 1H), 5.29-5.20 (m, 2H), 4.8 (ddt,  $J = 8.1, 6.1, 3.9$  Hz, 1H), 4.48 (t,  $J = 8.4$  Hz, 1H), 4.38 (dd,  $J = 8.3, 6.1$  Hz, 1H), 4.04 (m, 2H), 3.70-3.59 (m, 2H).

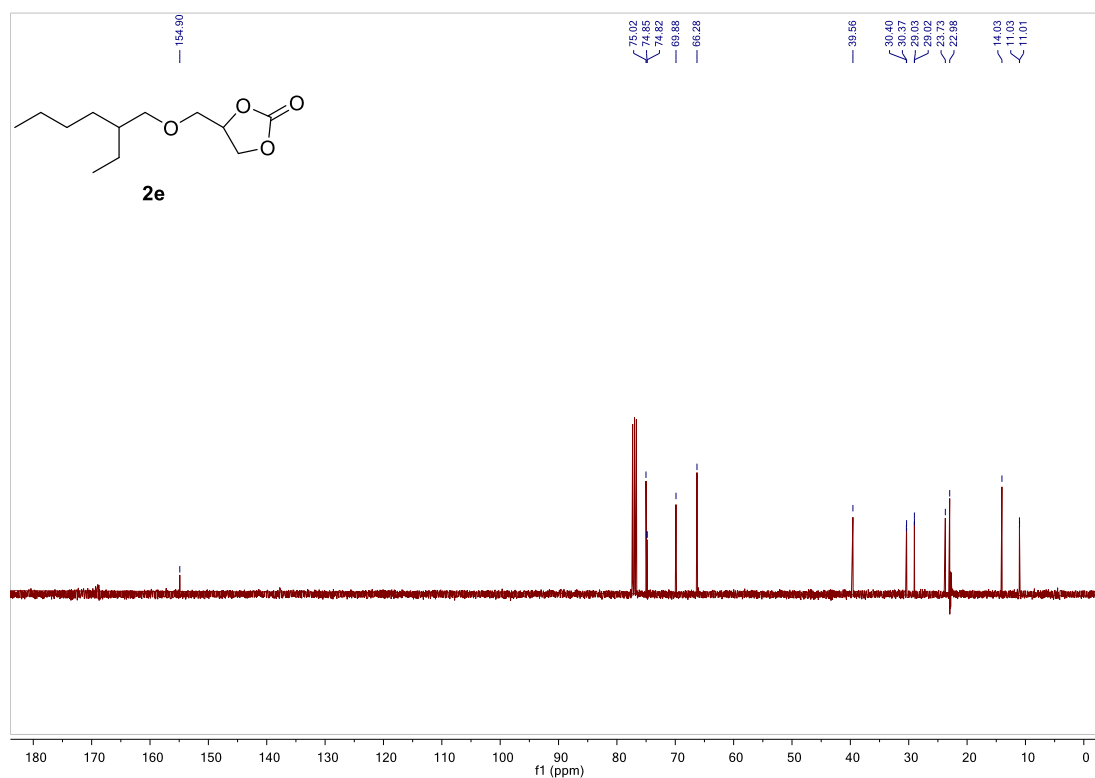


**2d.**  $^{13}\text{C}$  NMR (100 MHz,  $\text{CDCl}_3$ )  $\delta$  154.75, 133.60, 117.96, 74.95, 72.61, 68.81, 66.27.

A3.10  $^1\text{H}$  and  $^{13}\text{C}$  NMR spectra of isolated **PRODUCT 2e** (Table 3.5, entry 5).



**2e.**  $^1\text{H}$  NMR (400 MHz,  $\text{CDCl}_3$ )  $\delta$  4.82–4.76 (m, 1H), 4.50–4.37 (m, 2H), 3.62 (m, 2H), 3.39 (dd,  $J = 5.7, 1.9$  Hz, 2H), 1.55–1.45 (m, 1H), 1.40–1.20 (m, 8H), 0.88 (dt,  $J = 10.6, 7.0$  Hz, 6H).



**2e.**  $^{13}\text{C}$  NMR (100 MHz,  $\text{CDCl}_3$ )  $\delta$  154.90, 75.02, 74.85, 74.82, 69.88, 66.28, 39.56, 30.40, 30.37, 29.03, 29.02, 23.73, 22.98, 14.03, 11.03, 11.01.

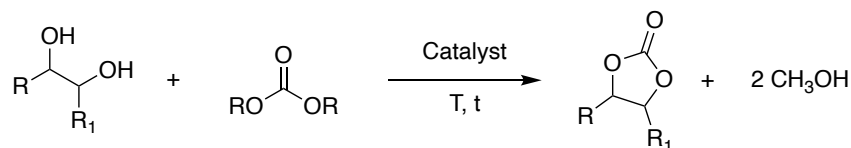
## CHAPTER 4

# SYNTHESIS OF CYCLIC CARBONATES FROM DIOLS AND DIMETHYL CARBONATE

### 4.1 HOMOGENEOUS CATALYSTS: DBU AS SWITCHABLE POLARITY CATALYST

#### 4.1.1 Introduction

The trans carbonation of a diol with a linear carbonate, also called Carbonate Interchange Reaction (CIR), **Scheme 4.1**, is an interesting, and currently much studied alternative, for the synthesis of cyclic carbonates (CCs). In fact, starting from 1,2-diols it is possible to obtain five-membered CCs, while starting from 1,3-diols are instead obtained six-membered CCs, used in the ring-opening polymerization (ROP).<sup>1,2</sup>



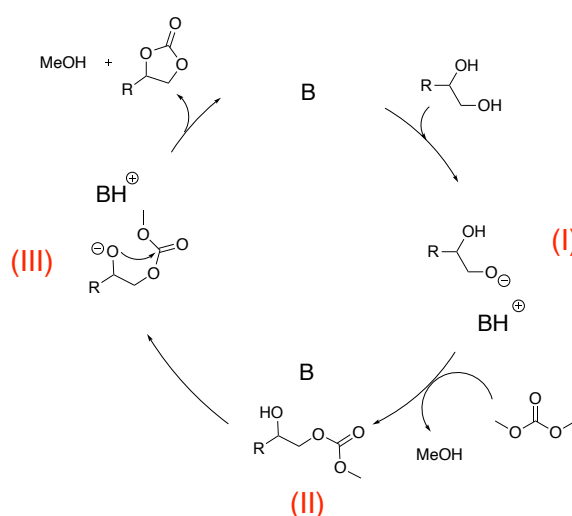
**Scheme 4.1** Trans carbonation of 1,2 diols from linear carbonates.

Although the synthesis of five-membered cyclic carbonates starting from epoxides is an advantageous method from many points of view (AE 100%, simplicity of very active catalysts, use of CO<sub>2</sub>, etc.), there are problems concerning the high instability and toxicity of different epoxides (i.e. ethylene oxide, propylene oxide, glycidol), that unfortunately are used to produce the most important CCs for the solvents market (i.e. ethylene carbonate, EC, propylene carbonate, PC, and glycerol carbonate, GC).<sup>3,4</sup> For this reason, the use of diols and dialkyl carbonates can represent a valid alternative to the use of epoxides. The diols do not present toxicity issues; some of them, such as glycerol (GLY), are waste products of the industrial supply chain, and dimethyl carbonate (DMC) is considered a green solvent, both for its properties and synthesis (see Chapter 1, section 1.7.2.1).<sup>5-7</sup>

The reaction involves the exchange of the carbonyl group between a carbonate and a diol, in the presence of a basic catalyst. Although the reaction temperatures used are lower for the

transcarbonation of ethylene carbonate (EC) with GLY (35-80 °C vs. 75-120 °C for the reaction with DMC), DMC could be preferentially selected by industries because the purification step of the GC is less energy consuming. Indeed, the boiling temperatures of DMC (90 °C) and methanol (65 °C) are much lower than those of EC (261 °C) and ethylene glycol EG (197 °C). In addition, reactions with DMC are usually carried out at atmospheric pressure while, for reactions from EC, a reduced pressure (35 mmHg) is often applied to remove EG and displace reaction equilibrium.<sup>8,9</sup>

As for the catalysts, alkaline compounds perform much better than acid ones. This behavior can be explained by the study of reaction mechanism, which in literature has been described in the synthesis of GC from GLY and DMC, but that can be generally extended to all the reactions with 1,2-diols (**Scheme 4.2**).<sup>6,7</sup> In presence of a base (B), the diol is initially deprotonated at the most reactive primary hydroxyl group (I). This nucleophilic anion attacks the carbonyl carbon of a DMC molecule leading to the formation of methanol (MeOH) and a methyl carbonate intermediate (II) which undergoes a cyclization reaction: an intramolecular nucleophilic substitution occurs, yielding GC and MeOH, and restoring the catalyst (III). Being the cyclization step (III) the rate-determining step of the overall process, basic catalysts activate the ring-closing reaction, through the deprotonation of the second hydroxyl group, while acid systems are less effective for the same process, not performing the deprotonation. It is also demonstrated that under comparable reaction conditions strong acids, like p-toluenesulfonic acid, gave limited yield, while with basic catalysts, particularly CaO and CaCO<sub>3</sub>, faster reactions with high yields could be carried out.<sup>6</sup>



**Scheme 4.2** Reaction mechanism for the synthesis of 5-member cyclic carbonates from diols and DMC.

In this context, the synthesis of GC from GLY is the most studied reaction and the one on which most catalysts have been tested; the methodology was scarcely extended to other functionalized 1,2-diols.<sup>10,11</sup> Since the CIR is an equilibrium, an excess of DMC, respect to the starting (generally 5-3 / 1), shifts the equilibrium to the products. The reaction can also favor the formation of the products by removing the MeOH, that is by-produced: MeOH forms an azeotropic mixture with the DMC with a boiling point of ca. 64 °C, containing 85 mol% MeOH and 15 mol% DMC. Nevertheless, under distillation conditions, DMC is continuously removed together with MeOH and for this reason is required in large excess. To selectively remove MeOH from the reaction mixture, several patents and papers have been reported.<sup>12</sup>

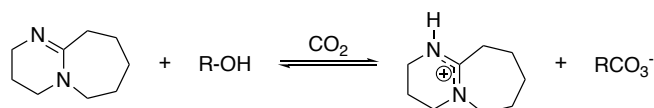
For the CIR of 1,2-diols and DMC, Sang-Hyun Pyo *et al.* published a catalyst-free protocol: higher temperature (110 °C) respect to the 90 °C usually present in literature, and a large excess of DMC (17 eq., compared to the usual 3-5) are required, and furthermore the MeOH produced must be removed by using 4Å molecular sieves.<sup>1</sup> Also Selva *et al.* tested both batch and continuous-flow, catalyst-free conditions, using in autoclave a range temperature of 120-220 °C.<sup>13</sup>

Various homogeneous inorganic bases, like KOH, NaOH and K<sub>2</sub>CO<sub>3</sub>, have been successfully tested in CIR, however, they led to some problems concerning the separation of catalysts: generally, a lot of water must be employed for washing the dissolved catalysts off the DMC and products. And in some cases water cannot be used because diols and carbonates are miscible.<sup>6</sup>

Typical organocatalysts described for the CIR with DMC include amines, amidines, guanidines, N-heterocyclic carbenes, phosphazenes, enzymes, organic salts and ionic liquids. In this context, in depth studies of continuous-flow conditions have been reported in literature.<sup>2,14-19</sup>

Among the organocatalysts used, one of the most reactive towards CIR proved to be 1,8-Diazabicyclo[5.4.0]undec-7-ene (DBU).<sup>15,20-23</sup> Munshi *et al.* used 0.1 mol% DBU for the synthesis of GC, obtaining best results (98% conversion of GLY with 96% selectivity to GC in 7.5 h, TON: 9408) with a molar ratio DMC:GLY 1:3, at 100 °C for 0.5 hours.<sup>20</sup> De Souza *et al.* described a continuous-flow process involving 1.5 mol% of DBU, 3 equiv. of DMC: GC was obtained with 80% conversion and 82% selectivity within 8 min at 120 °C.<sup>15</sup>

Interestingly, DBU, as other amines, is part of the so called “switchable polarity solvents”, from an idea of Jessop and co-workers. These bases can pass from a less-polar to a more-polar form when reacting with CO<sub>2</sub> in presence of water or alcohols (**Scheme 4.3**).

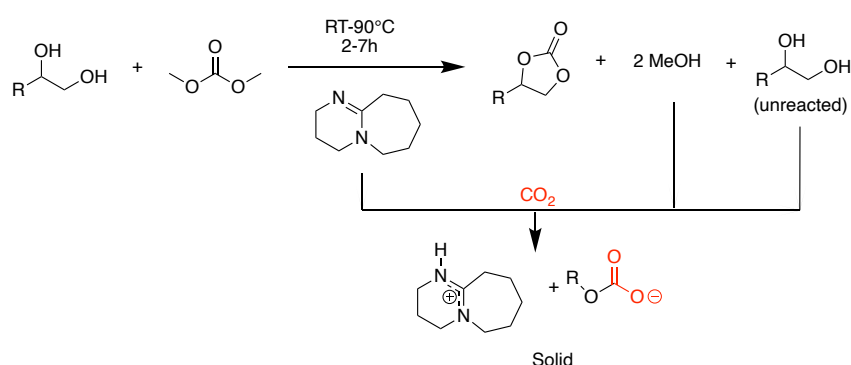


**Scheme 4.3** Polarity switch of DBU with CO<sub>2</sub> and alcohols.

Among the various applications, this concept was used in extraction processes, for the solubilization of cellulose and also for the recovery of organocatalysts in various synthesis.<sup>24–</sup>

34

In the present work DBU was used to catalyze the carbonation reactions of various diols with DMC. The final aim is to recover the catalyst, making it insoluble in the reaction mixture (where it acts as a homogeneous catalyst) by bubbling CO<sub>2</sub> into the reaction vial at the end of the reaction. In this way it is possible to recover the product, solubilized in DMC, and the solid catalyst, in its ionic form. Having MeOH as a byproduct of the CIR, the salt formed with the DBU and CO<sub>2</sub> could be formed both with MeOH and the unreacted diol, but also with adventitious water present in the non-anhydrous environment.<sup>35</sup> DBU can be subsequently brought back to its initial liquid form by heating the solidified catalyst at 60 °C for 2 hours, under vacuum, to release the CO<sub>2</sub> and the MeOH (**Scheme 4.4**).



**Scheme 4.4** Reaction scheme and catalyst recovery through CO<sub>2</sub> bubbling.

This concept has been used from *Cao et al.* in the synthesis of biodiesel: starting from triglycerides DBU can be used as base to catalyze the transesterification with MeOH to obtain

biodiesel (mainly composed of Fatty Acids Methyl Esters, or FAME). The catalyst can be then recovered through its reaction with MeOH and CO<sub>2</sub>, also favoring an easy separation of FAMES.<sup>23</sup> The step forward is the synthesis of GC from GLY, derived from biodiesel production, catalyzing it with DBU, then recovered with the CO<sub>2</sub>-assisted switchable polarity technique.<sup>22</sup> This procedure (catalysis with DBU and recovery through CO<sub>2</sub> addition) has also been applied in the synthesis of unsymmetrical linear carbonates.<sup>21</sup>

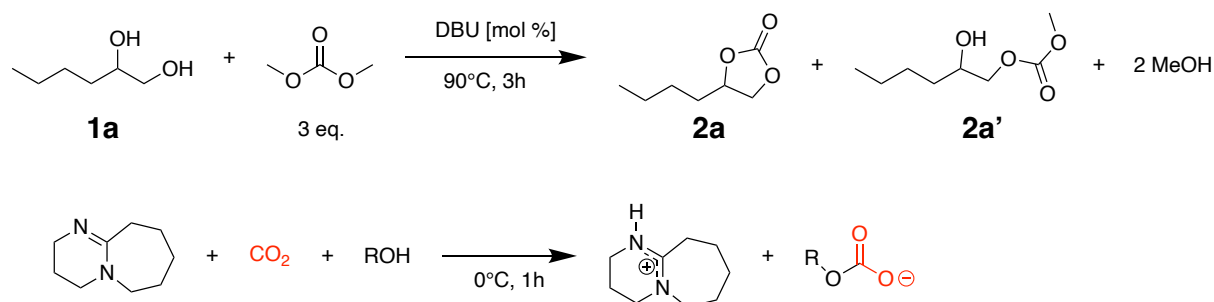
Nevertheless, a broad substrate scope in the DBU-catalyzed CIR for the synthesis of CCs, with a consequent recovery of DBU through CO<sub>2</sub> addition, has never been reported. Moreover, the gap the present work wants to fill, regards a study about a precise correlation between reaction conditions and catalyst recovery capacity.

#### 4.1.2 Results and discussions

The reaction of CIR starting from 1,2 hexanediol (**1a**) and DMC catalyzed by DBU was studied (**Table 4.1**) as model reaction (see experimental part). Different reaction conditions were tested (amount of DBU, temperature, reaction time, etc.). These reaction parameters had to be studied not only in terms of product yield but also looking at catalyst recovery at the end of the reaction; in fact it was deeply influenced by some of these variables, such as temperature, amount and reaction time.

##### DBU amount

As first reaction parameter, the amount of DBU was tested, and the main results are resumed in **Table 4.1**. The ratio **1a**/DMC was fixed at 1/3, which is the most common proportion found in literature. Also, the temperature was fixed at 90°C, that is the reflux temperature for DMC. The reactions were carried out in screw-capped tubes under autogenous pressure (see experimental part).

**Table 4.1** Test on DBU amount in the CIR of **1a** into **2a**.

Entry	DBU [mol %]	Conversion [%] <sup>c</sup>	Selectivity [%] <sup>c</sup>	DBU recovery [%] <sup>d</sup>
<b>1<sup>a</sup></b>	50	84	91	36
<b>2<sup>a</sup></b>	25	86	95	62
<b>3</b>	10	94	95	76
<b>4<sup>a,b</sup></b>	10	93	93	75
<b>5</b>	-	0	-	-

Reaction conditions: 2 mmol **1a** (249.2  $\mu\text{L}$ ), 3 eq. DMC (505.3  $\mu\text{L}$ ), 90°C, 3h, closed vial.

<sup>a</sup> Tested with a **1a**/DMC ratio of 1/5.

<sup>b</sup> Anhydrous DBU used

<sup>c</sup> Conversions and selectivity calculated by GC-MS (see experimental section).

<sup>d</sup> Calculated after re-dissolution of the salt.

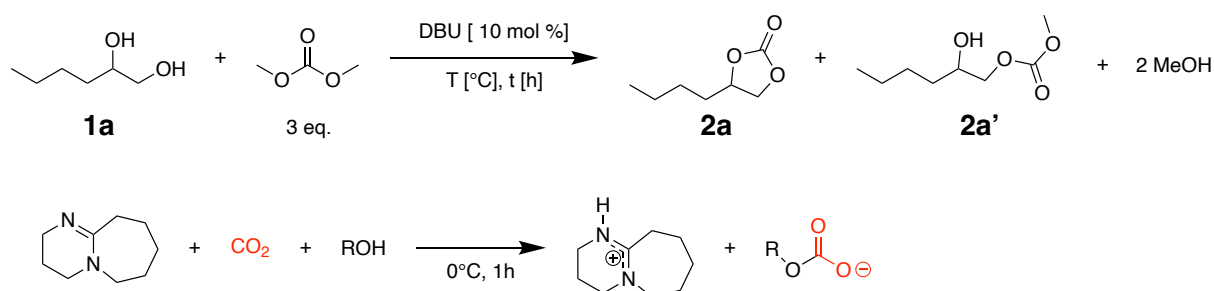
The highest amount of DBU tested was 50% (**Table 4.1**, entry 1): very good conversion and selectivity were obtained, but very poor DBU recovery. By decreasing the amount of DBU to 25% (**Table 4.1**, entry 2) and subsequently to 10% (**Table 4.1**, entry 3 and 4) an improvement is observed, both in terms of conversion and selectivity, but above all as DBU recovery. In fact, the recovery procedure took place by forming a solid salt of the DBU with the  $\text{CO}_2$ , bubbling the gas through a needle into the vial, at the end of the reaction. High amounts of DBU in the reaction system led to the instant formation of a solid when  $\text{CO}_2$  is blown. However, this also led to a greater viscosity of the system, which hinders the dispersion of the gas. A comparison was also made between the use of anhydrous and non-anhydrous DBU, not finding substantial differences (**Table 4.1**, entry 3 and 4). Although from literature lower quantities of DBU have been reported for the catalysis of these reactions, working on a very small scale (a 100% recovery of DBU would correspond to 30 mg), we did not use quantities lower than 10 mol%, rather aiming at a quantitative recovery of the catalyst.

### Temperature

As second reaction parameter, conversion on **1a** into **2a** was tested at different temperatures and the main results were resumed in Table 4.2. Also in this case the ratio **1a**/DMC was fixed at 1/3 and 10%

mol of DBU was used, as result of previous tests (see Table 4.1). Various reaction times have been varied as a function of a probable kinetics, for which slower reactions are expected at lower temperatures.

**Table 4.2** Tests on different temperatures in the CIR of **1a** into **2a**.



Entry	T [°C]	T [h]	Conversion [%] <sup>a</sup>	Selectivity [%] <sup>a</sup>	DBU recovery [%] <sup>b</sup>
<b>1</b>	90	3	94	95	76
<b>2</b>	50	3	75	93	-
<b>3</b>	50	7	91	95	96
<b>4</b>	rt	3	31	90	-
<b>5</b>	rt	7	54	92	-
<b>6</b>	rt	22	80	95	96

Reaction conditions: 2 mmol **1a** (249.2  $\mu\text{L}$ ), 3 eq. DMC (505.2  $\mu\text{L}$ ), 10% mol DBU (29.8  $\mu\text{L}$ ), closed vial.

<sup>a</sup> Conversions and selectivity calculated by GC-MS (see experimental section).

<sup>b</sup> Calculated after re-dissolution of the salt.

As already demonstrated, 90 °C is an ideal temperature to run CIR (**Table 4.2**, entry 1, see Appendix A4.1).

With the aim of using more sustainable conditions, CIR was tested at lower temperatures, observing that the reaction at 50 °C gave excellent conversions and selectivity (91% and 95% respectively) at longer reaction times (**Table 4.2**, entries 2 and 3). For the reaction at room temperature (rt), on the other hand, 22 h are necessary to obtain good conversions (**Table 4.2**, entries 4, 5 and 6). However, the most interesting aspect in the temperature study concerns with DBU recovery. In fact, it had already been observed that DBU, when heated for a prolonged time, underwent yellowing. The DBU, yellowed at 90 °C, formed the salt with CO<sub>2</sub> much slower and with much lower yields, compared to the DBU used at room temperature or with mild heating, such as at 50 °C. This behavior was due to DBU easy hydrolysis at higher temperature.<sup>36</sup> These observations were not made only in the context of the CIR study, but

also in blank tests, in which both DBU kept at rt and DBU heated at 90 °C were analyzed by <sup>1</sup>H-NMR (see Appendix A4.2), showing changing in heated sample spectrum. The two samples were also placed under a flow of CO<sub>2</sub>, and how is visible from **Figure 4.1**, the yellowed sample (heated to 90 °C) did not present a precipitate, while the one kept at room temperature did. Notably DBU and CO<sub>2</sub> are able to form a white precipitate, consistent with the formation of [DBUH<sup>+</sup>][HCO<sub>3</sub><sup>-</sup>], in the presence of adventitious water in the environment: this is the reason why (i) a precipitate has been observed also without the presence of an alcohol; (ii) no differences have been found using anhydrous or non-anhydrous DBU .<sup>35</sup>

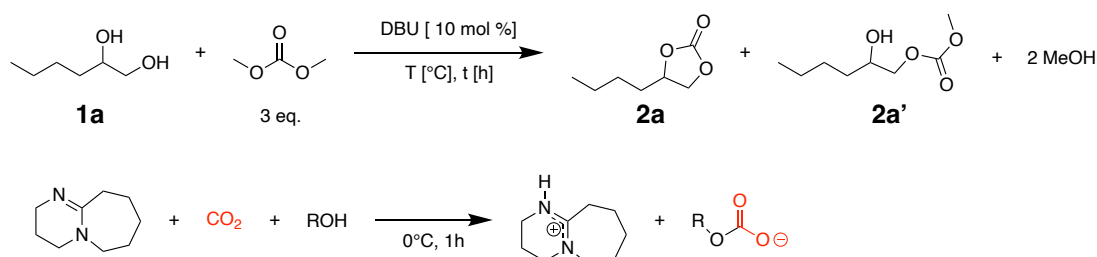


**Figure 4.1** Samples of DBU heated at 90°C and kept at rt after bubbling CO<sub>2</sub>.

### Catalyst recovery and reuse

After the solidification of the catalyst and its separation from the supernatant, composed by DMC and reaction products, the catalyst is heated to 60 °C under vigorous stirring and under vacuum, until the liquefaction and reformation of DBU (see experimental part). These conditions should also remove the MeOH used to form the salt, that in the subsequent cycle could shift the equilibrium to the reactants. The results on two cycles of CIR from **1a** and DMC are summarized in **Table 4.3**.

**Table 4.3.** Recycle tests at different temperatures in the CIR of **1a** into **2a**.



Entry	Cycle	T [°C]	T [h]	Conversion [%] <sup>a</sup>	Selectivity [%] <sup>a</sup>	DBU recovery [%] <sup>b</sup>
1	I	50	7	91	95	96
	II			89	93	92
2	I	90	3	94	95	76
	II			85	90	50

Reaction conditions: 2 mmol **1a** (249.2  $\mu$ L), 3 eq. DMC (505.2  $\mu$ L), 10% mol DBU (29.8  $\mu$ L), closed vial.

<sup>a</sup> Conversions and selectivity calculated by GC-MS (see experimental section).

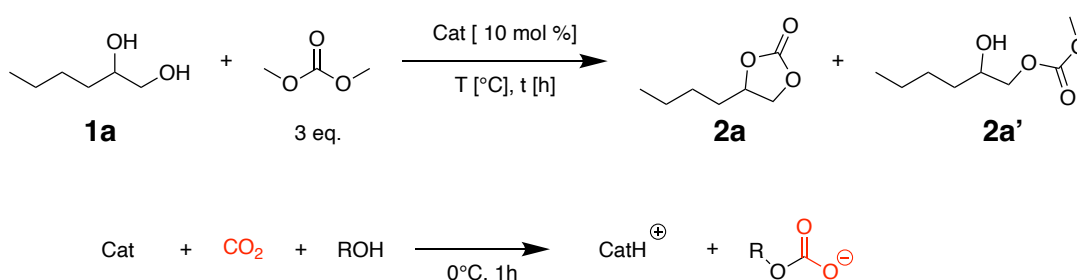
<sup>b</sup> Calculated after re-dissolution of the salt.

CIR reactions of **1a** to **2a** were carried out under the previously optimized conditions: 3 eq. DMC and 10% DBU. The DBU was tested and recycled at both 50 °C (**Table 4.3**, entry 1) and 90 °C (**Table 4.3**, entry 2). In the second cycles the activity was almost unchanged in both cases, with just a slight decrease. For recycling at 50 °C, the recovery of the DBU passed from 96% to 92% (**Table 4.3**, entry 1) for that at 90 °C from 76% to 50% (**Table 4.3**, entry 2). A probable cause of the decreased activity could be the presence in the catalyst of MeOH (that should be removed during the solubilization of the salt at 60 °C) or of the starting material, which shift the equilibrium of the reaction to the reactants.

#### Screening of basic catalysts

It is known from literature that DBU is the most effective organic basis for CIR but also 1,5,7-Triazabicyclo [4.4.0] dec-5-ene (TBD), 1,4-diazabicyclo [2.2.2] octane (DABCO) and triethylamine (TEA) have been tested as catalysts. TBD is a guanidine base while DABCO and TEA are amino bases, and their conjugate acids have pKa values of 15,<sup>37</sup> 8.72<sup>38</sup> and 10.68<sup>38</sup> respectively. The guanidine has a higher basicity than amidine: DBU's conjugate acid has a pKa = 14.2<sup>37</sup> in water, lower than TBD. Also in this case 1,2-hexanediol **1a** was used as a model substrate and the bases have been tested in equal conditions (**Table 4.4**).

**Table 4.4** Tests of different bases in the CIR of **1a** into **2a**.



Entry	Catalyst	T [°C]	T [h]	Conversion [%] <sup>a</sup>	Selectivity [%] <sup>a</sup>	Cat recovery [%] <sup>b</sup>
1	TDB	90	3	89	98	0
2	TEA	90	3	38	95	-
3	DABCO	90	3	82	93	80
4	DABCO	50	7	13	93	-

Reaction conditions: 2 mmol **1a** (249.2  $\mu$ L), 3 eq. DMC (505.2  $\mu$ L), 10% mol catalyst, closed vial.

<sup>a</sup> Conversions and selectivity calculated by GC-MS (see experimental section).

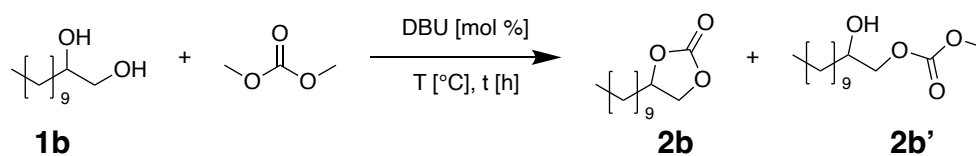
<sup>b</sup> Calculated after re-dissolution of the salt.

From **Table 4.4** we can observe how TBD (entry 1) catalyzes the reaction in 3 h with very good conversion and selectivity, however it does not react with CO<sub>2</sub> to form the salt. In entry 2, TEA was used as catalyst, but after 3h a conversion lower than 40% was obtained; moreover, this base is unable to carry out the switch reaction with CO<sub>2</sub>. As regards DABCO, it catalyzes the reaction at 90 °C with a conversion of 82% and a selectivity of 93% (**Table 4.4**, entry 3), being recovered with a yield of 80%. However, when the reaction was tested at 50 °C (**Table 4.4**, entry 4), only a 13% conversion is obtained after 7h, demonstrating that the DBU is a better organocatalyst for CIR.

### 1,2-dodecandiol

Together with the study on the conditions of CIR from **1a**, 1,2-hexandiol, also 1,2-dodecandiol (**1b**) was tested under the same condition (see experimental part). The aim was to evaluate the behavior of a more lipophilic diol modifying the reaction parameters in the same way. The most important results are summarized in **Table 4.5**.

**Table 4.5** Study of different conditions on CIR from **1b** and DMC.



Entry	DBU [mol %]	DMC [eq]	T [°C]	T [h]	Conversion [%] <sup>a</sup>	Selectivity [%] <sup>a</sup>	DBU recovery [%] <sup>b</sup>
1	5	5	90	3	93	90	59
2	25	3	90	3	92	92	58

<b>3</b>	10	1	90	3	91	92	63
<b>4</b>	-	5	90	4	0	-	-
<b>5</b>	10	3	50	7	89	99	71
<b>6</b>	10	3	RT	72	94	99	90

Reaction conditions: 2 mmol **1b** (404 mg), closed vial.

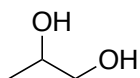
<sup>a</sup> Conversions and selectivity calculated by GC-MS (see experimental section).

<sup>b</sup> Calculated after re-dissolution of the salt.

In this case, a decrease in the percentage of DBU used (**Table 4.5** entries 1-3) did not lead to substantial differences in terms of conversion and selectivity. A slight increase in DBU recovery was obtained, but the values are lower, respect to those obtained in the CIR with **1a**. 1,2-dodecandiol, **1b**, and the corresponding carbonate, **2b**, are solid, thus making the reaction mix a much more viscous liquid, in which CO<sub>2</sub> blew more difficultly as the solid is formed. As expected, carrying out the reaction at 50°C for 7h (**Table 4.5** entry 5) and at RT for 3 days (**Table 4.5** entry 5), similar conversion and selectivity were obtained, but a marked improvement in DBU recovery.

After the study on two substrates with a lipophilic tail, **1a** and **1b**, the conditions studied were tested on other different substrates. Not only 1,2-diols but also 1-3 diols, to obtain 6-membered cyclic carbonates, were used. The most important results of the tests carried out on the other substrates are summarized in the following tables. <sup>1</sup>H NMR of isolated products and DBU after switch with CO<sub>2</sub> are reported in Appendix 4.1.

#### 1,2-propanediol **1c** (**Table 4.6**)



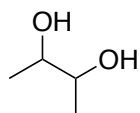
Entry	T [°C]	T [h]	Conversion [%] <sup>a</sup>	Selectivity [%] <sup>a</sup>	DBU recovery [%] <sup>b</sup>
<b>1</b>	90	4	69	81	55
<b>2</b>	50	24	51	84	97

Reaction conditions: 2 mmol **1c** (146.3 μL), 3 eq. DMC (505.2 μL), 10% mol DBU (29.8 μL), closed vial.

<sup>a</sup> Conversions and selectivity calculated by GC-MS (see experimental section).

<sup>b</sup> Calculated after re-dissolution of the salt.

### 2,3-butanediol **1d** (Table 4.7)



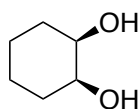
Entry	T [°C]	T [h]	Conversion [%] <sup>a</sup>	Selectivity [%] <sup>a</sup>	DBU recovery [%] <sup>b</sup>
1	90	6	88	97	75
2	50	24	73	93	91

Reaction conditions: 2 mmol **1d** (182  $\mu$ L), 3 eq. DMC (505.2  $\mu$ L), 10% mol DBU (29.8  $\mu$ L), closed vial.

<sup>a</sup> Conversions and selectivity calculated by GC-MS (see experimental section).

<sup>b</sup> Calculated after re-dissolution of the salt.

### cis-cyclohexane-1,2-diol **1e** (Table 4.8)



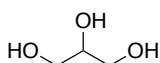
Entry	T [°C]	T [h]	Conversion [%] <sup>a</sup>	Selectivity [%] <sup>a</sup>	DBU recovery [%] <sup>b</sup>
1	90	6	60	90	57
2	50	24	51	92	81

Reaction conditions: 1 mmol **1e** (116 mg), 3 eq. DMC (253  $\mu$ L), 10% mol DBU (29.8  $\mu$ L), closed vial.

<sup>a</sup> Conversions and selectivity calculated by GC-MS (see experimental section).

<sup>b</sup> Calculated after re-dissolution of the salt.

### Glycerol **1f** (Table 4.9)



Entry	T [°C]	T [h]	Conversion [%] <sup>a</sup>	Selectivity [%] <sup>a</sup>	DBU recovery [%] <sup>b</sup>
1	90	2	85	94	90
2	50	2	85	95	95
3	RT	2	85	95	99

Reaction conditions: 2 mmol **1f** (146.2  $\mu$ L), 5 eq. DMC (842  $\mu$ L), 25% mol DBU (75  $\mu$ L), closed vial.

<sup>a</sup> Conversions and selectivity calculated by GC-MS (see experimental section).

<sup>b</sup> Calculated after re-dissolution of the salt.

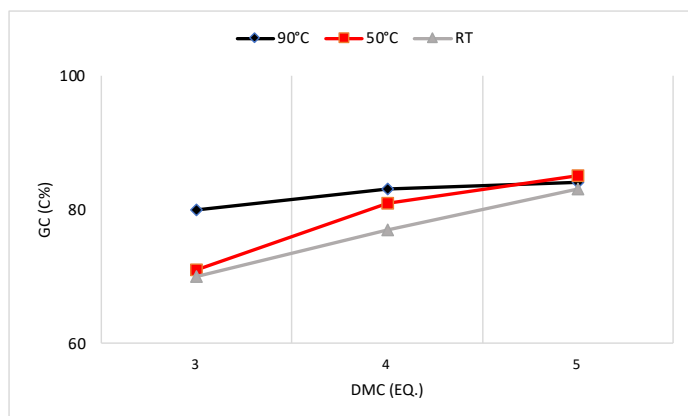
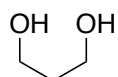


**Figure 4.2** Conversion of glycerol into glycerol carbonate (GC) varying temperatures and DMC eq.

### 1,3-propanediol **1g** (Table 4.10)



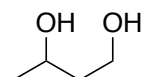
Entry	T [°C]	T [h]	Conversion [%] <sup>a</sup>	Selectivity [%] <sup>a</sup>	DBU recovery [%] <sup>b</sup>
1	90	6	78	0	-
2	50	24		0	-

Reaction conditions: 2 mmol **1g** (143.5  $\mu$ L), 3 eq. DMC (505.2  $\mu$ L), 10% mol DBU (29.8  $\mu$ L), closed vial.

<sup>a</sup> Conversions and selectivity calculated by GC-MS (see experimental section).

<sup>b</sup> Calculated after re-dissolution of the salt.

### 1,3-butanediol **1h** (Table 4.11)



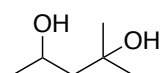
Entry	T [°C]	T [h]	Conversion [%] <sup>a</sup>	Selectivity [%] <sup>a</sup>	DBU recovery [%] <sup>b</sup>
1	90	6	67	0	-
2	50	24	52	0	-

Reaction conditions: 2 mmol **1d** (178.2  $\mu$ L), 3 eq. DMC (505.2  $\mu$ L), 10% mol DBU (29.8  $\mu$ L), closed vial.

<sup>a</sup> Conversions and selectivity calculated by GC-MS (see experimental section).

<sup>b</sup> Calculated after re-dissolution of the salt.

### 2-Methyl-2,4-pentanediol **1i** (Table 4.12)



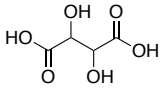
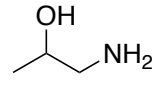
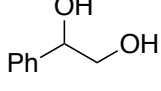
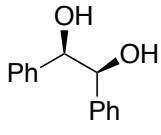
Entry	T [°C]	T [h]	Conversion [%] <sup>a</sup>	Selectivity [%] <sup>a</sup>	DBU recovery [%] <sup>b</sup>
1	90	24	74	25	72
2	50	72	51	30	84

Reaction conditions: 2 mmol **1i** (257  $\mu$ L), 3 eq. DMC (505.2  $\mu$ L), 10% mol DBU (29.8  $\mu$ L), closed vial.

<sup>a</sup> Conversions and selectivity calculated by GC-MS (see experimental section).

<sup>b</sup> Calculated after re-dissolution of the salt.

### Other substrates (Table 4.13)

Entry	Substrate	T [°C]	T [h]	Conversion [%] <sup>a</sup>	Selectivity [%] <sup>a</sup>	DBU recovery [%] <sup>b</sup>
1	 Tartaric Acid, 2mmol (300.2 mg), <b>1l</b>	90	24	0	-	-
2	 Amino-2-Propanol, 2 mmol (154.4 $\mu$ L), <b>1m</b>	90	6	95	0	-
3	 1-Phenyl-1,2-ethanediol, 2 mmol (276,32 mg), <b>1n</b>	50	48	51	85	87
4	 <i>Meso</i> -Hydrobenzoin 0.5 mmol (53.6 mg), <b>1o</b>	50	24	85	99	-

Reaction conditions: 3 eq. DMC (505.2  $\mu$ L), 10% mol DBU (29.8  $\mu$ L), closed vial.

<sup>a</sup> Conversions and selectivity calculated by GC-MS (see experimental section).

<sup>b</sup> Calculated after re-dissolution of the salt.

The CIRs having as starting materials **1c** (Table 4.6), **1d** (Table 4.7) and **1e** (Table 4.8) gave very similar results. The conversions of the reactions at 90 °C (entries 1) were always a little higher

than those of the reactions carried out at 50 °C. Selectivity was always quite similar when changing temperatures. The discriminating factor is the recovery of the DBU, more effective when the reactions were carried out at lower temperature.

Glycerol **1f** is a very important starting material, as its transformations have a wide interest in the industrial field. For this reason, a very in-depth study was carried out, and the most interesting results are summarized in **Table 4.9** and in **Figure 4.2**. It has been observed that, bringing the DBU equivalents from 3 to 5, the same results are obtained, in terms of conversion and selectivity, both in reactions carried out at 90 °C and at rt. In this case, blowing the CO<sub>2</sub> in the vial at the end of the reaction we did not obtain a solid salt but just a more polar liquid, no more miscible in DCM, which represented the salt that the DBU made with the unreacted glycerol (see Appendix 4.1, A4.7) and the other alcohols in the system. The recovery of DBU is high in all the cases, but quantitative for reactions carried out at rt. Notably, glycerol is not soluble in DMC at rt, but became miscible after few minutes from the beginning of the stirring.

The starting materials **1g**, **1h** and **1i** are 1,3-diols that, in the CIR with DMC, gave 6-membered cyclic carbonates. **1g** (**Table 4.10**) and **1h** (**Table 4.11**) gave good conversions but yielding only by-products as linear methyl carbonate with esterification of one or both OH: this is probably due to the wide conformational freedom on the C-C bonds. The starting **1i** (**Table 4.12**) also gave the cyclic product, probably because of the methyl groups on the carbons that: i) increase the electronic density of the O; ii) generate steric and conformational hindrance and therefore a greater possibility for the cyclic product. For reaction of **1i**, despite the good conversion, low selectivity was found by GC-MS analyses, not confirmed by <sup>1</sup>H NMR of the products after CO<sub>2</sub> switch; further analyses need to be done.

Other substates were tested (**Table 4.13**): tartaric acid, **1l**, which gave no product and amino-2-propanol, **1m**, which yield a very high conversion, but not cyclic carbamate; with 1-phenyl-1,2-ethanediol, **1n**, a conversion of 51% was obtained together with a good selectivity and catalyst recovery. *Meso*-hydrobenzoin, **1o**, gave very good conversion and selectivity, but the recovery of the catalyst was impossible to accomplish because the product precipitated at room temperature.

### 4.1.3 Conclusions

In the present study the CIR from diols and DMC were performed and the DBU used as catalyst was recovered in solid form by reaction with CO<sub>2</sub>. Different substrates and conditions were tested and good yields were obtained using 3-5 eq. of DMC and 10-25% of DBU. The temperature is a crucial factor for the recovery of the catalyst, in fact if at RT and 50 °C the conversions are lower in most cases, the recovery of the catalyst is much higher, compared to the reactions carried out at 90 °C: at that temperature DBU tends to hydrolyze, thus being less available to the formation of the ionic salt. The solid DBU is more easily separable from the liquid reaction mix; it can be reused while maintaining the same activity, after dissolving and removing the CO<sub>2</sub> and alcohol (obtained by heating and stirring under vacuum). These observations could lead to further evaluations on the use of switchable catalysts such as the DBU for other application.

### 4.1.4 Experimental section

#### Material

All chemicals and solvents were purchased from Sigma-Aldrich or Alfa Aesar and used without any further purification. CO<sub>2</sub> with  $\geq 99.5\%$  purity was purchased from Siad, Italy.

#### Representative procedure for CIR

The syntheses of the products catalyzed by DBU and other bases, were carried out in 10 ml-screw-capped tubes. Inside the test tube the starting material, the catalyst and DMC were added. The test tube is closed and heated under stirring at different temperature. At the end of the reaction an aliquot of the crude supernatant was silylated, diluted and analyzed through GC-MS.

The concentration of the starting materials was obtained directly from their respective peak areas in the gas chromatograph, as compared to peak's retention time of the standards. The conversion of the starting and the selectivity were calculated using these equations:

$$\text{Conversion, } C = (1a_{\text{initial}} + 1a_{\text{residual}}) / (1a_{\text{initial}}) \times 100$$

$$\text{Selectivity, } S = (2a) / (1a_{\text{initial}} - 1a_{\text{residual}}) \times 100$$

Reaction mixture and DBU salt, after CO<sub>2</sub> switch were also analyzed through <sup>1</sup>H-NMR to check the reaction selectivity (see Appendix 4.1).

### Silylation procedure

50 mL of silylating agent *N,O*-bis(trimethylsilyl)trifluoroacetamide and 1% chlorotrimethylsilane, (BSTFA + 1% TMCS), 100 mL of ethyl acetate and 20 mL of pyridine were added to 1–10 mg of sample into a GC-MS vial. The vial was heated at 60–80 °C for 30–40 min. The sample was then diluted with ethyl acetate before the injection.

### Catalysts recycle

At the end of the reaction the tubes were placed in an ice bath, the CO<sub>2</sub> is blown inside through a needle for about an hour. After the catalyst precipitation, the liquid supernatant of DMC, product and by-product was removed. The catalyst was washed twice with Et<sub>2</sub>O and then dried overnight under reduced pressure. It was analyzed through <sup>1</sup>H NMR to check its purity (see Appendix 4.1). Before its reuse it is heated at 60 °C under vigorous stirring and reduced pressure, until the liquid DBU is reformed.

### Instrumentation

GC-MS analyses of reaction mixtures were performed using an Agilent HP 6850 gas chromatograph connected to an Agilent HP 5975 quadrupole mass spectrometer. Analytes were separated on a HP-5MS fused-silica capillary column (stationary phase 5%-Phenyl)-methylpolysiloxane, 30 m, 0.25 mm i.d., 0.25 μm film thickness), with helium as the carrier gas (at constant pressure, 36 cm s<sup>-1</sup> linear velocity at 200 °C). Mass spectra were recorded under electron ionization (70 eV) at a frequency of 1 scan s<sup>-1</sup> within the 12–600 m/z range. The injection port temperature was 250 °C. The temperature of the column was kept at 50 °C for 5 min, then increased from 50 to 250 °C at 10 °C min<sup>-1</sup> and the final temperature of 250 °C was kept for 12 min.

<sup>1</sup>H NMR spectra were recorded on Varian 400 (400 MHz) spectrometer. <sup>13</sup>C NMR spectra were recorded on a Varian 400 (100 MHz) spectrometer. Chemical shifts are reported in ppm from TMS with the solvent resonance as the internal standard (deuteriochloroform: 7.26 ppm).

### Characterization data of isolated products and DBU (Spectra in Appendix 4.1)

**2a. 4-butyl-1,3-dioxolan-2-one** <sup>1</sup>H NMR (400 MHz, CDCl<sub>3</sub>) δ 4.68 (qd, *J* = 7.5, 5.5 Hz, 1H), 4.50 (t, *J* = 8.1 Hz, 1H), 4.04 (dd, *J* = 8.4, 7.2 Hz, 1H), 1.85 – 1.73 (m, 1H), 1.71 – 1.61 (m, 1H), 1.47 – 1.28 (m, 4H), 0.90 (t, *J* = 7.1 Hz, 3H).

**DBU. 1,5-diazabicyclo(5.4.0)undec-7-ene**  $^1\text{H}$  NMR (400 MHz,  $\text{CDCl}_3$ )  $\delta$  3.34 (dd,  $J = 11.7, 5.7$  Hz, 6H), 2.63 (t,  $J = 10.2$  Hz, 2H), 1.89 (dt,  $J = 11.9, 6.0$  Hz, 2H), 1.71 (s, 4H), 1.63 (s, 2H).

**2b. 4-decyl-1,3-dioxolan-2-one**  $^1\text{H}$  NMR (400 MHz,  $\text{CDCl}_3$ )  $\delta$  4.74 – 4.64 (m, 1H), 4.56 – 4.47 (m, 1H), 4.04 (dd,  $J = 8.4, 7.3$  Hz, 1H), 1.79 (tdd,  $J = 9.4, 5.9, 3.7$  Hz, 1H), 1.66 (ddd,  $J = 9.8, 9.3, 5.3$  Hz, 1H), 1.45 (ddd,  $J = 12.3, 10.6, 5.1$  Hz, 1H), 1.36 – 1.20 (m, 15H), 0.86 (t,  $J = 6.8$  Hz, 3H).

**2c. 4-methyl-1,3-dioxolan-2-one (propylene carbonate)**  $^1\text{H}$  NMR (400 MHz,  $\text{CDCl}_3$ )  $\delta$  4.83 (tq,  $J = 12.6, 6.3$  Hz, 1H), 4.53 (dd,  $J = 8.3, 7.8$  Hz, 1H), 4.00 (dd,  $J = 8.4, 7.3$  Hz, 1H), 1.47 (d,  $J = 6.3$  Hz, 3H).

**2d. 4,5-dimethyl-1,3-dioxolan-2-one**  $^1\text{H}$  NMR (400 MHz,  $\text{CDCl}_3$ )  $\delta$  4.88 – 4.78 (m, 1H), 1.39 – 1.31 (m, 3H).

**2e. hexahydrobenzo[d][1,3]dioxol-2-one**  $^1\text{H}$  NMR (400 MHz,  $\text{CDCl}_3$ )  $\delta$  4.73 – 4.63 (m, 2H), 1.87 (dd,  $J = 11.0, 5.3$  Hz, 4H), 1.69 – 1.49 (m, 4H)

**2f. 4-(hydroxymethyl)-1,3-dioxolan-2-one (glycerol carbonate)**  $^1\text{H}$  NMR (400 MHz,  $\text{CDCl}_3$ )  $\delta$  4.78 (m, 1H), 4.47 (dt,  $J = 14.7, 7.9$  Hz, 2H), 3.96 (d,  $J = 12.9$  Hz, 1H), 3.75 (d,  $J = 17.8$  Hz, 2H)

**2i. 4,4,6-trimethyl-1,3-dioxan-2-one**  $^1\text{H}$  NMR (400 MHz,  $\text{CDCl}_3$ )  $\delta$  4.61 (dtt,  $J = 12.3, 6.2, 3.1$  Hz, 1H), 1.92 (dd,  $J = 14.2, 3.1$  Hz, 1H), 1.79 – 1.69 (m, 1H), 1.38 (d,  $J = 6.2$  Hz, 6H), 1.40 (d,  $J = 6.2$  Hz, 3H)

**2n. 4-Phenyl-1,3-dioxolan-2-one**  $^1\text{H}$  NMR (400 MHz,  $\text{CDCl}_3$ )  $\delta$  7.49 – 7.19 (m, 5H), 5.64 (t,  $J = 8.0$  Hz, 1H), 4.82 – 4.72 (m, 1H), 4.35 – 4.26 (m, 1H).

## BIBLIOGRAPHY

- (1) Pyo, S.-H.; Hatti-Kaul, R. Chlorine-Free Synthesis of Organic Alkyl Carbonates and Five- and Six-Membered Cyclic Carbonates. *Adv. Synth. Catal.* **2016**, *358* (5), 834–839. <https://doi.org/10.1002/adsc.201500654>.
- (2) Pyo, S.-H.; Hatti-Kaul, R. Selective, Green Synthesis of Six-Membered Cyclic Carbonates by Lipase-Catalyzed Chemospecific Transesterification of Diols with Dimethyl Carbonate. *Adv. Synth. Catal.* **2012**, *354* (5), 797–802. <https://doi.org/10.1002/adsc.201100822>.
- (3) North, M.; Pasquale, R.; Young, C. Synthesis of Cyclic Carbonates from Epoxides and CO<sub>2</sub>. *Green Chem.* **2010**, *12* (9), 1514–1539. <https://doi.org/10.1039/C0GC00065E>.
- (4) Weil, C. S.; Condra, N.; Haun, C.; Striegel, J. A. Experimental Carcinogenicity and Acute Toxicity Of Representative Epoxides. *Am. Ind. Hyg. Assoc. J.* **1963**, *24* (4), 305–325. <https://doi.org/10.1080/00028896309343226>.
- (5) Okoye, P. U.; Hameed, B. H. Review on Recent Progress in Catalytic Carboxylation and Acetylation of Glycerol as a Byproduct of Biodiesel Production. *Renew. Sustain. Energy Rev.* **2016**, *53*, 558–574. <https://doi.org/10.1016/j.rser.2015.08.064>.
- (6) Ochoa-Gómez, J. R.; Gómez-Jiménez-Aberasturi, O.; Maestro-Madurga, B.; Pesquera-Rodríguez, A.; Ramírez-López, C.; Lorenzo-Ibarreta, L.; Torrecilla-Soria, J.; Villarán-Velasco, M. C. Synthesis of Glycerol Carbonate from Glycerol and Dimethyl Carbonate by Transesterification: Catalyst Screening and Reaction Optimization. *Appl. Catal. Gen.* **2009**, *366* (2), 315–324. <https://doi.org/10.1016/j.apcata.2009.07.020>.
- (7) Fiorani, G.; Perosa, A.; Selva, M. Dimethyl Carbonate: A Versatile Reagent for a Sustainable Valorization of Renewables. *Green Chem.* **2018**, *20* (2), 288–322. <https://doi.org/10.1039/C7GC02118F>.
- (8) Hirotsu, K.; 弘津健二; Kaneko, T.; 金子孝芳. Method for Producing 4-Hydromethyl-1,3-Dioxolan-2-One. JP2001172277A, June 26, 2001.
- (9) *Method for producing glycerol carbonate - Patent WO-03022829-A1 - PubChem.* <https://pubchem.ncbi.nlm.nih.gov/patent/WO-03022829-A1> (accessed 2022-01-24).
- (10) Nakatake, D.; Yokote, Y.; Matsushima, Y.; Yazaki, R.; Ohshima, T. A Highly Stable but Highly Reactive Zinc Catalyst for Transesterification Supported by a Bis(Imidazole) Ligand. *Green Chem.* **2016**, *18* (6), 1524–1530. <https://doi.org/10.1039/C5GC02056E>.
- (11) Yadav, G. D.; Surve, P. S. Solventless Green Synthesis of 4-O-Aryloxy Carbonates from Aryl/Alkyl-Oxy Propanediols and Dimethyl Carbonate over Nano-Crystalline Alkali Promoted Alkaline Earth Metal Oxides. *Catal. Sci. Technol.* **2013**, *3* (10), 2668–2676. <https://doi.org/10.1039/C3CY00204G>.
- (12) Tabanelli, T.; Cailotto, S.; Strachan, J.; Masters, A. F.; Maschmeyer, T.; Perosa, A.; Cavani, F. Process Systems for the Carbonate Interchange Reactions of DMC and Alcohols: Efficient Synthesis of Catechol Carbonate. *Catal. Sci. Technol.* **2018**, *8* (7), 1971–1980. <https://doi.org/10.1039/C8CY00119G>.
- (13) Guidi, S.; Calmanti, R.; Noè, M.; Perosa, A.; Selva, M. Thermal (Catalyst-Free) Transesterification of Diols and Glycerol with Dimethyl Carbonate: A Flexible Reaction for Batch and Continuous-Flow Applications. *ACS Sustain. Chem. Eng.* **2016**, *4* (11), 6144–6151. <https://doi.org/10.1021/acssuschemeng.6b01633>.
- (14) Gérardy, R.; Estager, J.; Luis, P.; Debecker, D. P.; Monbaliu, J.-C. M. Versatile and Scalable Synthesis of Cyclic Organic Carbonates under Organocatalytic Continuous Flow Conditions. *Catal. Sci. Technol.* **2019**, *9* (24), 6841–6851. <https://doi.org/10.1039/C9CY01659G>.
- (15) Nogueira, D. O.; Souza, S. P. de; Leão, R. A. C.; Miranda, L. S. M.; Souza, R. O. M. A. de. Process Intensification for Tertiary Amine Catalyzed Glycerol Carbonate Production: Translating Microwave Irradiation to a Continuous-Flow Process. *RSC Adv.* **2015**, *5* (27), 20945–20950. <https://doi.org/10.1039/C5RA02117K>.
- (16) Wang, Z.; Gérardy, R.; Gauron, G.; Damblon, C.; M. Monbaliu, J.-C. Solvent-Free Organocatalytic Preparation of Cyclic Organic Carbonates under Scalable Continuous Flow Conditions. *React. Chem. Eng.* **2019**, *4* (1), 17–26. <https://doi.org/10.1039/C8RE00209F>.
- (17) Ochoa-Gómez, J. R.; Gómez-Jiménez-Aberasturi, O.; Ramírez-López, C.; Belsué, M. A Brief Review on Industrial Alternatives for the Manufacturing of Glycerol Carbonate, a Green Chemical. *Org. Process Res. Dev.* **2012**, *16* (3), 389–399. <https://doi.org/10.1021/op200369v>.
- (18) Leão, R. A. C.; Souza, S. P. de; Nogueira, D. O.; Silva, G. M. A.; Silva, M. V. M.; Gutarra, M. L. E.; Miranda, L. S. M.; Castro, A. M.; Junior, I. I.; Souza, R. O. M. A. de. Consecutive Lipase Immobilization and Glycerol Carbonate Production under Continuous-Flow Conditions. *Catal. Sci. Technol.* **2016**, *6* (13), 4743–4748. <https://doi.org/10.1039/C6CY00295A>.
- (19) K. Munshi, M.; S. Biradar, P.; M. Gade, S.; H. Rane, V.; A. Kelkar, A. Efficient Synthesis of Glycerol Carbonate/Glycidol Using 1,8-Diazabicyclo [5.4.0] Undec-7-Ene (DBU) Based Ionic Liquids as Catalyst. *RSC Adv.* **2014**, *4* (33), 17124–17128. <https://doi.org/10.1039/C3RA47433J>.

- (20) Munshi, M. K.; Gade, S. M.; Mane, M. V.; Mishra, D.; Pal, S.; Vanka, K.; Rane, V. H.; Kelkar, A. A. 1,8-Diazabicyclo[5.4.0]Undec-7-Ene (DBU): A Highly Efficient Catalyst in Glycerol Carbonate Synthesis. *J. Mol. Catal. Chem.* **2014**, *391*, 144–149. <https://doi.org/10.1016/j.molcata.2014.04.016>.
- (21) Gu, Q.; Fang, J.; Xu, Z.; Ni, W.; Kong, K.; Hou, Z. CO<sub>2</sub> Promoted Synthesis of Unsymmetrical Organic Carbonate Using Switchable Agents Based on DBU and Alcohols. *New J. Chem.* **2018**, *42* (15), 13054–13064. <https://doi.org/10.1039/C8NJ01638K>.
- (22) Qing, Y.; Lu, H.; Liu, Y.; Liu, C.; Liang, B.; Jiang, W. Production of Glycerol Carbonate Using Crude Glycerol from Biodiesel Production with DBU as a Catalyst. *Chin. J. Chem. Eng.* **2018**, *26* (9), 1912–1919. <https://doi.org/10.1016/j.cjche.2018.01.010>.
- (23) Cao, X.; Xie, H.; Wu, Z.; Shen, H.; Jing, B. Phase-Switching Homogeneous Catalysis for Clean Production of Biodiesel and Glycerol from Soybean and Microbial Lipids. *ChemCatChem* **2012**, *4* (9), 1272–1278. <https://doi.org/10.1002/cctc.201200150>.
- (24) Samorì, C.; Barreiro, D. L.; Vet, R.; Pezzolesi, L.; F. Brilman, D. W.; Galletti, P.; Tagliavini, E. Effective Lipid Extraction from Algae Cultures Using Switchable Solvents. *Green Chem.* **2013**, *15* (2), 353–356. <https://doi.org/10.1039/C2GC36730K>.
- (25) Samorì, C.; Cespi, D.; Blair, P.; Galletti, P.; Malferrari, D.; Passarini, F.; Vassura, I.; Tagliavini, E. Application of Switchable Hydrophilicity Solvents for Recycling Multilayer Packaging Materials. *Green Chem.* **2017**, *19* (7), 1714–1720. <https://doi.org/10.1039/C6GC03535C>.
- (26) Samorì, C.; Basaglia, M.; Casella, S.; Favaro, L.; Galletti, P.; Giorgini, L.; Marchi, D.; Mazzocchetti, L.; Torri, C.; Tagliavini, E. Dimethyl Carbonate and Switchable Anionic Surfactants: Two Effective Tools for the Extraction of Polyhydroxyalkanoates from Microbial Biomass. *Green Chem.* **2015**, *17* (2), 1047–1056. <https://doi.org/10.1039/C4GC01821D>.
- (27) Großeheilmann, J.; Kragl, U. Simple and Effective Catalyst Separation by New CO<sub>2</sub>-Induced Switchable Organocatalysts. *ChemSusChem* **2017**, *10* (12), 2685–2691. <https://doi.org/10.1002/cssc.201700491>.
- (28) Großeheilmann, J.; Vanderveen, J. R.; Jessop, P. G.; Kragl, U. Switchable-Hydrophilicity Solvents for Product Isolation and Catalyst Recycling in Organocatalysis. *ChemSusChem* **2016**, *9* (7), 696–702. <https://doi.org/10.1002/cssc.201501654>.
- (29) Poole, H.; Gauthier, J.; Vanderveen, J. R.; Jessop, P. G.; Lee, R. Use of a Switchable-Hydrophilicity Solvent as Both a Solvent and a Catalyst in Aldol Condensation. *Green Chem.* **2019**, *21* (23), 6263–6267. <https://doi.org/10.1039/C9GC02593F>.
- (30) Yang, Y.; Song, L.; Peng, C.; Liu, E.; Xie, H. Activating Cellulose via Its Reversible Reaction with CO<sub>2</sub> in the Presence of 1,8-Diazabicyclo[5.4.0]Undec-7-Ene for the Efficient Synthesis of Cellulose Acetate. *Green Chem.* **2015**, *17* (5), 2758–2763. <https://doi.org/10.1039/C5GC00115C>.
- (31) Zhang, Q.; Oztekin, N. S.; Barrault, J.; De Oliveira Vigier, K.; Jérôme, F. Activation of Microcrystalline Cellulose in a CO<sub>2</sub>-Based Switchable System. *ChemSusChem* **2013**, *6* (4), 593–596. <https://doi.org/10.1002/cssc.201200815>.
- (32) Onwukamike, K. N.; Tassaing, T.; Grelier, S.; Grau, E.; Cramail, H.; Meier, M. A. R. Detailed Understanding of the DBU/CO<sub>2</sub> Switchable Solvent System for Cellulose Solubilization and Derivatization. *ACS Sustain. Chem. Eng.* **2018**, *6* (1), 1496–1503. <https://doi.org/10.1021/acssuschemeng.7b04053>.
- (33) Wolfs, J.; Meier, M. A. R. A More Sustainable Synthesis Approach for Cellulose Acetate Using the DBU/CO<sub>2</sub> Switchable Solvent System. *Green Chem.* **2021**, *23* (12), 4410–4420. <https://doi.org/10.1039/D1GC01508G>.
- (34) Xie, H.; Yu, X.; Yang, Y.; Zhao, Z. K. Capturing CO<sub>2</sub> for Cellulose Dissolution. *Green Chem.* **2014**, *16* (5), 2422–2427. <https://doi.org/10.1039/C3GC42395F>.
- (35) Heldebrant, D. J.; Jessop, P. G.; Thomas, C. A.; Eckert, C. A.; Liotta, C. L. The Reaction of 1,8-Diazabicyclo[5.4.0]Undec-7-Ene (DBU) with Carbon Dioxide. *J. Org. Chem.* **2005**, *70* (13), 5335–5338. <https://doi.org/10.1021/jo0503759>.
- (36) Hyde, A. M.; Calabria, R.; Arvary, R.; Wang, X.; Klapars, A. Investigating the Underappreciated Hydrolytic Instability of 1,8-Diazabicyclo[5.4.0]Undec-7-Ene and Related Unsaturated Nitrogenous Bases. *Org. Process Res. Dev.* **2019**, *23* (9), 1860–1871. <https://doi.org/10.1021/acs.oprd.9b00187>.
- (37) Kaupmees, K.; Trummal, A.; Leito, I. Basicities of Strong Bases in Water: A Computational Study. *Croat. Chem. Acta* **2014**, *87* (4), 385–395. <https://doi.org/10.5562/cca2472>.
- (38) Frenna, V.; Vivona, N.; Consiglio, G.; Spinelli, D. Amine Basicities in Benzene and in Water. *J. Chem. Soc. Perkin Trans. 2* **1985**, No. 12, 1865–1868. <https://doi.org/10.1039/P29850001865>.

## APPENDIX 4.1

### Contents

**A4.1**  $^1\text{H}$  NMR spectra of reaction mixture and DBU salt for conversion of 1a into 2a (Table 4.3, entry 2), after  $\text{CO}_2$  switch.

**A4.2** Comparison of  $^1\text{H}$  NMR spectra of DBU stirred at  $90^\circ\text{C}$  and at rt.

**A4.3**  $^1\text{H}$  NMR spectrum of reaction mixture and DBU salt for conversion of 1b into 2b (Table 4.5, entry 5), after  $\text{CO}_2$  switch.

**A4.4**  $^1\text{H}$  NMR spectrum of reaction mixture and DBU salt for conversion of 1c into 2c (Table 4.6, entry 1), after  $\text{CO}_2$  switch.

**A4.5**  $^1\text{H}$  NMR spectrum of reaction mixture and DBU salt for conversion of 1d into 2d (Table 4.7, entry 1), after  $\text{CO}_2$  switch.

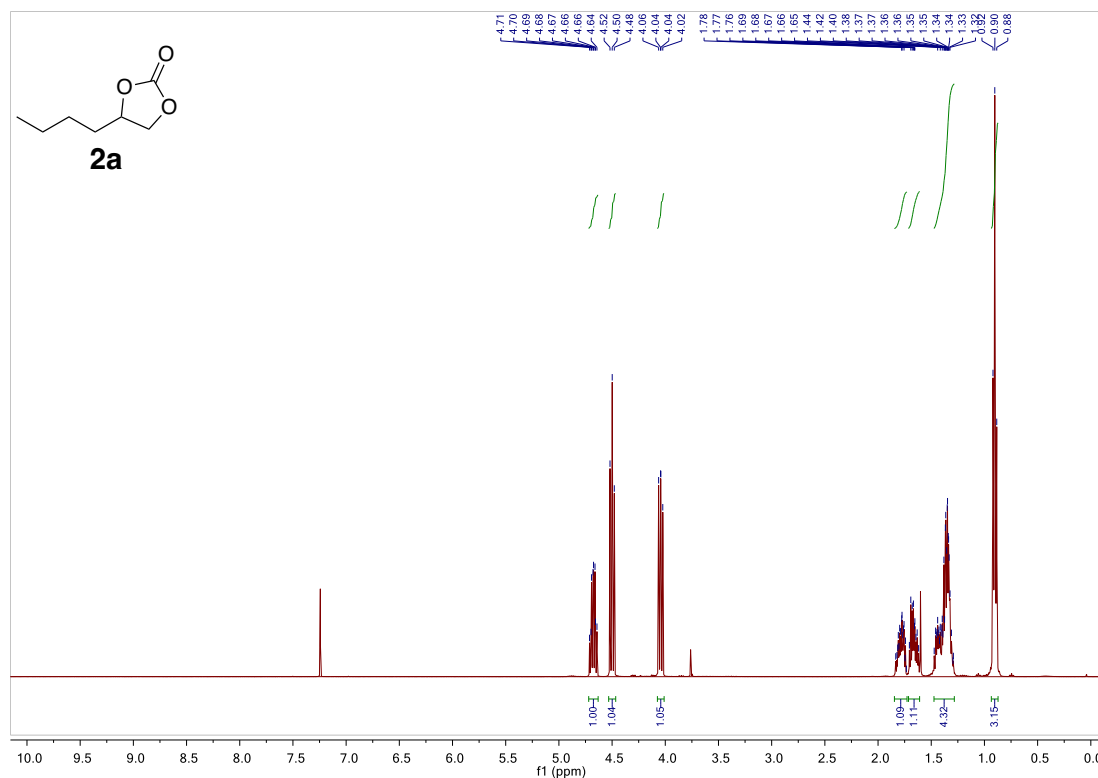
**A4.6**  $^1\text{H}$  NMR spectrum of reaction mixture and DBU salt for conversion of 1e into 2e (Table 4.8, entry 2), after  $\text{CO}_2$  switch.

**A4.7**  $^1\text{H}$  NMR spectrum of reaction mixture and DBU salt for conversion of 1f into 2f (Table 4.9, entry 1), after  $\text{CO}_2$  switch.

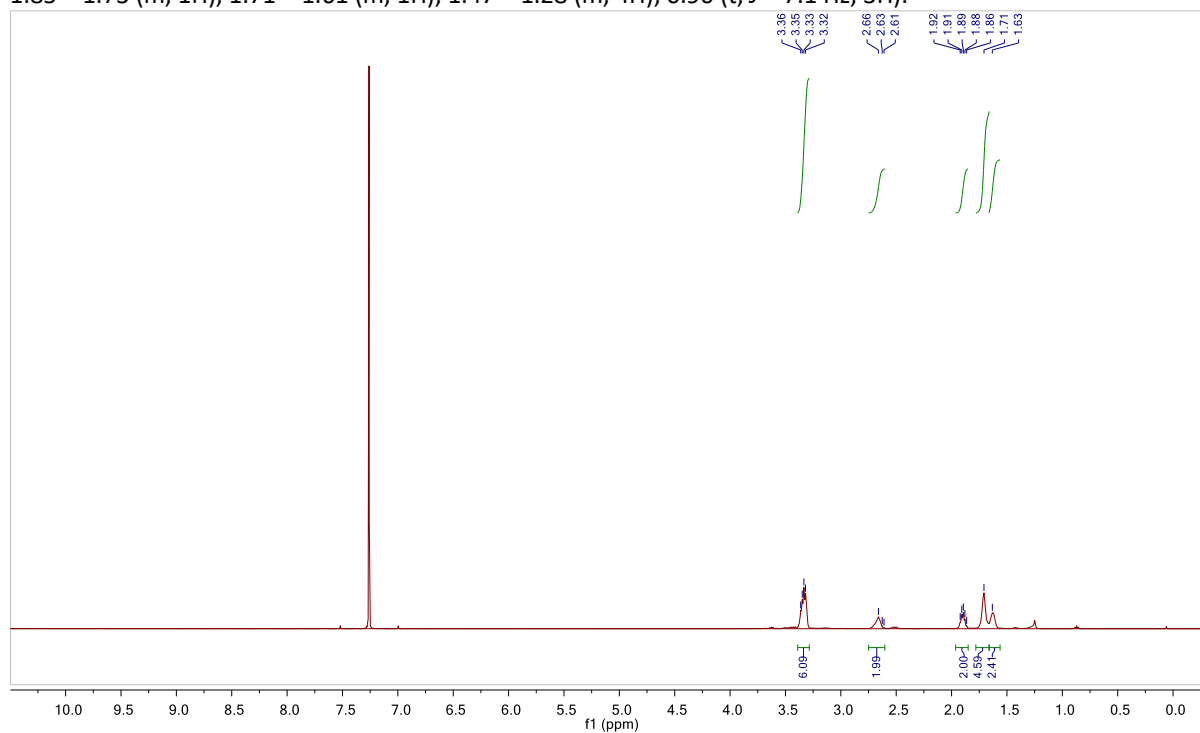
**A4.8**  $^1\text{H}$  NMR spectrum of reaction mixture and DBU salt for conversion of 1i into 2i (Table 4.12, entry 1), after  $\text{CO}_2$  switch.

**A4.9**  $^1\text{H}$  NMR spectrum of reaction mixture and DBU salt for conversion of 1n into 2n (Table 4.9 entry 3), after  $\text{CO}_2$  switch.

**A4.1**  $^1\text{H}$  NMR spectrum of reaction mixture and DBU salt for conversion of 1a into 2a (Table 4.2, entry 1), after  $\text{CO}_2$  switch.

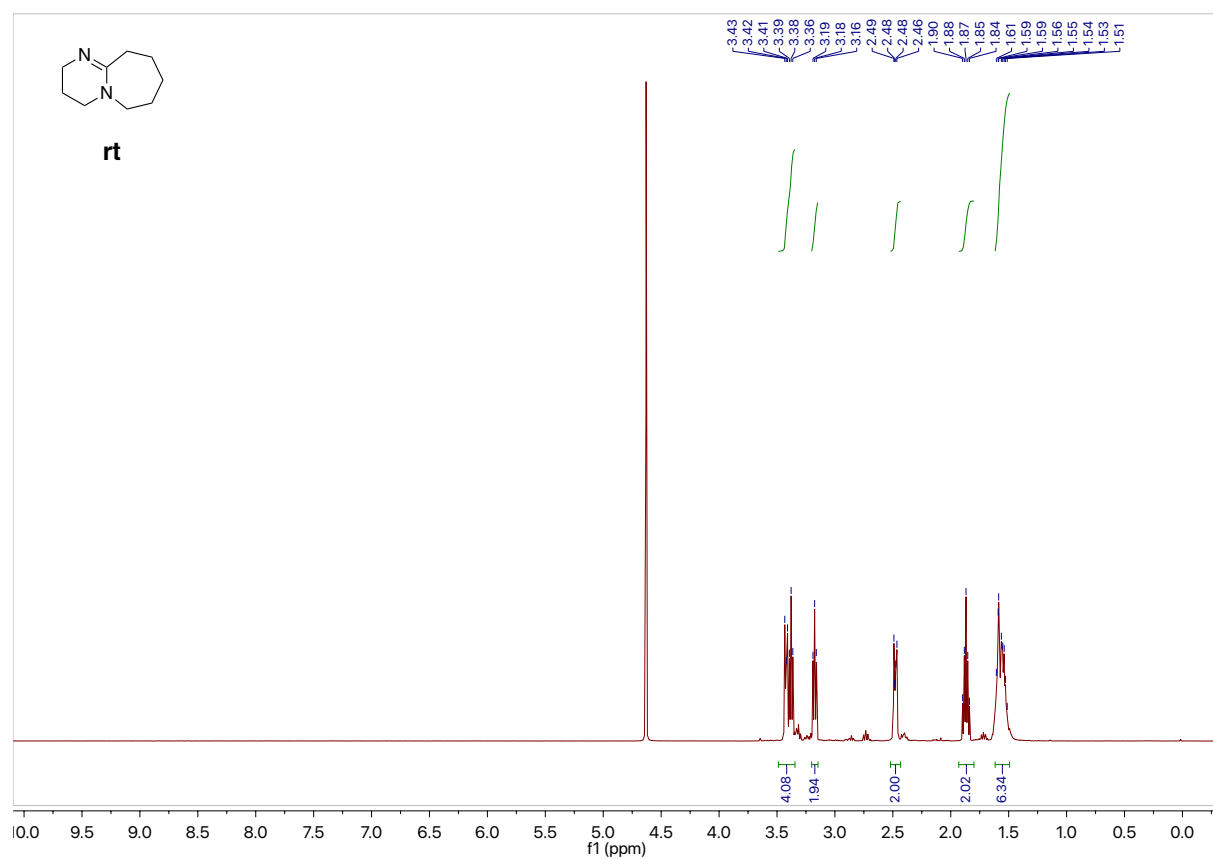
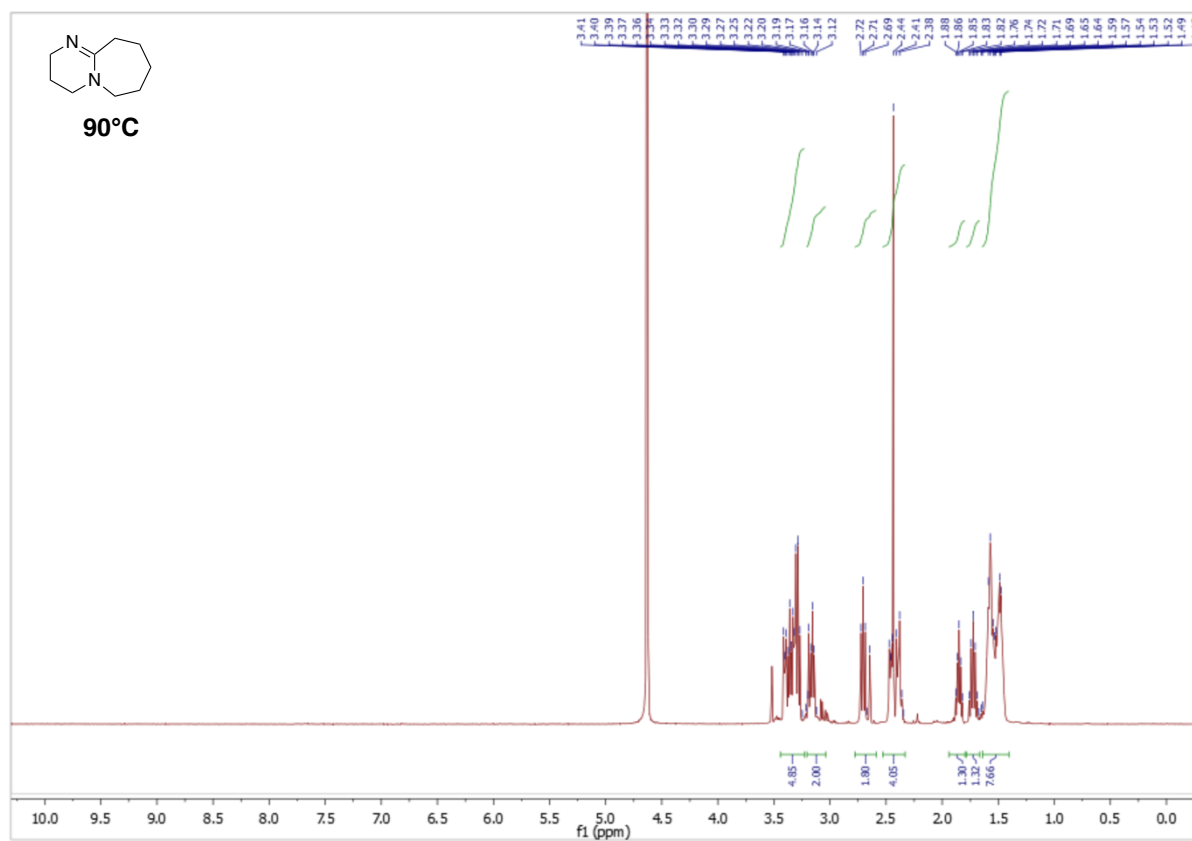


**2a.**  $^1\text{H}$  NMR (400 MHz,  $\text{CDCl}_3$ )  $\delta$  4.68 (qd,  $J = 7.5, 5.5$  Hz, 1H), 4.50 (t,  $J = 8.1$  Hz, 1H), 4.04 (dd,  $J = 8.4, 7.2$  Hz, 1H), 1.85 – 1.73 (m, 1H), 1.71 – 1.61 (m, 1H), 1.47 – 1.28 (m, 4H), 0.90 (t,  $J = 7.1$  Hz, 3H).

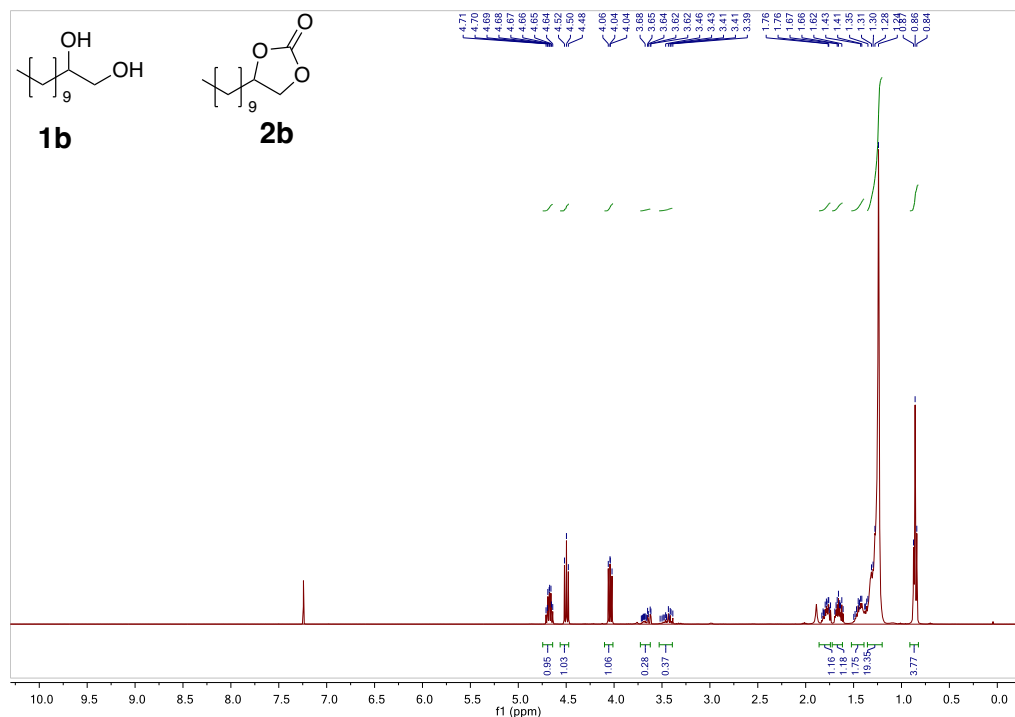


**DBU**  $^1\text{H}$  NMR (400 MHz,  $\text{CDCl}_3$ )  $\delta$  3.34 (dd,  $J = 11.7, 5.7$  Hz, 6H), 2.63 (t,  $J = 10.2$  Hz, 2H), 1.89 (dt,  $J = 11.9, 6.0$  Hz, 2H), 1.71 (s, 4H), 1.63 (s, 2H).

## A4.2 Comparison of $^1\text{H}$ NMR spectra of DBU stirred at $90^\circ\text{C}$ and at rt.

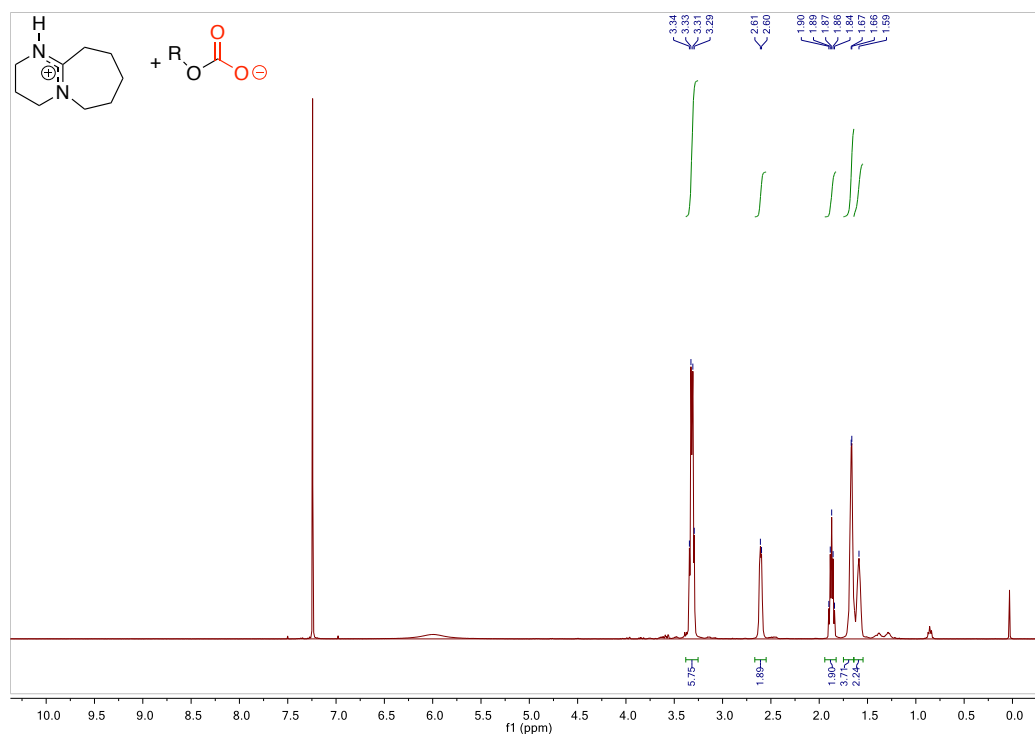


**A4.3**  $^1\text{H}$  NMR spectrum of reaction mixture and DBU salt for conversion of **1b** into **2b** (Table 4.5, entry 5), after  $\text{CO}_2$  switch.



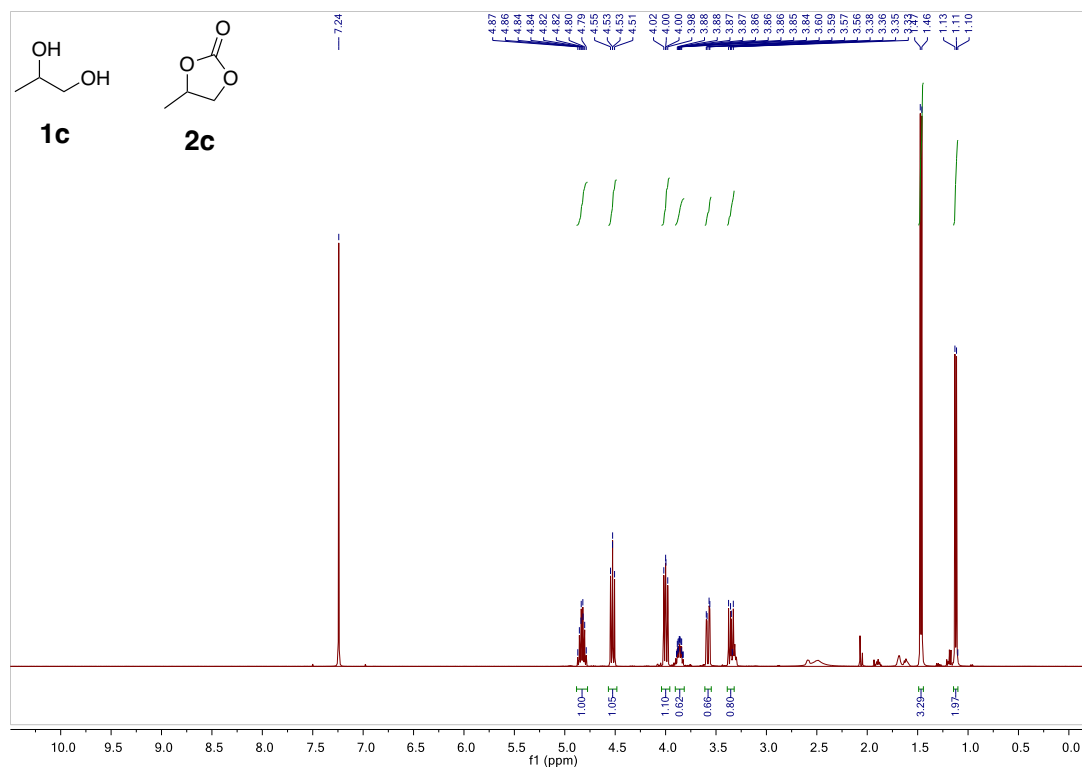
**2b**  $^1\text{H}$  NMR (400 MHz,  $\text{CDCl}_3$ )  $\delta$  4.74 – 4.64 (m, 1H), 4.56 – 4.47 (m, 1H), 4.04 (dd,  $J = 8.4, 7.3$  Hz, 1H), 1.79 (tdd,  $J = 9.4, 5.9, 3.7$  Hz, 1H), 1.66 (ddd,  $J = 9.8, 9.3, 5.3$  Hz, 1H), 1.45 (ddd,  $J = 12.3, 10.6, 5.1$  Hz, 1H), 1.36 – 1.20 (m, 15H), 0.86 (t,  $J = 6.8$  Hz, 3H).

**1b**  $^1\text{H}$  NMR (400 MHz,  $\text{CDCl}_3$ )  $\delta$  3.73 – 3.62 (m, 2H), 3.53 – 3.39 (m, 1H), 1.45 (ddd,  $J = 12.3, 10.6, 5.1$  Hz, 2H), 1.36 – 1.20 (m, 16H), 0.86 (t,  $J = 6.8$  Hz, 3H).



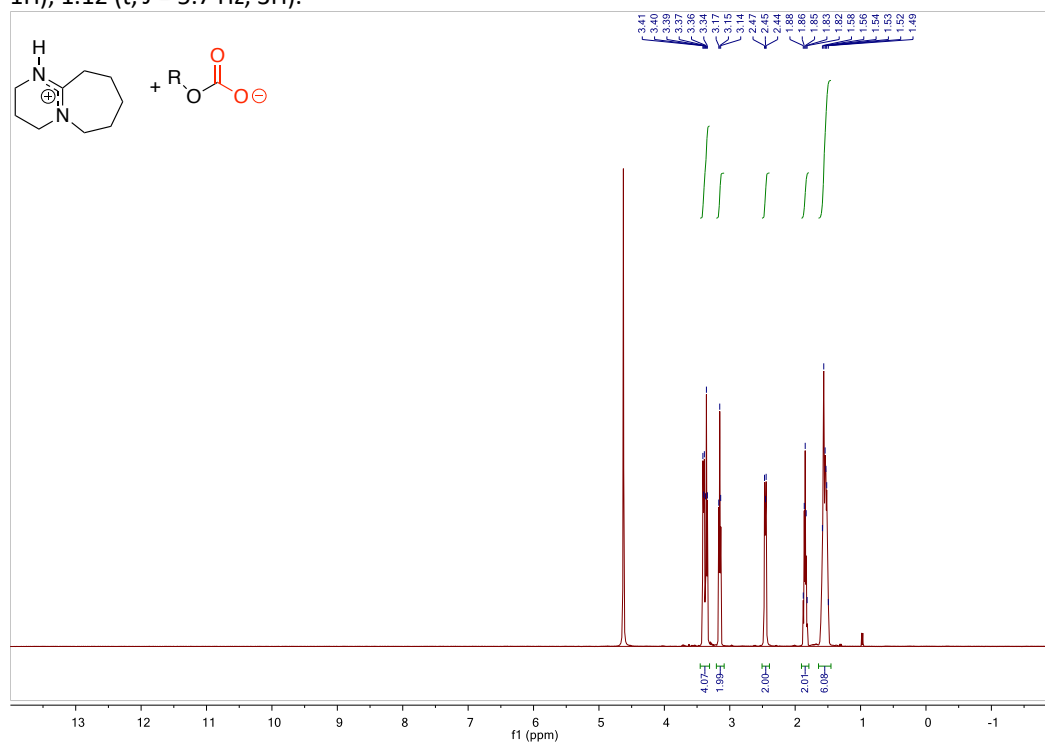
**DBU**  $^1\text{H}$  NMR (400 MHz,  $\text{CDCl}_3$ )  $\delta$  3.32 (q,  $J = 6.0$  Hz, 6H), 2.60 (d,  $J = 4.7$  Hz, 2H), 1.94 – 1.82 (m, 2H), 1.67 (d,  $J = 2.5$  Hz, 4H), 1.59 (s, 2H).

**A4.4**  $^1\text{H}$  NMR spectrum of reaction mixture and DBU salt for conversion of **1c** into **2c** (Table 4.6, entry 1), after  $\text{CO}_2$  switch.



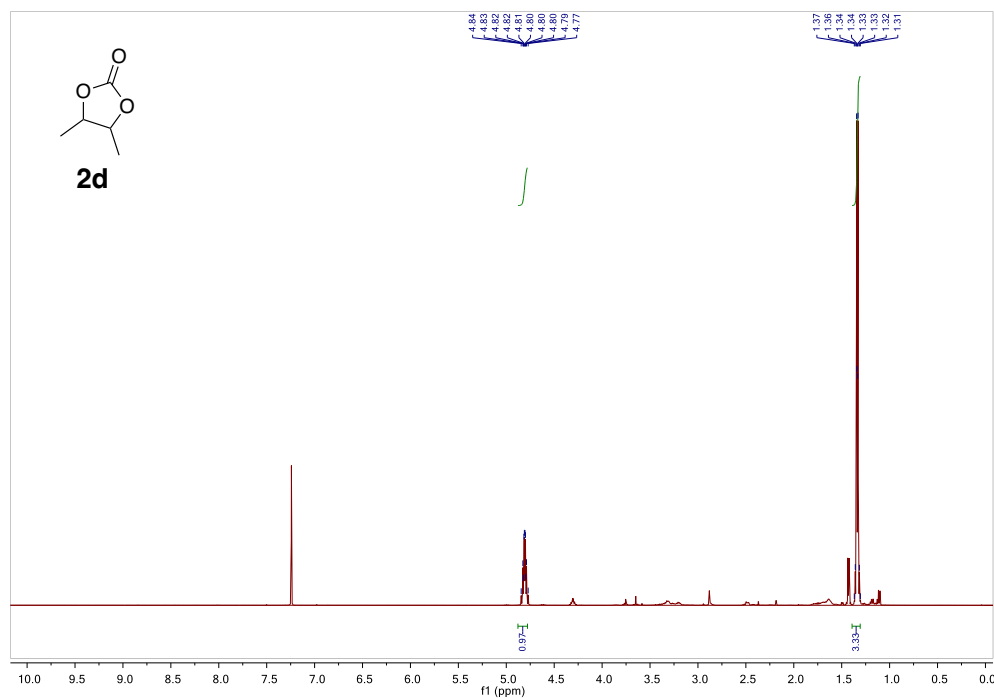
**2c.**  $^1\text{H}$  NMR (400 MHz,  $\text{CDCl}_3$ )  $\delta$  4.83 (tq,  $J = 12.6, 6.3$  Hz, 1H), 4.53 (dd,  $J = 8.3, 7.8$  Hz, 1H), 4.00 (dd,  $J = 8.4, 7.3$  Hz, 1H), 1.47 (d,  $J = 6.3$  Hz, 3H).

**1c.**  $^1\text{H}$  NMR (400 MHz,  $\text{CDCl}_3$ )  $\delta$  3.86 (ddq,  $J = 9.5, 7.7, 3.2$  Hz, 1H), 3.58 (dd,  $J = 11.1, 3.1$  Hz, 1H), 3.39 – 3.32 (m, 1H), 1.12 (t,  $J = 5.7$  Hz, 3H).

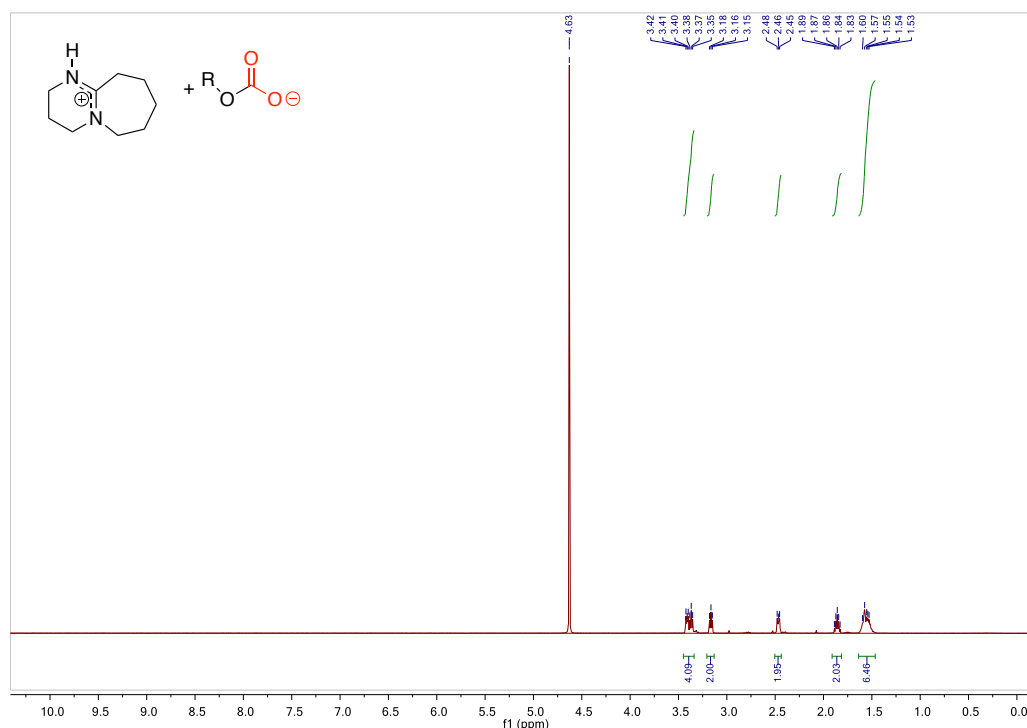


**DBU**  $^1\text{H}$  NMR (400 MHz,  $\text{D}_2\text{O}$ )  $\delta$  3.45 – 3.31 (m, 4H), 3.15 (t,  $J = 5.8$  Hz, 2H), 2.51 – 2.39 (m, 2H), 1.90 – 1.79 (m, 2H), 1.54 (dt,  $J = 15.0, 9.1$  Hz, 6H).

**A4.5**  $^1\text{H}$  NMR spectrum of reaction mixture and DBU salt for conversion of 1d into 2d (Table 4.7, entry 1), after  $\text{CO}_2$  switch.

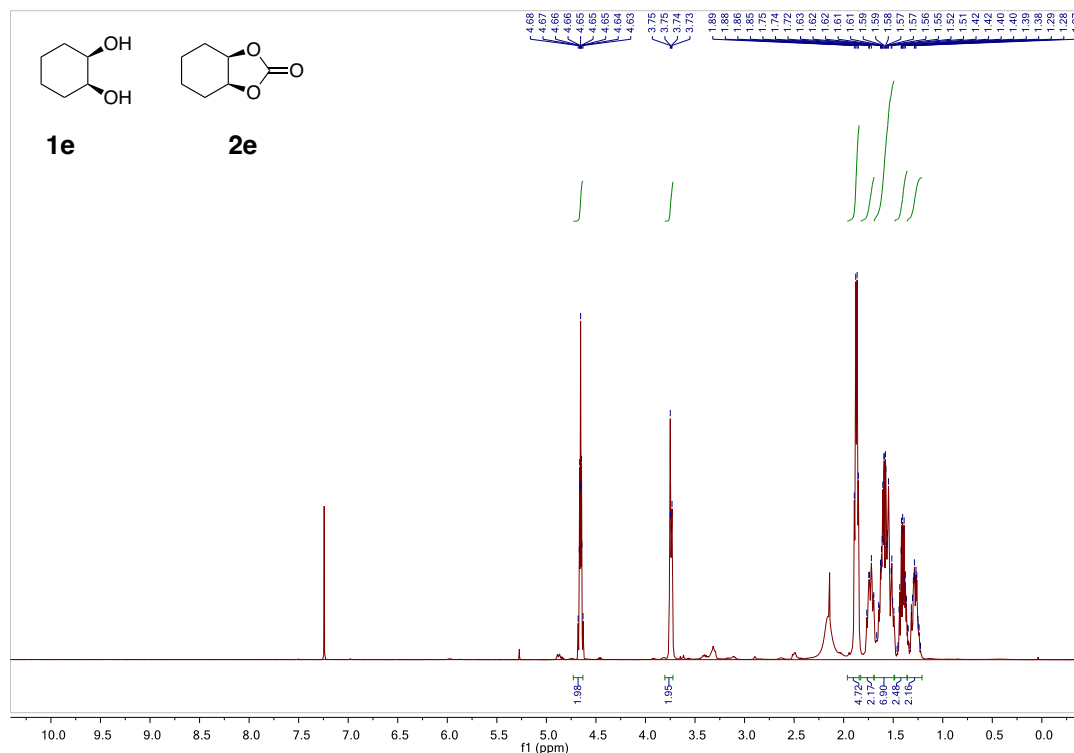


**2d.**  $^1\text{H}$  NMR (400 MHz,  $\text{CDCl}_3$ )  $\delta$  4.88 – 4.78 (m, 1H), 1.39 – 1.31 (m, 3H).



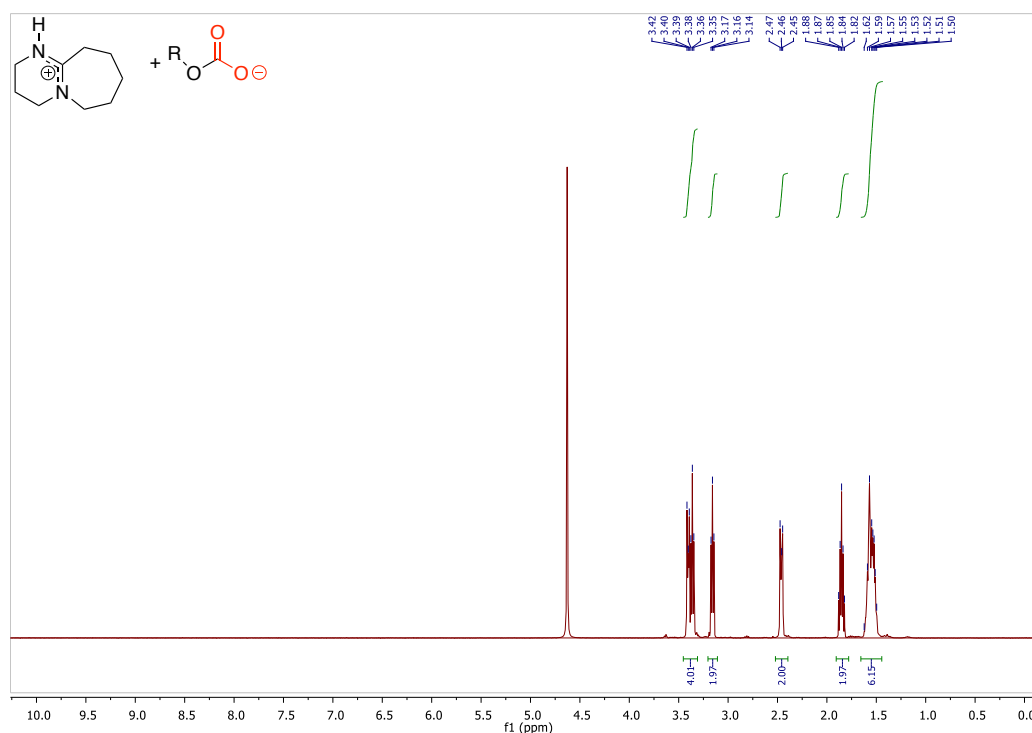
**DBU.**  $^1\text{H}$  NMR (400 MHz,  $\text{D}_2\text{O}$ )  $\delta$  3.45 – 3.34 (m, 4H), 3.16 (t,  $J = 5.8$  Hz, 2H), 2.50 – 2.44 (m, 2H), 1.91 – 1.81 (m, 2H), 1.64 – 1.46 (m, 6H).

**A4.6**  $^1\text{H}$  NMR spectrum of reaction mixture and DBU salt for conversion of **1e** into **2e** (Table 4.8, entry 2), after  $\text{CO}_2$  switch.



**2e.**  $^1\text{H}$  NMR (400 MHz,  $\text{CDCl}_3$ )  $\delta$  4.73 – 4.63 (m, 2H), 1.87 (dd,  $J = 11.0, 5.3$  Hz, 4H), 1.69 – 1.49 (m, 4H)

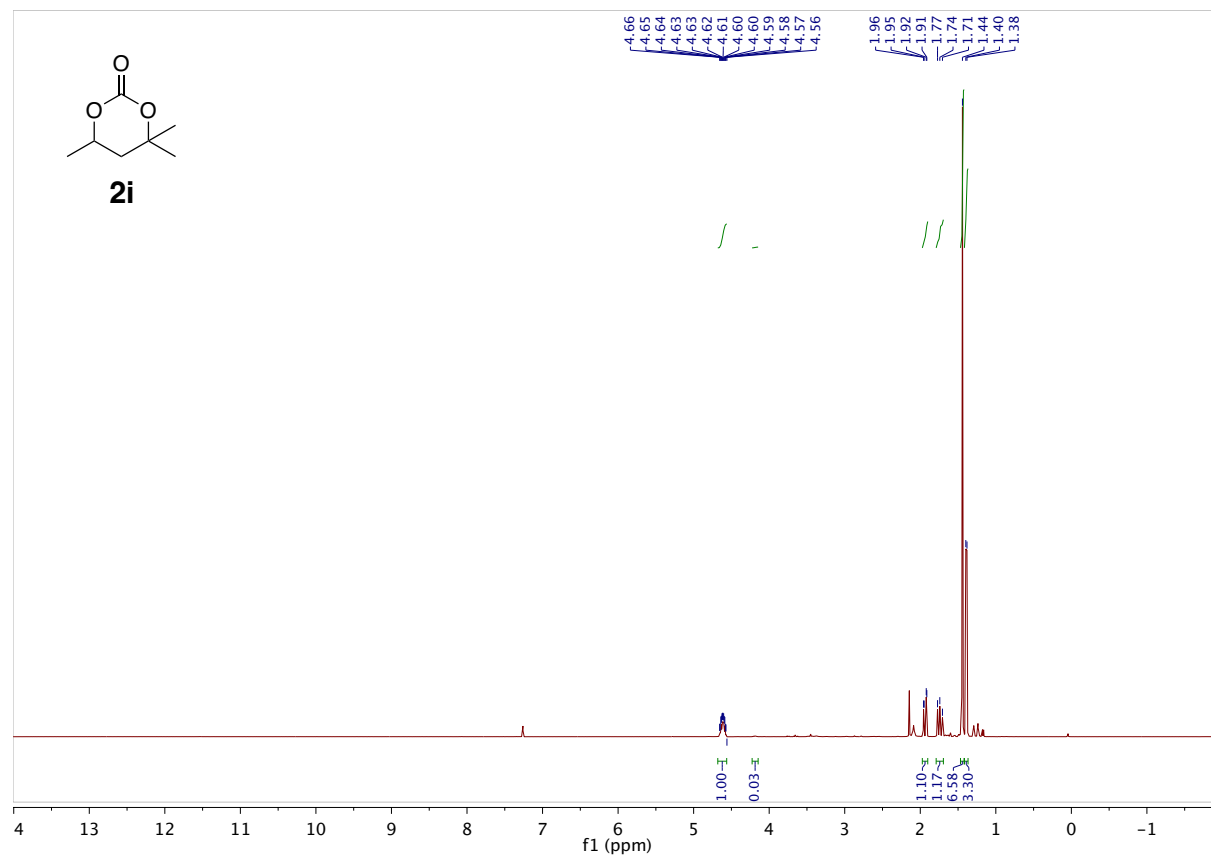
**1e.**  $^1\text{H}$  NMR (400 MHz,  $\text{CDCl}_3$ )  $\delta$  3.74 (dd,  $J = 5.1, 1.9$  Hz, 2H), 1.83 – 1.69 (m, 2H), 1.69 – 1.49 (m, 2H), 1.49 – 1.36 (m, 2H), 1.36 – 1.21 (m, 2H).



**DBU.**  $^1\text{H}$  NMR (400 MHz,  $\text{D}_2\text{O}$ )  $\delta$  3.45 – 3.31 (m, 4H), 3.16 (t,  $J = 5.8$  Hz, 2H), 2.52 – 2.39 (m, 2H), 1.91 – 1.78 (m, 2H), 1.66 – 1.44 (m, 6H).

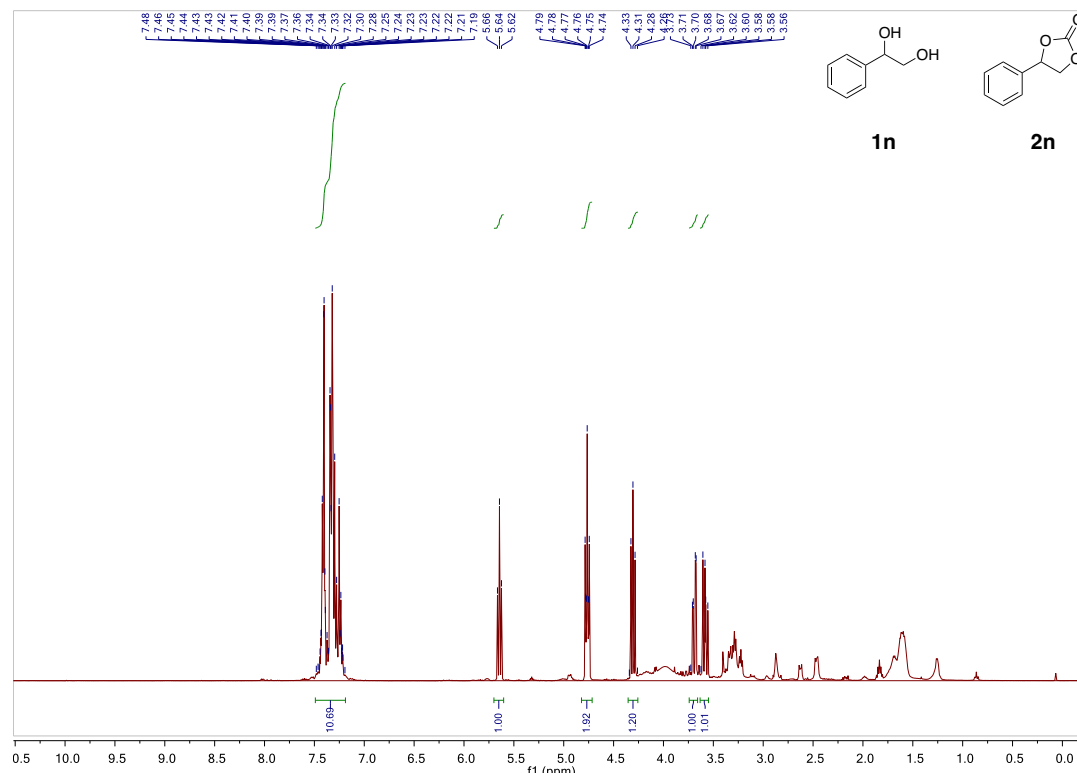


**A4.8**  $^1\text{H}$  NMR spectrum of reaction mixture and DBU salt for conversion of 1i into 2i (Table 4.12, entry 1), after  $\text{CO}_2$  switch.



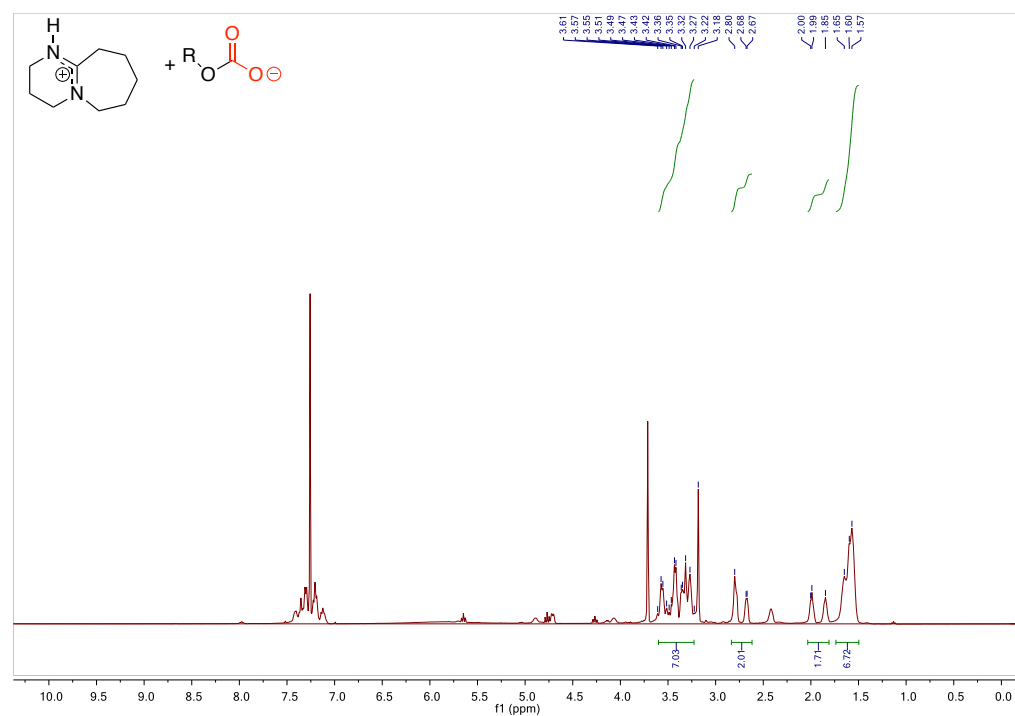
**2e.**  $^1\text{H}$  NMR (400 MHz,  $\text{CDCl}_3$ )  $\delta$  4.61 (dtt,  $J = 12.3, 6.2, 3.1$  Hz, 1H), 1.92 (dd,  $J = 14.2, 3.1$  Hz, 1H), 1.79 – 1.69 (m, 1H), 1.38 (d,  $J = 6.2$  Hz, 6H), 1.40 (d,  $J = 6.2$  Hz, 3H)

A4.9  $^1\text{H}$  NMR spectrum of reaction mixture and DBU salt for conversion of 1n into 2n (Table 4.9 entry 3), after  $\text{CO}_2$  switch.



**2n.**  $^1\text{H}$  NMR (400 MHz,  $\text{CDCl}_3$ )  $\delta$  7.49 – 7.19 (m, 5H), 5.64 (t,  $J = 8.0$  Hz, 1H), 4.82 – 4.72 (m, 1H), 4.35 – 4.26 (m, 1H).

**1n.**  $^1\text{H}$  NMR (400 MHz,  $\text{CDCl}_3$ )  $\delta$  7.49 – 7.19 (m, 5H), 4.82 – 4.72 (m, 1H), 3.74 – 3.66 (m, 1H), 3.63 – 3.55 (m, 1H).



**DBU**  $^1\text{H}$  NMR (400 MHz,  $\text{CDCl}_3$ )  $\delta$  3.60 – 3.23 (m, 6H), 2.83 – 2.62 (m, 2H), 2.03 – 1.81 (m, 2H), 1.74 – 1.50 (m, 6H).

## 4.2. HETEROGENEOUS CATALYSTS: CHAR-BASED BASIC CATALYSTS FROM POTATO STARCH

### 4.2.1 Introduction

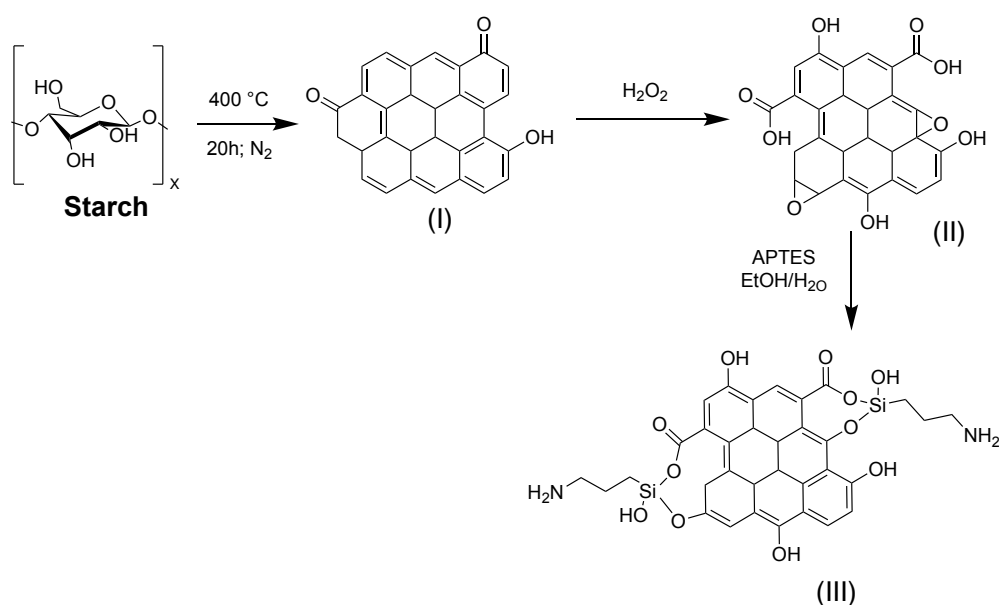
As stated in the previous chapter, the CIR of diols and DMC to obtain CCs has been performed using various basic catalysts, due to their superior performances respect to the acid ones. The key factor is the ability of a base to deprotonate the hydroxyl group in the rate determining step of the reaction that leads to the final cyclization (chapter 4.1, **Scheme 4.1**).<sup>1</sup>

Nevertheless, broad studies of both acid and basic catalyst in homogeneous and heterogeneous phase have been reported.<sup>2,3</sup> Among the acid heterogeneous catalysts, acid Amberlyst were unsuccessfully tested, obtaining very low conversion of glycerol (GLY) into glycerol carbonate (GC). Looking at heterogeneous basic catalysts, MgO, Amberlyst A26OH and Amberjet 4400 OH gave very scarce yields in the same reaction. CaO and CaCO<sub>3</sub> proved to be very active, instead, only after calcination at 900 °C. According to Ochoa-Gómez *et al.* the transcarbonation route from DMC with GLY is suitable for industrial production and involves uncalcined CaO as this heterogeneous catalyst is cheap and can be easily separated by filtration. In fact, although its performance is slightly worse than that of the calcined catalyst, due to the presence of impurities such as Ca(OH)<sub>2</sub> and CaCO<sub>3</sub>, the calcined catalyst is deactivated and must be regenerated after reaction. Interestingly also immobilized lipases, like *Candida antarctica lipase B* (CALB, Novozym 435) has been used to run this transesterification.<sup>4-6</sup> Also Mg/ZnO catalyst has been applied to GC synthesis obtaining a yield of 96%. Fishmeal biochar have been used for the reaction of GLY, using it without derivatization after the pyrolysis at 550-750 °C, obtaining GC in very good yields (99 %); the char was also recycled over five times with a slight decrease in reactivity.<sup>7,8</sup>

After using DBU as homogeneous catalyst and having developed a protocol to make it heterogeneous and easily separable, through the formation of its salt with CO<sub>2</sub>, the next goal was to use a totally heterogeneous catalyst. For this reason the char-based catalyst, developed for the synthesis of CCs from epoxides and CO<sub>2</sub>, was firstly tested on CIR from diols and DMC (see Chapter 3.2), by-passing the quaternarization step. Starting from the pyrolysis and oxidation of the potato starch, used as model starting material, two methods to obtain the amine functionalization on the char surface were developed. Then the optimized conditions, for CIR of 1,2-hexanediol (**1a**) and DMC, were found and the recyclability of the catalysts was checked.

## 4.2.2 Results and discussion

The first procedure, adopted to produce the basic catalysts from potato starch, resumed the method used to synthesize the catalysts described in Chapter 3.2. The changed protocol (see experimental section) is a 3-step synthetic pathway consisting of: a) carbonization of the starting material to give a char (I); b) oxidation of the char with H<sub>2</sub>O<sub>2</sub> to give an oxidized char (II); c) functionalization of (II) through the introduction of the amine moiety by the anchoring of APTES (III). (Scheme 4.1)



**Scheme 4.1** Synthetic pathway for APTES-functionalized char.

The potato starch was pyrolyzed at 400 °C for 15h: from previous observations we found that these conditions produced a char that could be well oxidized in the next step (see experimental part). In fact, higher temperatures generate a more carbonaceous and aromatic char, which is therefore more inert and difficult to oxidize.<sup>9,10</sup>

From previous research we found H<sub>2</sub>O<sub>2</sub> as best oxidizer in terms of oxidation conditions, cost, and safety (see chapter 3.2). Various catalysts applied in CIR were synthesized using different oxidation conditions and various methodologies to anchor (3-Aminopropyl)triethoxysilane (APTES) on the surface of the char (see experimental part): they are resumed in **Table 4.1**. For

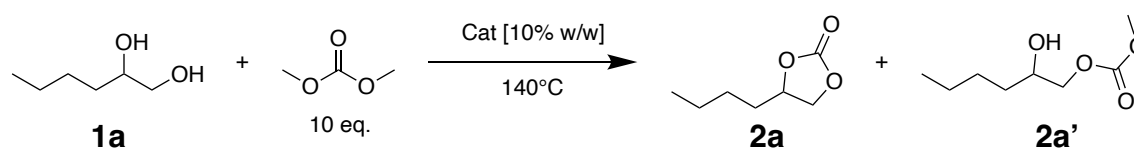
each catalyst (**A-F**) elemental composition (see experimental part), especially in term of nitrogen content, related to the derivatization with APTES, has been checked.

**Table 4.1** Elemental composition of the catalysts synthesized from potato starch over different reaction conditions (mean  $\pm$  standard deviation of three independent replicates).

Label	Conditions	N [%]	C [%]	H [%]
<b>A</b>	Starch Char (400 °C), H <sub>2</sub> O <sub>2</sub> (85 °C, 24 h) APTES 4,6% w/w (EtOH/H <sub>2</sub> O, 95/5, 85 °C, 4 h)	5.7 $\pm$ 0.3	38.2 $\pm$ 0.2	4.8 $\pm$ 0.2
<b>B</b>	Starch Char (400 °C), H <sub>2</sub> O <sub>2</sub> (85 °C, 24 h) APTES 4,6% w/w (EtOH/H <sub>2</sub> O, 90/10, 85 °C, 4 h)	6.4 $\pm$ 0.6	34.2 $\pm$ 0.1	4.9 $\pm$ 0.2
<b>C</b>	Starch Char (400 °C), H <sub>2</sub> O <sub>2</sub> (85 °C, 24 h) APTES 4,6% w/w (EtOH/H <sub>2</sub> O, 98/2, 85 °C, 4 h)	5.5 $\pm$ 0.3	36 $\pm$ 0.1	4.7 $\pm$ 0.1
<b>D</b>	Starch Char (400 °C), H <sub>2</sub> O <sub>2</sub> (85 °C, 24 h) APTES 4,6% w/w (EtOH, 85 °C, 4 h)	4.3 $\pm$ 0.1	41.9 $\pm$ 0.5	4.7 $\pm$ 0.3
<b>E</b>	Starch Char (400 °C), H <sub>2</sub> O <sub>2</sub> (85 °C, 6 h) APTES 4,6% w/w (EtOH/H <sub>2</sub> O, 95/5, 85 °C, 4 h)	1.3 $\pm$ 0.1	62.8 $\pm$ 0.2	3.34 $\pm$ 0.1
<b>F</b>	Starch Char (400 °C), H <sub>2</sub> O <sub>2</sub> (85 °C, 20 h) APTES 4,6% w/w (EtOH/H <sub>2</sub> O, 95/5, 85 °C, 4 h)	5.6 $\pm$ 0.2	40.1 $\pm$ 0.4	4.6 $\pm$ 0.4

Then the catalysts have been tested using as model reaction the CIR from 1,2-hexanediol (**1a**) and DMC, using the same conditions: 10 eq. of DMC, 10% w/w of the catalysts respect to the diol, at 140 °C. The reaction was conducted in a closed vial, under autogenous pressure. From the GC-analysis, together with the formation of the cyclic carbonate **2a**, also minor amounts of the linear methyl carbonate **2a'** was found. The comparison of the activity of the catalysts are resumed in **Table 4.2**.

**Table 4.2** Test of catalysts **A-F** in the synthesis of **1a** into **2a**.



Entry	Catalyst	Cycle	Time [h]	Conversion [%] <sup>a</sup>	Selectivity [%] <sup>a</sup>
1	<b>A</b>	I	6	98	98:2
		II	6	98	98:2
		III*	6	98*	98:2
2	<b>B</b>	I	6	0	-
		II	6	95*	96:4

3	C	I	6	0	-
		II*	20	93*	95:5
4	D	I	6	0	96:4
		II	6	10	97:3
5	E	I	10	0	-
6	F	I	2	95	95:5
		II*	2 10	0 95*	0 95:5

Reaction conditions: 1 mmol **1a** (124.6  $\mu$ L), 10 eq. DMC (842  $\mu$ L), catalyst (A-F) 10% w/w, 140°C, closed vial.

\*Catalyst in homogeneous phase.

<sup>a</sup>Conversions and selectivity calculated by GC-MS (see experimental section).

The tuning of the conditions for the synthesis of the catalysts **A-F** regarded both the oxidation time with H<sub>2</sub>O<sub>2</sub> (from 6 to 24 hours) and the ratio of EtOH/H<sub>2</sub>O used in functionalization with APTES (**Table 4.1**). An appropriate number of functional groups present on the char surface after oxidation is crucial to obtain a functionalization with APTES. The oxidation time required for a good grade of oxidation is >20 hours: catalyst **E** (**Table 4.1**), that reacted with H<sub>2</sub>O<sub>2</sub> for only 6 h, proved to have a very little amount of N, respect to the other catalysts, as demonstration of the low grade of functionalization with APTES. As expected, **E** was ineffective in CIR (**Table 4.2**, entry 5). The catalysts oxidated for longer time didn't present dramatic differences in CHN analyses (**A-D**, **F**) but the ratio EtOH/H<sub>2</sub>O used for amination proved to be crucial in their reactivity towards CIR: the optimum ratio was 95/5 (**A** and **F**). Catalysts **A** and **F** (whose only difference consists in 4 h of oxidation) had similar activity (**Table 4.2**, entries 1 and 6). Little amount of water in fact seemed to be mandatory to produce an active catalyst: water hydrolyzes the ethoxy groups of the APTES to hydroxyl group,<sup>11</sup> that can have a role in reaction mechanism, in stabilizing some reaction intermediates, in fact catalyst **D**, synthesized without water, was totally unactive toward CIR (**Table 4.2**, entry 4). Catalyst **B**, synthesized with a ratio EtOH/H<sub>2</sub>O of 90/10 was ineffective at the first cycle (**Table 4.2**, entry 2), giving good yields only in the second one (for the methods used in catalyst recycling, see experimental part). The same behavior was found for catalyst **C** (**Table 4.2**, entry 3), functionalized with a ratio EtOH/H<sub>2</sub>O of 98/2: probably in this case the amount of water was too low.

In any case, even the catalysts **A** and **F**, which seemed to have a greater reactivity in the first cycles, underwent to a probable deactivation or modification: the subsequent cycles needed longer reaction times (**Table 4.2** entry 1 and 6,) often becoming homogeneous with the reaction system. This deactivation of the catalyst was also suggested by the strong yellowing of the reaction solution and by the presence of many impurities found in the  $^1\text{H}$  NMR of the reaction crude.

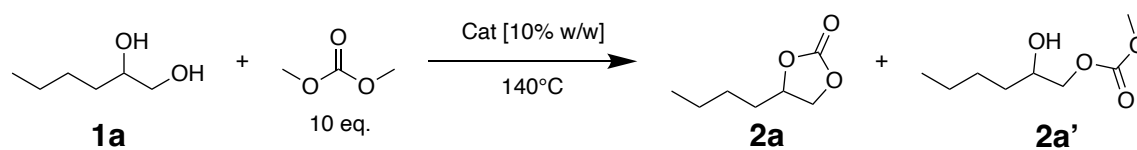
The strength and stability that the oxidized char derivatized with APTES had in the reaction with epoxides and  $\text{CO}_2$  (70 °C, 7h, neat reaction, see chapter 3.2), were not maintained under the harsher conditions here used for CIR (140 °C, 6-20h, in DMC). However, also with catalyst **A** and **F** the reaction didn't obtain good yields at temperatures < 130°C, even for prolonged reaction time.

For this reason, a char-based catalyst, oxidized in similar conditions, but functionalized with a different amino group, was synthesized.

Elemental analysis of the functionalized char over different reaction conditions were resumed in **Table 4.3**, while their test on CIRs of 1,2-hexanediol (**1a**) and DMC in **Table 4.4** (see experimental section). Equal conditions have been used to test the catalysts: 10 eq. of DMC, 10% w/w of the catalysts respect to the diol, at 140°C, in a closed vial.

**Table 4.3** Elemental composition of the catalysts synthesized from potato starch over different reaction conditions (mean  $\pm$  standard deviation of three independent replicates).

Label	Conditions	N [%]	C [%]	H [%]
<b>G</b>	Starch Char (400 °C), $\text{H}_2\text{O}_2$ 85 °C <b>16h</b> , 1,6-hexanediamine (130 °C, 17 h)	4.6 $\pm$ 0.1	55.4 $\pm$ 0.4	4.6 $\pm$ 0.1
<b>H</b>	Starch Char (400 °C), 1,6-hexanediamine (130 °C, 17 h)	0.82 $\pm$ 0.1	79.3 $\pm$ 0.2	2.4 $\pm$ 0.1
<b>I</b>	Starch Char (400 °C), $\text{H}_2\text{O}_2$ 85 °C <b>24h</b> , 1,6-hexanediamine (130 °C, 17 h)	5.7 $\pm$ 0.2	58.6 $\pm$ 0.7	5.0 $\pm$ 0.2
<b>J</b>	Starch Char (400 °C), $\text{H}_2\text{O}_2$ 85 °C 16h, <b>Ethylene diamine</b> (130 °C, 17 h)	7.3 $\pm$ 0.2	66.7 $\pm$ 0.6	4.1 $\pm$ 0.1
<b>K</b>	Starch Char (400 °C), $\text{H}_2\text{O}_2$ 85 °C 16h, <b>Ethanolamine</b> (130 °C, 17 h)	5.4 $\pm$ 0.1	67.9 $\pm$ 0.5	4.2 $\pm$ 0.1

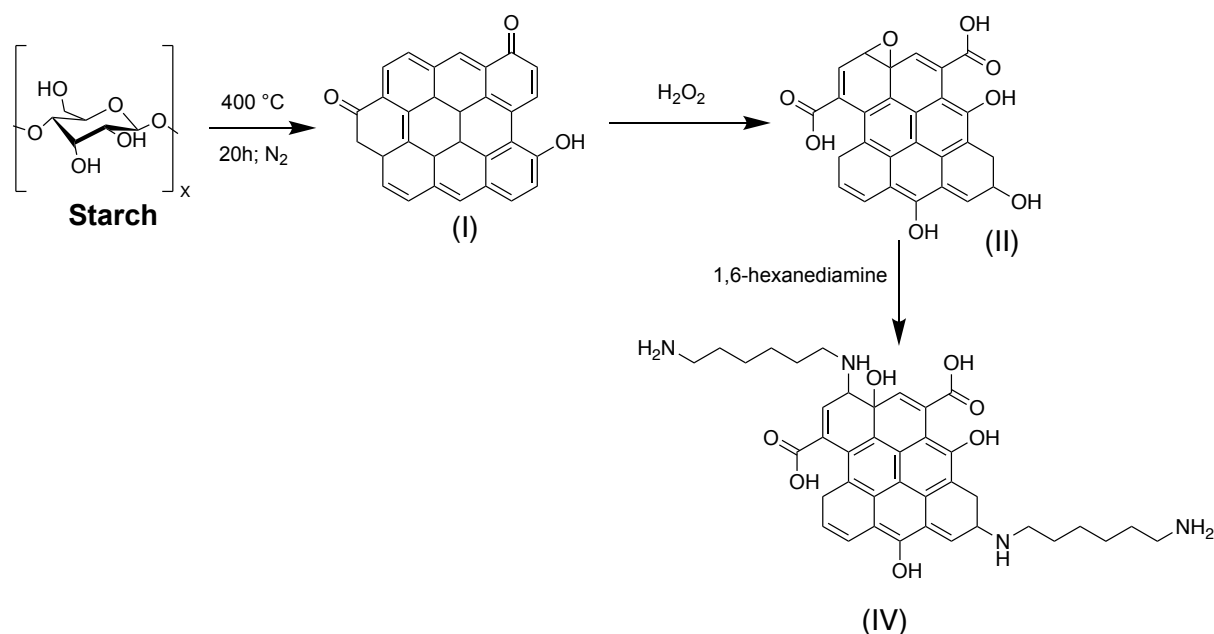
**Table 4.4** Test of catalysts **G-H** in the synthesis of **1a** into **2a**.

Entry	Catalyst	Conversion [%] <sup>a</sup>	Selectivity [%] <sup>a</sup>
1	G	95	96
2	H	0	0
3	I	71	96
4	J	0	0
5	K	0	0

Reaction conditions: 1 mmol **1a** (124.6  $\mu$ L), 10 eq. DMC (842  $\mu$ L), catalyst (G-K) 10% w/w, 140°C, closed vial.

<sup>a</sup> Conversions and selectivity calculated by GC-MS (see experimental section).

The tuning of the conditions to obtain the most reactive catalyst (resumed in **Table 4.3**), was mainly focused on the oxidizing step, since it was the factor that most affected the anchoring of the amine and the reactivity of the catalyst. It was found that using a solution of different amines in water at 130 °C for 17h, nitrogen content of the char increased (**Table 4.3, G,I-K**). Functionalizing the char directly after pyrolysis, by-passing oxidation, a low nitrogen content was detected (**Table 4.3, H**): oxidized chars have plenty of functional groups (carboxylic acids, aldehydes, ketones, epoxides, etc.) able to react with the amine, while the char after pyrolysis is highly aromatic and so inert. For this reason, catalyst **H** was inactive as catalyst for CIR (**Table 4.4**, entry 2). Interestingly, highly oxidized char incorporated a higher quantity of the amine (**Table 4.3, I**), but when used as catalyst in the CIR it was less active (**Table 4.4**, entry 3) than a lower oxidized char, **G** (**Table 4.4**, entry 1). Apparently, this behavior seems to be in contrast with the degree of functionalization, however it can be explained considering the hypothetical structure of the char (**Scheme 4.2**). We expected to obtain the final char as in structure (IV), with one -NH<sub>2</sub> bonded to the char and the other one remained primary amines, as a pendant. Highly oxidized char, having much more sites at step (II), on which 1,6-hexanediamine can be anchored, can lead to the bonding of both -NH<sub>2</sub> groups of the diamine. In this way, the amine groups will be sterically hindered on surface of the char, thus being less available and making the catalyst less active.



**Scheme 4.2** Synthetic pathway for 1,6-hexanediamine-functionalized char (hypothetical structure).

Ethanolamine and Ethylenediamine were also successfully anchored on the char surface (**Table 4.3, J and K**), but were not active at all in the CIR (**Table 4.4**, entries 4 and 5). This is probably due to the steric hinderance given by the short chain of the amines, that makes the primary amine too close to the char surface.

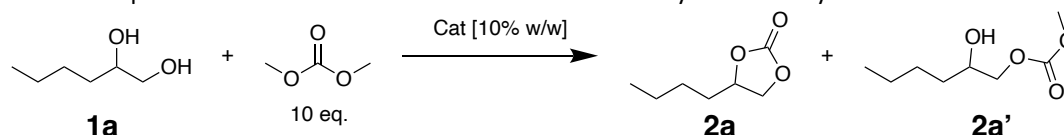
On the most reactive catalyst **G** elemental analysis (see experimental section) was made for the char after each reaction step (**Table 4.5**). After the pyrolysis process (I), the decrease in hydrogen is observed, due to the condensation of carbonaceous rings. Just a slight decrease in carbon content was found after oxidation (II). With amination (IV) a further decrease of the carbon component and obviously the amino component was present.

**Table 4.5** Elemental composition analyzed after each reaction step, for the synthesis of the functionalized char **G**, derived from potato starch (mean  $\pm$  standard deviation of three independent replicates).

Label	Reaction Step	N [%]	C [%]	H [%]
	Starting material	-	37.5 $\pm$ 0.7	6.4 $\pm$ 0.1
(I)	Step 1 - Pyrolysis	-	82.8 $\pm$ 0.3	2.8 $\pm$ 0.1
(II)	Step 2 - Oxidation	-	63.8 $\pm$ 0.2	3.0 $\pm$ 0.2
(IV)	Step 3 - Amination	4.6 $\pm$ 0.1	55.4 $\pm$ 0.4	4.6 $\pm$ 0.1

Conditions used for the activity evaluation of the differently functionalized catalysts for the CIR, were optimized using the most active catalyst **G** (Table 4.6), finding that 140 °C were necessary to obtain the highest yield and selectivity (Table 4.6, entry 5) and that 2h, instead of 4h, are enough to obtain similar results (Table 4.6, entry 6).

**Table 4.6** Optimization of the reaction conditions for the catalyst **G** in the synthesis of **1a** into **2a**.



Entry <sup>a</sup>	Catalyst amount [% w/w]	T [°C]	t [h]	Conversion [%] <sup>a</sup>	Selectivity [%] <sup>a</sup>
1	10	90	4	0	0
2	10	110	4	0	0
3	10	120	4	9	0
4	10	130	4	37	1
5	10	140	4	96	97
6	10	140	2	95	96

Reaction conditions: 1 mmol **1a** (124.6  $\mu$ L), 10 eq. DMC (842  $\mu$ L), catalyst **G** 10% w/w, closed vial.

<sup>a</sup> Conversions and selectivity calculated by GC-MS (see experimental section).

Catalyst **G** was also recycled (see experimental section) over five times without appreciable loss of catalytic activity (Figure 4.1)

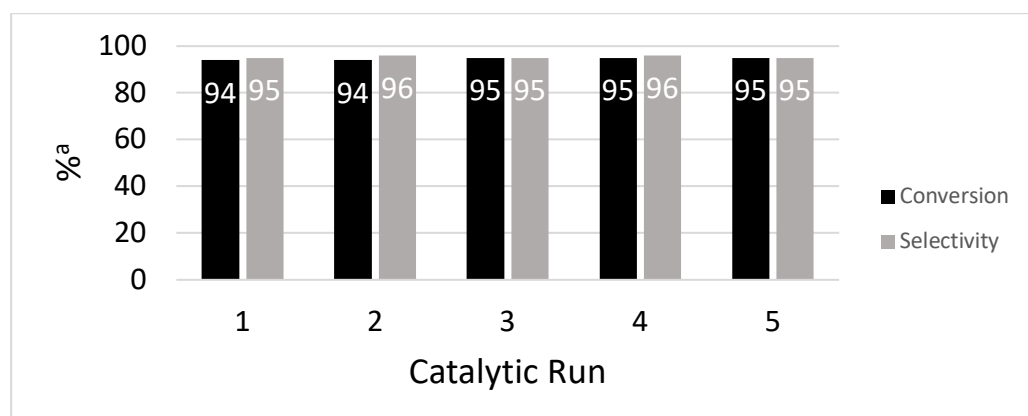


**Figure 4.1** Recycle of catalyst **G** in the synthesis of **1a** into **2a**.

Reaction conditions: 1 mmol **1a** (124.6  $\mu$ L), 10 eq. DMC (842  $\mu$ L), catalyst **G** 10% w/w, 140 °C, 2h, closed vial.

<sup>a</sup> Conversions and selectivity calculated by GC-MS (see experimental section).

### 4.2.3 Conclusions

Wanting to develop a heterogeneous basic catalyst to run CIR for the conversion of 1,2-hexanediol **1a** into its corresponding 5-membered cyclic carbonate, firstly some catalysts (**A-G**), synthesizing them with the same procedure used for the synthesis from epoxides and CO<sub>2</sub> (see chapter 3.2) were tested. Starting from pyrolyzed potato starch, various oxidation with H<sub>2</sub>O<sub>2</sub> and functionalization methods with APTES have been tested. Although some catalysts seemed active, their poor stability as heterogeneous catalysts and their non-recyclability led to the study other kind of functionalization. Always starting from the pyrolysis of potato starch, a derivatization including an oxidation step and an amination step, with 1,6-hexanediamine, has been optimized. The best performing catalyst, **G**, was studied in different conditions, obtaining very good conversion and selectivity in the CIR of **1a** into **2b**. It has also been recycled over five times without any loss of catalytic activity. Further studies, regarding the chemical-physical analyses of the materials obtained and the study of other substrates, are in progress.

### 4.2.4 Experimental section

#### Material

All chemicals and solvents were purchased from Sigma-Aldrich or Alfa Aesar and used without any further purification.

Catalyst synthesis: All the catalysts reported in this work (**A-K**) were synthesized following the 3-steps optimized experimental procedure reported as follows.

1. Pyrolysis of the starting material. Pyrolysis was conducted following a previously reported procedure.<sup>10</sup> Hence, potato starch (3g) was subjected to a bench-scale pyrolysis, using an apparatus consisting of a sliding sample carrier placed in a heated quartz tube connected to ice traps and a settling chamber. The quartz tube was heated by a cylindrical co-axial furnace and purged by 1.5 L min<sup>-1</sup> N<sub>2</sub> flow. Sample was moved into the heated zone of the quartz tube and heated for 15 h at 420 °C (measured temperature) under N<sub>2</sub> flow. The resulting char was collected, ground to powder in a mortar and used for the next steps without further purification. Yield: 15%

2. Oxidation of chars. In a 50 mL round bottomed flask, potato derived char (500 mg) was stirred in H<sub>2</sub>O<sub>2</sub> (25 mL) in various conditions. After that time, the reaction mixture was cooled to rt and a solution of HCl 1M (5 mL) was added, then the suspension was filtered and washed several times with H<sub>2</sub>O to recover the oxidized char (II), that was dried overnight at 70 °C under reduced pressure (100 mbar). Yield: 95%

3.1 APTES anchoring. In a 25 mL round bottomed flask equipped with a reflux condenser, oxidized char (80 mg) was added to a solution of aminopropyltriethoxysilane (APTES, 4.6 v/v%) in a mixture EtOH/H<sub>2</sub>O at various ratio (5 mL). The mixture was stirred at different temperatures for different time, then the solution was filtered and washed three times with EtOH (10 mL). The resulting amine-functionalized char was dried overnight at 70 °C under reduced pressure (100 mbar).

3.2 Diamine anchoring. In a 10 mL closed vial oxidized char (110 mg), Hexanediamine (200 mg) and H<sub>2</sub>O (1 mL) were stirred at 130 °C for 17h. The mixture was then cooled to rt and the suspension was filtered and washed with water several times (10 x 75 mL) to recover amine functionalized char (IV). Wet catalysts were dried overnight at 70 °C under reduced pressure (100 mbar). Yield: 99.9%

#### Representative procedure for the synthesis of 2a

The synthesis of **2a** (Table 4.2, 4.4 and 4.6) catalyzed with catalysts **A-K** was carried out in 10 ml-screw-capped tubes. Inside the test tube the starting material **1a** (1mmol), the catalyst (10% w/w) and DMC (10 equivalents) were added. The test tube was closed and heated under stirring at different temperature. At the end of the reaction, mix is centrifuged, and an aliquot of the crude supernatant was silylated, diluted and analyzed through GC-MS.

The concentrations **1a** and **2a** were obtained directly from their respective peak areas in the gas chromatograph, as compared to peak's retention time of **1a** and **2a** standards. The conversion of **1a** and the selectivity were calculated using these equations:

$$\text{Conversion, } C = (1a_{\text{initial}} + 1a_{\text{residual}}) / (1a_{\text{initial}}) \times 100$$

$$\text{Selectivity, } S = (2a) / (1a_{\text{initial}} - 1a_{\text{residual}}) \times 100$$

The product obtained can be isolated distilling DMC.

Crudes were also analyzed through <sup>1</sup>H NMR (see Appendix 4.2)

### Silylation procedure

50 mL of silylating agent N,O-bis(trimethylsilyl)trifluoroacetamide and 1% chlorotrimethylsilane, (BSTFA + 1% TMCS), 100 mL of ethyl acetate and 20 mL of pyridine were added to 1–10 mg of sample into a GC-MS vial. The vial was heated at 60–80 °C for 30–40 min. The sample was then diluted with ethyl acetate before the injection.

### Catalysts recycle

At the end of the reaction the mixture was centrifuged, and the liquid supernatant removed. The catalyst was washed twice with Et<sub>2</sub>O and then dried overnight under reduced pressure. The catalyst was weighted before starting a new cycle to check its total recovery.

### Instrumentation

GC-MS analyses of reaction mixtures were performed using an Agilent HP 6850 gas chromatograph connected to an Agilent HP 5975 quadrupole mass spectrometer. Analytes were separated on a HP-5MS fused-silica capillary column (stationary phase 5%-Phenyl)-methylpolysiloxane, 30 m, 0.25 mm i.d., 0.25 μm film thickness), with helium as the carrier gas (at constant pressure, 36 cm s<sup>-1</sup> linear velocity at 200 °C). Mass spectra were recorded under electron ionization (70 eV) at a frequency of 1 scan s<sup>-1</sup> within the 12–600 m/z range. The injection port temperature was 250 °C. The temperature of the column was kept at 50 °C for 5 min, then increased from 50 to 250 °C at 10 °C min<sup>-1</sup> and the final temperature of 250 °C was kept for 12 min.

<sup>1</sup>H NMR spectra were recorded on Varian 400 (400 MHz) spectrometers. <sup>13</sup>C NMR spectra were recorded on a Varian 400 (100 MHz) spectrometers. Chemical shifts are reported in ppm from TMS with the solvent resonance as the internal standard (deuteriochloroform: 7.26 ppm). The elemental composition of the starting materials, the chars at each derivatization step and the final catalysts was determined using an elemental analyzer (Thermo Scientific, Flash 2000, Organic Elemental Analyzer) through the flash combustion technique.

Characterization data of **2a** and **2a'**

**2a. 4-butyl-1,3-dioxolan-2-one**  $^1\text{H}$  NMR (400 MHz,  $\text{CDCl}_3$ )  $\delta$  4.68 (qd,  $J = 7.5, 5.5$  Hz, 1H), 4.50 (t,  $J = 8.1$  Hz, 1H), 4.04 (dd,  $J = 8.4, 7.2$  Hz, 1H), 1.84 – 1.73 (m, 1H), 1.71 – 1.61 (m, 1H), 1.48 – 1.28 (m, 4H), 0.91 (dd,  $J = 9.4, 4.7$  Hz, 3H).  $^{13}\text{C}$  NMR (100 MHz,  $\text{CDCl}_3$ )  $\delta$  155.03, 69.35, 33.54, 26.40, 22.22, 13.76.

## BIBLIOGRAPHY

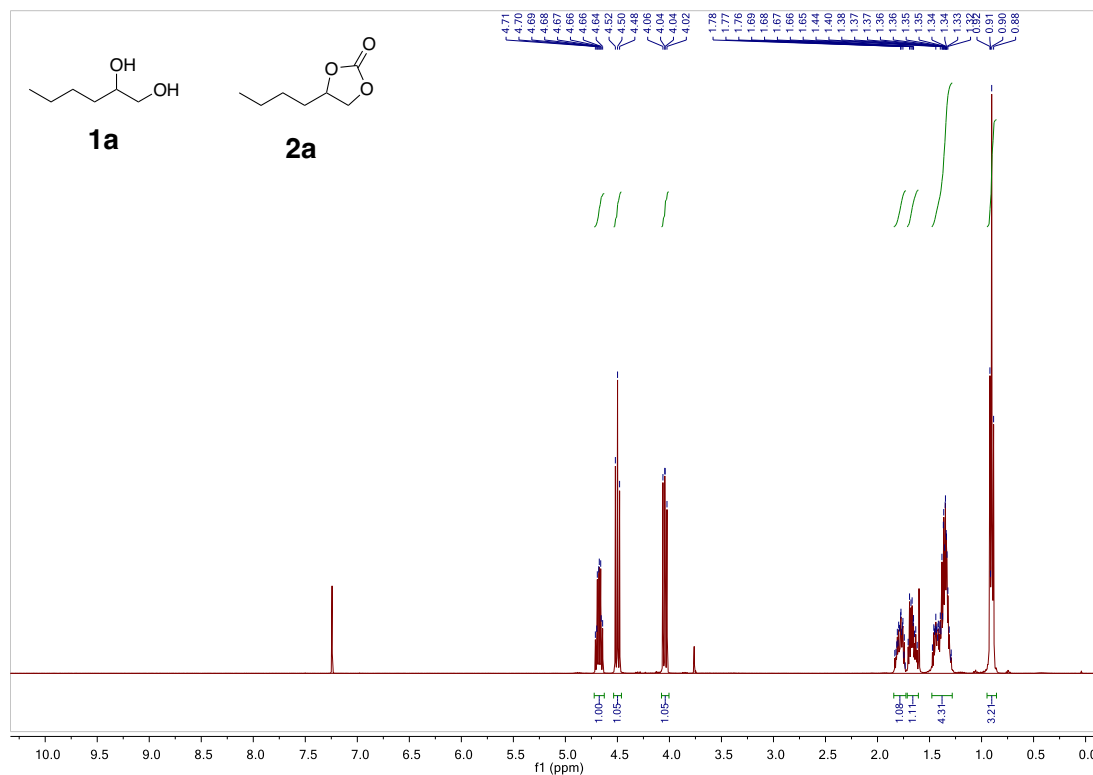
- (1) Fiorani, G.; Perosa, A.; Selva, M. Dimethyl Carbonate: A Versatile Reagent for a Sustainable Valorization of Renewables. *Green Chem.* **2018**, *20* (2), 288–322. <https://doi.org/10.1039/C7GC02118F>.
- (2) Ochoa-Gómez, J. R.; Gómez-Jiménez-Aberasturi, O.; Maestro-Madurga, B.; Pesquera-Rodríguez, A.; Ramírez-López, C.; Lorenzo-Ibarreta, L.; Torrecilla-Soria, J.; Villarán-Velasco, M. C. Synthesis of Glycerol Carbonate from Glycerol and Dimethyl Carbonate by Transesterification: Catalyst Screening and Reaction Optimization. *Appl. Catal. Gen.* **2009**, *366* (2), 315–324. <https://doi.org/10.1016/j.apcata.2009.07.020>.
- (3) de Caro, P.; Bandres, M.; Urrutigoity, M.; Cecutti, C.; Thiebaud-Roux, S. Recent Progress in Synthesis of Glycerol Carbonate and Evaluation of Its Plasticizing Properties. *Front. Chem.* **2019**, *7*, 308. <https://doi.org/10.3389/fchem.2019.00308>.
- (4) Kim, S. C.; Kim, Y. H.; Lee, H.; Yoon, D. Y.; Song, B. K. Lipase-Catalyzed Synthesis of Glycerol Carbonate from Renewable Glycerol and Dimethyl Carbonate through Transesterification. *J. Mol. Catal. B Enzym.* **2007**, *49* (1), 75–78. <https://doi.org/10.1016/j.molcatb.2007.08.007>.
- (5) Leão, R. A. C.; Souza, S. P. de; Nogueira, D. O.; Silva, G. M. A.; Silva, M. V. M.; Gutarra, M. L. E.; Miranda, L. S. M.; Castro, A. M.; Junior, I. I.; Souza, R. O. M. A. de. Consecutive Lipase Immobilization and Glycerol Carbonate Production under Continuous-Flow Conditions. *Catal. Sci. Technol.* **2016**, *6* (13), 4743–4748. <https://doi.org/10.1039/C6CY00295A>.
- (6) Du, Y.; Gao, J.; Kong, W.; Zhou, L.; Ma, L.; He, Y.; Huang, Z.; Jiang, Y. Enzymatic Synthesis of Glycerol Carbonate Using a Lipase Immobilized on Magnetic Organosilica Nanoflowers as a Catalyst. *ACS Omega* **2018**, *3* (6), 6642–6650. <https://doi.org/10.1021/acsomega.8b00746>.
- (7) Shikhaliyev, K.; Okoye, P. U.; Hameed, B. H. Transesterification of Biodiesel Byproduct Glycerol and Dimethyl Carbonate over Porous Biochar Derived from Pyrolysis of Fishery Waste. *Energy Convers. Manag.* **2018**, *165*, 794–800. <https://doi.org/10.1016/j.enconman.2018.04.001>.
- (8) Shikhaliyev, K.; Hameed, B. H.; Okoye, P. U. Utilization of Biochars as Sustainable Catalysts for Upgrading of Glycerol from Biodiesel Production. *J. Environ. Chem. Eng.* **2021**, *9* (2). <https://doi.org/10.1016/j.jece.2020.104768>.
- (9) Samorì, C.; Torri, C.; Fabbri, D.; Falini, G.; Faraloni, C.; Galletti, P.; Spera, S.; Tagliavini, E.; Torzillo, G. Unusual Catalysts from Molasses: Synthesis, Properties and Application in Obtaining Biofuels from Algae. *ChemSusChem* **2012**, *5* (8), 1501–1512. <https://doi.org/10.1002/cssc.201100822>.
- (10) Samorì, C.; Parodi, A.; Tagliavini, E.; Galletti, P. Recycling of Post-Use Starch-Based Plastic Bags through Pyrolysis to Produce Sulfonated Catalysts and Chemicals. *J. Anal. Appl. Pyrolysis* **2021**, *155* (October 2020), 105030. <https://doi.org/10.1016/j.jaap.2021.105030>.
- (11) Pinheiro, A. F. de M.; Nijmeijer, A.; Sripathi, V. G. P.; Winnubst, L. Chemical Modification/Grafting of Mesoporous Alumina with Polydimethylsiloxane (PDMS). *Eur. J. Chem.* **2015**, *6* (3), 287–295. <https://doi.org/10.5155/eurjchem.6.3.287-295.1258>.

## APPENDIX 4.2

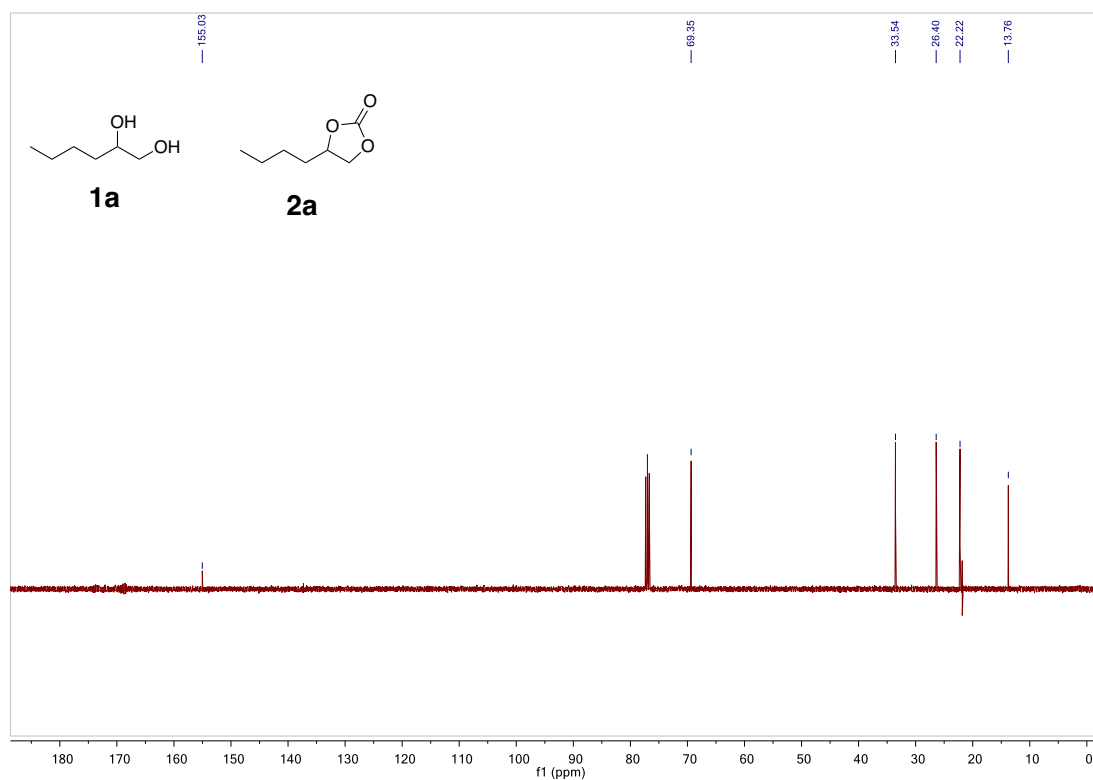
### Contents

A4.1.  $^1\text{H}$  NMR and  $^{13}\text{C}$  spectrum of reaction crude for conversion of **1a** into **2a** (Table 4.6, entry 5)

**A4.1.**  $^1\text{H}$  NMR and  $^{13}\text{C}$  spectrum of reaction crude for conversion of **1a** into **2a** (Table 4.6, entry 5)



**2a.**  $^1\text{H}$  NMR (400 MHz,  $\text{CDCl}_3$ )  $\delta$  4.68 (qd,  $J = 7.5, 5.5$  Hz, 1H), 4.50 (t,  $J = 8.1$  Hz, 1H), 4.04 (dd,  $J = 8.4, 7.2$  Hz, 1H), 1.84 – 1.73 (m, 1H), 1.71 – 1.61 (m, 1H), 1.48 – 1.28 (m, 4H), 0.91 (dd,  $J = 9.4, 4.7$  Hz, 3H).



**2a.**  $^{13}\text{C}$  NMR (100 MHz,  $\text{CDCl}_3$ )  $\delta$  155.03, 69.35, 33.54, 26.40, 22.22, 13.76

## CHAPTER 5

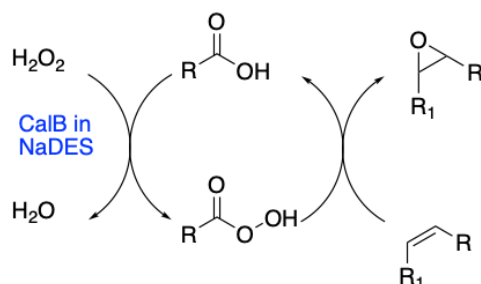
# LIPASE CATALYSED EPOXIDATIONS IN A SUGAR-DERIVED NATURAL DEEP EUTECTIC SOLVENT <sup>1</sup>

### 5.1 Introduction

Oxidation reactions have always been a major area of research due to their tremendous industrial applications. However, several oxidation processes present sustainability issues from the point of view of oxidants, catalysts and solvents used.<sup>2</sup> For example, a peracid is often used as the oxidizing agent,<sup>3</sup> but transportation and storage of organic peracids leads to significant safety issues and costs; when achievable, molecular oxygen or air are for sure the ideal oxidants, with hydrogen peroxide as the second-best choice, in terms of atom economy and versatility.<sup>4</sup> In this context, enzymes, that can work in sustainable solvents with mild oxidants, can contribute to increase the greenness of the oxidation reactions.<sup>5–13</sup> A very interesting system for obtaining peracids in situ is the chemoenzymatic system lipase/H<sub>2</sub>O<sub>2</sub> that continuously forms the peracids through a lipase-catalyzed perhydrolysis of carboxylic acids or their esters (**Scheme 5.1**).<sup>14–16</sup> A broad range of hydrolases has been investigated for the peracid formation and among them the lipase B from *Candida Antarctica* (CAL-B), immobilized onto an acrylic resin (Novozyme 435) is the most reactive.<sup>17</sup> This system has been successfully applied to epoxidations of alkenes (Prileshajev-epoxidation)<sup>18</sup> and other oxidations like Baeyer- Villiger (B-V) oxidations.

Epoxides are fundamental intermediates in organic synthesis, for example in the synthesis of cyclic carbonates and polycarbonates, when reacting with CO<sub>2</sub>. Despite their relevance, epoxides industrial synthesis is scarcely sustainable (both environmentally and economically). Epoxidation of some natural products is industrially carried out by the Prileshajev-epoxidation (epoxidation of an alkene with a peracid) using either preformed or in-situ-generated short chain peroxy acids.<sup>19,20</sup> Nevertheless, the need for a strong acid to catalyze peroxy acid formation in this process can result in unsatisfactory selectivity and undesirable side reactions via oxirane ring opening, leading to diols, hydroxyesters, and dimers. Prileshajev-epoxidation can be chemoenzymatically carried out on various substrates with CAL-B, a carboxylic acid as

precursor of the peracid, and H<sub>2</sub>O<sub>2</sub> as oxidant; this method allows an improvement in terms of sustainability, mild reaction conditions, limited side products and use of less toxic reagents.<sup>5,9,10,21</sup>



**Scheme 5.1** Chemoenzymatic pathway for epoxidations.

In addition to the type of catalyst and reagents, also reaction conditions and solvents used are key factors to define the greenness of the reaction system; to this purpose different green solvents have been exploited in chemoenzymatic oxidations, greatly contributing to the sustainability of the processes. They can be categorized into two main groups: (i) water and (ii) non-aqueous solvents like ionic liquids,<sup>22,23</sup> supercritical fluids and fluorinated solvents.<sup>24</sup> Deep Eutectic Solvents (DESs), described for the first time by Abbott *et al.* in 2001, are low melting mixtures based on a combination of readily available and inexpensive components, like quaternary ammonium salts as hydrogen bond acceptors (HBA), and acids, amides, amines, carbohydrates and alcohols as hydrogen bond donors (HBD).<sup>25</sup> They are liquid at or below 100 °C, thanks to H-bond interactions between the single components that create specific supramolecular structures. In 2013 Dai *et al.* reported numerous preparations of Natural Deep Eutectic Solvents (NaDESs) by using plant metabolites. Interestingly, when water is added to the mixtures, in different proportions according to the NaDES, it can be incorporated into this structure and becomes strongly bound, reducing the viscosity of the NaDES while retaining its original characteristics.<sup>26</sup>

The chemoenzymatic epoxidation systems described above have been studied in several solvents, including DESs,<sup>7,8,13,27–32</sup> in which it has been demonstrated that the enzymatic activity, stability, and selectivity can be enhanced.<sup>27,31,33–36</sup> Among the various NaDESs proposed by Dai *et al.*, this work focused on the only one sugar-derived and chlorine-free combination, composed by glucose, fructose, sucrose and water (1:1:1:11), that we called with the acronym GFS. To the best of our knowledge, the lipase/H<sub>2</sub>O<sub>2</sub> system was never

reported in a solvent like GFS and herein it is reported on its application in epoxidation from alkenes.

## 5.2 Results and discussion

The study of chemoenzymatic epoxidation of various alkenes is here reported (focusing for each of them on the enzyme amount, peracid precursors and H<sub>2</sub>O<sub>2</sub> amount and additions, and reaction time): cyclic alkenes (**Table 5.1**), poorly reactive stilbene (**Table 5.2**) and oleic acid (**Scheme 5.2**).

### Cyclic alkenes **1 a-1d**

Studying CAL-B mediated chemoenzymatic epoxidation in various NaDESs, Zhou *et al.* showed that amine-based DESs (i.e., choline chloride-urea, 1:2 molar ratio) significantly reduced the stability of CAL-B in a wide temperature range, whereas the polyol-based ones increased it.<sup>27</sup> For this reason, this study focused on polyol-based NaDESs. All the substrates tested are reported in **Table 5.1**. Cyclohexene **1a** (entry 1) was epoxidized with immobilised CAL-B (100 mg per 1.6 mmol of alkene), octanoic acid OA (one equivalent respect to the alkene), and H<sub>2</sub>O<sub>2</sub> (one equivalent respect to the alkene) in choline chloride-sorbitol (ChCl-Sorb), 1:1 molar ratio (400 mg), similarly to Zhou *et al.*<sup>27</sup> We observed a complete conversion of the starting material but a very low selectivity towards the epoxide; in fact the most of epoxide was converted into the chlorinated by-product and the diol after 20 h. This unexpected result encouraged the exclusive use of chloride-free, sugar-based NaDESs as the GFS.

We tested both solvents (ChCl-Sorb and GFS) in the same conditions with more easily detectable cyclododecene **1b** and we observed that GFS gave better conversions (entries 2 and 3); the same held true for other cyclic substrates (cyclooctene **1c** and limonene **1d**) (see Appendix Table A5.1, entries 1 and 5, and Table A5.2, entry 1). So, we decided to test various substrates to check the viability of the system. When Z/E mixtures were used in the starting alkene (as in **1b**), no diastereoselectivity was observed and the final product diastereomeric ratio reflected the diastereomeric distribution in the reagent.

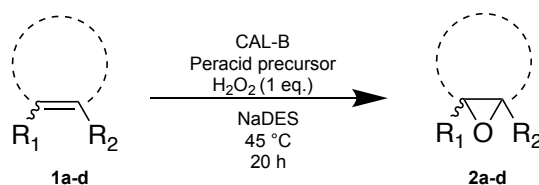
OA resulted the most reactive acid precursor under our conditions (entries 9-12), confirming the literature results, and its amount can be significantly lowered from 1 equivalent to 0.1 equivalents with all the substrates (entries 6, 8, 13, 14, 18). Considering aliphatic acids with different chain lengths, butyric acid BA (entry 10) gave very good results on **1c** while acetic

acid AA (entry 11) was poorly reactive; the biobased levulinic acid LA gave **2c** in good conversion (entry 12), prompting us to include 40 % of LA as a component of the GFS instead of water, with the aim of using it both as peracid precursor and solvent component; however in this case the epoxidation of cyclododecene **1b** was not satisfactory (entry 5). We also tested GFS-LA in combination with OA as peracid precursor on **1b**; results were good but lower than using GFS (entries 3 and 4). The same happened with **1c** (see Appendix, Table A5.1, entry 4). Dimethyl carbonate (DMC) was also tested as peracid precursor but without good results (see Appendix, Table A5.1, entries 1 and 3). The amount of the enzyme could be lowered till 30-25 U/mmol without significant loss of reactivity (entries 7 and 8, **1c** entry 14, **1d** entries 18 and 19).

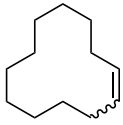
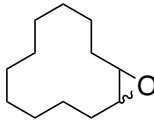
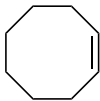
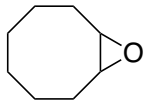
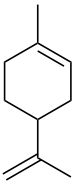
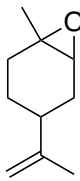
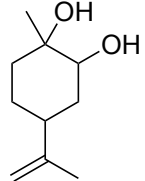
R-limonene **1d** is a very important biobased substrate, whose epoxy derivative has some relevance in the field of polymer synthesis.<sup>37</sup> Its internal double bond is much more reactive than the terminal one, being electron-richer; in all the tested conditions the product **2d** was obtained. Since the formation of the diol as by-product was initially observed (entry 15), milder conditions were tested on **1d**: i) halving the amount of NaDES; ii) keeping the temperature below 25 °C; iii) lowering addition rate of H<sub>2</sub>O<sub>2</sub>. All these conditions avoided the diol formation (entries 17 and 18). The use of a catalytic amount of acid precursor (entry 16) and a lower amount of the enzyme defined the best conditions to obtain **2d** in very good conversion (entry 18).

As expected from limonene results, terminal bonds of styrene and itaconic anhydride were not reactive in the mild condition we tested for the other substrates (see Appendix, Table A5.2, entries 5 and 6).

**Table 5.1.** Epoxidation of cyclic alkenes with chemoenzymatic method in NaDES.



Entry	Alkene	NaDES	CAL-B (U/mmol)	Peracid precursor [eq]	Product conversion [%] <sup>a</sup>	By-products conversion [%] <sup>a</sup>
	<b>1a</b>				<b>2a</b>	

						2 <sup>a'</sup>	2 <sup>a''</sup>
1	<b>1a</b>	ChCl-Sorb [1:1]	250	OA, 1	6	34	59
							-
2	<b>1b</b>	ChCl-Sorb [1:1]	250	OA, 1	68		
3	<b>1b</b>	GFS	250	OA, 1	71		
4	<b>1b</b>	GFS [1:1:1]-LA	250	OA, 1	64		
5	<b>1b</b>	GFS [1:1:1]-LA	250	LA	15		
6	<b>1b</b>	GFS	250	OA, 0.1	75		
7	<b>1b</b>	GFS	25	OA, 1	80		
8	<b>1b</b>	GFS	25	OA, 0.1	79 (77)		
							-
9	<b>1c</b>	GFS	250	OA, 1	>99		
10	<b>1c</b>	GFS	250	BA, 1	99		
11	<b>1c</b>	GFS	250	AA, 1	48		
12	<b>1c</b>	GFS	250	LA, 1	87		
13	<b>1c</b>	GFS	250	OA, 0.1	93		
14	<b>1c</b>	GFS	25	OA, 0.1	95 (91)		
							
15 <sup>c</sup>	<b>1d</b>	GFS	60	OA, 1	76		14
16 <sup>c</sup>	<b>1d</b>	GFS	60	OA, 0.1	73		16
17 <sup>c,d</sup>	<b>1d</b>	GFS	60	OA, 1	89		-
18 <sup>c,d</sup>	<b>1d</b>	GFS	30	OA, 0.1	96		-
19 <sup>c</sup>	<b>1d</b>	GFS	30	OA, 0.1	53		31

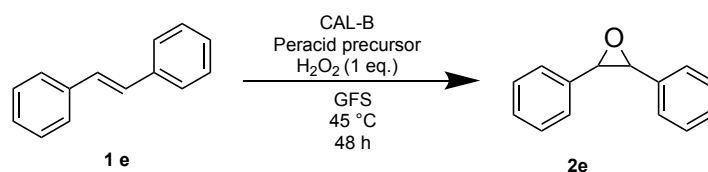
<sup>a</sup> Conversion by GC-MS, isolated yield in brackets; <sup>b</sup> diastereomeric ratio Z/E in **1b** and **2b** is always 2:1; <sup>c</sup> Room temperature (20 °C); <sup>d</sup> H<sub>2</sub>O<sub>2</sub> total amount divided into 4 portions added in 4 hours.

Acronyms: ChCl= choline chloride, Sorb = sorbitol, GFS = glucose, fructose, sucrose, H<sub>2</sub>O (1:1:1:11), OA= octanoic acid, LA= levulinic acid, AA = acetic acid, BA=butyric acid.

### Trans-Stilbene 1e

*Trans*-Stilbene **1e** is a challenging substrate because its double bond is electron-poor and it is poorly soluble in polar solvents like GFS. OA and other linear aliphatic carboxylic acids with shorter (hexanoic HA, butyric BA and acetic acid AA) and longer (dodecanoic acid, DA) chain lengths were tested as peracid precursors (Table 5.2). In all cases OA resulted the most effective acid precursor, but 1 equivalent was needed to obtain an effective conversion (entry 2). A decrease of the enzyme amount was possible, but a conversion of 75 % was reached only after 48 h (entry 4). Longer reaction times did not increase the conversion (see Appendix, Table A5.2, entries 4). Differently, the electron-poor, double bonds of crotonic acid and methyl crotonate were very difficult to be epoxidized (see Appendix, Table A5.2, entries 7 and 8) and we obtained just traces of the products. We also tested substrates carrying hydroxyl groups such as 1-octen-3-ol or *trans*-2-hexen- 1-ol but, as expected, the main product was the ester formed by OA and the alcohol under CAL-B catalysis (data not shown).

**Table 5.2** Epoxidation of *trans*-stilbene **1e** with chemoenzymatic method in GFS NaDES.



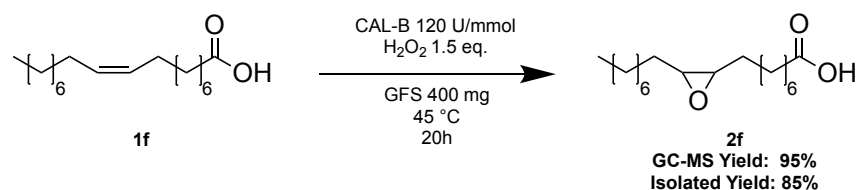
Entry	CAL-B [U/mmol]	Peracid precursor [eq]	2e conversion [%] <sup>a</sup>
1 <sup>b</sup>	250	OA, 1	60
2 <sup>b</sup>	250	OA, 0.1	traces
3	250	OA, 1	74 (70)
4	25	OA, 1	73
5	25	DA, 1	11
6	25	HA, 1	54
7	25	BA, 1	-
8	25	AA, 1	-

<sup>a</sup> Conversion by GC-MS, isolated yield in brackets; <sup>b</sup> time (20 h).

**Acronyms:** GFS = glucose, fructose, sucrose, water (1:1:1:11), OA= octanoic acid, DA = dodecanoic acid, HA= Hexanoic Acid, BA=butyric acid, AA = acetic acid.

### Oleic acid 1f

Oleic acid **1f** is a very interesting substrate since its epoxide (9,10-epoxystearic acid) is a highly valuable oleochemical due to its wide range of industrial applications, including cosmetics, personal care, and pharmaceutical products. The epoxidation worked very well and without the addition of OA (Scheme 5.2), thanks to an autocatalytic mechanism that formed the peroxy acid from the oleic acid itself.<sup>19</sup> A temperature of 45 °C was required not only to catalyze the reaction but also to avoid the product solidification. The conditions used are the same reported by the recent literature (temperature at maximum 50 °C, an excess of H<sub>2</sub>O<sub>2</sub>, short reaction time), except for the use of the solvent, which is generally toluene.<sup>38</sup> The epoxidation can also be carried out in a solvent-free system, but the process is more efficient for methyl oleate since the corresponding epoxide is liquid respect to solid 9,10-epoxystearic acid.<sup>39</sup>



**Scheme 5.2** Epoxidation of oleic acid with chemoenzymatic method in GFS.

### 5.3 Conclusions

We demonstrated that chemoenzymatic epoxidations using lipase CAL-B to form the active oxidant from carboxylic acid/H<sub>2</sub>O<sub>2</sub> pair can be performed in a sugar-based NaDES composed by an equimolar mixture of glucose, fructose, sucrose and water (GFS). Specific conditions to perform the reaction on selected substrates in good conversion and selectivity were found. The best conditions for epoxidations proved to be related to the substrate reactivity; reaction conditions were tuned and catalysts amounts decreased to obtain epoxides from poorly reactive and steric-hindered double bonds (as *trans*-stilbene) and to control the formation of byproducts in more reactive alkenes (like internal double bond of R-limonene).

## 5.4 Experimental section

### Materials

All chemicals and solvents were purchased from Sigma-Aldrich or Alfa Aesar and used without any further purification. CAL-B (Lipase B from *Candida antarctica*) immobilised on Immobead 150, recombinant from yeast, 4000 U/g was used.

### DESs preparation

The components were mixed with the appropriate stoichiometric ratios, heated at about 80–90 °C (120 °C for GFS) and magnetically stirred until homogeneous liquid was obtained; for GFS, distilled water (up to 30 wt %) was then added to get a homogeneous colorless liquid phase. All the DESs were cooled to rt (20 °C) before the use and stored in the fridge (4 °C).

### Representative procedure for enzymatic epoxidations of alkenes

In a 4-mL vial, the immobilised CAL-B (amounts reported in Tables 5.1–5.2 and Scheme 5.2) and 400 mg of DES (200mg for **1d**, 800mg for **1e**) were weighted, followed by the addition of 1.6mmol of alkene (0.8 mmol for **1f**), carboxylic acid (amounts reported in Tables 5.1–5.2 and Scheme 5.2) and 1 equivalent (eq) of H<sub>2</sub>O<sub>2</sub> (30% aqueous solution). For entries 17 and 18 in Table 5.1, H<sub>2</sub>O<sub>2</sub> has been added in 4 aliquots in 4h, for substrate **1f** 1.5 eq has been used. The vial was heated at 45 °C (or rt, 20 °C, for **1d**) for various reaction times, then crudes were extracted with cyclohexane or ethyl acetate and analysed by GC-MS. Extraction residues were checked after derivatization by silylation for the presence of other by-products. Conversions were calculated as ratios between products areas and total areas. <sup>1</sup>H and <sup>13</sup>C NMR spectra of some products have been acquired after purification of the crude by flash-column chromatography, some isolated yields are also reported. All products are known, they were recognized by comparison with standards or through mass spectra matching to what reported in NIST database.<sup>40</sup> Formation of by-products was checked by GC-MS and NMR.

### Silylation procedure

50mL of silylating agent N,O-bis(trimethylsilyl)trifluoroacetamide and 1% chlorotrimethylsilane, (BSTFA + 1% TMCS), 100 mL of CH<sub>3</sub>CN and 20 mL of pyridine were added

to 1–10mg of sample into a GC-MS vial. The vial was heated at 60-80 °C for 30-40 min. The sample was then diluted with CH<sub>3</sub>CN before the injection.

#### Purification procedure of selected products

Reaction mixtures were extracted with ethyl acetate or cyclohexane then washed with a NaHCO<sub>3</sub> solution to remove the octanoic acid (OA). After evaporating the solvent, the crude was purified by flash chromatography. The fractions containing the product were mixed, the solvent evaporated, and the purified products were analysed by GC-MS and NMR (see spectra in APPENDIX 5).

#### Instrumentation

GC-MS analysis of epoxides were performed using an Agilent HP 6850 gas chromatograph connected to an Agilent HP 5975 quadrupole mass spectrometer. Analytes were separated on a HP-5MS fused-silica capillary column (stationary phase 5%-phenyl)-methylpolysiloxane, 30 m, 0.25 mm i.d., 0.25 mm film thickness), with helium as the carrier gas (at constant pressure, 36 cm s<sup>-1</sup> linear velocity at 200 °C). Mass spectra were recorded under electron ionisation (70eV) at a frequency of 1 scan s<sup>-1</sup> within the 12600m/z range. The injection port temperature was 250 °C. The temperature of the column was kept at 50 °C for 5 min, then increased from 50 to 250 °C at 10 °C min<sup>-1</sup> and the final temperature of 250 °C was kept for 12 min. <sup>1</sup>H NMR spectra were recorded on Varian 400 (400 MHz) spectrometers. <sup>13</sup>C NMR spectra were recorded on a Varian 400 (100 MHz) spectrometers. Chemical shifts were reported in ppm from trimethylsilane (TMS) with the solvent resonance as the internal standard (deuteriochloroform: 7.26 ppm).

#### Characterization data of purified products (Spectra in Appendix 5)

**2b. Cyclododecene oxide** <sup>1</sup>H NMR (400 MHz, CDCl<sub>3</sub>) δ 2.89 (dd, *J* = 7.5, 6.0 Hz, 2H, *cis*-isomer), 2.70 (dd, *J* = 9.3, 2.1 Hz, 2H, *trans*-isomer), 2.22 – 2.13 (m, 2H, *trans*-isomer), 1.86 – 1.76 (m, 2H, *cis*-isomer), 1.65 – 1.17 (m, 34H), 1.04 (m, 2H, *trans*-isomer). <sup>13</sup>C NMR (100 MHz, CDCl<sub>3</sub>) δ 59.91, 58.16, 31.38, 26.65, 25.90, 25.53, 25.03, 24.05, 23.99, 23.86, 23.44, 22.42.

**2c. Cyclooctene oxide**  $^1\text{H}$  NMR (400 MHz,  $\text{CDCl}_3$ )  $\delta$  2.89 (qd,  $J = 4.3, 2.6$  Hz, 2H), 2.18 – 2.09 (m, 2H), 1.67 – 1.43 (m, 8H), 1.27 (dtd,  $J = 13.6, 10.0, 3.6$  Hz, 2H).  $^{13}\text{C}$  NMR (100 MHz,  $\text{CDCl}_3$ )  $\delta$  55.60, 26.87, 26.52, 26.25, 25.55

**2e. *Trans*-stilbene oxide**  $^1\text{H}$  NMR (400 MHz,  $\text{CDCl}_3$ )  $\delta$  7.42 – 7.32 (m, 10H), 3.87 (s, 2H).  $^{13}\text{C}$  NMR (100 MHz,  $\text{CDCl}_3$ )  $\delta$  137.06, 128.54, 128.30, 125.46, 62.83

**2f. 9,10-epoxystearic acid**  $^1\text{H}$  NMR (400 MHz,  $\text{CDCl}_3$ )  $\delta$  2.92 (s, 2H), 2.35 (t,  $J = 7.5$  Hz, 2H), 1.72 – 1.58 (m, 2H), 1.56 – 1.20 (m, 24H), 0.89 (t,  $J = 6.8$  Hz, 3H).  $^{13}\text{C}$  NMR (100 MHz,  $\text{CDCl}_3$ )  $\delta$  179.54, 57.27, 57.22, 33.92, 31.82, 29.51, 29.49, 29.27, 29.18, 29.12, 28.91, 27.77, 27.73, 26.55, 26.51, 24.59, 22.63, 14.06

## BIBLIOGRAPHY

- (1) Vagnoni, M.; Samorì, C.; Pirini, D.; Paz, M. K. V. D.; Gidey, D. G.; Galletti, P. Lipase Catalysed Oxidations in a Sugar-Derived Natural Deep Eutectic Solvent. *Biocatal. Biotransformation* **2021**.
- (2) Cavani, F.; Teles, J. H. Sustainability in Catalytic Oxidation: An Alternative Approach or a Structural Evolution? *ChemSusChem* **2009**, *2* (6), 508–534. <https://doi.org/10.1002/cssc.200900020>.
- (3) Swern, Daniel. Organic Peroxides. *Chem. Rev.* **1949**, *45* (1), 1–68. <https://doi.org/10.1021/cr60140a001>.
- (4) Burek, B. O.; Bormann, S.; Hollmann, F.; Bloh, J. Z.; Holtmann, D. Hydrogen Peroxide Driven Biocatalysis. *Green Chem.* **2019**, *21* (12), 3232–3249. <https://doi.org/10.1039/C9GC00633H>.
- (5) Niku-Paavola, M.-L.; Viikari, L. Enzymatic Oxidation of Alkenes. *J. Mol. Catal. B Enzym.* **2000**, *10* (4), 435–444. [https://doi.org/10.1016/S1381-1177\(99\)00117-4](https://doi.org/10.1016/S1381-1177(99)00117-4).
- (6) Constable, D. J. C.; Dunn, P. J.; Hayler, J. D.; Humphrey, G. R.; Johnnie L. Leazer, J.; Linderman, R. J.; Lorenz, K.; Manley, J.; Pearlman, B. A.; Wells, A.; Zaks, A.; Zhang, T. Y. Key Green Chemistry Research Areas—a Perspective from Pharmaceutical Manufacturers. *Green Chem.* **2007**, *9* (5), 411–420. <https://doi.org/10.1039/B703488C>.
- (7) Gorke, J. T.; Srienc, F.; Kazlauskas, R. J. Hydrolase-Catalyzed Biotransformations in Deep Eutectic Solvents. *Chem. Commun.* **2008**, No. 10, 1235–1237. <https://doi.org/10.1039/B716317G>.
- (8) Kotlewska, A. J.; Rantwijk, F. van; Sheldon, R. A.; Arends, I. W. C. E. Epoxidation and Baeyer–Villiger Oxidation Using Hydrogen Peroxide and a Lipase Dissolved in Ionic Liquids. *Green Chem.* **2011**, *13* (8), 2154–2160. <https://doi.org/10.1039/C1GC15255F>.
- (9) Silva, W. S. D.; Lapis, A. A. M.; Suarez, P. A. Z.; Neto, B. A. D. Enzyme-Mediated Epoxidation of Methyl Oleate Supported by Imidazolium-Based Ionic Liquids. *J. Mol. Catal. B Enzym.* **2011**, *68* (1), 98–103. <https://doi.org/10.1016/j.molcatb.2010.09.019>.
- (10) Hollmann, F.; Arends, I. W. C. E.; Buehler, K.; Schallmeyer, A.; Bühler, B. Enzyme-Mediated Oxidations for the Chemist. *Green Chem.* **2011**, *13* (2), 226–265. <https://doi.org/10.1039/C0GC00595A>.
- (11) Qin, Y.-Z.; Li, Y.-M.; Zong, M.-H.; Wu, H.; Li, N. Enzyme-Catalyzed Selective Oxidation of 5-Hydroxymethylfurfural (HMF) and Separation of HMF and 2,5-Diformylfuran Using Deep Eutectic Solvents. *Green Chem.* **2015**, *17* (7), 3718–3722. <https://doi.org/10.1039/C5GC00788G>.
- (12) Yin, J.; Wang, J.; Li, Z.; Li, D.; Yang, G.; Cui, Y.; Wang, A.; Li, C. Deep Desulfurization of Fuels Based on an Oxidation/Extraction Process with Acidic Deep Eutectic Solvents. *Green Chem.* **2015**, *17* (9), 4552–4559. <https://doi.org/10.1039/C5GC00709G>.
- (13) Yang, S.-L.; Duan, Z.-Q. Insight into Enzymatic Synthesis of Phosphatidylserine in Deep Eutectic Solvents. *Catal. Commun.* **2016**, *82*, 16–19. <https://doi.org/10.1016/j.catcom.2016.04.010>.
- (14) Björkling, F.; Godtfredsen, S. E.; Kirk, O. Lipase-Mediated Formation of Peroxycarboxylic Acids Used in Catalytic Epoxidation of Alkenes. *J. Chem. Soc. Chem. Commun.* **1990**, No. 19, 1301–1303. <https://doi.org/10.1039/C39900001301>.
- (15) Yadav, G. D.; Devi, K. M. Enzymatic Synthesis of Perlauric Acid Using Novozym 435. *Biochem. Eng. J.* **2002**, *10* (2), 93–101. [https://doi.org/10.1016/S1369-703X\(01\)00164-4](https://doi.org/10.1016/S1369-703X(01)00164-4).
- (16) Busto, E.; Gotor-Fernández, V.; Gotor, V. Hydrolases: Catalytically Promiscuous Enzymes for Non-Conventional Reactions in Organic Synthesis. *Chem. Soc. Rev.* **2010**, *39* (11), 4504–4523. <https://doi.org/10.1039/C003811C>.
- (17) Ortiz, C.; Ferreira, M. L.; Barbosa, O.; Santos, J. C. S. dos; Rodrigues, R. C.; Berenguer-Murcia, Á.; Briand, L. E.; Fernandez-Lafuente, R. Novozym 435: The “Perfect” Lipase Immobilized Biocatalyst? *Catal. Sci. Technol.* **2019**, *9* (10), 2380–2420. <https://doi.org/10.1039/C9CY00415G>.
- (18) Aouf, C.; Durand, E.; Lecomte, J.; Figueroa-Espinoza, M.-C.; Dubreucq, E.; Fulcrand, H.; Villeneuve, P. The Use of Lipases as Biocatalysts for the Epoxidation of Fatty Acids and Phenolic Compounds. *Green Chem.* **2014**, *16* (4), 1740–1754. <https://doi.org/10.1039/C3GC42143K>.
- (19) Klaas, M. R. G.; Warwel, S. Complete and Partial Epoxidation of Plant Oils by Lipase-Catalyzed Perhydrolysis 1 Based Partly on a. **1999**. [https://doi.org/10.1016/S0926-6690\(98\)00023-5](https://doi.org/10.1016/S0926-6690(98)00023-5).
- (20) Hilker, I.; Bothe, D.; Prüss, J.; Warnecke, H.-J. Chemo-Enzymatic Epoxidation of Unsaturated Plant Oils. *Chem. Eng. Sci.* **2001**, *56* (2), 427–432. [https://doi.org/10.1016/S0009-2509\(00\)00245-1](https://doi.org/10.1016/S0009-2509(00)00245-1).
- (21) Moreira, M. A.; Nascimento, M. G. Chemo-Enzymatic Epoxidation of (+)-3-Carene. *Catal. Commun.* **2007**, *12* (8), 2043–2047. <https://doi.org/10.1016/j.catcom.2007.02.032>.
- (22) Moniruzzaman, M.; Kamiya, N.; Goto, M. Activation and Stabilization of Enzymes in Ionic Liquids. *Org. Biomol. Chem.* **2010**, *8* (13), 2887–2899. <https://doi.org/10.1039/B926130C>.
- (23) Elgharbawy, A. A. M.; Moniruzzaman, M.; Goto, M. Recent Advances of Enzymatic Reactions in Ionic Liquids: Part II. *Biochem. Eng. J.* **2020**, *154*, 107426. <https://doi.org/10.1016/j.bej.2019.107426>.

- (24) Hobbs, H. R.; Thomas, N. R. Biocatalysis in Supercritical Fluids, in Fluorous Solvents, and under Solvent-Free Conditions. *Chem. Rev.* **2007**, *107* (6), 2786–2820. <https://doi.org/10.1021/cr0683820>.
- (25) Abbott, A. P.; Capper, G.; Davies, D. L.; Munro, H. L.; Rasheed, R. K.; Tambyrajah, V. Preparation of Novel, Moisture-Stable, Lewis-Acidic Ionic Liquids Containing Quaternary Ammonium Salts with Functional Side Chains. *Chem. Commun.* **2001**, No. 19, 2010–2011. <https://doi.org/10.1039/B106357J>.
- (26) Dai, Y.; van Spronsen, J.; Witkamp, G.-J.; Verpoorte, R.; Choi, Y. H. Natural Deep Eutectic Solvents as New Potential Media for Green Technology. *Anal. Chim. Acta* **2013**, *766*, 61–68. <https://doi.org/10.1016/j.aca.2012.12.019>.
- (27) Zhou, P.; Wang, X.; Yang, B.; Hollmann, F.; Wang, Y. Chemoenzymatic Epoxidation of Alkenes with *Candida Antarctica* Lipase B and Hydrogen Peroxide in Deep Eutectic Solvents. *RSC Adv.* **2017**, *7* (21), 12518–12523. <https://doi.org/10.1039/C7RA00805H>.
- (28) Durand, E.; Lecomte, J.; Baréa, B.; Piombo, G.; Dubreucq, E.; Villeneuve, P. Evaluation of Deep Eutectic Solvents as New Media for *Candida Antarctica* B Lipase Catalyzed Reactions. *Process Biochem.* **2012**, *47* (12), 2081–2089. <https://doi.org/10.1016/j.procbio.2012.07.027>.
- (29) Drożdż, A.; Erfurt, K.; Bielas, R.; Chrobok, A. Chemo-Enzymatic Baeyer–Villiger Oxidation in the Presence of *Candida Antarctica* Lipase B and Ionic Liquids. *New J. Chem.* **2015**, *39* (2), 1315–1321. <https://doi.org/10.1039/C4NJ01976H>.
- (30) Ranganathan, S.; Zeitlhofer, S.; Sieber, V. Development of a Lipase-Mediated Epoxidation Process for Monoterpenes in Choline Chloride-Based Deep Eutectic Solvents. *Green Chem.* **2017**, *19* (11), 2576–2586. <https://doi.org/10.1039/C7GC01127J>.
- (31) Gotor-Fernández, V.; Paul, C. E. Deep Eutectic Solvents for Redox Biocatalysis. *J. Biotechnol.* **2019**, *293*, 24–35. <https://doi.org/10.1016/j.jbiotec.2018.12.018>.
- (32) Ma, Y.; Li, P.; Li, Y.; Willot, S. J.-P.; Zhang, W.; Ribitsch, D.; Choi, Y. H.; Verpoorte, R.; Zhang, T.; Hollmann, F.; Wang, Y. Natural Deep Eutectic Solvents as Multifunctional Media for the Valorization of Agricultural Wastes. *ChemSusChem* **2019**, *12* (7), 1310–1315. <https://doi.org/10.1002/cssc.201900043>.
- (33) Ülger, C.; Takaç, S. Kinetics of Lipase-Catalysed Methyl Gallate Production in the Presence of Deep Eutectic Solvent. *Biocatal. Biotransformation* **2017**, *35* (6), 407–416. <https://doi.org/10.1080/10242422.2017.1359573>.
- (34) Oh, Y.; Park, S.; Yoo, E.; Jo, S.; Hong, J.; Kim, H. J.; Kim, K. J.; Oh, K. K.; Lee, S. H. Dihydrogen-Bonding Deep Eutectic Solvents as Reaction Media for Lipase-Catalyzed Transesterification. *Biochem. Eng. J.* **2019**, *142*, 34–40. <https://doi.org/10.1016/j.bej.2018.11.010>.
- (35) Guajardo, N.; Ahumada, K.; Domínguez de María, P.; Schrebler, R. A. Remarkable Stability of *Candida Antarctica* Lipase B Immobilized via Cross-Linking Aggregates (CLEA) in Deep Eutectic Solvents. *Biocatal. Biotransformation* **2019**, *37* (2), 106–114. <https://doi.org/10.1080/10242422.2018.1492567>.
- (36) Nian, B.; Cao, C.; Liu, Y. How *Candida Antarctica* Lipase B Can Be Activated in Natural Deep Eutectic Solvents: Experimental and Molecular Dynamics Studies. *J. Chem. Technol. Biotechnol.* **2020**, *95* (1), 86–93. <https://doi.org/10.1002/jctb.6209>.
- (37) Auriemma, F.; De Rosa, C.; Di Caprio, M. R.; Di Girolamo, R.; Ellis, W. C.; Coates, G. W. Stereocomplexed Poly(Limonene Carbonate): A Unique Example of the Cocrystallization of Amorphous Enantiomeric Polymers. *Angew. Chem. Int. Ed.* **2015**, *54* (4), 1215–1218. <https://doi.org/10.1002/anie.201410211>.
- (38) Milchert, E.; Malarczyk, K.; Kłós, M. Technological Aspects of Chemoenzymatic Epoxidation of Fatty Acids, Fatty Acid Esters and Vegetable Oils: A Review. *Molecules* **2015**, *20* (12), 21481–21493. <https://doi.org/10.3390/molecules201219778>.
- (39) Orellana-Coca, C.; Törnvall, U.; Adlercreutz, D.; Mattiasson, B.; Hatti-Kaul, R. Chemo-Enzymatic Epoxidation of Oleic Acid and Methyl Oleate in Solvent-Free Medium. *Biocatal. Biotransformation* **2005**, *23* (6), 431–437. <https://doi.org/10.1080/10242420500389488>.
- (40) Informatics, N. O. of D. and. *NIST Chemistry WebBook*. <https://webbook.nist.gov/chemistry/> (accessed 2022-05-11). <https://doi.org/10.18434/T4D303>.

## APPENDIX 5

### Contents

A5.1 Additional results about epoxidations of cyclic alkenes.

A5.2 Additional results about epoxidations of *trans*-stilbene (**1e**) and linear alkenes.

A5.3  $^1\text{H}$  and  $^{13}\text{C}$  NMR spectra of isolated PRODUCT 2b (Cyclododecene oxide), Table 5.1, entry 8.

A5.4  $^1\text{H}$  and  $^{13}\text{C}$  NMR spectra of isolated PRODUCT 2c (Cyclooctene oxide), Table 5.1, entry 14.

A5.5  $^1\text{H}$  and  $^{13}\text{C}$  NMR spectra of isolated PRODUCT 2e (*trans*-stilbene oxide), Table 5.2, entry 3.

A5.6  $^1\text{H}$  and  $^{13}\text{C}$  NMR spectra of isolated PRODUCT 2f (9,10-epoxystearic acid), Scheme 5.2.

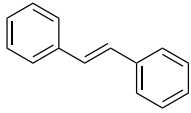
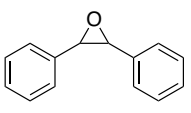
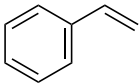
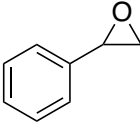
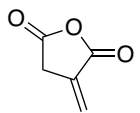
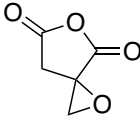
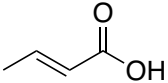
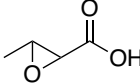
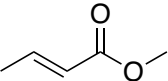
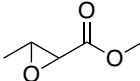
### A5.1 Additional results about epoxidations of cyclic alkenes.

Entry	Alkene	NaDES	CAL-B (U/mmol)	Peracid precursor (eq)	Product Conversion (%) <sup>a</sup>
1	<b>1b<sup>b</sup></b>	ChCl-Sorb [1:1]	250	DMC, 1	13
2	<b>1b<sup>b</sup></b>	ChCl-LA [1:2]	250	LA	5
3	<b>1b<sup>b</sup></b>	GFS [1:1:1] -LA	250	DMC, 1	25
4	<b>1c</b>	GFS [1:1:1] -LA	250	OA, 1	63
5	<b>1d<sup>c</sup></b>	ChCl-Sorb [1:1]	30	OA, 0.1	68

<sup>a</sup> Conversion by GC-MS; <sup>b</sup> diastereomeric ratio Z/E in **1b** and **2b** is always 2:1; <sup>c</sup> Room temperature (20 °C).

Acronyms: ChCl= choline chloride, Sorb = sorbitol, GFS = glucose, fructose, sucrose, DMC= dimethyl carbonate, OA= octanoic acid, LA= levulinic acid.

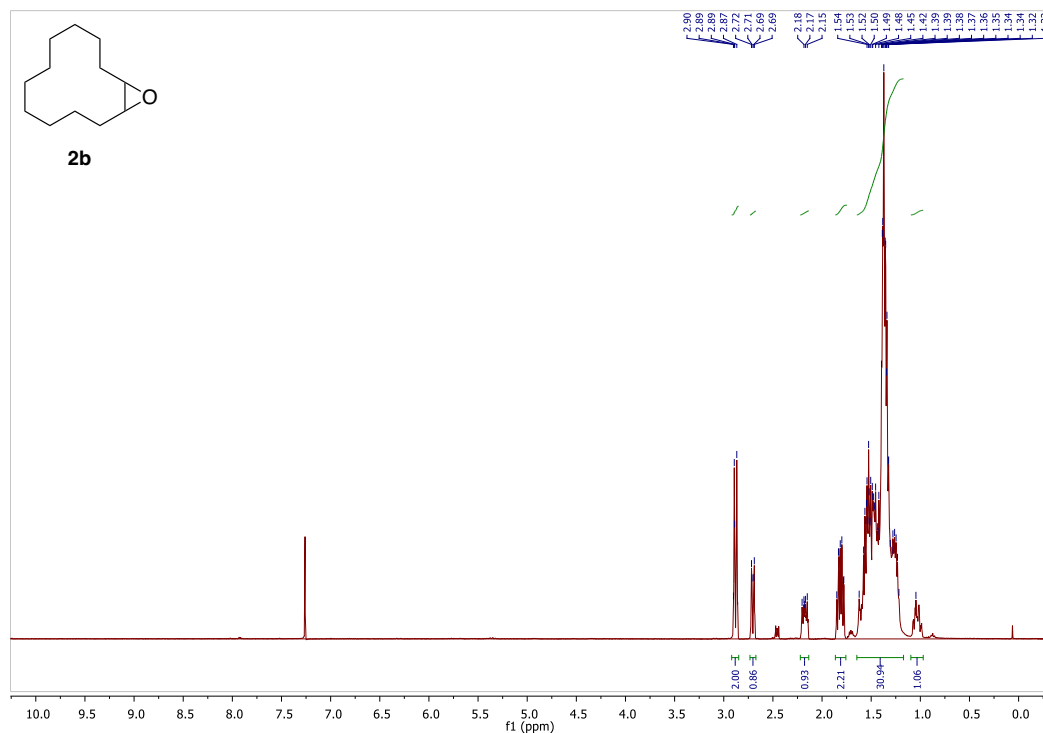
## A5.2 Additional results about epoxidations of *trans*-stilbene (**1e**) and other linear alkenes.

Entry	Alkene	NaDES	CAL-B (U/mmol)	Peracid precursor (eq)	time (h)	Product Conversion (%) <sup>a</sup>
	 <b>1e</b>					 <b>2e</b>
1	<b>1e</b>	ChCl-Sorb [1:1]	250	OA, 1	20	15
2	<b>1e</b>	GFS [1:1:1] -LA	250	OA, 1	20	8
3	<b>1e</b>	GFS	25	OA, 1	20	39
4	<b>1e</b>	GFS	25	OA, 1	72	76
5		GFS	100	OA, 10	70	 12
6		GFS	various	various	various	 -
7		GFS	various	various	various	 traces
8		GFS	various	various	various	 traces

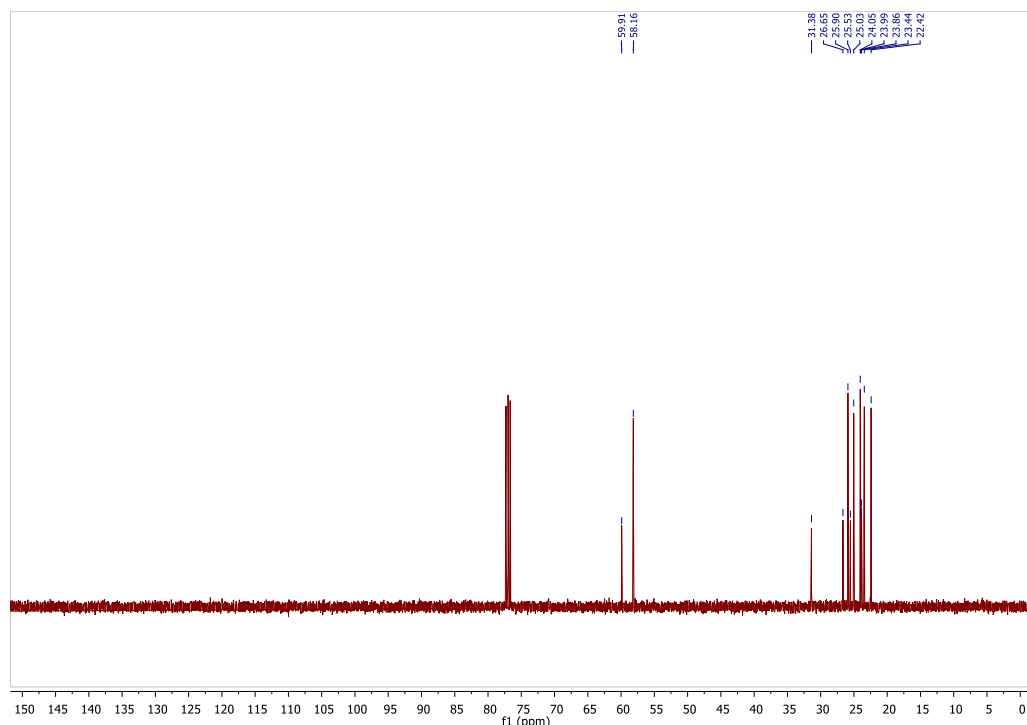
<sup>a</sup> Conversion by GC-MS.

Acronyms: ChCl= choline chloride, Sorb = sorbitol, GFS = glucose, fructose, sucrose, DMC= dimethyl carbonate, OA= octanoic acid, LA= levulinic acid.

A5.3  $^1\text{H}$  and  $^{13}\text{C}$  NMR spectra of isolated **PRODUCT 2b** (Cyclododecene oxide), Table 5.1, entry 8.

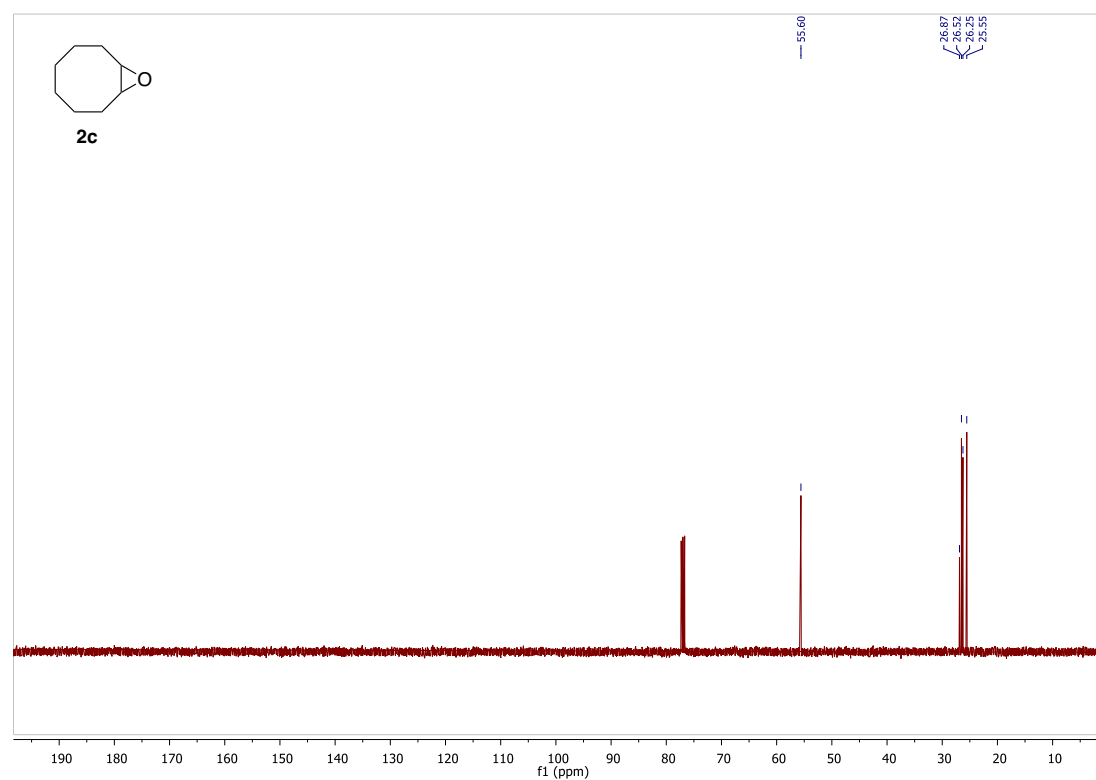
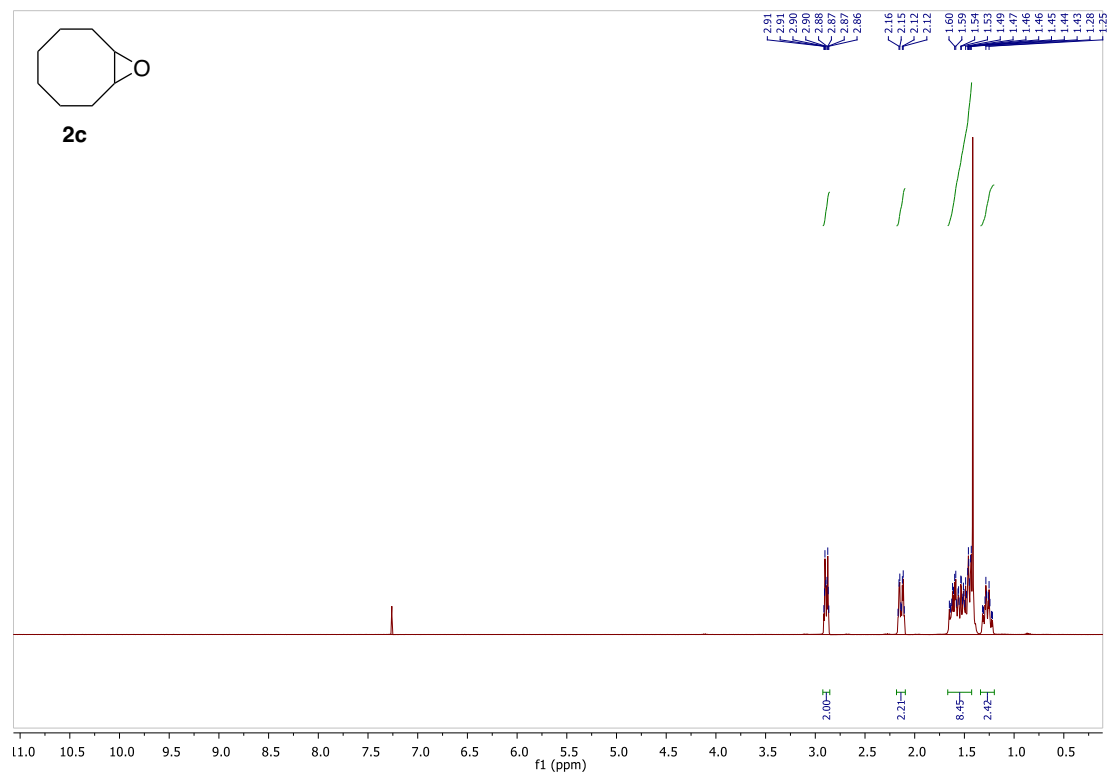


$^1\text{H}$  NMR (400 MHz,  $\text{CDCl}_3$ )  $\delta$  2.89 (dd,  $J = 7.5, 6.0$  Hz, 2H, *cis*-isomer), 2.70 (dd,  $J = 9.3, 2.1$  Hz, 2H, *trans*-isomer), 2.22 – 2.13 (m, 2H, *trans*-isomer), 1.86 – 1.76 (m, 2H, *cis*-isomer), 1.65 – 1.17 (m, 34H), 1.04 (m, 2H, *trans*-isomer).

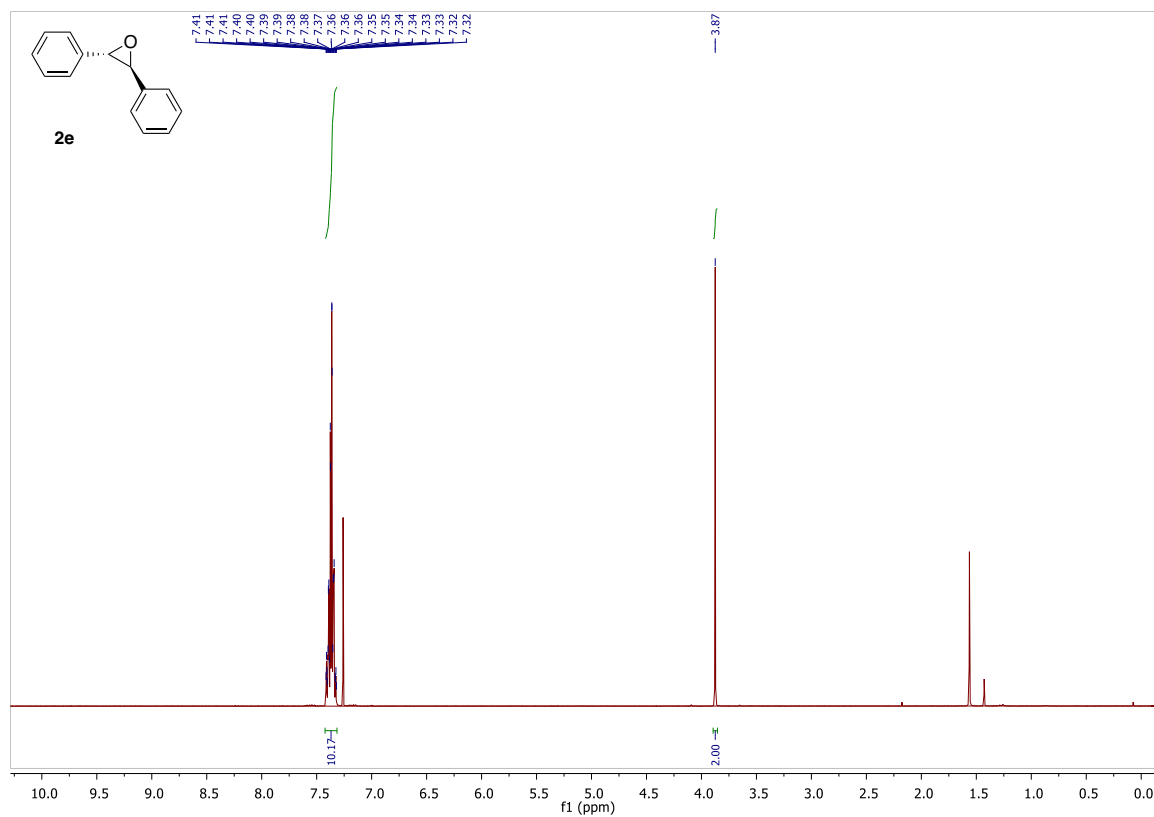


$^{13}\text{C}$  NMR (100 MHz,  $\text{CDCl}_3$ )  $\delta$  59.91, 58.16, 31.38, 26.65, 25.90, 25.53, 25.03, 24.05, 23.99, 23.86, 23.44, 22.42.

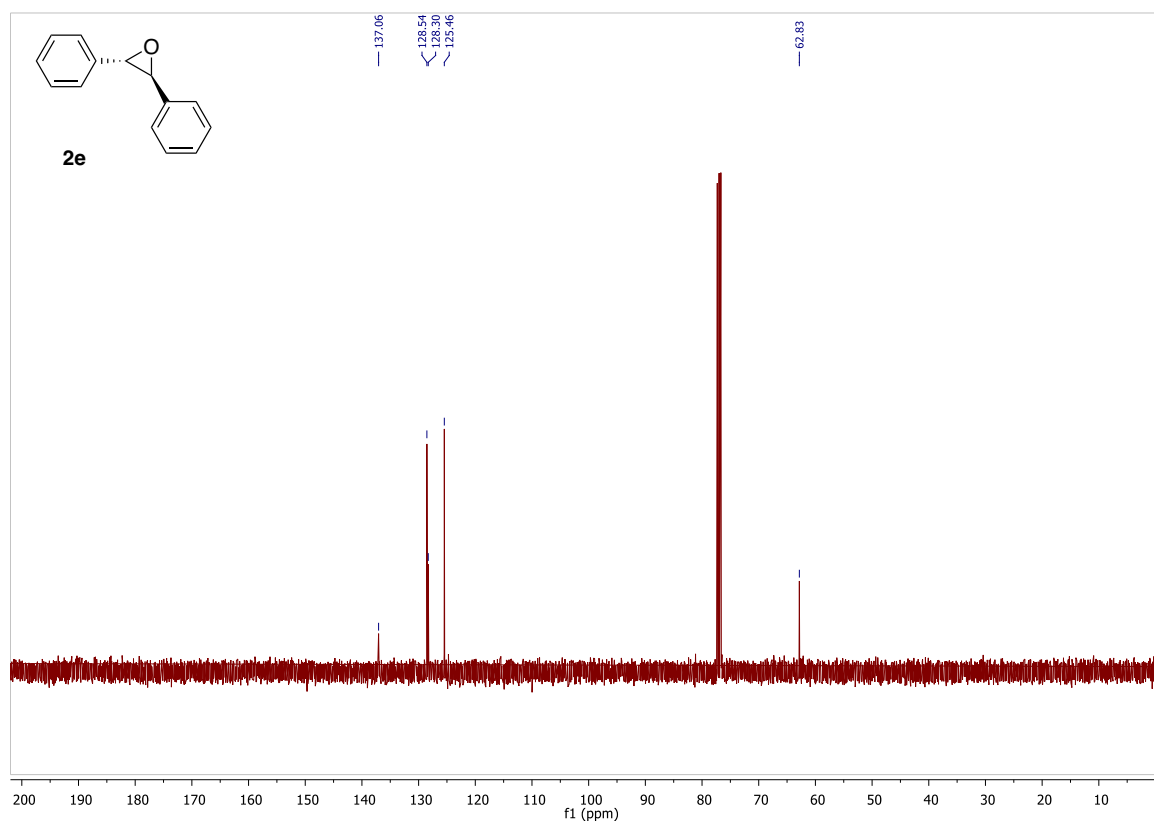
A5.4  $^1\text{H}$  and  $^{13}\text{C}$  NMR spectra of isolated PRODUCT 2c (Cyclooctene oxide), Table 5.1, entry 14.



A5.5  $^1\text{H}$  and  $^{13}\text{C}$  NMR spectra of isolated **PRODUCT 2e** (*trans*-stilbene oxide), Table 5.2, entry 3.

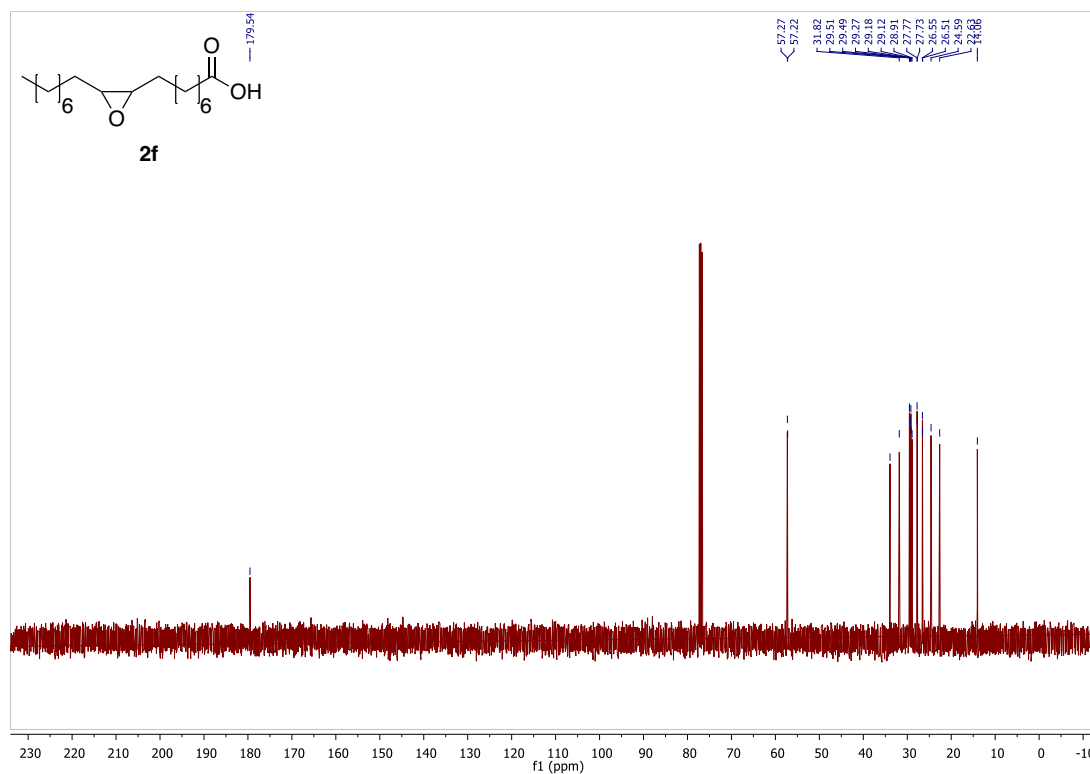
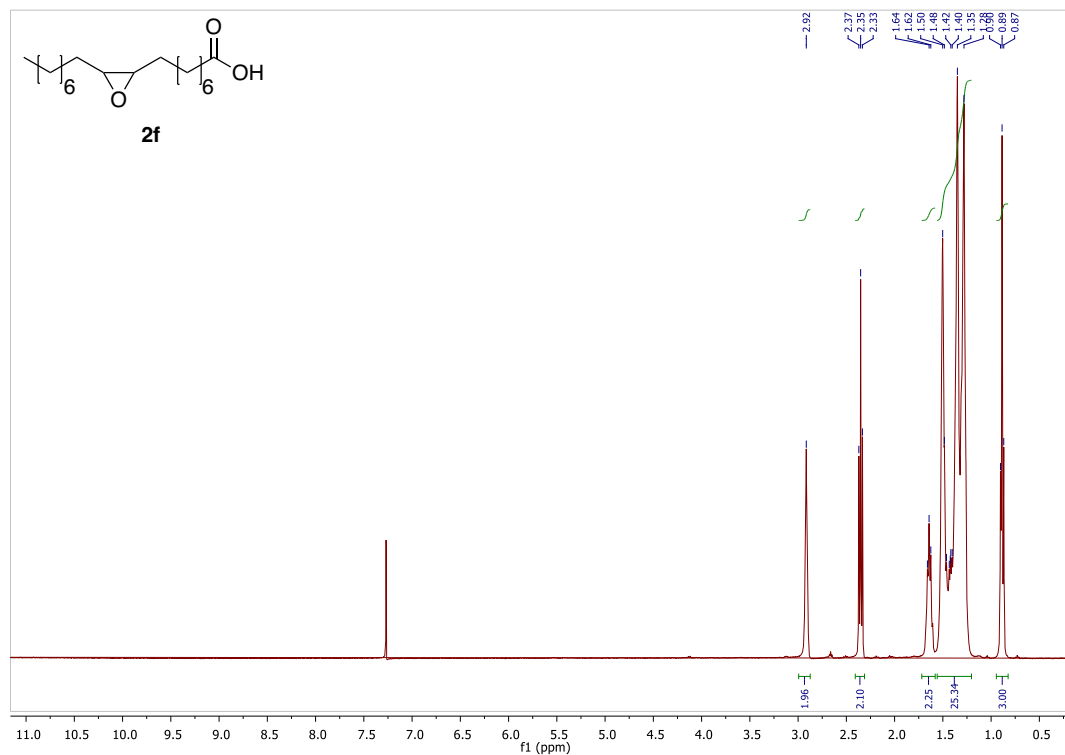


$^1\text{H}$  NMR (400 MHz,  $\text{CDCl}_3$ )  $\delta$  7.42 – 7.32 (m, 10H), 3.87 (s, 2H).



$^{13}\text{C}$  NMR (100 MHz,  $\text{CDCl}_3$ )  $\delta$  137.06, 128.54, 128.30, 125.46, 62.83

A5.6  $^1\text{H}$  and  $^{13}\text{C}$  NMR spectra of isolated PRODUCT 2f (9,10-epoxystearic acid), Scheme 5.2.



**Published as:** Vagnoni, M.; Samorì, C.; Pirini, D.; Paz, M. K. V. D.; Gidey, D. G.; Galletti, P. Lipase Catalysed Oxidations in a Sugar-Derived Natural Deep Eutectic Solvent. *Biocatal. Biotransformation* **2021**. <https://doi.org/10.1080/10242422.2021.1913126>

## CHAPTER 6

# EXTRACTION OF ASTAXANTHIN FROM *HAEMATOCOCCUS PLUVIALIS* WITH HYDROPHOBIC DEEP EUTECTIC SOLVENTS BASED ON OLEIC ACID <sup>1</sup>

### 6.1 Introduction

Microalgae are microorganisms that are gaining a lot of interest since in the appropriate growing conditions they can achieve high CO<sub>2</sub> uptake rates. The absorbed CO<sub>2</sub> is involved in their metabolism, making them a great source of biomass with high added value: fuels, human food supplement, animal feed additive, polyunsaturated fatty acids, antioxidants, coloring agents and pigments and fertilizers. Astaxanthin (3,3'-dihydroxy-β,β-carotene-4,4'-dione) is a secondary carotenoid belonging to the class of xanthophylls and biosynthesized by the microalga *Haematococcus pluvialis*. It is also produced by the yeast *Phaffia rhodozyma* and accumulated by marine invertebrates, birds and by a variety of living organisms. *H. pluvialis* accumulates the astaxanthin, bounded with long-chain fatty acids (monoesters), **Figure 6.1**, in specific hydrophobic deposits in the cytoplasm composed of (neutral) lipid droplets (e.g. triglycerides).<sup>2,3</sup>

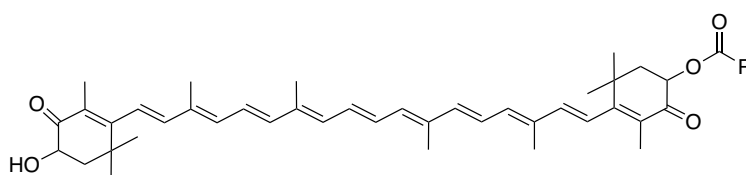


**Figure 6.1** Astaxanthin mono esterified.

The extraction and purification of astaxanthin from *H. pluvialis* is not a trivial process: i) the known chemical instability of astaxanthin (oxidation) when exposed to high temperatures, oxygen, light, and extreme pH environments can affect and compromise its practical use;<sup>4</sup> ii) the presence of lipidic droplets all around astaxanthin molecules with similar solubility behavior hampers their effective separation; iii) the rigid cellular structures of *H. pluvialis* cysts creates a physical barrier that can decrease the efficiency of the extraction; iv) the need of

harvesting and dewatering algal cells before the extraction makes the entire recovery energy-intensive.

The recovery of natural astaxanthin has been accomplished with a variety of solvents, from hazardous traditional organic compounds to safer solvents (e.g. ethyl acetate, acetone, ethanol),<sup>5</sup> to unconventional (but sometimes highly-costly) alternatives<sup>6</sup> like supercritical CO<sub>2</sub>, vegetable oils, ionic liquids, or deep eutectic solvents.<sup>7-13</sup> Regardless of the kind of solvent, the dewatering of the algal biomass, its pre-treatment to weaken the cell walls (i.e. cell disruption), the solvent removal to recover astaxanthin, and the color fading and loss of biological activity are unavoidable issues.

Ionic liquids have been widely used in the recovery of astaxanthin from natural matrices including *H. pluvialis*,<sup>14</sup> as “weakening” agents to increase the cell membrane permeability<sup>7,15-18</sup> and as real lipophilic solvents.<sup>14,19-22</sup> In all these cases no protocol has never been applied directly to algal cultures. Moreover, since ILs are not volatile (apart of the distillable CO<sub>2</sub>-based alkyl carbamate ILs developed by Khoo *et al.*<sup>14</sup>), the solvent removal/separation to recover astaxanthin is a critical issue, performed by the addition of an anti-solvent that was then distilled to regenerate the IL itself<sup>20,21</sup> or by a further liquid/liquid extraction.<sup>22</sup> It is worth mentioning that the inherent toxicity of most IL components prevents their use without any separation from the extracted astaxanthin.

As already stated, Deep eutectic solvents (DESs) have become quite popular in the scenario of green extractions, especially if composed of non-toxic and biocompatible hydrogen bond donors and acceptors (HBD and HBA, respectively).<sup>23</sup> DESs have been initially considered as “improved ILs” in terms of sustainability, but the characteristics that these two families of solvents have in common are important but a few, like the non-volatility and the tunability of the properties as a function of different combinations of the components. In analogy with ILs, both hydrophilic<sup>13,24</sup> and hydrophobic<sup>11,25</sup> DESs have been used so far for the recovery of astaxanthin from natural matrices, mainly from crustacean waste. If hydrophilic and water-soluble eutectic mixtures of choline chloride and diols/carboxylic acids act as “adjuvants” for weakening algal cell wall and enhancing a subsequent astaxanthin extraction, hydrophobic DESs can work as real solvents for astaxanthin itself.<sup>26</sup> The only class of hydrophobic DESs exploited so far as solvents for extracting astaxanthin are terpene-based mixtures, characterized by a low viscosity in comparison to hydrophilic DESs and other phosphonium-based hydrophobic DESs:<sup>11,25</sup> perillyl alcohol, camphor, eucalyptol, and menthol were used

mixed with myristic acid, and the mixture menthol-myristic acid was the most efficient one in the extraction of astaxanthin from crab waste.<sup>11</sup>

A common feature to both hydrophilic and hydrophobic DESs is their low or absent volatility: if this property confers an intrinsic safety for the operators and the environment, it is also true that this strictly influences their application since DESs are inseparable from the compounds they dissolve.<sup>27</sup> For this reason, the use of eutectic mixtures composed of safe components is mandatory for developing “bioactive compounds-DES” formulations exploitable in applications for humans. Menthol-fatty acids hydrophobic DESs meet this criterion<sup>28</sup> with the additional benefit of being Therapeutic DESs (TheDES)<sup>29</sup> since both menthol and fatty acids are anti-inflammatory and antimicrobial compounds.<sup>28,30</sup>

In this work terpene-based hydrophobic DESs were applied to the recovery of natural astaxanthin from *H. pluvialis* by exploiting the unique features of three novel mixtures based on oleic acid mixed with DL-menthol (named MAO), thymol (TAO), and geraniol (GAO), here used for the first time:

- being water-immiscible, the three DESs were applied directly to *H. pluvialis* cultures, developing a novel protocol in which the harvesting, dewatering and pre-treatment of the algal cells were avoided, thus decreasing the overall energy consumption and economics of the extraction process;<sup>9</sup>
- being composed of non-volatile components, the three DESs were not separated from the extracted astaxanthin but directly incorporated into bioactive formulations, overcoming the difficulties and energy consumption of astaxanthin recovery from non-volatile solvents using an anti-solvent;<sup>11</sup>
- being composed of edible and Generally Recognized As Safe (GRAS) components, already in use as food additives, the three DESs were used to prepare formulations that could be exploited in the food industry as carriers of natural astaxanthin, approved by both the United States Food and Drug Administration (USFDA) and the European Commission as food colorant/dye;
- being composed of oily components (oleic acid), known to improve the stability and the bioavailability in humans of natural astaxanthin, the three DESs could act as stabilizing agents for natural astaxanthin.<sup>31</sup>

The study of the chemical-physical properties of DES here reported was done by the group prof. M. Tiecco of the University of Perugia (Italy), while the cultivation of algal cultures and

the analysis of algal vitality were carried out by the group of Prof. L. Pezzolesi of University of Bologna.

## 6.2 Results and discussion

### Hydrophobic DESs preparation and solid-liquid phase diagrams

The study of the chemical-physical properties of DES was done in collaboration with the group of prof. M. Tiecco of the University of Perugia (Italy).

Three oleic acid-based mixtures composed of natural and edible components approved by the Flavor and Extract Manufacturers Association (FEMA) as GRAS flavor ingredients (oleic acid: FEMA N° 2815; DL-menthol: FEMA N° 2665; thymol: FEMA N° 3066; geraniol: FEMA N° 2507) were here prepared with the aim of providing an improvement towards the use of hydrophobic DESs.<sup>32</sup> The solid-liquid phase diagrams of the three mixtures were initially defined and compared with the theoretical melting curves (**Figure 6.2**).<sup>33</sup> This approach was necessary to define the identity of the liquid mixtures; in this case, this was particularly important since oleic acid itself is a liquid (m.p. = 16°C), so the resulting mixtures could be solutions rather than eutectic systems. Moreover, a shift of the eutectic point from the theoretical one, in terms of both molar ratio of the components and melting point, is necessary to define the mixtures as “deep eutectic solvents”.<sup>34</sup> This shift indicates that the interactions occurring between the different molecules have intensities like the ones occurring between the same species; therefore, the mixtures have a non-ideal behavior.<sup>35</sup>

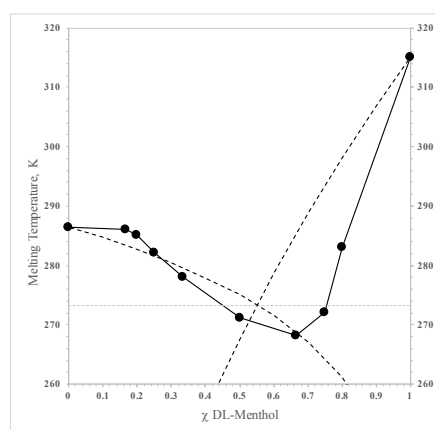


**Figure 6.2** Eutectic profiles, experimental melting points (dots) and theoretical curves (dashed lines) vs molar ratio of the DESs (a-c); experimental activity coefficients  $\gamma$  of the DESs (d-f).

All the three mixtures can be considered as DESs as the eutectic points observed differed from the theoretical curves both in terms of eutectic ratio and melting points.<sup>36</sup> MAO had a eutectic

point at 2:1 (DL-menthol:oleic acid) molar ratio with a melting point of -5°C (oleic acid m.p. = 16°C; DL-menthol m.p. = 42°C) while the ideal curve showed a minimum at about 0°C and approximately 1:1 molar ratio of the components. TAO had a eutectic point at 3:1 molar ratio (thymol/oleic acid) with a melting point of -4°C (thymol m.p. = 49°C); in this case, a higher shift from the theoretical curve was observed (about 7°C and 1/2 molar ratio). GAO had a peculiar and uncommon solid-liquid diagram with a eutectic point at 13:1 molar ratio (geraniol:oleic acid) with a melting point of -31°C (geraniol m.p. = -15°C). However, even the theoretical curve showed a minimum at a high value of the molar ratio (0.85 molar fraction of geraniol) with a temperature of about -18°C. All the DESs showed shifts from ideal values of activity in correspondence to the eutectic points. If MAO showed the fewest difference from the ideal curve in the melting point profile, TAO and GAO showed high differences from the ideal behavior. All these liquid systems can be considered as Type V DESs because they are composed of non-ionic molecules. Moreover, they are hydrophobic because both the components are scarcely soluble in water (<0.01 mM oleic acid; <3 mM DL-menthol; 6 mM thymol; 5 mM geraniol) and their water content (i.e. 2.9 wt% for TAO, 0.94 wt% for MAO, and 2.6 wt% for GAO) was in agreement with literature data on hydrophobic DESs.<sup>37</sup>

Mixtures of terpenes (such as geraniol, thymol, and menthol) with carboxylic acids have been already reported and discussed in the literature;<sup>32</sup> however, in those mixtures, only small shifts of the experimental melting points from the theoretical ones are reported. Differently, in all the oleic acid mixtures here reported, larger differences were observed; this suggests that the hydrogen-bonding networks established in oleic acid-based mixtures are significantly different in intensity to the ones reported for other carboxylic acids. Three other non-eutectic but liquid mixtures of oleic acid were also prepared to understand whether the “eutecticity” could give superior extraction performances: i) thymol:oleic acid in a molar ratio 1:1, ii) geraniol:oleic acid in a molar ratio 2:1, and iii) L- $\alpha$ -phosphatidylcholine:oleic acid in a weight ratio 95:5.

#### Extraction of astaxanthin from freeze-dried *H. pluvialis* biomass

The three hydrophobic DESs here studied were applied to the extraction of astaxanthin from *H. pluvialis* and compared with the single (liquid) components (oleic acid and geraniol) in terms of astaxanthin recovery. From a qualitative point of view, all the hydrophobic phases here

tested gave an identical carotenoid profile to what achieved through traditional organic solvents (cyclohexane:acetone:ethanol mixture) (**Figure 6.3**).

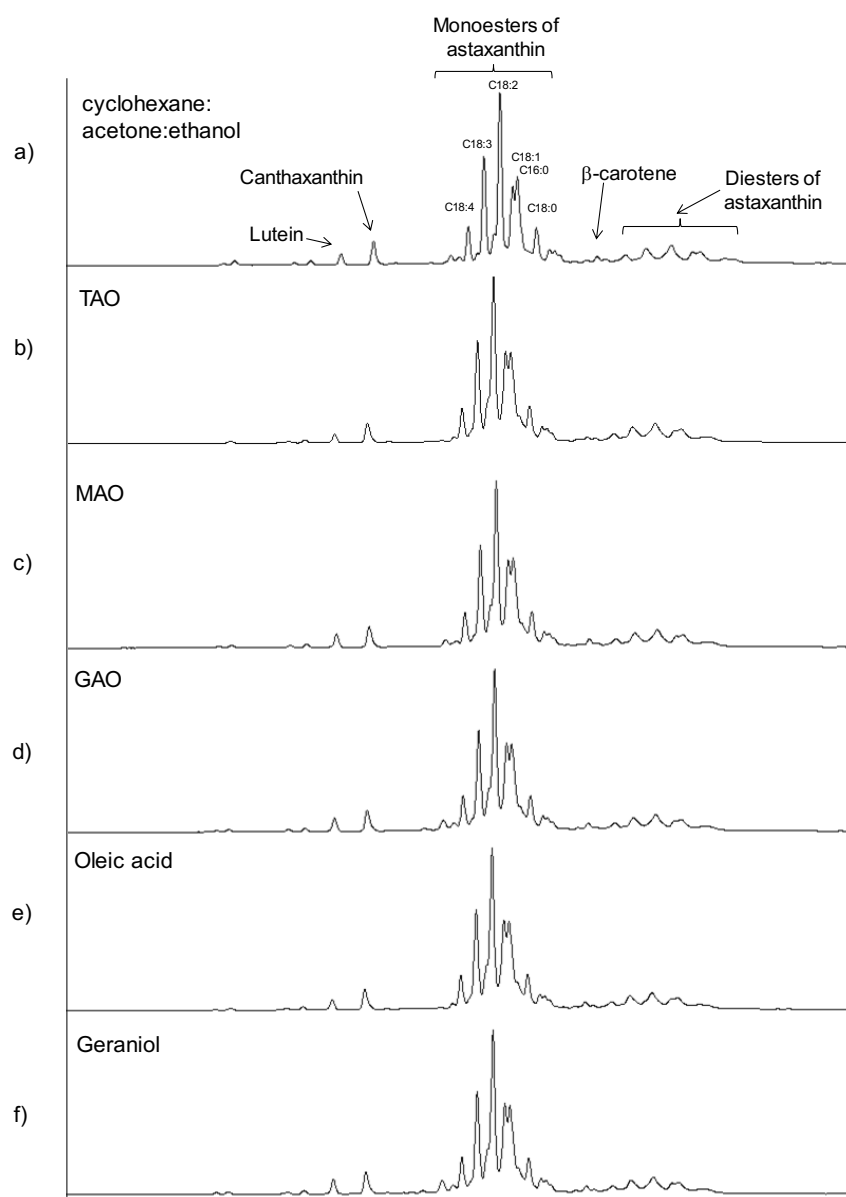


**Figure 6.3** Carotenoid profile obtained with a) cyclohexane:acetone:ethanol mixture 2:1:1 v/v/v; b) thymol:oleic acid 3:1, TAO; c) DL-menthol:oleic acid 2:1, MAO; d) geraniol:oleic acid 13:1, GAO; e) oleic acid, f) and geraniol.

All the chromatograms obtained by HPLC UV-Vis at 470 nm were predominantly characterized by the peaks of astaxanthin monoesters, identified by LC-MS on the basis of the molecular weight: monoesters of linoleic (C18:2) and linolenic acid (C18:3) were the most abundant peaks, followed by oleic (C18:1) and stearidonic acid (C18:4) monoesters (**Figure 6.3**). The monoester with palmitic acid (C16:0) was the only C16-ester detected, in line with previous findings.<sup>9</sup> Minor signals ascribable to astaxanthin diesters, lutein, canthaxanthin, and  $\beta$ -

carotene were found in all the extracts. The ratio between astaxanthin monoesters and diesters was  $4.8 \pm 0.3$ , in line with the literature<sup>38</sup> and independent from the solvent used and the kinetics, highlighting that no specific selectivity occurred in the extraction of the two forms of astaxanthin biosynthesized by *H. pluvialis*. The NMR spectra of the extract obtained with the cyclohexane:acetone:ethanol mixture (see Appendix, A6.1) revealed also the presence of unsaturated triglycerides that constitute the lipidic droplets known to create hydrophobic deposits in the hydrophilic environment of the cytoplasm,<sup>2,3</sup> and from which astaxanthin is hardly separable even after flash chromatography (see Appendix, A6.2). Therefore, independently from the solvent used for the extraction, the extracts resulted composed of a mixture of carotenoids, in which the monoesters of astaxanthin dominate, and polyunsaturated fatty acids: all of these components can play a synergic role and confer superior properties to the extract than isolated astaxanthin.<sup>39</sup>

From a quantitative point of view, the performance of the three hydrophobic DESs was similar, giving a recovery of astaxanthin of about 60% in 6 h (**Figure 6.4**). MAO was the only one that showed slower kinetics of extraction since in 1 h the recovery of astaxanthin was almost half of that obtained with TAO and GAO. After 24 h, TAO gave the best extraction performances ( $83 \pm 13\%$ ), followed by MAO ( $74 \pm 4\%$ ), and GAO ( $66 \pm 6\%$ ). Geraniol tested alone behaved similarly to GAO, while oleic acid was the worst hydrophobic phase among the tested ones ( $41 \pm 7\%$  of recovery after 6 h), even after prolonged extraction times (24 h,  $64 \pm 10\%$ ). This suggests that the combination of oleic acid in a DES mixture with all the three terpenes here used effectively improves its extraction ability, probably due to a reduction of oleic acid viscosity or to an increase in “affinity” for astaxanthin, thanks to  $\pi$ - $\pi$  stacking interactions between the conjugated systems of terpenes (but not DL-menthol) and that of astaxanthin. On the other hand, the extraction performances of the non-eutectic mixtures of oleic acid here prepared (see Appendix, A6.3, with the data for thymol:oleic acid in a molar ratio 1:1 and geraniol:oleic acid in a molar ratio 2:1) were worse than the corresponding DESs (TAO and GAO) over a long period; in particular, the recovery of astaxanthin with TAO was 1.4 times higher than a non-eutectic mixture of oleic acid and thymol. The mixture L- $\alpha$ -phosphatidylcholine and oleic acid (95:5 ratio by weight), known as OSMOS<sup>TM</sup> solvent, was the worst solvent among the ones tested (52% after 24 h), presumably because of higher viscosity than the terpenes mixtures.

The effect of the temperature on the extraction performances was evaluated on TAO, the best solvent among the tested ones. Increasing the extraction temperature from rt to 60°C improved the kinetics and the overall performances, giving an astaxanthin recovery of 75±0.7% after 6 h, 1.2 times higher than what was obtained at rt and higher than all the solvents here tested. Therefore, this temperature was chosen to investigate two other biomass/TAO ratios (i.e. 5 and 10 wt%, see Appendix, A6.4). The recovery after 6 h did not substantially change, regardless of the used ratio (70.9±2.8% at 10 wt% and 84.9±3.7% at 5 wt%), underlying that it is possible to minimize the amount of solvent used without changing the extraction performances (higher ratios were not tested since the viscosity of the “biomass-TAO” solution hampered an efficient separation of the extracted biomass by centrifugation).

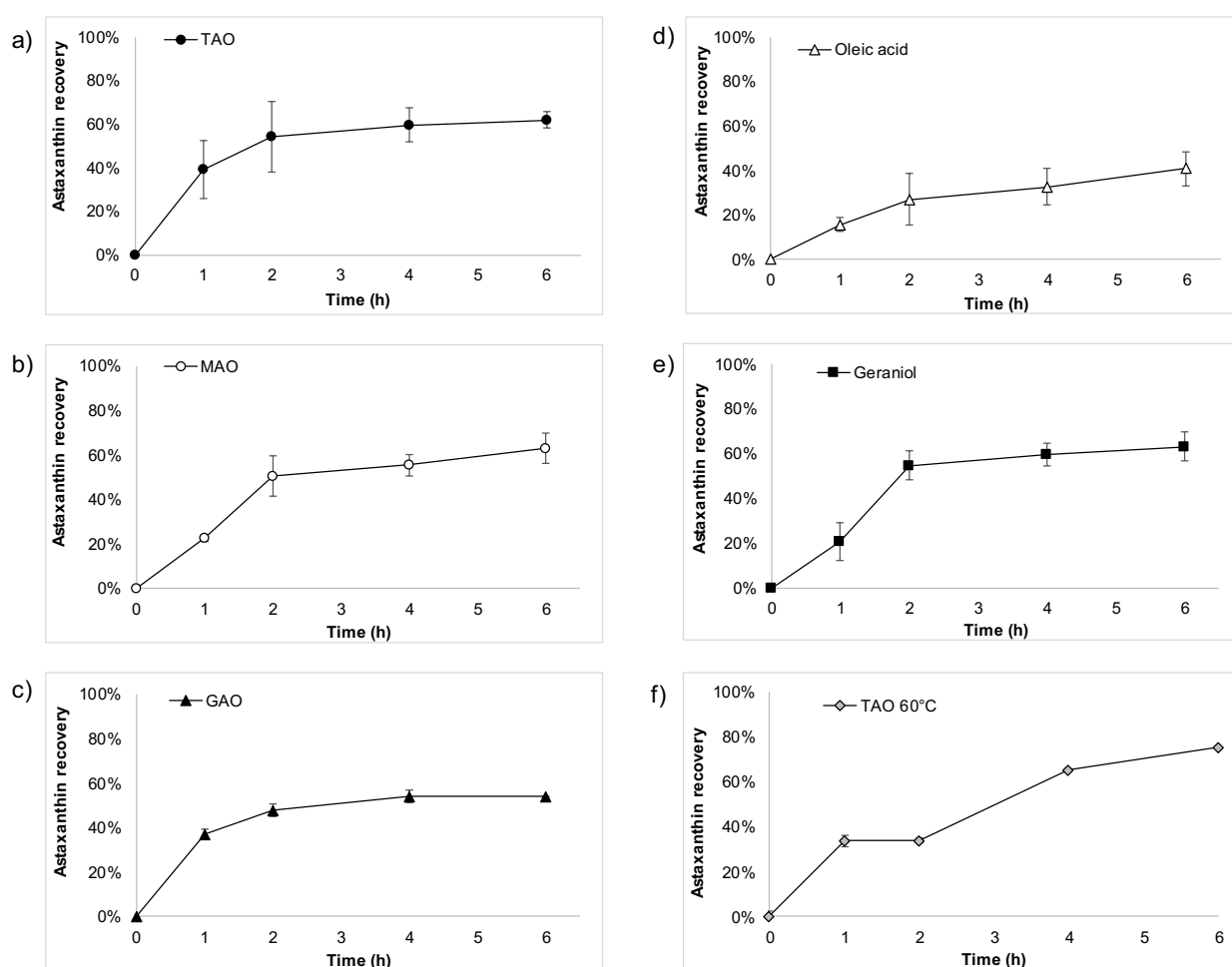


**Figure 6.4** Astaxanthin recovery from *H. pluvialis* freeze-dried biomass with a) thymol:oleic acid 3:1, TAO; b) DL-menthol:oleic acid 2:1, MAO; c) geraniol:oleic acid 13:1, GAO; d) oleic acid, e) geraniol, and f) thymol:oleic acid 3:1, TAO at 60°C. Data are expressed on the basis of the percentage of astaxanthin content in *H. pluvialis* cells, as mean ± standard deviation of two independent experiments on different freeze-dried algal biomass.

### Extraction of astaxanthin from *H. pluvialis* cultures

All the three hydrophobic DESs here tested formed a biphasic system with water and were therefore applicable in a direct extraction of astaxanthin from *H. pluvialis* culture. The possibility of by-passing algae harvesting and dewatering is for sure economically appealing even if extracting astaxanthin from algal cultures is more challenging than extracting astaxanthin from freeze-dried biomass because astaxanthin is accumulated inside algal cells surrounded by a strong and multilamellar cell wall and by a large volume of water. The kinetics of the liquid-liquid extraction with the three hydrophobic DESs and their single (liquid) components was here tested (**Figure 6.5**). In parallel, the algal vitality was analyzed by measuring the residual photosynthetic efficiency after the extraction at specific time frames (see Appendix, A6.5). This evaluation was done to verify the “algal-compatibility” of such hydrophobic solvents in keeping *H. pluvialis* cells alive and reusable for continuous production of astaxanthin.<sup>9</sup>

All the three DESs (**Figure 6.5** a-c) followed the same kinetics of extraction: the recovery of astaxanthin increased from values of about 10% achieved in 1 h, up to 30% after 6 h; the “hampering” effect created by water to the contact between solvent and algal cells was evident since the recovery, in this case, was half of what achieved from *H. pluvialis* pellet in the same time frame (**Figure 6.4** a-c). After 48 h, the recovery of astaxanthin reached values of 56, 58 and 68% with MAO, TAO, and GAO, respectively. Diversely from what occurred in the extraction of astaxanthin from algal pellets, oleic acid showed the same extraction pattern of DESs, while geraniol gave the best performance under these conditions (three-times higher astaxanthin recovery than DESs in 1 h, and 44% of recovery in 6 h). Qualitatively, the extracts recovered from algal cultures showed some differences with the extracts obtained from algal pellets (see Appendix, A6.6): the chromatograms were dominated by the signal of astaxanthin monoesters, but lutein and  $\beta$ -carotene were almost undetectable. The ratio between astaxanthin monoesters and diesters ( $6.0\pm 0.2$ ), was higher than what was observed in the extracts from freeze-dried biomass ( $4.8\pm 0.3$ ), but it is known that several biological factors related to algal growth and physiology (like the cultivation period, cysts age, growth medium composition)<sup>38</sup> influence this number and in the present case *H. pluvialis* cultures used for obtaining the pellet came from a different batch than the ones used for the liquid-liquid extraction.

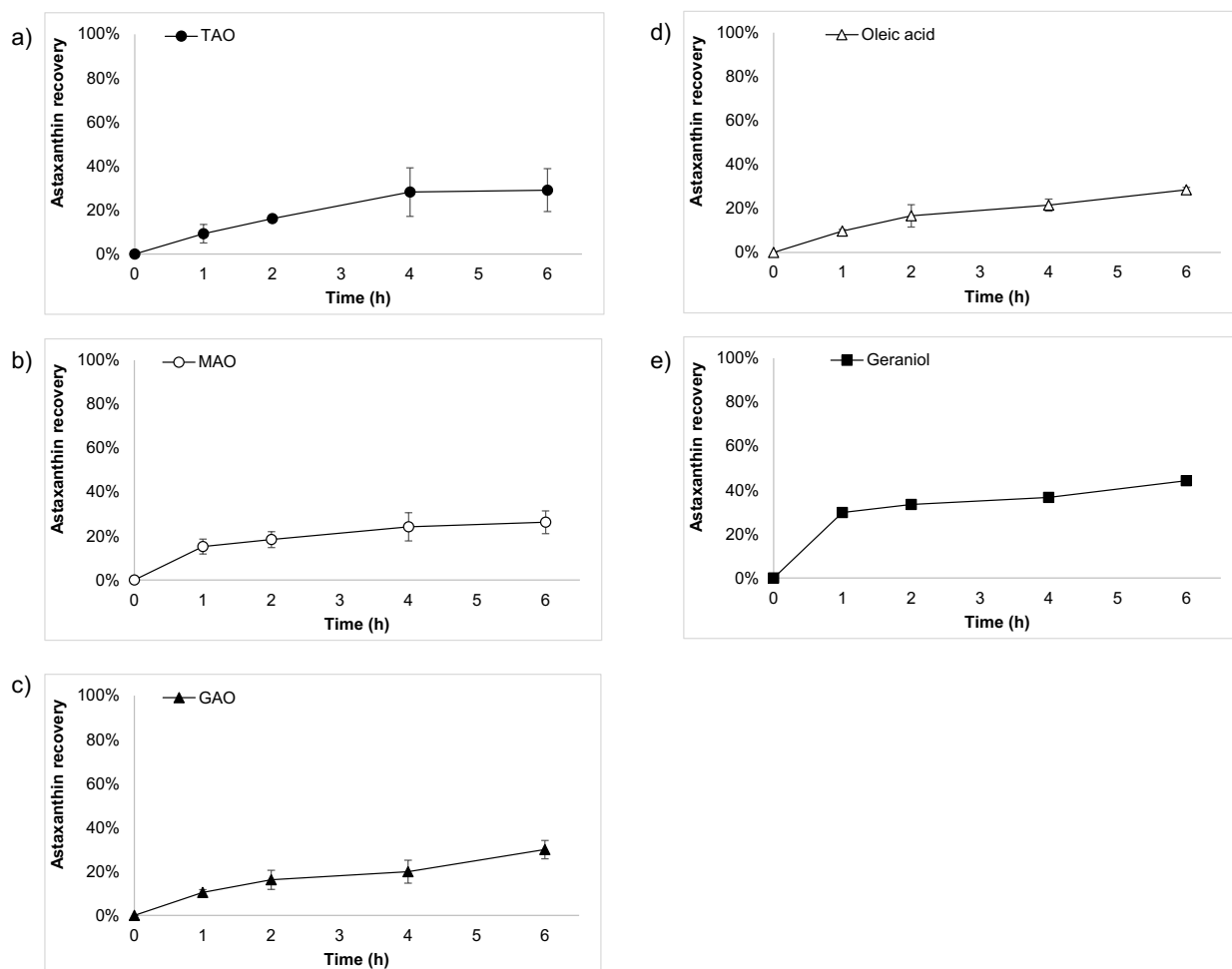


**Figure 6.5** Astaxanthin recovery from *H. pluvialis* cultures with a) thymol:oleic acid 3:1, TAO; b) DL-menthol:oleic acid 2:1, MAO; c) geraniol:oleic acid 13:1, GAO; d) oleic acid, and e) geraniol. Data are expressed based on the percentage of the astaxanthin content in *H. pluvialis* cells, as mean  $\pm$  standard deviation of two independent experiments on different algal biomass.

Even if after 1 and 4 h of contact algal cells seemed intact and still rich in astaxanthin or empty under a light microscope (see Appendix, A6.8), after 1h no photosynthetic activity was observed for the culture put in contact with TAO, GAO, and geraniol, while the viability of cells extracted with MAO was 50% for the first hour of extraction, before dropping down to 0% after 4 h (see Appendix, A6.5). In analogy to what was already observed for vegetable oils, oleic acid was the most algae-compatible compound, maintaining 80% of algal viability within the first hour of extraction and about 30% even after 6 h of extraction (see Appendix, A6.5).<sup>40</sup> NMR spectroscopy analysis of the algal cultures after 6 h of contact with the various hydrophobic solvents here tested helped in explaining such behavior: in the case of the three DESs, the presence of the terpenic component of the eutectic mixtures was detected (geraniol >> thymol ~ DL-menthol, see Appendix, A6.7), while oleic acid (tested alone or as a component of the DESs) was almost undetectable and largely below the molar ratio of the mixtures used

in the extraction step; this suggested that the hydrophobic DESs here used were not completely water-stable.<sup>41</sup> Therefore, the algal cell mortality could be related to the toxicity towards algae of each terpene (the growth inhibition of DL-menthol, thymol, and geraniol on freshwater algae after 72 h of exposition is reported to be in the range of 0.1 mM). These data demonstrated that preserving the viability of algal cells after contact with solvents is even more challenging than extracting algal metabolites directly from algal culture.

#### Light-stability test and antioxidant activity

The instability of astaxanthin to light, oxygen, and self-oxidation is a serious issue that can affect its practical use, especially for what concerns the Z-isomers, less thermodynamically stable than the all-E-isomers and more prone to isomerize in response to heat and light; different solvent media (e.g. vegetable oils enriched in oleic acid like sunflower, soybean, sesame, and rice bran) and additives (e.g. the antioxidants  $\alpha$ -tocopherol and ascorbic acid) have shown their positive effect in improving astaxanthin stability and preventing its degradation during 6-week storage in the dark.<sup>42,43</sup> Since the hydrophobic DESs here used contain both oleic acid and terpenes that are known to have antioxidant properties that could have a synergic effect, the stability of extracted astaxanthin contained in DESs, oleic acid, and geraniol was tested under the effect of light, one of the main oxidative factor together with temperature and oxygen (**Figure 6.6**).<sup>44</sup>

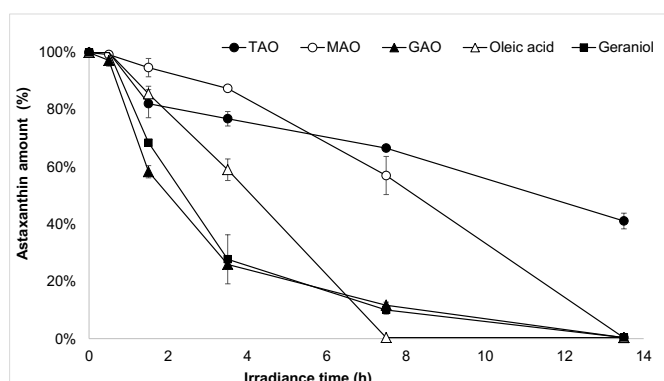


**Figure 6.6** Effect of light as oxidative factor on astaxanthin contained in DESs, oleic acid, and geraniol.

All samples except for TAO extract showed a complete astaxanthin degradation at the end of the 13.5 h irradiance. GAO and geraniol extracts followed the same kinetics of degradation, with an astaxanthin content that rapidly decreased (after 3.5 h, more than 70% of the initial astaxanthin content was degraded). In oleic acid a decrease with a constant rate was

observed, reaching a complete degradation after 7.5 h of exposure to light. MAO and TAO extracts performed the best, maintaining the astaxanthin amount above 50% after 7.5 h. After 13.5 h in TAO 40% of the initial astaxanthin content was maintained (**Figure 6.7 b**), demonstrating TAO superior potential to stabilize astaxanthin due to the antioxidant properties of thymol, higher than those of geraniol and menthol.<sup>45</sup> The antioxidant activity of TAO alone was 30-times higher than that of MAO (**Figure 6.7**, black bars), while oleic acid did not have any antioxidant activity at all. This finding can be attributed to the unique antioxidant properties of thymol, a well-known <sup>1</sup>O<sub>2</sub> quencher and anti-lipid peroxidation agent, suggested as a valid natural replacement for synthetic antioxidant food additives.<sup>46–48</sup> Moreover, it is known that a whole carotenoid extract that contains astaxanthin is more antioxidant than astaxanthin alone, thanks to the synergism that occurs in the extract between astaxanthin and the polyunsaturated lipidic droplets strictly associated with astaxanthin itself; moreover, astaxanthin monoester has a stronger total antioxidant capacity than astaxanthin in the free form.<sup>39</sup> This could explain the large increase of the antioxidant potential of all the tested solvents (black bars) observed after the extraction process (white bars). However, after the exposition to light, only TAO was capable to maintain such property (grey bars), suggesting TAO as the most promising extractant, carrier and stabilizer of natural astaxanthin among the tested DESs, useful for the development of food additives.

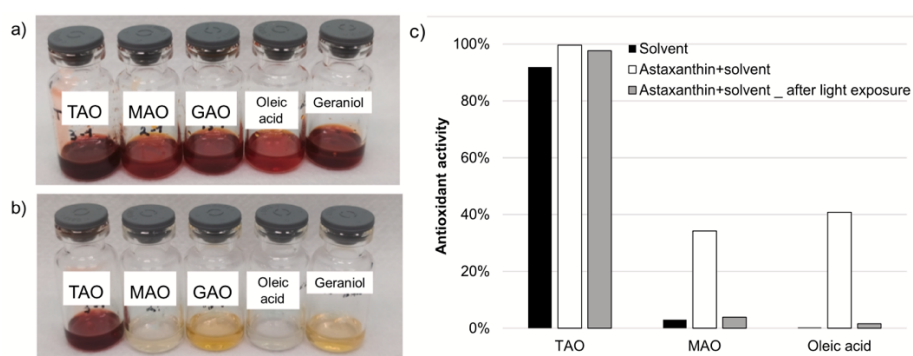


**Fig. 6.7** Extracts of astaxanthin in TAO, MAO, GAO, oleic acid, and geraniol after a) the extraction from *H. pluvialis* freeze-dried cells, and b) 13.5 h of light irradiance. Antioxidant activity of TAO, MAO, and oleic acid tested alone or as extracts of astaxanthin (c).

### 6.3 Conclusions

Three novel DESs based on oleic acid and thymol (TAO), DL-menthol (MAO) and geraniol (GAO) have been here prepared for the first time and applied to the extraction of astaxanthin from *H. pluvialis*. All of them gave good recovery percentages without any thermal, mechanical or

chemical pre-treatment; the extraction of dried biomass gave an astaxanthin recovery of about 60% in 6 h, independently from the DES used and significantly higher than the recovery of 40% achieved with oleic acid alone. Increasing the extraction temperature increased the recovery up to 75% under the same time frame, while the performances did not vary with the biomass/solvent ratio used.

A liquid-liquid extraction directly from algal cultures, by-passing dewatering and harvesting steps, known to be energy-intensive and largely impacting on the overall economics of algal-based process/productions, has been here demonstrated. In this case, the three DESs behaved similarly, giving a recovery of about 30% in 6 h and 60-70% in 48 h. Although the three DESs behaved similarly in terms of extraction efficiency, they had completely different antioxidant potential and stabilizing power of astaxanthin: the eutectic mixture composed of thymol and oleic acid was the best in this sense, maintaining the astaxanthin amount above 40% after 13.5 h of light exposure thanks to the 30-times higher antioxidant potential of thymol in comparison to DL-menthol and geraniol. This finding suggests the possibility to exploit astaxanthin extracts in TAO as improved antioxidant formulations that could be used for human-related applications thanks to the biocompatibility of all the GRAS ingredients of such formulations.

## **6.4 Experimental section**

### Materials

All solvents and chemicals used in this study were purchased from Sigma-Aldrich (Germany) and were used without purification (purities  $\geq 98\%$ ). Free astaxanthin, canthaxanthin, and lutein standards (purities  $\geq 95\%$ ) were purchased from Sigma-Aldrich (Germany).

### Solid-Liquid phase determination and Deep Eutectic Solvents (DESs) preparation

All the hydrophobic DESs (DL-menthol:oleic acid, thymol:oleic acid, geraniol:oleic acid) characterization was based on the comparison between the experimental and the theoretical solid-liquid phase diagrams. The experimental solid-liquid phase curves were obtained by measuring the melting points of the different samples at the different molar ratios with a thermometer via immersion of the samples in an ice/NaCl mixture or solid

CO<sub>2</sub>/acetone mixture in a Dewar. The melting temperatures were evaluated in triplicate to avoid any kinetic effect on the melting of the mixtures.

The solid-liquid theoretical curves were determined by using equation (1) that represents the solid-liquid equilibrium curve in a eutectic mixture (Rowlinson, 1970):

$$\ln(\chi_i \cdot \gamma_i) = \frac{\Delta_m h_i}{R} \cdot \left( \frac{1}{T_{m,i}} - \frac{1}{T} \right) + \frac{\Delta_m C p_i}{R} \cdot \left( \frac{T_{m,i}}{T} - \ln \frac{T_{m,i}}{T} - 1 \right) \quad (1)$$

where  $\chi_i$  is the mole fraction of component i,  $\gamma_i$  is its activity coefficient in the liquid phase,  $\Delta_m h_i$  and  $T_{m,i}$  are its melting enthalpy and temperature, respectively,  $\Delta_m C p_i$  is its heat capacity change upon melting, R is the ideal gas constant, and T is the absolute temperature of the system. This equation can be simplified by considering the heat capacity change upon the melting of a substance as negligible, therefore equation (2) was used:

$$\ln(\chi_i \cdot \gamma_i) = \frac{\Delta_m h_i}{R} \cdot \left( \frac{1}{T_{m,i}} - \frac{1}{T} \right) \quad (2)$$

The theoretical melting temperatures were determined from the theoretical curves by considering the activity coefficients  $\gamma_i = 1$ . The eutectic points were determined as the minimum in the experimental curves and they were compared to the theoretical ones.

The experimental  $\gamma_i$  values were determined via equation (3) by using the experimentally observed melting temperatures:

$$\gamma_i = \frac{\exp\left[\frac{\Delta_m h_i}{R} \left( \frac{1}{T_{m,i}} - \frac{1}{T} \right)\right]}{\chi_i} \quad (3)$$

The three DESs were then prepared by mixing appropriate molar ratios of oleic acid and the three terpenes to give MAO (DL-menthol:oleic acid, 2:1), TAO (thymol:oleic acid, 3:1), and GAO (geraniol:oleic acid, 13:1). The mixtures were heated at 60°C and magnetically stirred until homogeneous liquids were obtained. Particular attention was given to ensure homogeneous heating and prevent terpenes sublimation by limiting the headspace. The water content of the three DESs was measured via Karl-Fisher titration (684 KF Coulometer, Metrohm, US).

Three other mixtures were also prepared in the same way and then tested, to compare the extraction efficiency of eutectic and non-eutectic mixtures of oleic acid: i) thymol:oleic acid in a molar ratio 1:1, ii) geraniol:oleic acid in a molar ratio 2:1, and iii) L- $\alpha$ -phosphatidylcholine:oleic acid in a weight ratio 95:5.

### Haematococcus pluvialis cultivation

*H. pluvialis* (strain HP5, isolated in July 2014 in a freshwater sample collected in Ravenna, Italy) was cultivated in triplicate in a 1 L air-insufflated bottle using a modified BBM medium at a temperature of  $21\pm 1^\circ\text{C}$ , a light intensity of  $90\text{-}100\ \mu\text{mol}$  of photons per  $\text{m}^2\ \text{s}^{-1}$  and a 16 h light:8 h dark cycle. Under these conditions, the cells were kept in a vegetative phase until a dry weight of  $0.7\ \text{g}\ \text{L}^{-1}$  was reached. Then, the cultures were stressed under high light intensity ( $450\text{-}500\ \mu\text{mol}$  of photons per  $\text{m}^2\ \text{s}^{-1}$ ) and nutrient starvation by 3-times dilution of the algal culture.<sup>9</sup> When mature aplanospores (red cysts) were obtained, astaxanthin was extracted through two different procedures: extraction from freeze-dried algal biomass and from algal culture.

### Extraction of astaxanthin from freeze-dried *H. pluvialis* biomass

Algal culture (100 mL) with an astaxanthin content of 1.6 wt% was collected and centrifuged at  $2550\ \text{x}\ \text{g}$  for 10 min at  $4^\circ\text{C}$ . The supernatant was removed, the algal pellet was freeze-dried and then extracted at rt for 6 h with DESs, oleic acid, and geraniol (50 mg of biomass with 2 mL of solvent, i.e. 2.5 wt%). At the end of such time, the extracts were centrifuged at  $2550\ \text{x}\ \text{g}$  for 10 min to separate the extracted biomass from the liquid phases, then recovered by pipetting. Aliquots of the recovered liquid phases (0.02 mL) were withdrawn at specific time frames (1, 2, 4, and 6 h), diluted in DMSO (0.08 mL) and methanol (0.4 mL), and analyzed by HPLC-UV vis at 470 nm, as described below to determine the astaxanthin content. The same extraction procedure was also applied varying specific conditions to evaluate their effect on the kinetics and overall extraction performances:

- i) at rt with three non-eutectic mixtures of oleic acid: i) thymol:oleic acid in a molar ratio 1:1, ii) geraniol:oleic acid in a molar ratio 2:1, and iii) L- $\alpha$ -phosphatidylcholine:oleic acid in a weight ratio 95:5;
- ii) at  $60^\circ\text{C}$  with TAO;
- iii) at  $60^\circ\text{C}$  with two other biomass/TAO ratios: 50 mg biomass/1 mL TAO (i.e. 5 wt%), and 50 mg biomass/0.5 mL TAO (i.e. 10%).

### Extraction of astaxanthin from *H. pluvialis* culture

Algal culture (3 mL) with a cell density of  $1.3\ \text{g}\ \text{L}^{-1}$  and an astaxanthin content of 2.7 wt% was put in contact with DESs, oleic acid, and geraniol (1 mL) and gently stirred with a magnetic bar

at 50-100 rpm for 6 h. At the end of such time, the biphasic mixtures were centrifuged at 2550 x g for 10 min to separate the algal cultures from the liquid solvents, lastly recovered by pipetting. Aliquots of the recovered solvent phases (0.02 mL) were withdrawn at specific time frames (1, 2, 4, and 6 h), diluted in DMSO (0.08 mL) and methanol (0.4 mL), and analyzed by HPLC-UV vis at 470 nm, as described below to determine the astaxanthin content. *H. pluvialis* vitality before and after the extraction experiments was evaluated through pulse-amplitude modulated (PAM) fluorometry measurements in terms of kinetics and parameters of Photosystem II (PSII)<sup>9</sup>. The model used was 101-PAM (H. Walz, Effeltrich, Germany) connected to a PDA-100 data acquisition system, high power LED Lamp Control unit HPL-C and LED-Array-Cone HPL-L470 to supply saturated pulses, US-L655 and 102-FR to provide far-red light and light measurement, respectively. Before and after the extraction experiments, aliquots of algal cultures were placed in cuvettes (10 × 10 mm) mounted on an optical unit ED-101US/M. Measurement of the photosynthetic efficiency was derived from the maximum quantum yield of PSII ( $\Phi_{PSII}$ ), calculated from the following equation (4):

$$\Phi_{PSII} = \frac{F_m - F_0}{F_m} \quad (4)$$

The minimal fluorescence ( $F_0$ ) was measured on dark-adapted cultures for 20 min, by using modulated light of low intensity ( $2 \mu\text{mol m}^{-2} \text{s}^{-1}$ ). Then, a short saturating pulse of  $3000 \mu\text{mol m}^{-2} \text{s}^{-1}$  for 0.8 s induced the maximal fluorescence yield ( $F_m$ ). Photosynthetic activity (%) was calculated by dividing the maximum quantum yield of PSII ( $\Phi_{PSII}$ ) after the extraction by the maximum quantum yield of PSII ( $\Phi_{PSII}$ ) of the culture before the extraction.

#### Astaxanthin analysis

To determine the astaxanthin content in the algal cells subjected to the extraction experiments, a freeze-dried algal pellet (50 mg) was extracted twice with a mixture of cyclohexane/ethanol/acetone (2/1/1, 5 mL) for 48 h at rt. An aliquot of solvent (0.02 mL) was withdrawn, diluted in DMSO (0.08 mL) and methanol (0.4 mL), and analyzed by HPLC-UV-vis at 470 nm. Liquid chromatography analysis was performed using an HPLC system (Agilent 1200 series, Agilent Technologies Italia S.p.A, Milan, Italy) coupled with a UV-vis diode array detector. The separation was performed using an XBridge C8 column 137 Å, 3.5  $\mu\text{m}$ , 4.6 mm x 150 mm (Waters, Milford, MA, US) maintained at 30°C, with an injected volume of 5  $\mu\text{L}$ . The mobile phase was constituted as follows: H<sub>2</sub>O (solvent A) and methanol (solvent B).

Chromatographic separation was achieved at a  $0.7 \text{ mL min}^{-1}$  flow rate under gradient elution conditions: 80–100% B from 0 to 10 min, 100% B from 10 to 18 min, 100-80% B from 18 to 20 min; all the changes in the mobile phase composition were linear. The astaxanthin content in the cells was determined using a calibration curve prepared with standard astaxanthin in the free form ( $2.5\text{-}20 \mu\text{g mL}^{-1}$ ). The astaxanthin recovery (%) was determined by dividing the astaxanthin amount extracted with DESs, oleic acid, and geraniol, by the astaxanthin content in the algal cells (determined as described before with the mixture of cyclohexane/acetone/ethanol). The qualitative identification of the astaxanthin monoesters in the extracts was carried out through HPLC-MS analyses performed on an Agilent 1260 Infinity II system coupled to an electrospray ionization mass spectrometer (positive-ion mode,  $m/z = 100\text{-}3000$  amu, fragmentor 30 V). The column was the same used for HPLC/UV-Vis analysis, the mobile phase was modified by adding trifluoroacetic acid 0.1% v/v to both solvents. Chromatographic separation was achieved at a  $0.4 \text{ mL min}^{-1}$  flow rate under gradient elution conditions: 80–100% B from 0 to 10 min, 100% B from 10 to 30 min, 100-80% B from 30 to 32 min. Chemstation software was used for data processing.

#### NMR-analysis

To check the amount of TAO, MAO, GAO, and geraniol lost in aqueous phase, 1 mL of each solvent was added to 1 mL of  $\text{D}_2\text{O}$ ; after 6 h of contact between the two phases,  $^1\text{H}$  NMR quantitative analysis was performed by using 3-(trimethylsilyl)propionic-2,2,3,3- $\text{d}_4$  acid (TMSP), sodium salt as internal standard. Spectra were recorded in  $\text{D}_2\text{O}$  using a 5 mm probe on a VARIAN Mercury 400 spectrometer (400 MHz). Chemical shifts have been reported in ppm from tetramethyl silane (TMS).

$^1\text{H}$  NMR spectra of the extract obtained through cyclohexane:acetone:ethanol mixture from *H. pluvialis* freeze-dried biomass was recorded after solvent evaporation and performed on a Varian 400 (400 MHz) spectrometer. Chemical shifts are reported in ppm from TMS with the solvent resonance as the internal standard ( $\text{CDCl}_3$ : 7.26 ppm).

$^1\text{H}$  NMR and  $^{13}\text{C}$  NMR spectra before and after the extraction of freeze-dried biomass were registered on calibrated highly concentrated samples ( $50 \mu\text{l}$  of liquids in  $500 \mu\text{l}$  of  $\text{CDCl}_3$ ) on a Bruker DRX Advance 400 spectrometer equipped with a BBFO probe and on a Bruker Advance III HD. All the spectra were calibrated on solvents signals.

### Light-stability test and DPPH assay

Oxidation tests were performed on the extracts obtained from freeze-dried *H. pluvialis* biomass to evaluate the potential of the different hydrophobic solvents here used to stabilize and preserve astaxanthin. Samples were exposed to light radiation under controlled conditions employing sun simulating OSRAM ULTRA-VITALUX 300W UV-A lamp (220-230  $\mu\text{E m}^{-2} \text{s}^{-1}$ , OSRAM spa, Milan, Italy). Aliquots of solvent (0.02 mL) were withdrawn at specific time frames (0.5, 1.5, 3.5, 7.5 and 13.5 h), diluted in DMSO (0.08 mL) and methanol (0.4 mL), and analyzed by HPLC-UV vis at 470 nm, as described above to determine the astaxanthin content. The astaxanthin stability was expressed as the percentage of astaxanthin amount at specific ageing time with respect to the astaxanthin content in the corresponding unaged sample.

The antioxidant activity of the obtained extracts was evaluated using the 2,2-diphenyl-1-picrylhydrazyl (DPPH) free radical scavenging assay (Blois, 1958). An aliquot (25  $\mu\text{L}$ ) of the sample was dissolved in ethanol to obtain 2 mL solutions, then 500  $\mu\text{L}$  of these solutions were mixed with 500  $\mu\text{L}$  of 0.06 mM DPPH solution (in ethanol). After 30 min of incubation at rt in the dark, the absorbance at 517 nm was measured with JASCO V-650 UV/Vis spectrophotometer (Jasco, Tokyo, Japan). The DPPH free radical scavenging activity was calculated in terms of the percentage of inhibition of the free radicals by using the following equation (5):

$$\text{DPPH scavenging activity } \% = \frac{A_C - (A_S - A_B)}{A_C} \quad (5)$$

Where:  $A_S$  indicates the absorbance of the sample,  $A_C$  is the absorbance of the control (prepared by diluting 500  $\mu\text{L}$  of DPPH solution in 500  $\mu\text{L}$  of ethanol) and  $A_B$  is the absorbance of blank (prepared by mixing 500  $\mu\text{L}$  of sample solution with 500  $\mu\text{L}$  of ethanol).

## BIBLIOGRAPHY

- (1) Pitacco, W.; Samori, C.; Pezzolesi, L.; Gori, V.; Grillo, A.; Tiecco, M.; Vagnoni, M.; Galletti, P. Extraction of Astaxanthin from *Haematococcus Pluvialis* with Hydrophobic Deep Eutectic Solvents Based on Oleic Acid. *Food Chem.* **2022**, *379*, 132156. <https://doi.org/10.1016/j.foodchem.2022.132156>.
- (2) Solovchenko, A. E. Recent Breakthroughs in the Biology of Astaxanthin Accumulation by Microalgal Cell. *Photosynth. Res.* **2015**, *125* (3), 437–449. <https://doi.org/10.1007/s11120-015-0156-3>.
- (3) Shah, M. M. R.; Liang, Y.; Cheng, J. J.; Daroch, M. Astaxanthin-Producing Green Microalga *Haematococcus Pluvialis*: From Single Cell to High Value Commercial Products. *Front. Plant Sci.* **2016**, *7* (APR2016). <https://doi.org/10.3389/fpls.2016.00531>.
- (4) Liu, X.; McClements, D. J.; Cao, Y.; Xiao, H. Chemical and Physical Stability of Astaxanthin-Enriched Emulsion-Based Delivery Systems. *Food Biophys.* **2016**, *11* (3), 302–310. <https://doi.org/10.1007/s11483-016-9443-6>.
- (5) Vechio, H.; Mariano, A. B.; Vieira, R. B. A New Approach on Astaxanthin Extraction via Acid Hydrolysis of Wet *Haematococcus Pluvialis* Biomass. *J. Appl. Phycol.* **2021**, *33* (5), 2957–2966. <https://doi.org/10.1007/s10811-021-02495-z>.
- (6) de Souza Mesquita, L. M.; Martins, M.; Pisani, L. P.; Ventura, S. P. M.; de Rosso, V. V. Insights on the Use of Alternative Solvents and Technologies to Recover Bio-Based Food Pigments. *Compr. Rev. Food Sci. Food Saf.* **2021**, *20* (1), 787–818. <https://doi.org/10.1111/1541-4337.12685>.
- (7) Desai, R. K.; Streefland, M.; Wijffels, R. H.; Eppink, M. H. M. Novel Astaxanthin Extraction from *Haematococcus Pluvialis* Using Cell Permeabilising Ionic Liquids. *Green Chem.* **2016**, *18* (5), 1261–1267. <https://doi.org/10.1039/c5gc01301a>.
- (8) Krichnavaruk, S.; Shotipruk, A.; Goto, M.; Pavasant, P. Supercritical Carbon Dioxide Extraction of Astaxanthin from *Haematococcus Pluvialis* with Vegetable Oils as Co-Solvent. *Bioresour. Technol.* **2008**, *99* (13), 5556–5560. <https://doi.org/10.1016/j.biortech.2007.10.049>.
- (9) Samori, C.; Pezzolesi, L.; Galletti, P.; Semeraro, M.; Tagliavini, E. Extraction and Milking of Astaxanthin from: *Haematococcus Pluvialis* Cultures. *Green Chem.* **2019**, *21* (13). <https://doi.org/10.1039/c9gc01273g>.
- (10) Machmudah, S.; Shotipruk, A.; Goto, M.; Sasaki, M.; Hirose, T. Extraction of Astaxanthin from *Haematococcus Pluvialis* Using Supercritical CO<sub>2</sub> and Ethanol as Entrainer. *Ind. Eng. Chem. Res.* **2006**, *45* (10), 3652–3657. <https://doi.org/10.1021/ie051357k>.
- (11) Rodrigues, L. A.; Pereira, C. V.; Leonardo, I. C.; Fernández, N.; Gaspar, F. B.; Silva, J. M.; Reis, R. L.; Duarte, A. R. C.; Paiva, A.; Matias, A. A. Terpene-Based Natural Deep Eutectic Systems as Efficient Solvents to Recover Astaxanthin from Brown Crab Shell Residues. *ACS Sustain. Chem. Eng.* **2020**, *8* (5), 2246–2259. <https://doi.org/10.1021/acssuschemeng.9b06283>.
- (12) Gao, J.; You, J.; Kang, J.; Nie, F.; Ji, H.; Liu, S. Recovery of Astaxanthin from Shrimp (*Penaeus Vannamei*) Waste by Ultrasonic-Assisted Extraction Using Ionic Liquid-in-Water Microemulsions. *Food Chem.* **2020**, *325* (December 2019), 126850. <https://doi.org/10.1016/j.foodchem.2020.126850>.
- (13) Chandra Roy, V.; Ho, T. C.; Lee, H. J.; Park, J. S.; Nam, S. Y.; Lee, H.; Getachew, A. T.; Chun, B. S. Extraction of Astaxanthin Using Ultrasound-Assisted Natural Deep Eutectic Solvents from Shrimp Wastes and Its Application in Bioactive Films. *J. Clean. Prod.* **2021**, *284*. <https://doi.org/10.1016/j.jclepro.2020.125417>.
- (14) Khoo, K. S.; Ooi, C. W.; Chew, K. W.; Foo, S. C.; Lim, J. W.; Tao, Y.; Jiang, N.; Ho, S.-H.; Show, P. L. Permeabilization of *Haematococcus Pluvialis* and Solid-Liquid Extraction of Astaxanthin by CO<sub>2</sub>-Based Alkyl Carbamate Ionic Liquids. *Chem. Eng. J.* **2021**, *411*, 128510. <https://doi.org/10.1016/j.cej.2021.128510>.
- (15) Bi, W.; Tian, M.; Zhou, J.; Row, K. H. Task-Specific Ionic Liquid-Assisted Extraction and Separation of Astaxanthin from Shrimp Waste. *J. Chromatogr. B* **2010**, *878* (24), 2243–2248. <https://doi.org/10.1016/j.jchromb.2010.06.034>.
- (16) Choi, S.-A.; Oh, Y.-K.; Lee, J.; Sim, S. J.; Hong, M. E.; Park, J.-Y.; Kim, M.-S.; Kim, S. W.; Lee, J.-S. High-Efficiency Cell Disruption and Astaxanthin Recovery from *Haematococcus Pluvialis* Cyst Cells Using Room-Temperature Imidazolium-Based Ionic Liquid/Water Mixtures. *Bioresour. Technol.* **2019**, *274*, 120–126. <https://doi.org/10.1016/j.biortech.2018.11.082>.
- (17) Liu, Z.-W.; Yue, Z.; Zeng, X.-A.; Cheng, J.-H.; Aadil, R. M. Ionic Liquid as an Effective Solvent for Cell Wall Deconstructing through Astaxanthin Extraction from *Haematococcus Pluvialis*. *Int. J. Food Sci. Technol.* **2019**, *54* (2), 583–590. <https://doi.org/10.1111/ijfs.14030>.
- (18) Liu, Z.-W.; Zeng, X.-A.; Cheng, J.-H.; Liu, D.-B.; Aadil, R. M. The Efficiency and Comparison of Novel Techniques for Cell Wall Disruption in Astaxanthin Extraction from *Haematococcus Pluvialis*. *Int. J. Food Sci. Technol.* **2018**, *53* (9), 2212–2219. <https://doi.org/10.1111/ijfs.13810>.

- (19) Fan, Y.; Niu, Z.; Xu, C.; Yang, L.; Chen, F.; Zhang, H. Biocompatible Protic Ionic Liquids-Based Microwave-Assisted Liquid-Solid Extraction of Astaxanthin from *Haematococcus Pluvialis*. *Ind. Crops Prod.* **2019**, *141*, 111809. <https://doi.org/10.1016/j.indcrop.2019.111809>.
- (20) Gao, J.; You, J.; Kang, J.; Nie, F.; Ji, H.; Liu, S. Recovery of Astaxanthin from Shrimp (*Penaeus Vannamei*) Waste by Ultrasonic-Assisted Extraction Using Ionic Liquid-in-Water Microemulsions. *Food Chem.* **2020**, *325*, 126850. <https://doi.org/10.1016/j.foodchem.2020.126850>.
- (21) Gao, J.; Fang, C.; Lin, Y.; Nie, F.; Ji, H.; Liu, S. Enhanced Extraction of Astaxanthin Using Aqueous Biphasic Systems Composed of Ionic Liquids and Potassiumphosphate. *Food Chem.* **2020**, *309*, 125672. <https://doi.org/10.1016/j.foodchem.2019.125672>.
- (22) Praveenkumar, R.; Lee, K.; Lee, J.; Oh, Y.-K. Breaking Dormancy: An Energy-Efficient Means of Recovering Astaxanthin from Microalgae. *Green Chem.* **2015**, *17* (2), 1226–1234. <https://doi.org/10.1039/C4GC01413H>.
- (23) Dai, Y.; van Spronsen, J.; Witkamp, G. J.; Verpoorte, R.; Choi, Y. H. Natural Deep Eutectic Solvents as New Potential Media for Green Technology. *Anal. Chim. Acta* **2013**, *766*, 61–68. <https://doi.org/10.1016/j.aca.2012.12.019>.
- (24) Zhang, H.; Tang, B.; Row, K. H. A Green Deep Eutectic Solvent-Based Ultrasound-Assisted Method to Extract Astaxanthin from Shrimp Byproducts. *Anal. Lett.* **2014**, *47* (5), 742–749. <https://doi.org/10.1080/00032719.2013.855783>.
- (25) Lee, Y. R.; Row, K. H. Comparison of Ionic Liquids and Deep Eutectic Solvents as Additives for the Ultrasonic Extraction of Astaxanthin from Marine Plants. *J. Ind. Eng. Chem.* **2016**, *39*, 87–92. <https://doi.org/10.1016/j.jiec.2016.05.014>.
- (26) Florindo, C.; Branco, L.; Marrucho, I. Quest for Green-Solvent Design : From Hydrophilic to Hydrophobic ( Deep ) Eutectic Solvents. *ChemSusChem* **2019**, *12*, 1549–1559. <https://doi.org/10.1002/cssc.201900147>.
- (27) Samorì, C.; Mazzei, L.; Ciurli, S.; Cravotto, G.; Grillo, G.; Guidi, E.; Pasteris, A.; Tabasso, S.; Galletti, P. Urease Inhibitory Potential and Soil Ecotoxicity of Novel “Polyphenols-Deep Eutectic Solvents” Formulations. *ACS Sustain. Chem. Eng.* **2019**, *7* (18). <https://doi.org/10.1021/acssuschemeng.9b03493>.
- (28) Silva, J. M.; Pereira, C. V.; Mano, F.; Silva, E.; Reis, R. L.; Sa, I.; Paiva, A.; Matias, A. A.; Duarte, A. R. C. Therapeutic Role of Deep Eutectic Solvents Based on Menthol and Saturated Fatty Acids on Wound Healing. *ACS Appl. Biomater.* **2019**, *2*, 4346–4355. <https://doi.org/10.1021/acsabm.9b00598>.
- (29) Silva, J. M.; Reis, R. L.; Paiva, A.; Duarte, A. R. C. Design of Functional Therapeutic Deep Eutectic Solvents Based on Choline Chloride and Ascorbic Acid. *ACS Sustain. Chem. Eng.* **2018**, *6* (8), 10355–10363. <https://doi.org/10.1021/acssuschemeng.8b01687>.
- (30) Van Osch, D. J. G. P.; Dietz, C. H. J. T.; Van Spronsen, J.; Kroon, M. C.; Gallucci, F.; Van Sint Annaland, M.; Tuinier, R. A Search for Natural Hydrophobic Deep Eutectic Solvents Based on Natural Components. *ACS Sustain. Chem. Eng.* **2019**, *7* (3), 2933–2942. <https://doi.org/10.1021/acssuschemeng.8b03520>.
- (31) Ambati, R. R.; Moi, P. S.; Ravi, S.; Aswathanarayana, R. G. Astaxanthin: Sources, Extraction, Stability, Biological Activities and Its Commercial Applications - A Review. *Mar. Drugs* **2014**, *12* (1), 128–152. <https://doi.org/10.3390/md12010128>.
- (32) Martins, M. A. R.; Crespo, E. A.; Pontes, P. V. A.; Silva, L. P.; Bülow, M.; Maximo, G. J.; Batista, E. A. C.; Held, C.; Pinho, S. P.; Coutinho, J. A. P. Tunable Hydrophobic Eutectic Solvents Based on Terpenes and Monocarboxylic Acids. *ACS Sustain. Chem. Eng.* **2018**, *6* (7), 8836–8846. <https://doi.org/10.1021/acssuschemeng.8b01203>.
- (33) Kollau, L. J. B. M.; Vis, M.; Van Den Bruinhorst, A.; De With, G.; Tuinier, R. Activity Modelling of the Solid-Liquid Equilibrium of Deep Eutectic Solvents. *Pure Appl. Chem.* **2019**, *91* (8), 1341–1349. <https://doi.org/10.1515/pac-2018-1014>.
- (34) Pontes, P. V. A.; Crespo, E. A.; Martins, M. A. R.; Silva, L. P.; Neves, C. M. S. S.; Maximo, G. J.; Hubinger, M. D.; Batista, E. A. C.; Pinho, S. P.; Coutinho, J. A. P.; Sadowski, G.; Held, C. Measurement and PC-SAFT Modeling of Solid-Liquid Equilibrium of Deep Eutectic Solvents of Quaternary Ammonium Chlorides and Carboxylic Acids. *Fluid Phase Equilibria* **2017**, *448*, 69–80. <https://doi.org/10.1016/j.fluid.2017.04.007>.
- (35) Ashworth, C. R.; Matthews, R. P.; Welton, T.; Hunt, P. A. Doubly Ionic Hydrogen Bond Interactions within the Choline Chloride-Urea Deep Eutectic Solvent. *Phys. Chem. Chem. Phys.* **2016**, *18* (27), 18145–18160. <https://doi.org/10.1039/c6cp02815b>.
- (36) Maha M. Abdallah, Simon Müller, Andrés González de Castilla, Pavel Gurikov, Ana A. Matias, Maria do Rosário Bronze, N. F. Physicochemical Characterization and Simulation of the Eutectic Solvent Systems. **2021**.
- (37) Tiecco, M.; Cappellini, F.; Nicoletti, F.; Del Giacco, T.; Germani, R.; Di Profio, P. Role of the Hydrogen Bond Donor Component for a Proper Development of Novel Hydrophobic Deep Eutectic Solvents. *J. Mol. Liq.*

- 2019**, *281*, 423–430. <https://doi.org/10.1016/j.molliq.2019.02.107>.
- (38) Grewe, C.; Griehl, C. Time- and Media-Dependent Secondary Carotenoid Accumulation in *Haematococcus Pluvialis*. *Biotechnol. J.* **2008**, *3* (9–10), 1232–1244. <https://doi.org/10.1002/biot.200800067>.
- (39) Tan, Y.; Ye, Z.; Wang, M.; Manzoor, M. F.; Aadil, R. M.; Tan, X.; Liu, Z. Comparison of Different Methods for Extracting the Astaxanthin from *Haematococcus Pluvialis*: Chemical Composition and Biological Activity. *Molecules* **2021**, *26* (12), 3569. <https://doi.org/10.3390/molecules26123569>.
- (40) Samorì, C.; Pezzolesi, L.; Galletti, P.; Semeraro, M.; Tagliavini, E. Extraction and Milking of Astaxanthin from *Haematococcus Pluvialis* Cultures. *Green Chem.* **2019**, *21* (13), 3621–3628. <https://doi.org/10.1039/C9GC01273G>.
- (41) Florindo, C.; Branco, L. C.; Marrucho, I. M. Development of Hydrophobic Deep Eutectic Solvents for Extraction of Pesticides from Aqueous Environments. *Fluid Phase Equilibria* **2017**, *448*, 135–142. <https://doi.org/10.1016/j.fluid.2017.04.002>.
- (42) Honda, M.; Kageyama, H.; Hibino, T.; Osawa, Y.; Kawashima, Y.; Hirasawa, K.; Kuroda, I. Evaluation and Improvement of Storage Stability of Astaxanthin Isomers in Oils and Fats. *Food Chem.* **2021**, *352* (February), 129371. <https://doi.org/10.1016/j.foodchem.2021.129371>.
- (43) Anarjan, N.; Nehdi, I. A.; Tan, C. P. Protection of Astaxanthin in Astaxanthin Nanodispersions Using Additional Antioxidants. *Molecules* **2013**, *18* (7), 7699–7710. <https://doi.org/10.3390/molecules18077699>.
- (44) Armenta, R. E.; Isabbl, G. L. Stability Studies on Astaxanthin Extracted from Fermented Shrimp Byproducts. *J. Agric. Food Chem.* **2009**, *57* (14), 6095–6100. <https://doi.org/10.1021/jf901083d>.
- (45) Ruberto, G.; Baratta, M. T. Antioxidant Activity of Selected Essential Oil Components in Two Lipid Model Systems. *Food Chem.* **2000**, *69* (2), 167–174. [https://doi.org/10.1016/S0308-8146\(99\)00247-2](https://doi.org/10.1016/S0308-8146(99)00247-2).
- (46) Aeschbach, R.; Löliger, J.; Scott, B. C.; Murcia, A.; Butler, J.; Halliwell, B.; Aruoma, O. I. Antioxidant Actions of Thymol, Carvacrol, 6-Gingerol, Zingerone and Hydroxytyrosol. *Food Chem. Toxicol.* **1994**, *32* (1), 31–36. [https://doi.org/10.1016/0278-6915\(84\)90033-4](https://doi.org/10.1016/0278-6915(84)90033-4).
- (47) Alam, K.; Nagi, M. N.; Badary, O. A.; Al-shabanah, O. A.; Al-rikabi, A. C.; Al-bekairi, A. M. THE PROTECTIVE ACTION OF THYMOL AGAINST CARBON TETRACHLORIDE HEPATOTOXICITY IN MICE. *Pharmacol. Res.* **1999**, *40* (2), 159–163. <https://doi.org/10.1006/phrs.1999.0472>.
- (48) Kruk, I.; Michalska, T.; Lichszteld, K.; Kładna, A.; Aboul-Enein, H. Y. The Effect of Thymol and Its Derivatives on Reactions Generating Reactive Oxygen Species. *Chemosphere* **2000**, *41* (7), 1059–1064. [https://doi.org/10.1016/S0045-6535\(99\)00454-3](https://doi.org/10.1016/S0045-6535(99)00454-3).

## APPENDIX 6

### Contents

**A6.1**  $^1\text{H}$ -NMR spectrum of the extract obtained through cyclohexane:acetone:ethanol mixture.

**A6.2**  $^1\text{H}$ -NMR spectrum of a fraction of the purified extract obtained through cyclohexane: acetone: ethanol mixture.

**A6.3** Table of Astaxanthin recovery from *H. pluvialis* freeze-dried biomass with different compounds.

**A6.4** Astaxanthin recovery from *H. pluvialis* freeze-dried biomass after 6 h with TAO, varying the biomass/TAO ratio.

**A6.5** Residual photosynthetic activity of *H. pluvialis* cells after the contact with MAO and oleic acid.

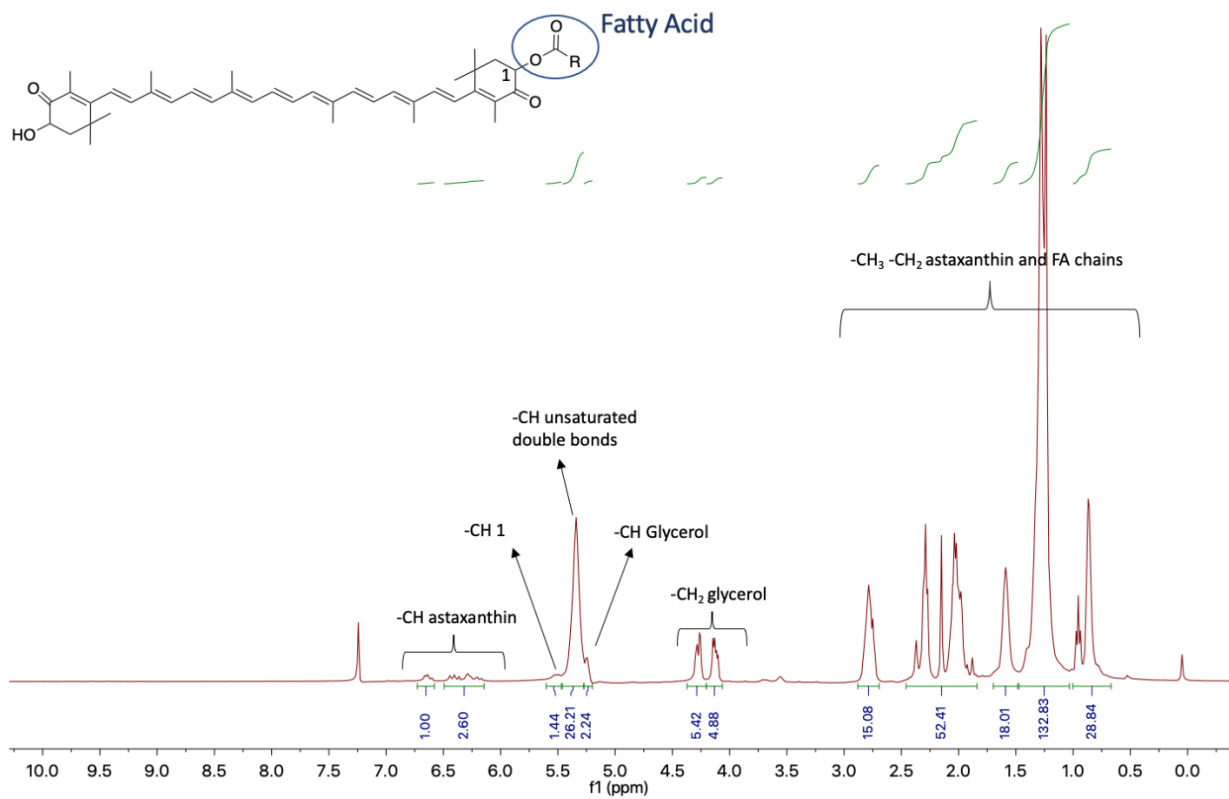
**A6.6** Comparison of the carotenoid profile obtained with TAO from freeze-dried biomass and from the culture.

**A6.7**  $^1\text{H}$  NMR spectra of DES after 6 h contact with water.

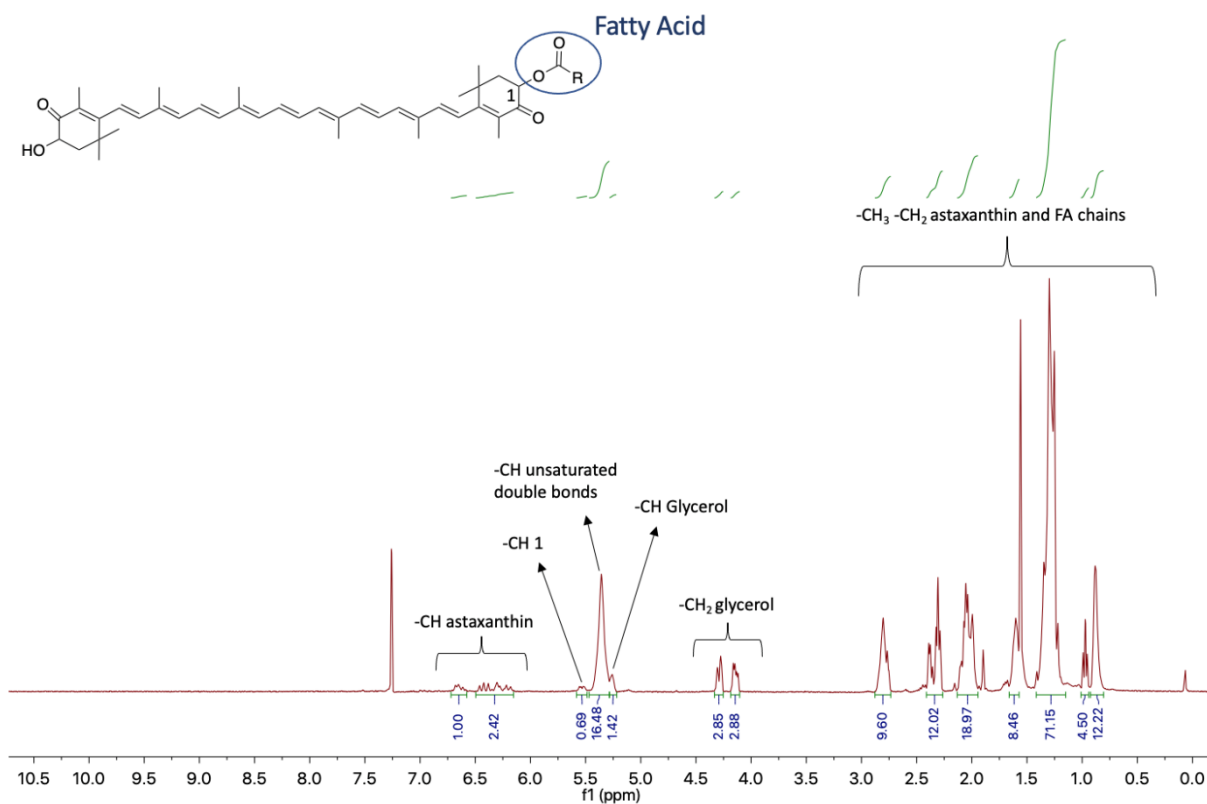
**A6.8** Optical microscope pictures of *H. pluvialis* cysts after extraction with DES.

**A6.9**  $^1\text{H}$  NMR and  $^{13}\text{C}$  NMR spectra of TAO before and after the extraction of freeze-dried biomass.

### A6.1 <sup>1</sup>H-NMR spectrum of the extract obtained through cyclohexane:acetone:ethanol mixture.



**A6.2**  $^1\text{H-NMR}$  spectrum of a fraction of the purified extract obtained through cyclohexane: acetone: ethanol mixture. Purification was made by flash-column chromatography (cyclohexane-ethyl acetate, 99:1-70:30).

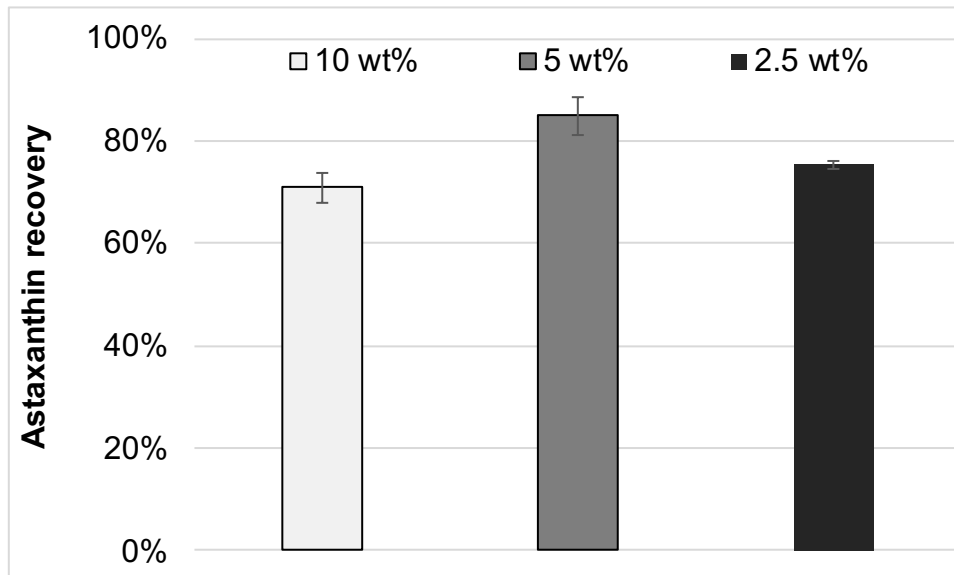


**A6.3** Astaxanthin recovery from *H. pluvialis* freeze-dried biomass with MAO; TAO; GAO; oleic acid; geraniol; non-eutectic mixture of thymol and oleic acid in a 1:1 molar ratio; non-eutectic mixture of geraniol and oleic acid in a 2:1 molar ratio; non-eutectic mixture of L- $\alpha$ -phosphatidylcholine:oleic acid in a 95:5 weight ratio. Data are expressed based on the percentage of the astaxanthin content in *H. pluvialis* cells, as mean of two independent experiments on different freeze-dried algal biomass.

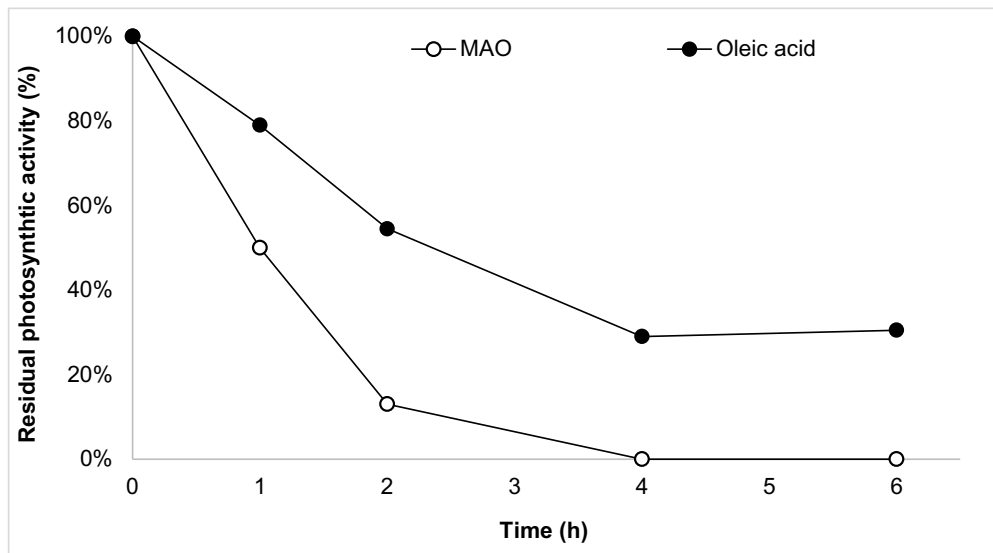
Solvent acronym	Component 1	Component 2	Molar ratio	Astaxanthin recovery (%)			
				1 h	2 h	4 h	24 h
MAO	DL-menthol	Oleic acid	2:1	22	50	55	74
TAO	Thymol	Oleic acid	3:1	39	54	60	83
-	Thymol	Oleic acid	1:1	46	57	58	61
GAO	Geraniol	Oleic acid	13:1	37	48	54	66
-	Geraniol	Oleic acid	2:1	51	53	54	57
-	L- $\alpha$ -phosphatidylcholine	Oleic acid	95:5*	35	46	51	52
-	Oleic acid	-	-	16	27	33	64
-	Geraniol	-	-	21	55	60	62

\*Weight ratio

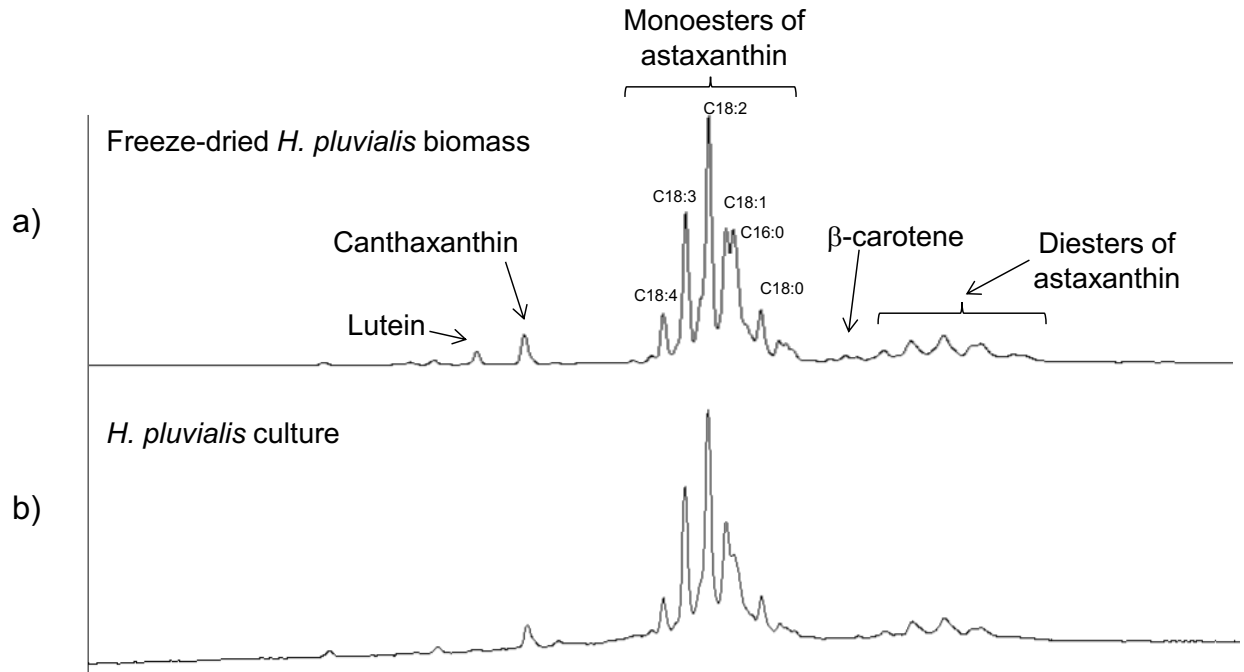
**A6.4** Astaxanthin recovery from *H. pluvialis* freeze-dried biomass after 6 h with TAO, varying the biomass/TAO ratio (2.5, 5 and 10 wt%). Data are expressed based on the percentage of the astaxanthin content in *H. pluvialis* cells, as mean of two independent experiments on different freeze-dried algal biomass.



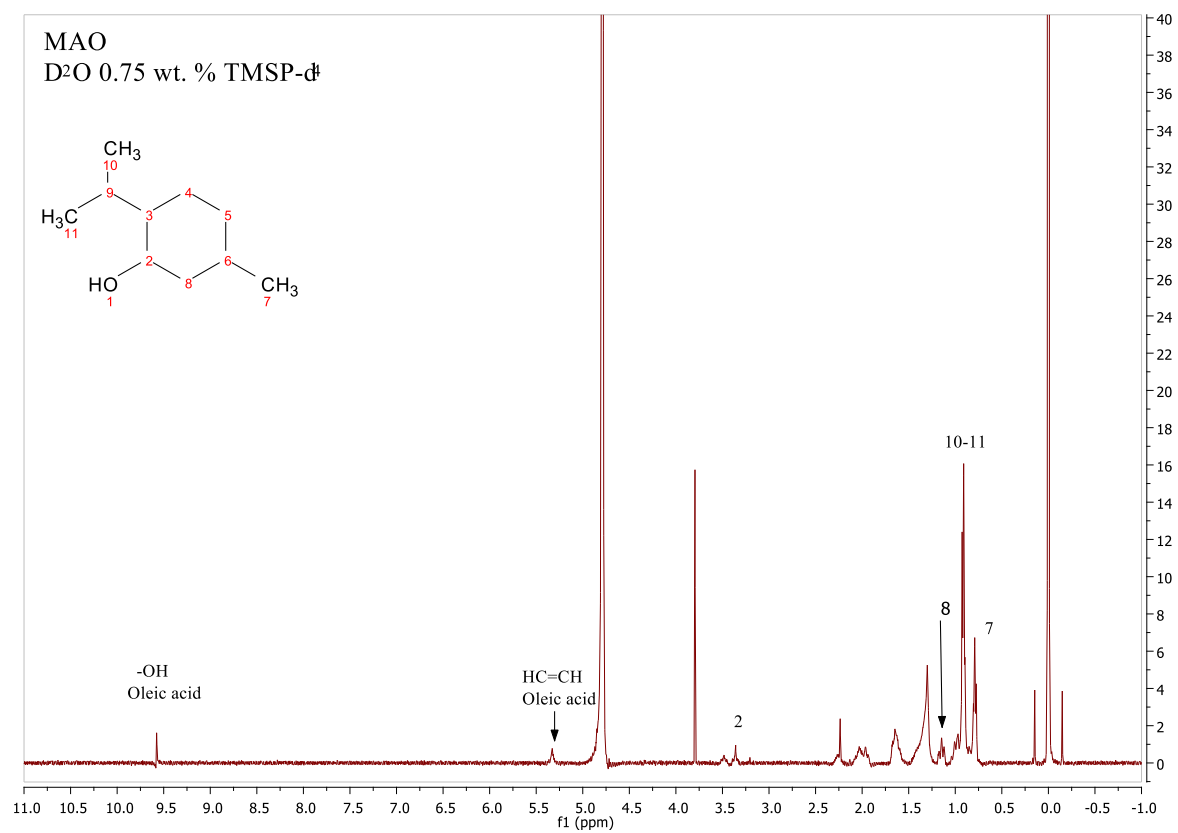
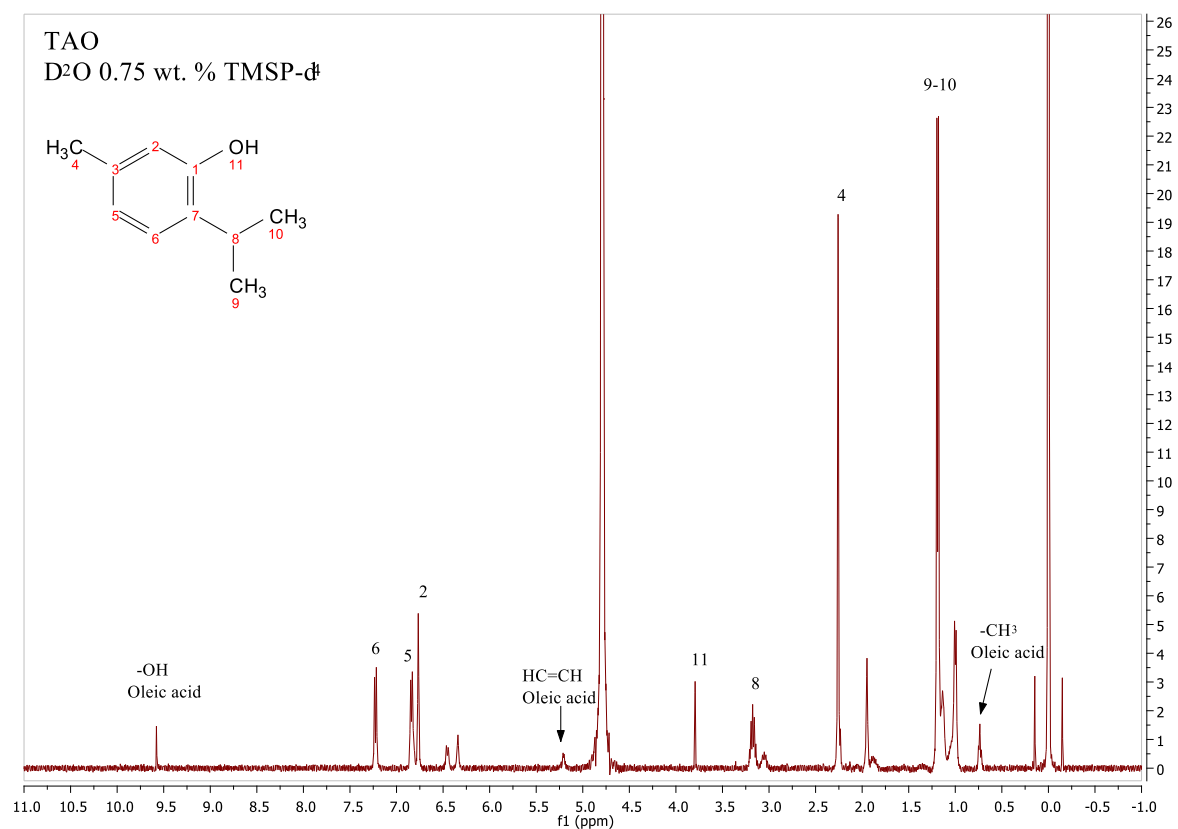
**A6.5** Residual photosynthetic activity of *H. pluvialis* cells after the contact with MAO and oleic acid for 1, 2, 4, and 6 h. Data are expressed on the basis of the percentage of the photosynthetic activity of the same culture without the extraction.

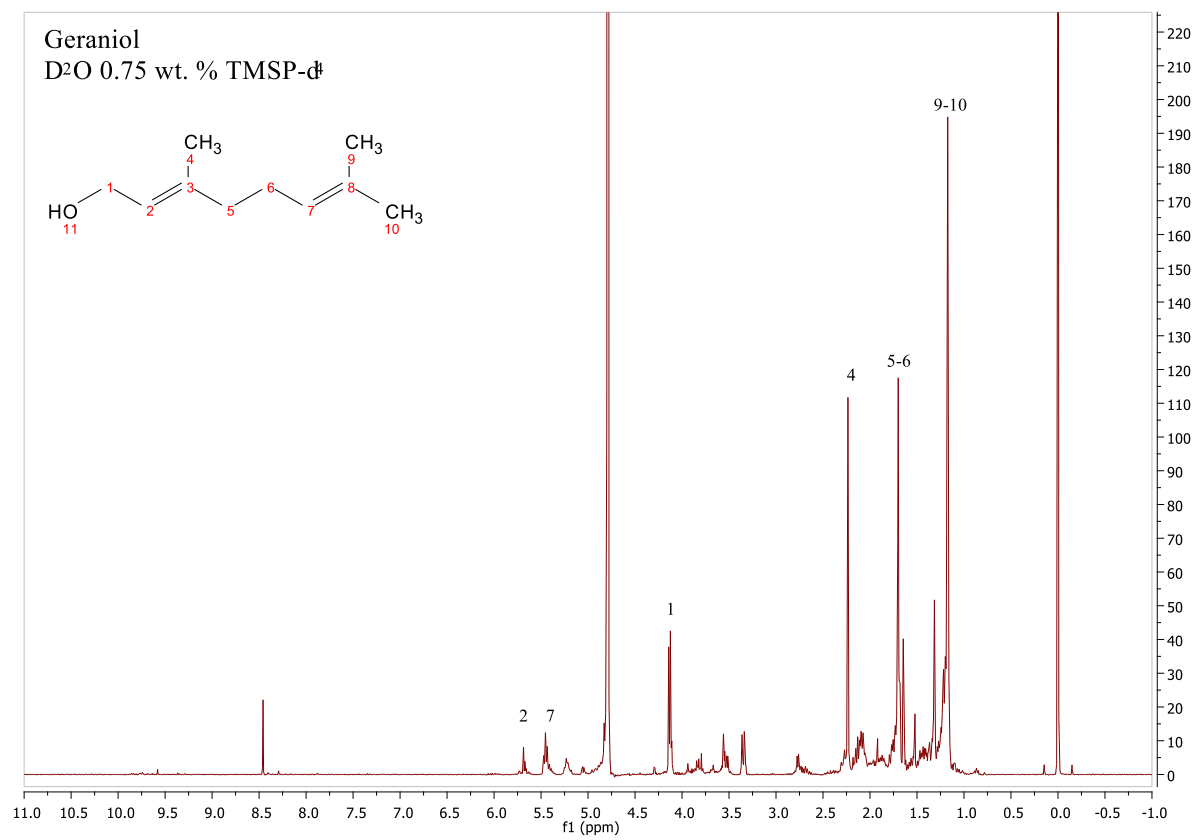
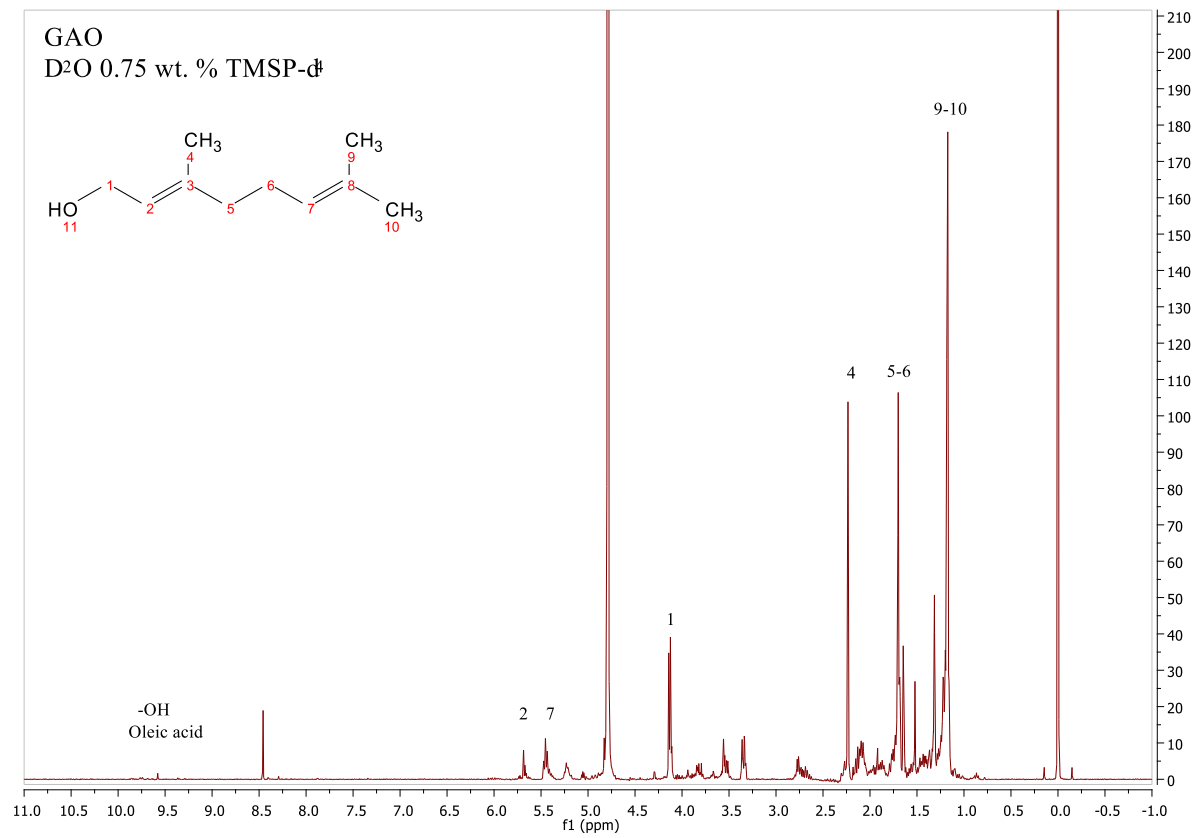


**A6.6** Comparison of the carotenoid profile obtained with TAO from a) freeze-dried *H. pluvialis* biomass and b) *H. pluvialis* culture.

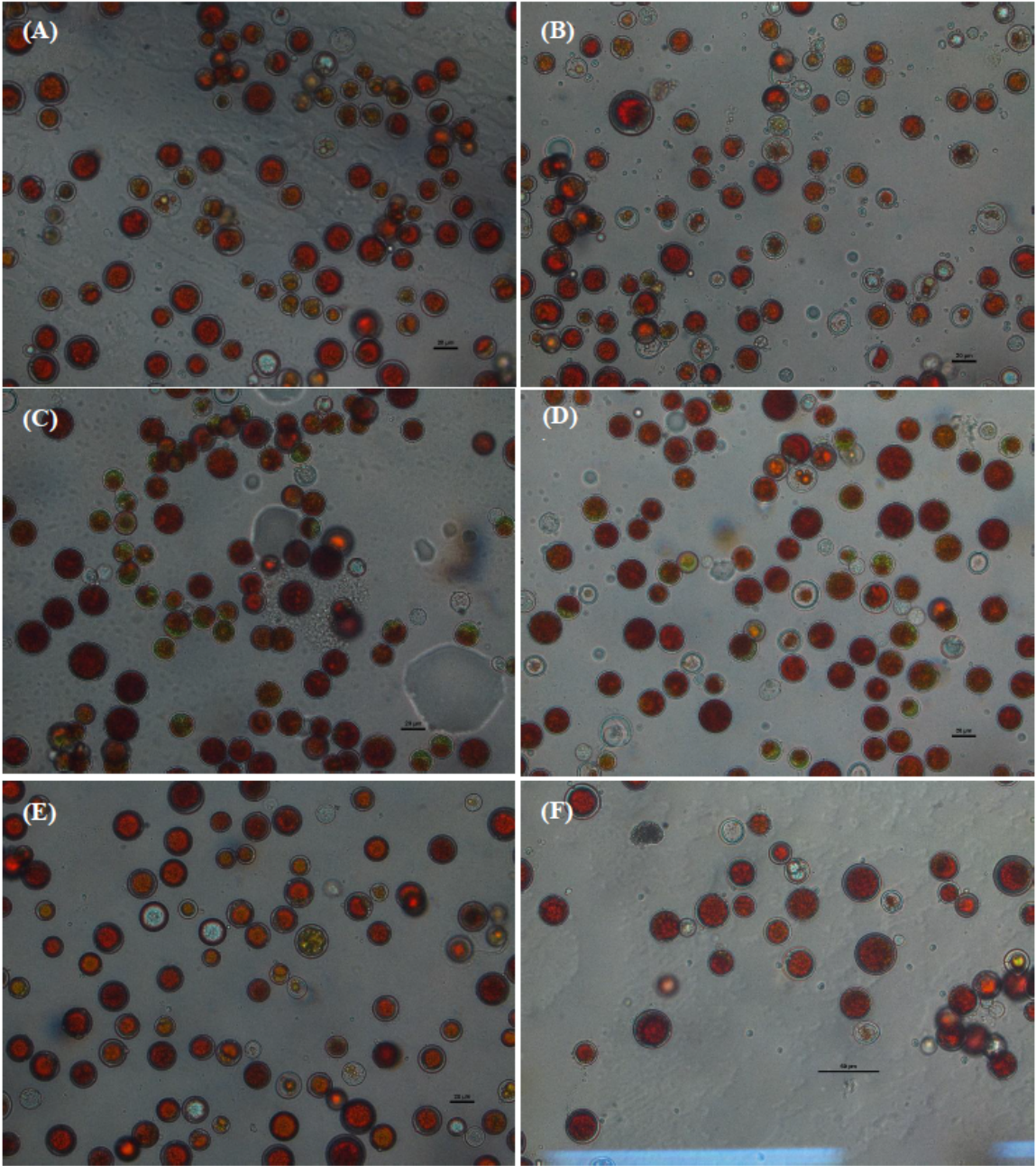


## A6.7 <sup>1</sup>H NMR spectra of DES after 6 h contact with water.

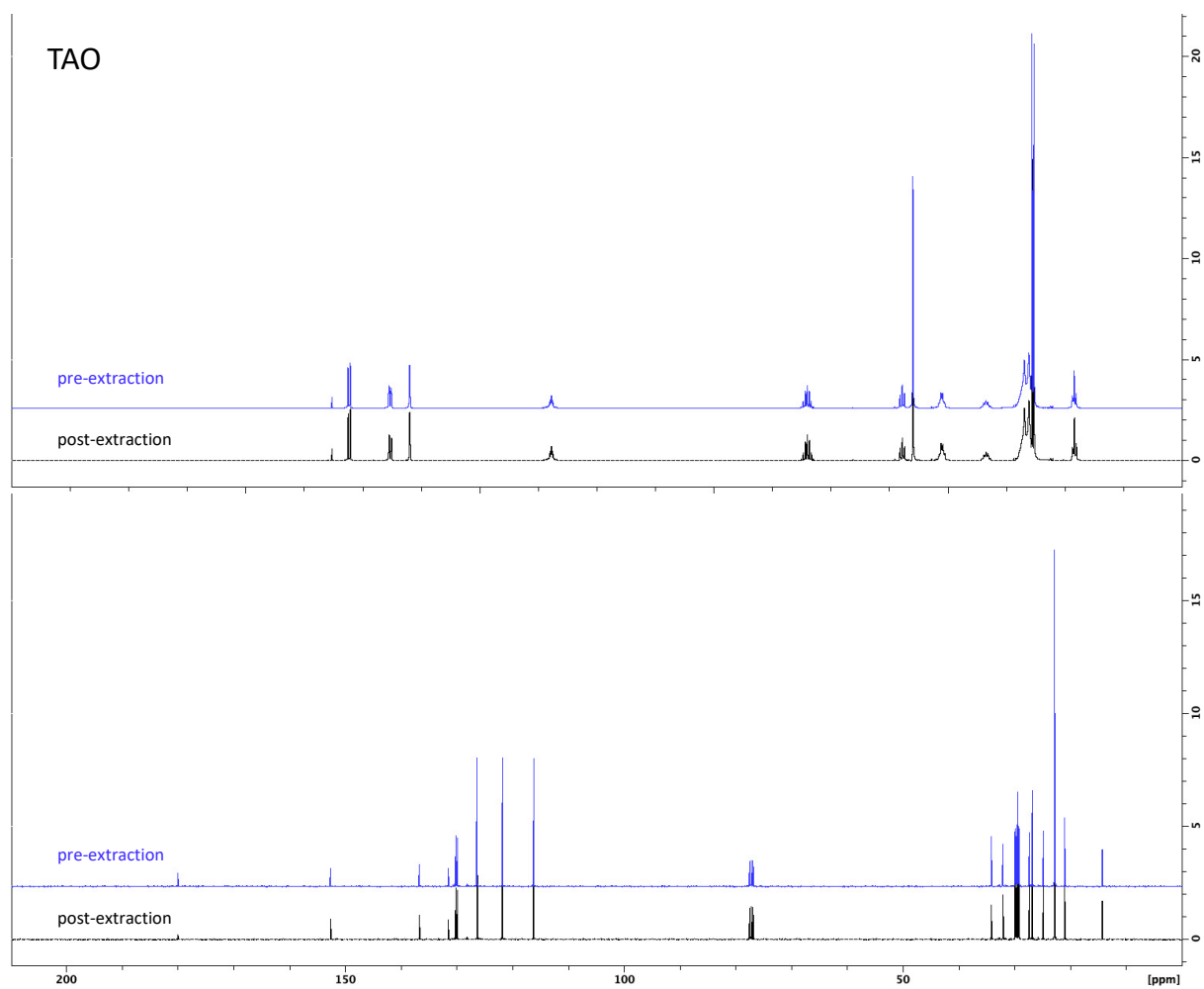




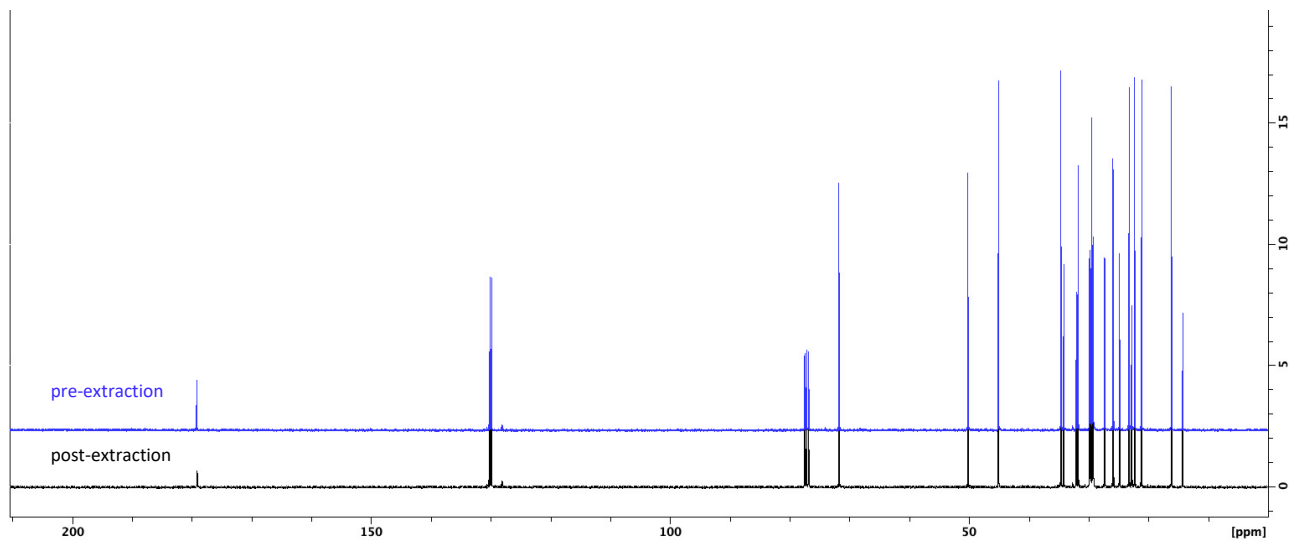
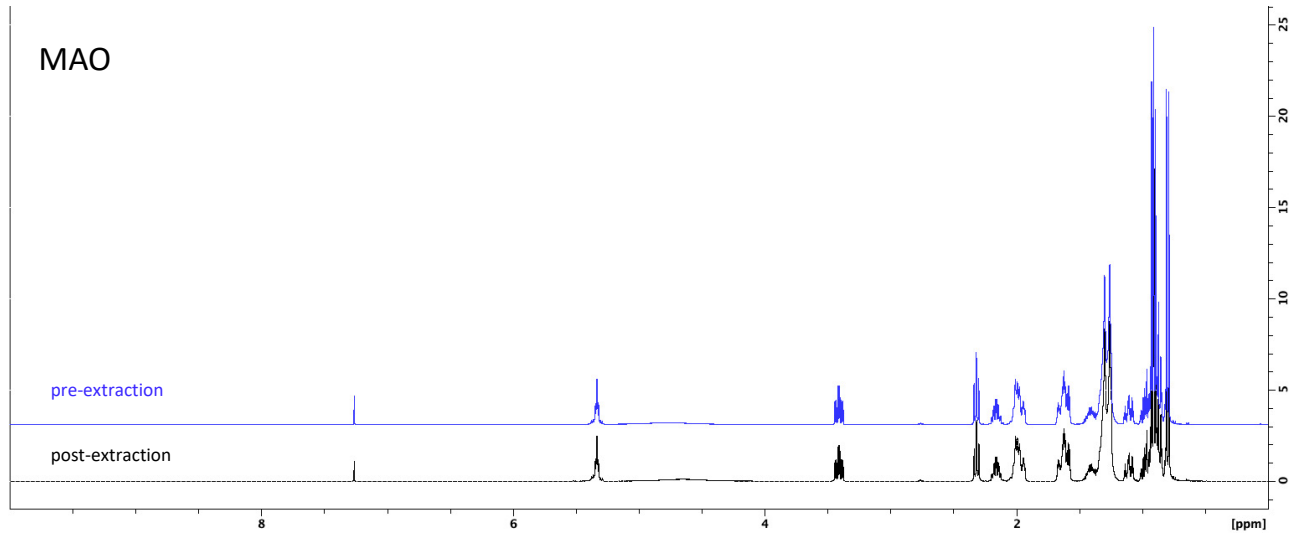
A6.8 Optical microscope pictures (32x magnification) of *H. pluvialis* cysts after liquid-liquid extraction with A) GAO after 1 h; B) GAO after 4 h; C) MAO after 1 h; D) MAO after 4 h; E) TAO after 1 h; F) TAO after 4 h. Scale bar is 50  $\mu\text{m}$  for F), and 20  $\mu\text{m}$  for the other pictures.

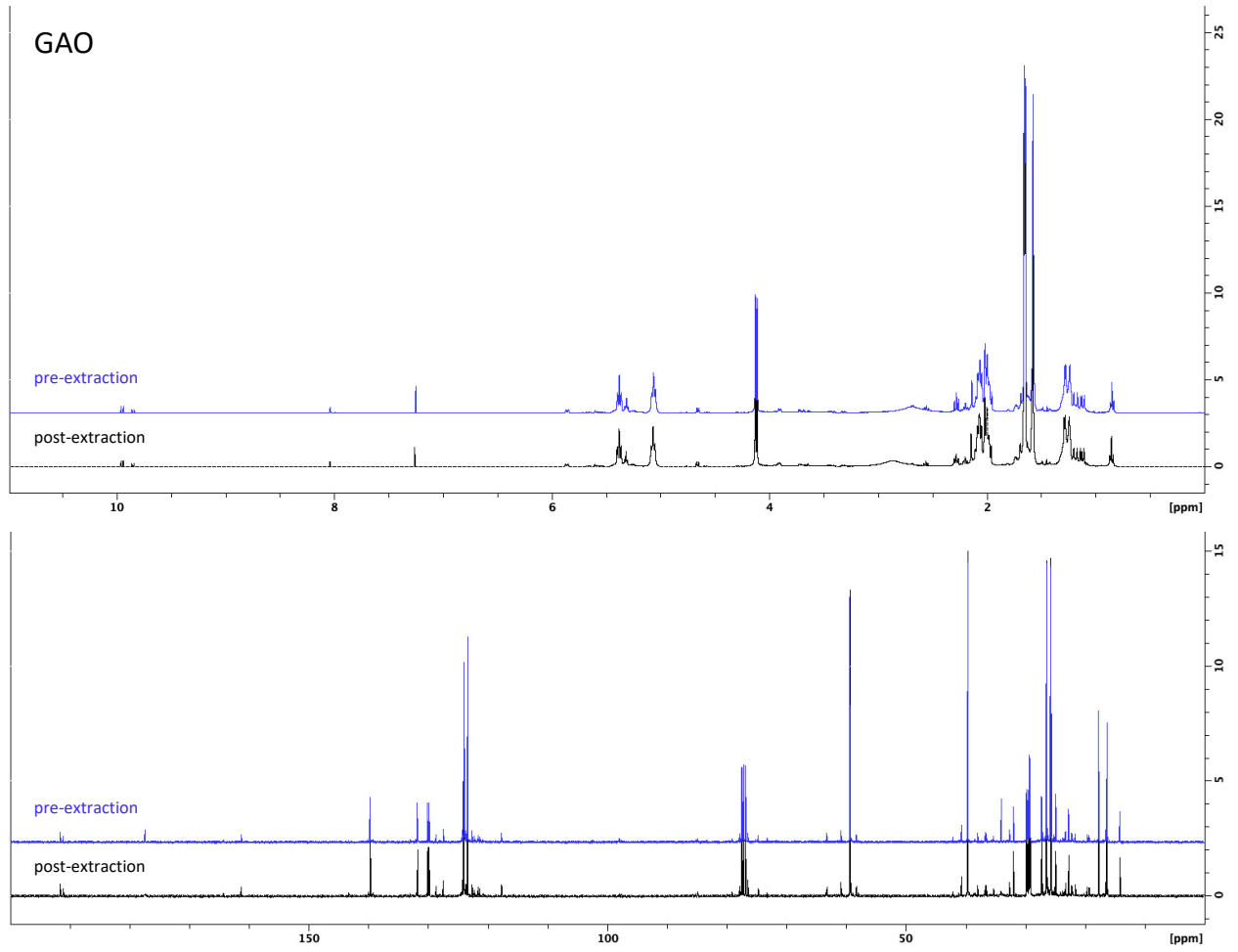


## A6.9 $^1\text{H}$ NMR and $^{13}\text{C}$ NMR spectra of DES.



# MAO





**Published as:** Pitacco, W.; Samorì, C.; Pezsolesi, L.; Gori, V.; Grillo, A.; Tiecco, M.; Vagnoni, M.; Galletti, P. Extraction of Astaxanthin from *Haematococcus Pluvialis* with Hydrophobic Deep Eutectic Solvents Based on Oleic Acid. *Food Chem.* **2022**, *379*, 132156. <https://doi.org/10.1016/j.foodchem.2022.132156>.